Towards a personalised medicine strategy to reduce prostate cancer risk in men

Eliza Yankova (BSc)

A thesis presented to Ulster University for the degree of Doctor of Philosophy

Northern Ireland Centre for Stratified Medicine
School of Biomedical Sciences
Faculty of Life and Health Sciences
Ulster University

May 2018

I confirm that the word count of the thesis is less than 100,000 words.

Table of Contents

List of Figures

List of Figures is Appendices

List of Tables

Acknowledgements

I would like to thank Dr Andrew McDowell and Prof Tony Bjourson. This work was supported by £11.5M grant awarded to Professor Tony Bjourson from European Union Regional Development Fund (ERDF) EU Sustainable Competitiveness Programme for N. Ireland; Northern Ireland Public Health Agency (HSC R&D) & Ulster University. I would also like to thank Prof Christopher Mitchell and Prof Lorraine Marin for providing some of the cell lines used in this study.

A massive thank you to Dr David Gibson. The completion of this thesis would have been impossible without his guidance.

Thank you to all the staff in the Northern Ireland Centre for Stratified Medicine and C-TRIC for all your help. Special thank you to Dr Geraldine Horigan for being there for me over the last few months.

A big thank you to everyone I have met during this PhD adventure.

Thank you to Phil Egan, you have taught me so much.

Thank you to Tan Ahmed and Lee McCahon for listening to my problems and giving the best advice, both in science and in general.

Thank you, Ruairidh and Kevin, I am proud of you.

Thank you, Chris, for all the laughter.

And a special thank you to Andrew Parton for all the advice, support and amazing memories from the last three years; thank you for helping me get here.

Thank you, mum and dad – Отново ще имам време за разговори по Скайп.

Thank you to Mrs Neli Vitanova – Благодаря за вдъхновението.

Thank you to Dr Jeremy Ross, you showed me how fun and exciting science can be.

And thank you to Sam, you can have your girlfriend back (soon).

Abstract

Prostate cancer is the second most common cancer in men. Studies now indicate a strong association of the disease with chronic bacterial infection, which may ultimately induce oncogenesis. It has been shown that *P. acnes* is the predominant organism isolated from prostatectomy samples and is significantly associated with organ inflammation. Further evidence suggests that *P. acnes* is able to chronically infect the prostate gland and *in vitro* experiments clearly indicate its potential to drive oncogenic changes. This thesis investigates the oncogenic potential of specific prostate-derived *P. acnes* phylogenetic types, with the ultimate aim of developing risk stratification approaches for the development of the disease.

In vitro infection models were used to compare the effects of different phylogenetic types of *P. acnes* on prostate epithelial cells. Soft agar assays and quantitative PCR (qPCR) were used to investigate the molecular expression profiles associated with endothelial-mesenchymal transition (EMT) and inflammation during bacterial infection. Cells infected with phylotype IA_1 were able to form colonies in soft agar assays, indicating cellular transformation. Additionally, qPCR results showed a decrease in the expression of the EMT marker E-cadherin. These findings were supported by immunostaining experiments. Furthermore, qPCR expression analysis revealed that phylotype IA_1 infection induces changes suggestive of apoptosis resistance, increased proliferation and androgen-independent growth, all characteristics of advanced treatment-resistant cancer. In contrast, cells infected with type III strain exhibited expression changes consistent with anti-cancer behaviour, including increased apoptosis and androgen-dependent signalling.

These findings highlight the strain-specific response to infection and suggest the attractive possibility that infection with *P. acnes* may be a modifiable risk factor for prostate cancer. Since some phylotypes of *P. acnes* may be oncogenic, while others are cancer-protective, the development of a screening test to identify the presence of infection may therefore prove valuable to stratify patients at risk of oncogenesis.

Abbreviations

1,3-BPG	1,3-bisphosphoglyceric acid
22Rv1	Prostate carcinoma cell line
22Rv1	Prostate cancer cell line
ACACA	Acetyl-coenzyme A carboxylase alpha
ACKR3	Atypical chemokine receptor 3 (also called CXCR-7)
ACTB	Beta actin
ADAM17	ADAM metallopeptidase domain 17 (also called TACE)
AE	QIAGEN QIAamp DNA Mini Kit elution buffer
AKT	Protein kinase B (protein/gene)
AL	QIAGEN QIAamp DNA Mini Kit lysis buffer
AMP	Adenosine monophosphate
AMPK	AMP-activated protein kinase
ANGPT2	Angiopoietin-2
APC	Adenomatous polyposis coli
AR	Androgen receptor
ARNTL	Aryl hydrocarbon receptor nuclear translocator-like
aroE	Shikimate 5-dehydrogenase
ATCC	American Type Culture Collection
ATP	Adenosine triphosphate
ATPase	Adenosine triphosphatase
atpD	ATP synthase beta chain
AW1	QIAGEN QIAamp DNA Mini Kit wash buffer
AW2	QIAGEN QIAamp DNA Mini Kit wash buffer

B2M	Beta-2-microglobulin
BAX	BCL-2-associated X protein
BC3	QIAGEN 5X Reverse Transcription Buffer 3
BCL2	B-cell lymphoma 2 (protein/gene)
β-ME	β-mercaptoethanol
β-TrCP	F-box/WD repeat-containing protein 1A
BHI	Brain heart infusion
bHLH	Basic helix-loop-helix
BIM	BCL-2-like protein 11
BPH	Bovine pituitary extract
BR	Broad range
BRCA2	Breast cancer 2, tumours suppressor gene
BrdU	Bromodeoxyuridine (5-bromo-2-deoxyuridine)
BSA	Bovine serum albumin
CagA	*H. pylori* cytotoxin-associated gene A
CAMKK1	Calcium/calmodulin-dependent protein kinase kinase 1, alpha
CAMP	Christie-Atkins-Munch-Peterson co-haemolytic factor
cAMP	Cyclic adenosine monophosphate
CAMSAP1	Calmodulin regulated spectrin-associated protein 1
CASP3	Caspase 3, apoptosis-related cysteine peptidase
CAV1	Caveolin-1
CAV2	Caveolin-2
CC	Clonal complex
CCNA1	Cyclin A1

CCND1	Cyclin D1
CCND2	Cyclin D2
CD	Cluster of differentiation
CDH1	E-cadherin (epithelial)
CDH2	N-cadherin (neuronal)
CDK	Cyclin-dependent kinase
CDKN2A	Cyclin-dependent kinase inhibitor 2A, also known as $p16^{ink4a}$
cDNA	Complementary DNA
CFTR	Cystic fibrosis transmembrane conductance regulator
CFU	Colony forming unit
CI	Confidence interval
CK1	Casein kinase 1
CLN3	Ceroid-lipofuscinosis, neuronal 3
CLOCK	Circadian locomotor output cycles kaput
CoA	Coenzyme A
COX-1/*COX1*	Cyclooxygenase-1 (protein/gene), also called PTGS1
COX-2/*COX2*	Cyclooxygenase-2 (protein/gene), also called PTGS2
CP/CPSS	Chronic prostatitis/chronic pelvic pain syndrome
CREB1	cAMP responsive element binding protein 1
CRPC	Castration resistant prostate cancer
Ct or Cp	Cycle threshold
CXCL	Chemokine (C-X-C motif) ligand
CXCR	C-X-C motif chemokine receptor
DAPI	4',6-diamidino-2-phenylindole, dihydrochloride

DAXX	Death-domain associated protein
DDX11	DEAD/H (Asp-Glu-Ala-Asp/His) box polypeptide 11
DHT	5α-dihydrotestosterone
DKK3	Dickkopf Wnt signalling pathway inhibitor homolog 3
DLC1	Deleted in liver cancer 1
DLL4	Delta-like protein 4
DMSO	Dimethyl sulfoxide
DNA	Deoxyribonucleic acid
DNA-PK	DNA-dependent protein kinase
dNTP	Deoxynucleotide
DRE	Digital rectal examination
DU145	Prostate cancer cell line
Dvl	Dishevelled
E	Efficiency
EB	QIAGEN QIAquick PCR Purification Kit elution buffer
E-box	Enhancer box
ECM	Extracellular matrix
ECT2	Epithelial cell transforming sequence 2 oncogene
EDNRB	Endothelin receptor type B
EDTA	Ethylenediaminetetraacetic acid
EGF	Epidermal growth factor
EGFP	Enhanced green fluorescent protein
EGFR	Epidermal growth factor receptor
EGR3	Early growth response 3

ELISA	Enzyme-linked immunosorbent assay
EMT	Epithelial–mesenchymal transition
EPCAM	Epithelial cell adhesion molecule, mutated in Lynch syndrome
ERG	V-ets erythroblastosis virus E26 oncogene homolog (avian)
ERK	Extracellular signal-regulated kinases
erm(X)	Erythromycin resistance gene
ETV1	Ets variant 1
FACS	Fluorescence-activated cell sorting
FadA	*Fusobacterium* adhesin A
FAS	Fatty acid synthase
FASN	Fatty acid synthase (gene, encodes FAS)
FBS	Foetal bovine serum
FFPE	Formalin-fixed paraffin-embedded
FGF	Fibroblast growth factors
FOXM1	Forkhead box protein M1
FOXO1	Forkhead box protein O1
FSH	Follicle stimulating hormone
G_1-phase	Gap/Growth phase 1
G_2-phase	Gap/Growth phase 2
GAPDH	Glyceraldehyde 3-phosphate dehydrogenase
GBS	Group B Streptococci, e.g. *S. agalactiae*
GCA	Grancalcin, EF-hand calcium binding protein
GE	QIAGEN genomic DNA elimination buffer
gehA	*P. acnes* gene encoding lipase

gmk	Guanylate kinase
GnRH	Gonadotropin-releasing hormone
GPX3	Glutathione peroxidase 3 (plasma)
GSK3	Glycogen synthase kinase 3
GSTP1	Glutathione S-transferase pi 1
GTPase	Guanosine triphosphatase
guaA	GMP synthase
HAL	Histidine ammonia-lyase
HDMEC	Human dermal microvascular endothelial cells
HER2	Receptor tyrosine-protein kinase erbB-2
HGDC	Human Genomic DNA Contamination Control
HIF-1	Hypoxia-inducible factor 1
HMEC-1	Human microvascular endothelial cell line
HMGCR	3-hydroxy-3-methylglutaryl-CoA reductase
HPG	Hypothalamic-pituitary-gonadal axis
HPRT	Hypoxanthine-guanine phosphoribosyltransferase
HPV	Human papilloma virus
HRP	Horseradish peroxidase
HS	High sensitivity
IF	Immunofluorescence
IFNγ	Interferon gamma
IGF-1/IGF1	Insulin-like growth factor 1 (somatomedin C)
IGFBP5	Insulin-like growth factor binding protein 5
IKK	IκB kinase

IL	Interleukin
IL1R	Interleukin 1 receptor
IL-1β/IL1B	Interleukin 1 beta (protein/gene)
IL-6/IL6	Interleukin 6 (protein/gene)
IL6R	Interleukin 6 receptor
IL-8/IL8	Interleukin 8 (protein/gene)
IntDen	Integrated density
IκB	Inhibitor of κB
JAK	Janus kinase
JNK	c-Jun N-terminal kinase
KLHL13	Kelch-like 13 (*Drosophila*)
KLK	Kallikrein
KLK3	Kallikrein-related peptidase 3 (PSA)
KSFM	Keratinocyte serum-free medium
LDH	Lactate dehydrogenase
lepA	GTP-binding protein
LGALS4	Lectin, galactoside-binding, soluble, 4
LH	Luteinizing hormone
LnCAP	Prostate cancer cell line
LOXL1	Lysyl oxidase-like 1
LRP	lipoprotein receptor-related protein
LSGS	Low serum growth supplements
MAD	Mothers against decapentaplegia in *Drosophila*
MAPK	Mitogen-activated protein kinase

MAPKAPK	Mitogen-activated protein kinase-activated protein kinase
MAPKK	Mitogen-activated protein kinase
MAPKKK	Mitogen-activated protein kinase kinase kinase (also called MAP3K)
MAX	MYC associated factor X
Mcl-1	Myeloid cell leukaemia 1, BCL2 family apoptosis regulator
MCP-1	Monocyte chemoattractant protein-1 (CCL2)
M-CSF	Macrophage colony-stimulating factor
MDM2	Mouse double minute 2 homolog
MEK	MAPK/ERK Kinase, aka MAP2K
MET	Mesenchymal-epithelial transition
MGMT	O-6-methylguanine-DNA methyltransferase
MKI67	Marker of proliferation Ki-67
MLH1	*mutL* homolog 1, mutated in Lynch syndrome
MLST	Multilocus sequence typing
MMP	Matrix metalloproteinase
MNK	Menkes' protein, also known as ATP7A
MOI	Multiplicity of infection
M-PER	Mammalian protein extraction reagent
M-phase	Mitotic phase
MPS	Massive parallel sequencing
MSH2	*mutS* homolog 2, mutated in Lynch syndrome
MSH6	*mutS* homolog 6, mutated in Lynch syndrome
MSK	Mitogen and stress-activated protein kinase
MSR-1	Macrophage scavenger receptor-1

MSX1	Msh homeobox 1
MTO1	Mitochondrial translation optimization 1 homolog
mTOR	Mechanistic target of rapamycin
mTORC	Mechanistic target of rapamycin complex
MTT	3-(4,5-Dimethylthiazol-2-yl)-2,5-Diphenyltetrazolium Bromide
NAD+	Nicotinamide adenine dinucleotide (oxidized)
NADH	Nicotinamide adenine dinucleotide (reduced)
NCTC	National Collection of Type Cultures
NDRG3	NDRG family member 3
NEMO	Nuclear factor-kappa B Essential Modulator
NF-κB	Nuclear factor of kappa light polypeptide gene enhancer in B-cells
NF-κB1	NF-κB family member class I, p105, becomes p50 when processed
NF-κB2	NF-κB family member class I, p100, becomes p52 when processed
NIK	NF-κB inducing kinase
NK	Nature killer cells
NKX3-1	NK3 homeobox 1
NLRP3	Cryopyrin, inflammasome component
NormIntDen	Normalised integrated density
NRIP1	Nuclear receptor interacting protein 1
NSAID	Non-steroidal anti-inflammatory drug
OD	Optical density
$p16^{INK4a}$	Cyclin-dependent kinase inhibitor 2A, also known as CDKN2A
P2	QIAGEN Primer and External Control Mix
p53	Tumour protein p53

P53AIP1	p-53-regulated apoptosis-inducing protein 1
PAmce	Putative cell invasion-associated protein
Pap60	Putative cell invasion-associated protein
PB	QIAGEN QIAquick PCR Purification Kit binding buffer
PBS	Phosphate buffered saline
PBST	PBS-Tween
PC	Positive control
PC-3	Metastatic (bone) human prostate carcinoma cell line
PCR	Polymerase chain reaction
PDGF	Platelet-derived growth factor
PDGFR	Platelet-derived growth factor receptor
PDK1	3-phosphoinositide-dependent protein kinase-1
PDLIM4	PDZ and LIM domain 4
PDPK1	3-phosphoinositide dependent protein kinase-1
PE	QIAGEN QIAquick PCR Purification Kit wash buffer
PES1	Pescadillo homolog 1, containing BRCT domain (zebrafish)
PFKFB2	6-phosphofructo-2-kinase/fructose-2,6-biphosphatase
PH	Prolyl hydroxylases
PhIP	2-Amino-1-methyl-6-phenylimidazo[4,5-b]pyridine
PI3K	Phosphatidylinositol-4,5-bisphosphate 3-kinase
PIA	Proliferative inflammatory atrophy
PIN	Prostatic intraepithelial neoplasia, mutated in Lynch syndrome
PIP_3	Phosphatidylinositol (3,4,5)-trisphosphate
PlGF	Placental growth factor

PMH	Progressive macular hypomelanosis
PMS2	PMS1 homolog 2, mutated in Lynch syndrome
PPP2R1B	Protein phosphatase 2, regulatory subunit A, beta
PRKAB1	Protein kinase, AMP-activated, beta 1 non-catalytic subunit
PSA	Prostate specific antigen
PTEN	Phosphatase and tensin homolog
PTGS	Prostaglandin-endoperoxide synthase, also known as COX-2
PTGS1	Prostaglandin-endoperoxide synthase 1, also called COX-1
PTGS2	Prostaglandin-endoperoxide synthase 2, also called COX-2
qPCR	Quantitative/real-time polymerase chain reaction
RAF	**R**apidly **a**ccelerated **f**ibrosarcoma proto-oncogene
RARB	Retinoic acid receptor, beta
RAS	**Ra**t **s**arcoma gene
RASSF1	Ras association (RalGDS/AF-6) domain family member 1
Rb	Retinoblastoma
RBM39	RNA binding motif protein 39
RE3	QIAGEN Reverse Transcriptase Enzyme Mix 3
recA	Recombinase A protein
RelA	NF-κB family member class II, p65
RelB	NF-κB family member class II
RLT	QIAGEN RNeasy Plus Mini-Kit lysis buffer
RNA	Ribonucleic acid
RNase	Ribonuclease
RNASEL	2’-5—oligoadenylate dependent ribonuclease L

RNAseq	RNA sequencing
ROS	Reactive oxygen species
RPE	QIAGEN RNeasy Plus Mini-Kit wash buffer
RPLP0	Ribosomal protein, large, P0
RPMI-1640	Roswell Park Memorial Institute - 1640 medium
rRNA	Ribosomal RNA
RSK	Ribosomal s6 kinase
RT	Reverse transcription
RTK	Receptor tyrosine kinase
RT-PCR	Reverse-transcription polymerase chain reaction
RW1	QIAGEN RNeasy Plus Mini-Kit wash buffer
RWPE-1	Non-cancerous human prostate epithelial cell line
SCAF11	SR-related CTD-associated factor 11
SEM	Standard error of the mean
SEPT7	Septin 7
SFRP1	Secreted frizzled-related protein 1
SHBG	Sex hormone-binding globulin
SHP	SH2 domain-containing phosphatase
S-HRP	Streptavidin-horseradish peroxidase conjugate
SLC5A8	Solute carrier family 5 (iodide transporter), member 8
sma	Small body gene in *C. elegans*
SMAD	Portmanteau of *sma* (in *C. elegans*) and MAD (in *Drosophila*)
SNAI1	Snail family zing finger 1 (Snail)
SNAI2	Snail family zing finger 2 (Slug)

SOCS3	Suppressor of cytokine signalling 3
sodA	Superoxide dismutase
SOX4	SRY (sex determining region Y)-box 4
S-phase	Synthesis phase
SREBF1	Sterol regulatory element binding transcription factor 1
ST	Sequence type
STAT	Signal transducer and activator of transcription
STI	Sexually transmitted infection
STK11	Serine/threonine kinase 11
SUPT7L	Suppressor of Ty 7
TACE	Tumour necrosis factor-α conversing enzyme (also called ADAM17)
TBP	TATA-binding protein
TCA	Tricarboxylic acid cycle, also called Krebs cycle or Citric acid cycle
TFPI2	Tissue factor pathway inhibitor 2
TGFB1I1	Transforming growth factor beta 1 induced transcript 1
TGFBR	Transforming growth factor beta receptor
TGF-β/TGFB	Transforming growth factor beta (protein/gene)
Th_1	Type 1 helper T cells
THP-1	Acute monocytic leukaemia cell line
TIMP	Tissue inhibitor of metalloproteinases
TLR	Toll-like receptor
tly	Putative haemolysin gene
TMB	3,3',5,5'-Tetramethylbenzidine
TMPRSS2	Transmembrane protease, serine 2

TNFR	Tumour necrosis factor receptor
TNFRSF10D	TNF superfamily, member 10d, decoy with truncated death domain
TNF-α/TNF	Tumour necrosis factor (protein/gene)
TNM	Tumour/node/metastasis staging system
TP53	Tumour protein p53
TRADD	Tumour necrosis factor receptor type 1-associated DEATH domain
TRAF	TNF receptor associated factor
TRUS	Transrectal ultrasound
TSP-1	Thrombospondin-1
TUNEL	Terminal deoxynucleotidyl transferase (**T**dT) d**U**TP **N**ick-**E**nd **L**abelling
TWIST1	Twist-related protein 1
U	Unit
UPEC	Uropathogenic *Escherichia coli*
USP5	Ubiquitin specific peptidase 5 (isopeptidase T)
VacA	*H. pylori* vacuolating cytotoxin A
VEGF	Vascular endothelial growth factor
VEGFR	Vascular endothelial growth factor receptor
VIM	Vimentin
ZIP1	Zinc transporter protein 1
ZNF185	Zinc finger protein 185 (LIM domain)

Declaration

I hereby declare that for 2 years following the date on which the thesis is deposited in Research Student Administration of Ulster University, the thesis shall remain confidential with access or copying prohibited. Following expiry of this period I permit:

1. The Librarian of the University to allow the thesis to be copied in whole or in part without reference to me on the understanding that such authority applies to the provision of single copies made for study purposes or for inclusion within the stock of another library.
2. The thesis to be made available through the Ulster Institutional Repository and/or EThOS under the terms of the Ulster eTheses Deposit Agreement which I have signed.

IT IS A CONDITION OF USE OF THIS THESIS THAT ANYONE WHO CONSULTS IT MUST RECOGNISE THAT THE COPYRIGHT RESTS WITH THE UNIVERSITY AND THEN SUBSEQUENTLY TO THE AUTHOR ON THE EXPIRY OF THIS PERIOD AND THAT NO QUOTATION FROM THE THESIS AND NO INFORMATION DERIVED FROM IT MAY BE PUBLISHED UNLESS THE SOURCE IS PROPERLY

Chapter 1:
General Introduction

The main topic of this thesis is the role of *Propionibacterium acnes* infection in prostate oncogenesis. This chapter provides a comprehensive introduction to prostate anatomy and pathophysiology, the bacterium of interest *P. acnes*, and concludes with a summary of studies investigating the relationship between *P. acnes* and prostate cancer. The potential for this knowledge to be applied in the field of stratified medicine is also highlighted.

1.1. *Prostate cancer*

1.1.1. Prostate anatomy and physiology

The human prostate is a walnut-shaped accessory gland of the male reproductive tract. It is located in the pelvis, below the bladder and anterior to the rectum. The gland is composed of luminal secretory epithelial cells, basal cells, and neuroendocrine cells (Figure 1.1.A) (McNeal, 1981; di Sant'Agnese, 1998). The stroma of the prostate includes smooth muscle cells, myofibroblasts, lymphatic cells and nerves, as well as inflammatory cells (Bartsch et al., 1979).

McNeal (1981) proposed the currently accepted prostate zonal anatomy concept with four anatomical zones – peripheral zone, central zone, transition zone, and anterior fibromuscular stroma, as seen in Figure 1.1.B. (McNeal, 1981). The peripheral zone is the largest zone of the prostate, comprising roughly 70% of the gland, and is the origin of 68% of prostate adenocarcinomas (McNeal et al., 1988). The central zone, located around the ejaculatory ducts, expanding upwards towards the base of the bladder, represents 20-25% of the prostate volume. It is associated with a densely packed stroma and large and irregular glands. Finally, the transition zone forms 5-10% of the gland, and it has two pear-shaped lobes that surround the urethra; the transition zone is associated with 26% of adenocarcinomas (McNeal et al., 1988).

The production of semen by the testes, epididymis, and male accessory glands (including the prostate gland) is vital for human reproduction. Semen is composed of 2-5% spermatozoa, 65-75% seminal vesicle fluid (e.g. prostaglandins, fructose), 20-30% prostatic fluid (including zinc ions (Zn^{2+}), citrate, kallikreins) and about 1% bulbourethral fluid (mucins, galactose, sialic acid) (Verze et al., 2016). The role of the prostate is key to male fertility, as the chemical compounds it adds to seminal fluid are at the core of

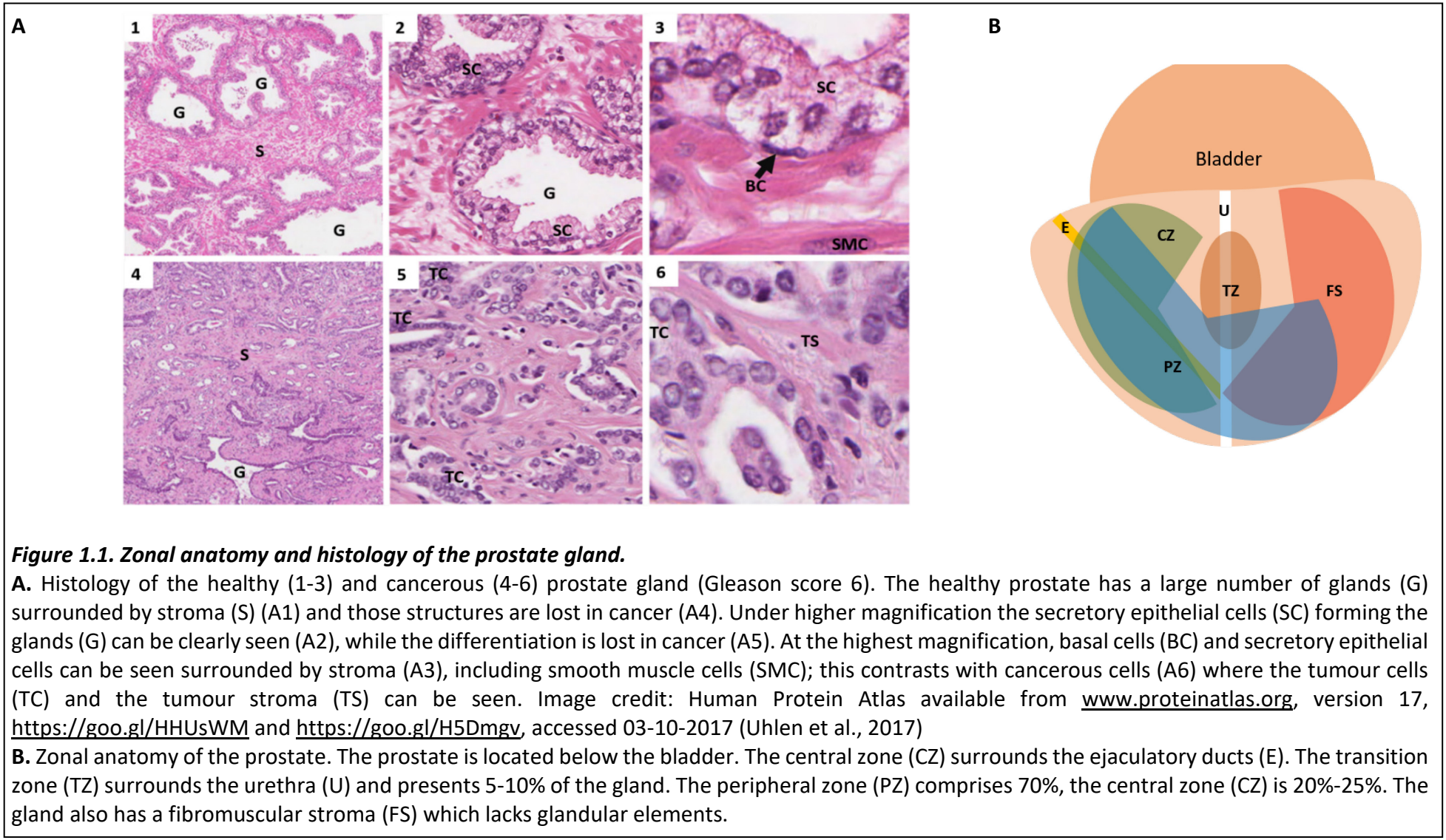

Figure 1.1. Zonal anatomy and histology of the prostate gland.

A. Histology of the healthy (1-3) and cancerous (4-6) prostate gland (Gleason score 6). The healthy prostate has a large number of glands (G) surrounded by stroma (S) (A1) and those structures are lost in cancer (A4). Under higher magnification the secretory epithelial cells (SC) forming the glands (G) can be clearly seen (A2), while the differentiation is lost in cancer (A5). At the highest magnification, basal cells (BC) and secretory epithelial cells can be seen surrounded by stroma (A3), including smooth muscle cells (SMC); this contrasts with cancerous cells (A6) where the tumour cells (TC) and the tumour stroma (TS) can be seen. Image credit: Human Protein Atlas available from www.proteinatlas.org, version 17, https://goo.gl/HHUsWM and https://goo.gl/H5Dmgv, accessed 03-10-2017 (Uhlen et al., 2017)

B. Zonal anatomy of the prostate. The prostate is located below the bladder. The central zone (CZ) surrounds the ejaculatory ducts (E). The transition zone (TZ) surrounds the urethra (U) and presents 5-10% of the gland. The peripheral zone (PZ) comprises 70%, the central zone (CZ) is 20%-25%. The gland also has a fibromuscular stroma (FS) which lacks glandular elements.

molecular processes involved in ejaculation, sperm activation and capacitation (Gilany et al., 2015).

Human prostate epithelial cells, which form the glandular structures within the prostate, accumulate large amounts of Zn^{2+} ions (roughly 4% of the total zinc in the body) (Verze et al., 2016). The zinc ions inhibit the first step of the Krebs cycle: the conversion of citric acid to isocitrate by the enzyme aconitase (Franklin et al., 2005). Due to their truncated Krebs cycle, healthy prostate epithelial cells are energy inefficient, have low levels of respiration, and lower levels of reactive oxygen species (ROS) than most other cells in the body; it has been suggested that the normally lower level of ROS in prostate epithelial means they are less tolerable to elevation in ROS levels (Dakubo et al., 2006). It is worth noting, that while in most cases cells go from energy efficient healthy cells to energy inefficient malignant cells, the opposite is true for prostate epithelial cells: they normally have poor energy efficiency but become energy efficient when cancerous (Costello and Franklin, 2000). An early sign of this transformation is the decreased expression or loss of *ZIP1*, a Zn^{2+} transporter protein (Costello and Franklin, 2006; Johnson et al., 2010).

The kallikreins (KLKs) secreted by the prostate are a subgroup of 15 serine proteases, with the most notable example being the prostate specific antigen (PSA), encoded by the *KLK3* gene), which play a role in sperm motility and liquefy sperm by directly targeting the gel proteins semenogelin-1 and semenogelin-2 (Lilja, 1985; Lilja et al., 1987; Lilja et al., 2008). Zn^{2+} ions have an inhibitory role on kallikreins while within the prostatic tissue. After ejaculation, semenogelin-rich seminal vesicle fluid is mixed with prostatic secretions; semenogelins and fibronectin form a gelatinous mass that is liquefied within a few minutes by the activated kallikreins, and it allows the movement of sperm towards the fallopian tube (Verze et al., 2016)

1.1.2. Prostate disease

As the prostate plays a key role in the male reproductive system, it is important to study any issues within the organ which may interfere with its function. The focus of this thesis is prostate cancer and, more specifically, the role of chronic infection in prostate oncogenesis; however, a brief introduction to other prostate-related diseases is necessary to highlight the impact they have on the function of the gland and how they differ from prostate cancer.

1.1.2.1. Prostatitis

Prostatitis, or inflammation of the prostate gland, according to the current National Institute of Health definition can be divided into four categories: acute bacterial prostatitis, chronic bacterial prostatitis, chronic prostatitis/chronic pelvic pain syndrome, or asymptomatic inflammatory prostatitis (Krieger et al., 1999).

1.1.2.1.1. Acute bacterial prostatitis

Acute bacterial prostatitis is rare, and occurs as a result of ascending urinary tract infections, or as a direct intervention to the prostate gland, for example following a prostate biopsy (Millan-Rodriguez et al., 2006; Wagenlehner et al., 2013). The bacteria most commonly associated with acute prostatitis include *Escherichia coli* (including uropathogenic *E. coli*, also known as UPEC), *Pseudomonas aeruginosa*, *Klebsiella* spp.; if the condition is intervention-related, there is a higher number of mixed cultures (Krieger et al., 2008; Yoon et al., 2012).

1.1.2.1.2. Chronic prostatitis/chronic pelvic pain syndrome

The aetiology of chronic prostatitis/chronic pelvic pain syndrome (CP/CPPS) is unknown. Symptoms of the syndrome include pelvic discomfort, erectile dysfunction and issues with urination (Khan et al., 2017).

1.1.2.1.3. Chronic prostatitis

E. coli has also been implicated in causing chronic prostate infections, while other studies suggest that Gram-positive cocci, such as *Enterococcus faecalis*, *Staphylococcus* spp., *Streptococcus agalactiae*, predominate (Weidner et al., 1991; Bundrick et al., 2003). Chronic prostatitis is commonly found in both benign prostatic hyperplasia (BPH) and prostate cancer (Gerstenbluth et al., 2002).

1.1.2.1.4. Asymptomatic inflammatory prostatitis

Asymptomatic inflammatory prostatitis differs from the previously described categories of prostatitis, as patients have no symptoms of infection. The two signs that a patient has an asymptomatic infection are elevated PSA and the presence of leukocytes if the prostate is examined histologically. This type of prostatitis is commonly seen in men with benign prostatic hyperplasia and prostate cancer (Nickel et al., 1999). Chronic inflammation has been suggested to play a role in prostate cancer, and the potential

role in *P. acnes* in chronic inflammation leading to prostate oncogenesis will be further discussed in Section 1.3.

1.1.2.2. Benign prostatic hyperplasia

BPH is a non-cancerous hyperplasia of epithelial and stromal cells of the prostate's transition zone (McNeal, 1968; McNeal, 1988). The condition is not thought to be a precursor of prostate cancer (Kristal et al., 2010). While the number of cells increases, they retain their morphology. BPH is seen in 25% of 50-year olds and 90% of 80-year-olds; however, symptoms are only seen in 10% of cases (Bushman, 2009). The hyperplasia of epithelial cells causes an enlargement of the prostate which can lead to a number of lower urinary tract symptoms, including difficulty urinating and increased frequency (Barry et al., 1992). Increased cardiovascular risk, chronic infection of the prostate gland, and changes in androgen levels have been suggested as possible causes, although the aetiology is currently unknown (Kim et al., 2016).

1.1.2.3. Proliferative inflammatory atrophy

Proliferative intraepithelial atrophy (PIA) (illustrated in Figure 1.2.B) is a rare condition represented by inflammation-associated atrophy and post-atrophic hyperplasia, and has been shown to merge with adenocarcinoma lesions (Wang et al., 2009). It has been suggested that PIA is a possible prostate cancer precursor via prostatic intraepithelial neoplasia (PIN), as PIA lesions are commonly merged with PIN (Putzi and De Marzo, 2000).

1.1.2.4. Prostatic intraepithelial neoplasia

Prostatic intraepithelial neoplasia (PIN) is presented by clusters of luminal epithelial cells with the appearance of cancerous cells (e.g. enlarged nuclei with prominent nucleoli) but a preserved basal layer, see Figure 1.2.C (Presti, 2007). It has been reported that the incidence of PIN increases with age and is seen in 7-8% of men in their 20s and 63-86% (dependent on race, with rates being higher in African-Americans) of 70-year-olds (Merrimen et al., 2013). It has been suggested that high-grade PIN is a precursor of prostate adenocarcinoma (Haussler, 1999). While PIN and invasive cancers display frequent multifocal co-occurrence, previous studies disagree on whether PIN predates cancer, as would be expected if it was in fact a precursor of oncogenesis (Sanchez-Chapado et al., 2003; Soos et al., 2005).

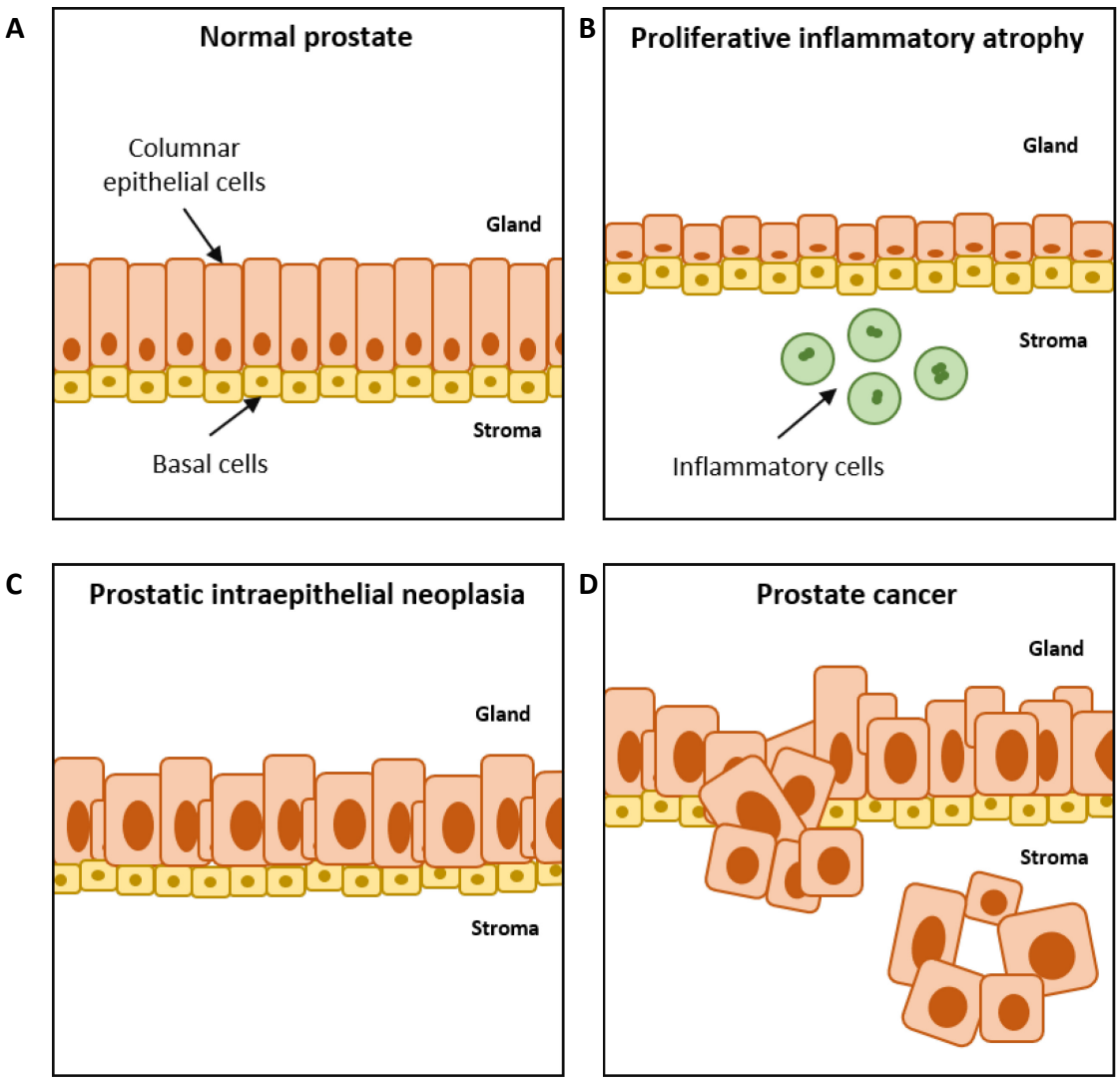

Figure 1.2. Changes seen in prostate disease.

A. The normal prostate is composed of columnar secretory epithelial cells forming the glands and is outlined by basal cells.

B. Proliferative inflammatory atrophy is associated with proliferating epithelial cells which fail to differentiate into columnar secretory cells. The PIA areas are also associated with chronic inflammation.

C. In prostatic intraepithelial neoplasia, the cells possess some morphological similarities to cancerous cells, including enlarged nuclei, however, they have a preserved basal layer.

D. With prostate cancer, in addition to changes in morphology, the cells infiltrate the surrounding stroma and this migration can progress to metastasis, if not identified early. Adapted from Nelson et al. (2003).

1.1.2.5. Prostate cancer

This thesis is primarily focused on investigating the role of chronic infection, specifically infection with *Propionibacterium acnes*, in the development of prostate cancer. Before considering the role of infection in oncogenesis, however, it is important to present the risk factors for the disease, as well as diagnosis and treatment options available.

1.1.2.5.1. Incidence of prostate cancer

In the UK in 1993, prostate cancer accounted for 16% of cancer diagnoses; by 2014 the number had increased to 26%, making prostate cancer the most commonly diagnosed cancer in men with the projection that the percentage would rise further (Smittenaar et al., 2016). Prostate cancer is the most common cancer diagnosed in European men (Arnold et al., 2015). It is estimated that in US men prostate cancer will have accounted for 19% of cancer diagnoses in 2017, and will be responsible for 8% of deaths (Siegel et al., 2017). Over the last decade in the US, especially early 2010s, there was a rapid decrease of the number of prostate cancer diagnoses (more than 10% annually between 2010 and 2013), which was mainly due to changes of screening recommendations by the US Preventive Services Task Force (Siegel et al., 2017). The changes were suggested mainly due to concerns of over-diagnosis and unnecessary treatment (Moyer, 2012).

Newly developed prostate cancer usually displays symptoms that do not differ from BPH, including difficulties in urination, increased frequency or decreased urine flow. As the cancer progresses, it may become metastatic which is the main cause of death; the most common metastasis sites include bone (90%, associated with severe pain), lung (46%) and liver (25%) (Bubendorf et al., 2000). Another complication of advanced prostate cancer is cachexia, also called wasting syndrome; it is associated with weight loss, loss of appetite, loss of muscle mass, and fatigue. It has been suggested that inflammatory cytokines (e.g. interleukin-6 (IL-6) and tumour necrosis factor α (TNF-α)) are involved in promoting cachexia in cancer patients. In animal models, IL-6 can drive cachexia via Signal transducer and activator of transcription 3 (STAT3) activation (Bonetto et al., 2011). In prostate cancer patients, increased IL-6 levels are associated with poor prognosis, with the cytokine being produced by both immune and cancer cells (Kuroda et al., 2007).

1.1.2.5.2. Risk factors

Risk factors for the development of prostate cancer include age, family history, race, diet and other environmental factors.

Age is the most important risk factor for prostate cancer, and post-mortem studies have shown that 30% of men over the age of 50 have prostate cancer, with the percentage rising to 70% in men over the age of 70 (Hoffman, 2011).

Family history is a major risk factor for the development of prostate cancer. Twin studies have revealed that prostate tumours have a stronger hereditary link than any other malignancy (Gronberg et al., 1994; Ahlbom et al., 1997). If a first-degree relative has been diagnosed the calculated risk ratio is 2.1 (Hemminki, 2012). Furthermore, if one, two or three first-degree relatives are diagnosed with prostate cancer, a man's risk of developing the disease increases 2-fold, 5-fold and 11-fold, respectively (Steinberg et al., 1990). Familial prostate cancers are more likely to be diagnosed earlier than sporadic cancers, and have a significantly better 10-year cancer specific survival (92% for familial cancers compared to 69% for sporadic cancers) (Plonis et al., 2015; Raheem et al., 2015; Randazzo et al., 2016).

It has been shown that men with the Lynch syndrome (a cancer disorder associated with germline mutations of mismatch repair genes EPCAM, MLH1, MSH2, MSH6, or PMS2) are five times more likely to develop prostate cancer that non-carriers and those cancers are not more likely to be of the aggressive variety (Haraldsdottir et al., 2014). Another example of familial prostate cancer, carriers of BRCA2 mutations, are at increased risk of developing early onset prostate cancer (up to 7 years earlier onset than non-hereditary cancer of the prostate) and those cancers are more likely to be aggressive and have poor survival rates (4-year median survival post-diagnosis) (Narod et al., 2008; Castro et al., 2013).

Incidence of prostate cancer is lower in Asia, compared with the US and Western Europe (Hsing et al., 2000). If men of Asian origin immigrate to the west, their risk of developing cancer of the prostate increases, strongly suggesting than lifestyle and environment play and important role in the disease (Haenszel and Kurihara, 1968; Shimizu et al., 1991; Whittemore et al., 1995). In the US, African Americans are at a doubled risk of prostate cancer death compared to Caucasians, with a 60% higher incidence of the disease

(Howlader et al., 2011). African American men are usually diagnosed on average 1.2 years earlier than white men and are twice as likely to be diagnosed before the age of 45, yet they have a higher mortality rate (Karami et al., 2007; Robbins et al., 2015).

Animal fats and red meats heave been implicated as a potential driver of prostate oncogenesis (Giovannucci et al., 1993; Gann et al., 1994; Lemarchand et al., 1994). Notably, meats cooked at high temperature form a number of carcinogens, one of which (2-amino-1-methyl-6-phenylimidazo[4,5-b]pyridine or PhIP) has been shown to cause prostate cancer in rats (Gross et al., 1993; Stuart et al., 2000).

On the other hand, it has been suggested that some vegetables might have a cancer protective role (Chan and Giovannucci, 2001). A notable example is that high plasma levels of lycopene (an antioxidant associated with increased intake of tomatoes) has been linked with a reduced risk of prostate cancer (Rowles et al., 2017). Other antioxidants connected with decreased prostate cancer risk include vitamin E and selenium; however, a recent randomised controlled trial showed that vitamin E, selenium, or both used in a combination did not prevent prostate cancer in the cohorts examined (Nelson et al., 2003; Lippman et al., 2009).

A meta-analysis on alcohol use and relative risk of prostate cancer showed that there is a statistically significant link between consumption of small amounts of alcohol (between 1.3 and 24 g per day) and increased prostate cancer morbidity and mortality (Zhao et al., 2016).

Metabolic syndrome is not significantly associated with prostate cancer risk, but two of its components (high waist circumference and hypertension) have shown a significant link (Esposito et al., 2013).

Epidemiological studies suggest that a prior history of prostatitis related to sexually transmitted infections (STIs), such as human papilloma virus, syphilis and gonorrhoea, leads to an increased risk of prostate cancer development, although they highlight the possibility for detection and recall bias (Dennis and Dawson, 2002; Dennis et al., 2002)

1.1.2.5.3. Diagnosis

1.1.2.5.3.1. Prostate specific antigen

PSA is a serine protease encoded by the *KLK3* gene, and is produced by prostate epithelial cells. Together with other KLKs it plays a role in sperm liquification and motility.

Increased PSA levels in the blood are not a consequence of increased production of PSA by the prostate, but are thought to be a result of physical changes in the gland that lead to the PSA leaking into the bloodstream, as during prostate cancer development there is actually a significant decrease in *KLK3* expression (Qiu et al., 1990; Lilja et al., 2008).

The use of PSA as a sole biomarker for prostate cancer in not considered to be ideal. While a serum PSA value above 4 ng/ml is regarded as elevated, results between 4 and 10 ng/ml are considered to be within the test's "grey zone" and are associated with low levels of sensitivity (at 23%) and specificity (93%) (Thompson et al., 2005). As many prostate cancers are not life threatening and clinically significant, it is thought that PSA testing leads to over-diagnosis of clinically non-significant disease (Gilgunn et al., 2013). Furthermore, increased levels of PSA are not specific to prostate cancer but can also be due to BPH or prostatitis (Pinsky et al., 2006; Azab et al., 2012). Despite this, a recent study highlighted that PSA-screening decreases the risk of prostate cancer related death by 25 to 32% (Tsodikov et al., 2017). There is, however, a need for a more reliable diagnostic test than the current PSA analysis.

Novel diagnostic tests aimed at increased specificity and sensitivity are currently under development. Both tests (one using the prostate health index mathematical formula and the other using a panel four KLKs) are hoped to decrease the number of unnecessary biopsies currently performed due to inadequate performance of the PSA test (Loeb and Catalona, 2014; Bryant et al., 2015).

The current EU guidelines recommend testing of all men above the age of 50 (45 if family history is present or the man is of African origin); while optimal testing intervals have not been studied the current recommendation for follow-up is 2 years for men who are at a higher risk, and 8 years otherwise (Mottet et al., 2017).

1.1.2.5.3.2. Digital rectal examination

Digital rectal examination (DRE) is a routinely used procedure, where the prostate is felt for any asymmetry or nodule formation, as well as enlargement or hardening of the prostate gland as a whole; however, cancers detected via DRE are usually at an advanced stage (Stewart et al., 2017).

1.1.2.5.3.3. Transrectal ultrasound guided prostate biopsy

Transrectal ultrasound (TRUS) guided biopsy is a technique used for cancer diagnosis. The decision whether biopsy is required is based on either elevated PSA levels, an abnormal DRE, or the presence of both. The ultrasound probe is inserted into the rectum while a biopsy sample is taken from the prostate transrectally or transperineally. The currently employed biopsy method is called the "extended method", as it includes 10 or 12 core biopsies taken along the length of the gland, bilaterally and far from the periphery (Mottet et al., 2017). There is no significant difference between detection rates of transrectal and transperineal biopsies, but transperineal biopsies have a mild detection advantage if the patient's PSA levels were in the "grey zone".

The risks associated with TRUS and a prostate biopsy include haematuria (66% of the cases), haematospermia (38%), rectal bleeding (<28%) (Efesoy et al., 2013).

1.1.2.5.3.4. Gleason scoring and tumour staging

While prostate cancer is suspected after DRE and/or elevated PSA, the diagnosis is based on histopathological analysis of the biopsy (Mottet et al., 2017).

The Gleason grading system is used for assessing the aggressiveness of the tumour (Gleason and Mellinger, 1974). The glandular histology of the biopsy is studied and graded based on five different growth and differentiation patterns. A score of 1 is given for differentiated patterns, and a score of 5 for the least differentiated. For cancer biopsies, the European Association of Urology guidelines advise that the Gleason score consists of the sum of the grade of the most prevalent pattern and the grade of the highest scored pattern (Mottet et al., 2017). For radical prostatectomy samples the Gleason score is calculated by summing the lowest and the highest scoring patterns that take up at least 5% of the sample (Heidenreich et al., 2011; Mottet et al., 2017). The higher the score, the more progressed the tumour is. An example of a tumour with a

Gleason score 6 can be seen in Figure 1.1.A, and a general illustration comparing prostate cancer to pre-malignant prostate conditions can be seen in Figure 1.2.D.

TNM (tumour, node, metastasis) staging assesses the tumour (whether it is palpable, visible, organ confined), whether adjacent lymph nodes have been affected and whether metastasis is present (either to non-adjacent lymph nodes, bone or other organs). A tumour at stage T1N0M0 would be clinically insignificant, while a tumour staged T4N1M1b (non-organ confined, spread to regional lymph nodes with proof of bone metastasis) would be associated with a poor prognosis (Cheng et al., 2012).

1.1.2.5.4. Treatment

1.1.2.5.4.1. Monitoring

There are two types of monitoring approaches currently in use.

Active surveillance is employed in younger patients with life expectancy of over 10 years. It is used in patients who have low-risk prostate cancer and aims to decrease toxicity due to treatment without endangering the patient's life (Mottet et al., 2017). Regular assessments, such as DRE, PSA and biopsies, follow the disease progression, and a switch to active treatment is usually based on changes in the tumour staging after a biopsy (Klotz et al., 2010).

"Watchful waiting" is recommended for frail patients, who have a life expectancy of less than ten years due to age or co-morbidities. It aims to reduce treatment related toxicity and side effects. Studies have shown that if a patient has a Charlson comorbidity index of 2 or more, tumour aggressiveness does not have a significant impact on overall survival (Albertsen et al., 2011).

1.1.2.5.4.2. Radical prostatectomy

Radical prostatectomy (the surgical removal of the prostate and surrounding lymph nodes) is used for the eradication of organ-contained disease. The surgery can be performed as an open surgery, laparoscopy (performed via small incisions, using a laparoscope) or as a robot-assisted prostatectomy. While there is no evidence that one procedure is superior to the others, robotic surgery has been shown to carry a lower risk of complications during the procedure (Ramsay et al., 2012). Common side effect of radical prostatectomy are erectile dysfunction and incontinence (Mottet et al., 2017).

1.1.2.5.4.3. Radiation therapy

Brachytherapy is used as a common treatment for localised prostate cancer. Initially developed in the 1970s, a radioactive isotope of iodine (^{125}I) was inserted into the prostate (Whitmore et al., 1972). At this stage, however, the delivery method did not guarantee consistent dosage and lead to serious complications. When TRUS was developed, the guided implantation of the radioactive isotope was made possible, which lead to accurate delivery and allowed for the identification of patient subgroups that would benefit most from the treatment (Ragde et al., 2000).

With the development of higher energy accelerators and advancement in tomography methods, external beam radiotherapy (the delivery of high doses of radiation to deep-seated cancers from outside the body) became a possibility (Denmeade and Isaacs, 2002). Several randomised trials have demonstrated the benefits of combining androgen deprivation therapy with radiation therapy (as both lead to the death of prostate epithelial cells, including cancerous cells), such as improvement of overall survival and increased relapse-free time (Pilepich et al., 1995; Bolla et al., 1997; Pilepich et al., 1997).

1.1.2.5.4.4. Hormonal therapy

While the treatments above are chosen for organ confined tumours, hormonal therapy is recommended for advanced metastatic cancers.

1.1.2.5.4.4.1. Hypothalamic-pituitary-gonadal axis and the androgen receptor

To understand the action of androgen-deprivation therapy, a brief introduction to the hypothalamic–pituitary–gonadal (HPG) axis and the role of androgens in the male physiology is necessary. The hypothalamus produces the gonadotropin-releasing hormone (GnRH) which has a direct effect on the pituitary gland, activating the release of luteinizing hormone (LH) and follicle stimulating hormone (FSH). FSH acts on the Sertoli cells of the testis and drives the production androgen-binding protein necessary for testosterone transport in the blood; also via the Sertoli cells, FSH has a direct effect on germ cells by stimulating spermatogenesis. LH stimulates testosterone production in the Leydig cells of the testis. Elevated levels of testosterone can lead to the inhibition of the process though a complex negative feedback loop (Figure 1.3) (Norman and Henry, 2015).

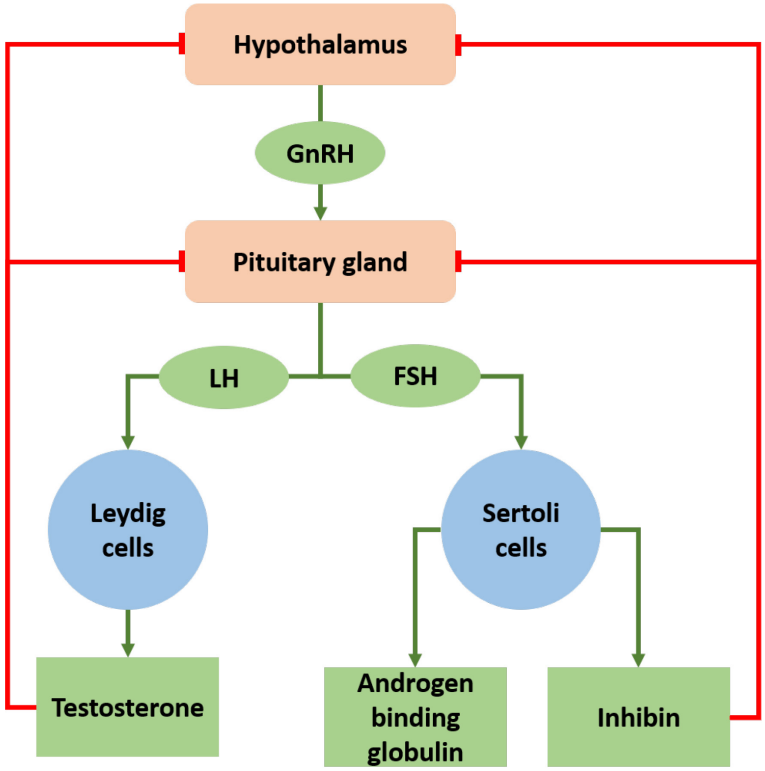

Figure 1.3. HPG axis.
Gonadotropin-releasing hormone (GnRH) is produced by the hypothalamus and acts on the pituitary gland, leading to the production of luteinizing hormone (LH) and follicle stimulating hormone (FSH). LH acts on the Leydig cells in the testis to produce testosterone, while FSH stimulate androgen binding globulin and inhibin production from the Sertoli cells. The produced inhibin and testosterone can act as negative feedback inhibitors on the HPG axis.

The androgen receptor (AR) is a nuclear receptor of 3C subclass, and it functions as a ligand-dependent transcription factor (Lu et al., 2006). AR, inactivated by chaperone proteins, is present in the cytoplasm diffusely (Figure 1.4) (Centenera et al., 2008). When bound to an androgen ligand, such as testosterone or the higher affinity 5α-dihydrotestosterone (DHT), the AR is released from its chaperone proteins (Edwards and Bartlett, 2005). Once freed, the AR changes conformation, forms a homodimer and is translocated to the nucleus where it undergoes post-translational modification (Centenera et al., 2008). The activated dimer AR then binds to DNA at sequences called androgen-responsive elements. Following, transcriptional co-factors and activators are summoned to the site, and initiate the process (Shang et al., 2002; Centenera et al., 2008). The AR mediates a number of basic prostate cell functions such as zinc levels and *KLK3* expression, thus PSA can be used to monitor disease progression, and response to treatment, especially androgen deprivation therapy (Ryan et al., 2006; Verze et al., 2016).

1.1.2.5.4.4.2. Castration sensitive cancers

The standard treatment for metastatic prostate cancer in the last few decades has been androgen deprivation therapy, either by surgical castration via bilateral orchiectomy (removal of both testes) or chemical castration via GnRH analogue treatment. (Yamaoka et al., 2010)

The most common goal of hormonal therapy is to deprive the androgen receptor of its ligand. To achieve this, drugs target GnRH and release of LH from the pituitary, which in turn prevents testosterone production (Wong et al., 2014). This is followed by a brief surge in testosterone levels (called testosterone flare), but testosterone production in the testes is inhibited and testosterone concentration in the serum of chemically castrated men reaches levels comparable to those of men who have undergone surgical castration (van Poppel and Nilsson, 2008).

Animal studies have shown that when androgen deprivation therapy is used, the loss of ligand leads to a loss of signalling which causes death in most secretory epithelial cells, as androgen is required for their survival; when androgen signalling is restored, a rapid regrowth of the gland was observed (English et al., 1987; Evans and Chandler, 1987).

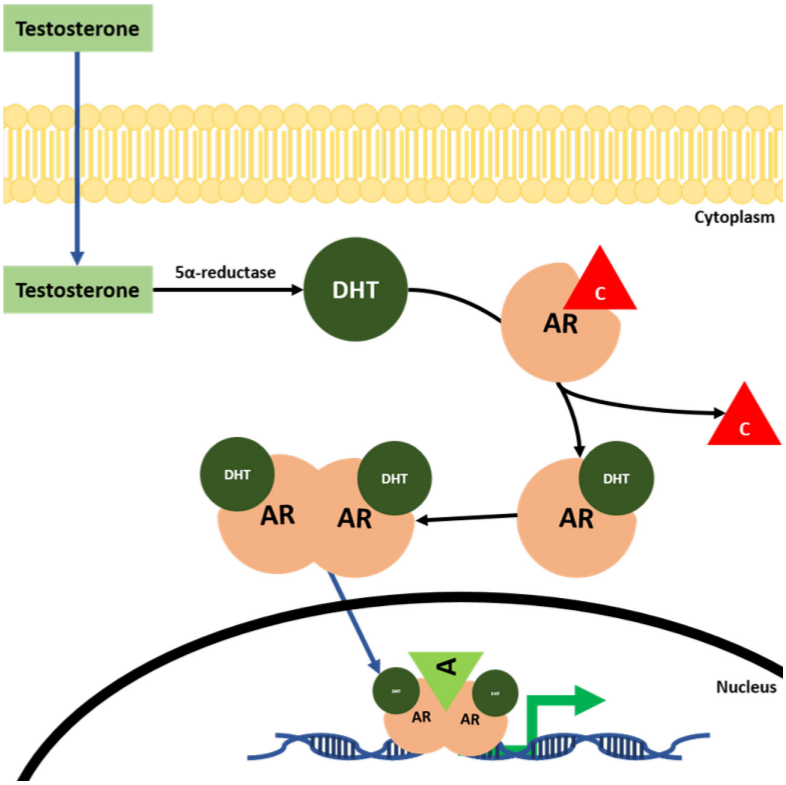

Figure 1.4. Androgen receptor activation.

Once testosterone enters the cells, it is converted to a more active form DHT by 5α-reductase. The androgen receptor (AR) is found in the cytoplasm bound to inhibiting chaperone proteins (C). Once DHT binds AR, C are removed, leading to active AR which forms dimers and translocates to the nucleus, where it binds DNA and summons activators (A) which help it initiate transcription of molecules involved in a range of cellular functions.

AR antagonists are sometimes used in combination with drugs targeting GnRH; these antagonists actively target the AR by recruiting co-repressors (rather than co-activators) that lead to conformational changes in the receptor, preventing transcriptional activation (Knudsen and Penning, 2010).

A recent study has shown that abiraterone plus prednisone added to androgen deprivation therapy in newly diagnosed, castration-sensitive, metastatic prostate cancer, leads to prolonged overall survival and prolonged progression-free survival (Fizazi et al., 2017).

1.1.2.5.4.4.3. Castration-resistant cancer

Despite the initial positive response to androgen deprivation therapy, most metastatic prostate cancers progress to androgen-independent growth, also known as castration resistant prostate cancer (CRPC) (Tucci et al., 2015). Once resistance to androgen deprivation therapy is developed, the CRPC is associated with poor prognosis, with docetaxel being the standard of care, demonstrating prolonged survival in CRPC patients. It has, however, been associated with severe side effects, e.g. anaemia, diarrhoea, sensory neuropathy (Tannock et al., 2004). A more recently discovered drug, abiraterone (androgen biosynthesis inhibitor) has demonstrated promising results both as a treatment in naïve CRPC patients, and in patients previously treated with docetaxel (Huggins et al., 1941; de Bono et al., 2011).

Multiple factors have been suggested as facilitators of androgen deprivation therapy resistance, including androgen receptor signalling through androgens produced in the adrenal glands, increased androgen production within the tumour, mutations in the androgen receptor and within the androgen signalling pathway, reviewed in detail by Knudsen and Penning (2010) (Stanbrough et al., 2006; Montgomery et al., 2008). Nuclear-factor kappa B (NF-κB) is a potent activator of inflammatory response and has been implicated in oncogenesis, as it can promote proliferation, metastasis and angiogenesis, while inhibiting apoptosis (Karin et al., 2002). In the context of prostate cancer, NF-κB and the AR show a direct correlation, with *in vitro* data suggesting that AR-expression is modulated by NF-κB, highlighting a possible pathway for inflammation to drive not only CRPC but oncogenesis as a whole (Zhang et al., 2009).

1.1.2.5.5. Prostate microflora

Using ultra-deep pyro sequencing, a study evaluated the prevalent bacterial species in radical prostatectomy samples, showing no significant difference between tumour and non-tumour sites analysed (Cavarretta et al., 2017). The study did, however, give insight into the bacterial taxa present in the prostate, with the most prevalent genus being *Propionibacteria*. Multiple explanations are possible for the presence of *P. acnes* in the prostate, including ascension via the urethra, as studies have shown that the bacterium is present in the genitourinary tract; an alternative explanation could be that the bacterium is sexually transmitted, as it has also been cultured from both healthy women and women with vaginosis (Thomason et al., 1984; Shannon et al., 2006a; Cavarretta et al., 2017).

Two studies, using massive parallel sequencing (MPS) and RNA sequencing, analysed prostate cancer samples for the presence of microorganisms. The MPS study demonstrated the presence of different bacterial species with *P. acnes* being isolated from 95% of samples (Yow et al., 2017). The second study showed that *P. acnes* is present in both cancerous and benign adjacent tissue, and is not seen in healthy controls; it also demonstrated the differences between the organisms present in prostate samples from Chinese and Western patients (Chen and Wei, 2015). A change in the prostate microflora could explain why prostate cancer incidence in Asian men increases if they relocate to the West.

1.2. Propionibacterium acnes

P. acnes has been associated with a number of chronic diseases over the years and most recently it has been suggested that it could be a key factor in oncogenesis in a subgroup of prostate cancers. Before exploring the evidence for its role in prostate cancer, we will highlight some aspects of *P. acnes* biology and its role in disease.

P. acnes is a pleomorphic rod-shaped Gram-positive anaerobic-to-microaerophilic microorganism. It is a part of the normal human skin microflora, with about half of the bacteria normally found on the skin being anaerobes, including *P. acnes* (Tancrede, 1992). Other *Propionibacteria* species found on the skin include *P. granulosum* and *P. avidum*. In addition to the skin, *P. acnes* can also be isolated from the gastrointestinal and genitourinary tracts (including the prostate gland), as well as the oral cavity. *P. acnes*

is found in the pilosebaceous units of sebaceous glands and produces lipases that degrade the triglycerides from sebum (the lipid-rich product of the glands) to free fatty acids (Marples et al., 1971). The free fatty acids then contribute to the acidity of the skin, thus discouraging the growth of common pathogens such as *Staphylococcus aureus* and *Streptococcus pyogenes* and promoting the growth of coagulase-negative bacteria and *Corynebacterium* spp. (Grice and Segre, 2011).

1.2.1. Genetic Divisions

In recent years, the investigation of *P. acnes* has shifted focus from researching the involvement of the organism in the development of acne to investigating the possibility that some phylogenetic types may be associated with a specific disease, while others may be associated with health. Using a combination of 16S rRNA sequencing and multilocus sequence typing (MLST) there are now six confirmed phylogroups of *P. acnes*: IA_1, IA_2, IB, IC, II and III. The initial split of *P. acnes* into two distinct phenotypes I and II was based on agglutination differences and the pattern of sugars in the cell walls: type I contains galactose, glucose and mannose, while type II only has glucose and mannose (Johnson and Cummins, 1972). More recently McDowell et al. (2005) confirmed that the two phenotypes are phylogenetically distinct groups using the non-ribosomal housekeeping gene *recA* (encoding a DNA-dependent ATPase) and a putative haemolysin/FtsJ-like methyltransferase gene *tly*, with type I later divided into subtypes IA and IB (Valanne et al., 2005). Subtype IA was then further split into IA_1 and IA_2, based on high resolution MLST and whole genome sequencing analysis (Vörös et al., 2012). Additionally, subtype IC was proposed following phylogenetic and whole genome analysis with isolates from this group displaying antibiotic resistance to erythromycin and tetracycline (McDowell et al., 2012b). Finally, type III *P. acnes* was identified based on cell morphology, antibody reactivity and phylogenetic analysis of *recA* (McDowell et al., 2008). More recently, a reclassification of the *Propionibacterium* family and renaming of *P. acnes* to *Cutibacterium acnes* was proposed (Scholz and Kilian, 2016).

1.2.2. Virulence factors

Several whole genome sequences of different types of *P. acnes* have been published, giving insight not only in the phylogenetic relationships between the different types of the bacterium but also identifying a range of putative virulence factors (Bruggemann et

al., 2004; Hunyadkurti et al., 2011; Horvath et al., 2012; McDowell et al., 2012b; Vörös et al., 2012).

1.2.2.1. Christie-Atkins-Munch-Petersen factors

Christin-Atkins-Munch-Petersen (CAMP) reaction is a synergistic reaction first observed with Group B Streptococci (GBS, e.g. *Streptococcus agalactiae*) producing complete haemolysis only in the presence of β-toxin/sphingomyelinase C-producing *Staphylococcus aureus* (Christie et al., 1944). Five similar homologues were discovered in *P. acnes*, and it has been suggested that during an acne infection, when phagocytosed by the macrophage, *P. acnes* uses the host lysosomal acid sphingomyelinase, thus enhancing the activity of CAMP factor and escaping phagocytosis (Nakatsuji et al., 2011). All five CAMP factors are present in different types but they show differences in expression, e.g. CAMP factor 1 production was seen in types IB and II, but not in type IA, and CAMP factor 2 production was higher in IA, compared to IB and II (Valanne et al., 2005). The proposed mechanisms of action for the action of CAMP factors in GBS is the formation of 1.6 to 2.7 nm pores in the cell membrane, leading to increased osmotic pressure and eventually to cell lysis (Lang and Palmer, 2003).

1.2.2.2. Lipase

P. acnes has been shown to release extracellular lipases that hydrolyse triglycerides from sebum to release free fatty acids which are then thought to aid colonization by assisting adherence, and may also reduce the invasion of other, more pathogenic bacteria, by altering pH. Additionally, it has been proposed that free glycerol is also released from the hydrolysis of triglycerides, and that it is utilized as a carbon source by *P. acnes*. (Ingham et al., 1981; Miskin et al., 1997). An example of a lipase produced by *P. acnes* is the product of *gehA*, which encodes a 339 amino acid CG rich signalling peptide (Miskin et al., 1997).

1.2.2.3. Biofilm formation

Biofilm formation is the irreversible attachment of microorganisms to a surface and the formation of an extracellular matrix, resulting in phenotype alteration and increased antimicrobial resistance, most commonly associated with medical device infections, e.g. prosthetic joints. *P. acnes* is shown to have three separate clusters encoding genes involved in extracellular polysaccharide synthesis, indicating that it has the ability to form biofilms. It has been shown that a mature biofilm can be formed within 24 to 48-

hour incubation and that lipase activity is higher in *P. acnes* biofilm, compared to planktonic cells (Bruggemann et al., 2004; Coenye et al., 2007a). Electron microscope study of the *P. acnes* biofilm showed that it forms a layer 10 μm thick with a filamentous structure, and unlike other bacterial species, biofilm formation was inhibited by plasma, which could be a possible explanation why *P. acnes* infection is more often seen in prosthetic join infection and cerebrospinal fluid shunts, compared to heart valves (Holmberg et al., 2009a).

1.2.2.4. Other virulence factors

The production of porphyrins has also been suggested as a means for *P. acnes* to cause skin damage as a result of increased oxygen tension; molecular oxygen reacts with the released porphyrins and causes cell damage via free oxygen radicals (Bruggemann et al., 2004).

Hoeffler (1977) reported the presence of chondroitin sulphatase, hyaluronidase and DNase in some *P. acnes* strains, with a widely-reported gelatinase activity. The presence of a bacteriocin-like substance with bacteriostatic activity, called acnecin, has also been reported (Fujimura and Nakamura, 1978). In addition to the different virulence factors, *P. acnes* has alterations in the peptidoglycan layer structure, namely unsubstituted glucosamine residues, which are responsible for lysozyme resistance (Kamisango et al., 1982).

1.2.3. Stimulation of the immune system

P. acnes has been proven to be a strong driver of immune response and its ability to do so has previously been used as an anti-cancer treatment. Multiple animal experiments have shown that when murine cancer models (including melanoma, mastocytoma, mammary carcinoma, sarcoma) were injected with *P. acnes* of an unknown phylotype, there was evidence of delayed growth and even protection from cancer progression (Woodruff and Boak, 1966; Millman et al., 1977; Tsuda et al., 2011). A suggested explanation is that *P. acnes* activates a T_h1 immune response which in turn summons cytotoxic T cells and natural killer (NK) cells to the site, thus exhibiting anti-tumour activity (Tsuda et al., 2011).

1.2.4. Antibiotic resistance

Due to the widespread use of antimicrobials as treatment for acne, *P. acnes*, which used to be susceptible to antibiotic treatment, has developed resistance mechanisms (Wang et al., 1977). The main resistance mechanism adopted by *P. acnes* are point mutations and the antimicrobials that it is most commonly resistant to are erythromycin and tetracycline, which used to be the two main treatments for acne. Tetracycline resistance is often due to nucleotide substitution of guanine with cytosine at base 1058 of the 16S rRNA, and resistance to erythromycin is a result of point mutation at bases 2057, 2058 or 2059 in the 23S rRNA, or the mobile gene element transposon *Tn5432* carrying *erm(X)* resistance gene (Ross et al., 1997; Ross et al., 1998; El-Mahdy et al., 2010). *P. acnes* also shows intrinsic resistance to metronidazole, which is usually used to treat anaerobic infections (Denys et al., 1983).

1.2.5. *P. acnes* and disease

In addition to being associated with the normal microflora, *P. acnes* has been linked to a number of diseases, e.g. acne vulgaris, prosthetic joint infections, sarcoidosis, endophthalmitis, prostate cancer, etc. (Homma et al., 1978; Somani et al., 1997; Cohen et al., 2005; Zeller et al., 2007).

1.2.5.1. Acne

P. acnes is known as the causative agent of acne, although the exact mechanism of its involvement in the development of acne is unclear. Circumstantial evidence supports this idea, as antibiotic treatment of acne improves the condition, and if resistance to antibiotics is generated, the condition then recurs. Studies have shown an association of phylogenetic type IA_1 with acne (McDowell et al., 2013). As reviewed by Dessinioti and Katsambas (2010), there are numerous mechanisms in which *P. acnes* may be involved in epidermal colonization and subsequent inflammation associated with acne, for example, it may activate toll-like-receptors which in turn initiate NF-κB-response, regulating the expression of immune response genes.

1.2.5.2. Medical implant infections

P. acnes, previously disregarded as a contaminant if isolated from implants, is associated with chronic low-grade infection related to implants as often as *Staphylococcus aureus* (Tunney et al., 1998). *P. acnes* forms a firm biofilm on the biomaterial and isolates from deep infections demonstrate better biofilm formation compared to isolates from

healthy skin (Soderquist et al., 2010). Infection with type I was seen in 63% of cases and 37% were linked to type II, with the percentages being similar in the case of aseptic failure, 67% and 33% respectively (Sampedro et al., 2009). A more recent study shows that the association of types IB, II and III with prosthetic hip infections is higher compared to type IA (McDowell et al., 2011). The main symptom of a *P. acnes* infection of the orthopaedic implant is pain which makes the condition difficult to diagnose accurately (Sampedro et al., 2009). The treatment of *P. acnes* infection related to implants presents a challenge, as the bacteria grow in a biofilm, and as a result the resistance to some antibiotics (e.g. cefamandole, vancomycin, and ciprofloxacin) increases. An additional challenge for the treatment of orthopaedic implant infections is that there is no single antibiotic that is effective against both *P. acnes* and *S. aureus*, which are the two most common isolates. Furthermore, the slow growth of *P. acnes* and long incubation period of at least 7 days, means that it is possible for cultures to be discarded before growth is visible (Ramage et al., 2003; Dodson et al., 2010). In the case of shoulder arthroplasty, Dodson et al. (2010) suggest that the axillary region should be isolated with an antimicrobial drape, to avoid contamination, and that the usual blood tests (erythrocyte sedimentation rate, white blood cell count, C-reactive protein) are not good indicators of *P. acnes* infection. Zeller et al. (2007) point out that macrophage and lymphocyte infiltrations would reflect the immune response in slow-developing prosthetic joint infections, and not neutrophilic infiltration.

P. acnes has been related to both native and prosthetic heart valves. The cases of endocarditis linked to *Propionibacterium* spp., are usually associated with a long history and lack clinical signs of infection. The mortality rates of *Propionibacteria*-related endocarditis vary between 9.1% and 46%, which highlights the importance of evaluating the presence of bacteria in patient blood and the importance of not dismissing positive culture results (Mohsen et al., 2001; Clayton et al., 2006).

1.2.5.3. Sarcoidosis

Sarcoidosis is a systemic granulomatous disease, with the organs most commonly affected being the lungs and lymph nodes. The aetiology of the disease is unknown but it is suggested that it results from an antigen-driven response to an exogenous agent in genetically predisposed patients (Hunninghake et al., 1999). *P. acnes* was the first organism isolated from sarcoid lesions (cultured from 78% of biopsy samples) and has

thus been implicated as having a role in the development of the disease (Abe et al., 1984). In following studies, both *P. acnes* and *P. granulosum* were isolated from sarcoidosis samples from different countries, averaging at 89% and 60%, respectively (Eishi et al., 2002). It was later shown that there is no difference between the phenotypes and genotypes of sarcoid and non-sarcoid isolates, however, a correlation between the amino acid profiles of genes *PAmce* and *Pap60* and invasiveness was found, indicating that the two genes may be involved in cell invasion, although the study did not prove the direct involvement of *P. acnes* in sarcoidosis (Furukawa et al., 2009)

P. acnes can exist as dormant and cell wall-deficient forms in macrophages, in the form of Hamazaki-Wesenberg bodies, which can be activated and proliferate in cells at the site of latent infection. The newly formed small round bodies are infective *P. acnes* and when released from the macrophages they can still lead to infection (Eishi, 2013).

1.2.5.4. Sciatica

Sciatica is the term used for any pain related to compression or irritation of the sciatic nerve, including lower back pain. It has been proposed that *P. acnes* plays a role in sciatica. The bacterium was isolated from 84% (16/19) of culture positive samples (53% culture positive, 19/56) from patients who had undergone microdiscectomy (Stirling et al., 2001). Further studies used antibiotic therapy in an uncontrolled trial with patients diagnosed with Type 1 Modic changes (bone oedema), and the results at follow-up showed significant improvement, strongly suggesting bacterial involvement; these findings were confirmed in a controlled double-blind study (Albert et al., 2008; Albert et al., 2013).

1.2.5.5. Progressive macular hypomelanosis

Progressive macular hypomelanosis (PMH) is a condition associated with skin discolouration, mainly on the front and the back of the trunk. It has been suggested that *P. acnes* plays a role in the disease, and it was recently shown that phylogenetic type III *P. acnes* is significantly associated with the hypomelanotic lesions (Westerhof et al., 2004; Barnard et al., 2016)

1.2.5.6. Endophthalmitis

P. acnes is also involved in certain eye infections. Endophthalmitis as a result of a *P. acnes* infection is considered a diagnostic and therapeutic challenge. Examples of

infections include chronic postoperative endophthalmitis with the inflammation producing a white plaque in the capsular bag of the eye, typically inducing recurrent infections, or endophthalmitis following cataract extraction and posterior chamber intraocular lens, with symptoms including decreased vision, anterior chamber reaction, a white intracapsular plaque and pain, and is once again associated with reoccurrence (Aldave et al., 1999; Csukas et al., 2004).

1.2.5.7. Primary biliary cirrhosis

Using *P. acnes*-specific polymerase chain reaction (PCR), it was suggested that the bacterium is involved in granuloma formation and 56% of periportal hepatocytes in primary biliary cirrhosis (Harada et al., 2001). It is not clear what the exact mechanism of granuloma formation is but it is suggested that immunomodulation by *P. acnes* may be involved (Harada et al., 2001).

1.3. *P. acnes and prostate cancer*

1.3.1. Chronic inflammation and cancer

The prostate is an immunocompetent organ, meaning that small numbers of immune cells are present at all times (90% $CD8^+$ T-lymphocytes, as well as B-lymphocytes, mast cells, macrophages) (Di Carlo et al., 2007; De Nunzio et al., 2011). In contrast, inflammatory infiltrate, consisting of $CD3^+$ T cells and macrophages is often seen in both the epithelial and stromal cells of radical prostatectomy samples and prostate biopsies (Wagenlehner et al., 2007).

It has been observed that both acute and chronic multifocal inflammation can be seen in prostatectomy samples. This inflammation is not just confined to the area of the tumour, and can also be seen in malignancy-free tissue, indicating that it is not simply an immune response to the cancer cells (Blumenfeld et al., 1992). Chronic inflammation plays an important role in oncogenesis by causing cellular damage via the products of inflammatory cells, e.g. reactive nitrogen and oxygen species which lead to DNA damage.

The involvement of infection in prostate oncogenesis has long been suggested and is supported by circumstantial evidence. In addition to the potential role of acute prostatitis related to STIs, single nucleotide polymorphisms in genes involved in the innate immune response to infection, such as 2'-5-oligoadenylate dependent

ribonuclease L (*RNASEL*), macrophage scavenger receptor-1 (*MSR-1*) and toll-like receptors, are also suggested as risk factors for prostate oncogenesis. *RNASEL* is one of the best studied prostate-associated loci and encodes a ribonuclease involved in interferon signalling in viral infections; *MSR-1* encodes a homotrimeric "scavenger" receptor class A, expressed mainly in the macrophages, and has the ability to bind a variety of ligands, including Gram-positive and Gram-negative bacteria, apoptotic cells, and oxidised high and low density lipoproteins (Gonzalgo and Isaacs, 2003; De Marzo et al., 2007).

Examples of chronic inflammation being linked to oncogenesis include hepatitis C infection of the liver, leading to hepatocellular carcinoma, *Helicobacter pylori* infection and the development of gastric cancer and *Fusobacterium* spp. and colorectal and pancreatic cancer (Ernst and Gold, 2000; Coussens and Werb, 2002; Keku et al., 2013; Mitsuhashi et al., 2015).

1.3.1.1. Gastric carcinoma and Helicobacter pylori

H. pylori is a Gram-negative microaerophilic bacterium which colonizes the human stomach and gastrointestinal tract. The link between *H. pylori* and gastric carcinoma was first highlighted by a number of large epidemiological studies which showed the organism was more frequently present in patients with gastric cancer compared to control groups (Parsonnet et al., 1991; Talley et al., 1991). The bacterium has a number of virulence factors which are linked to an increased risk of developing stomach cancer, e.g. cytotoxin-associated gene A (CagA) is a bacterial protein that activates numerous oncogenesis promoting pathways in epithelial cells, including β-catenin signalling and phosphatidylinositol-4,5-bisphosphate 3-kinase/protein kinase B (PI3K/Akt) signalling (Franco et al., 2005; Nagy et al., 2009). Another example is vacuolating cytotoxin A (VacA), which is a toxin capable of suppressing T cell development (Gebert et al., 2003). The role of *H. pylori* in gastric carcinoma has been reviewed in detail by Amieva and Peek (2016). The development of a vaccine against *H. pylori* aimed at prevention of gastric carcinoma has been proposed (Chui et al., 2005).

1.3.1.2. Bacteria and colorectal cancer

The genus *Fusobacteria* is represented by Gram-negative, anaerobic, non-spore forming bacilli and is found as a part of the normal microflora of the oropharynx. Studies have discovered multiple links between colorectal cancer and *Fusobacteria*. *Fusobacterium*

spp. were shown to be present at increased levels in colorectal adenoma (benign precursor to adenocarcinoma) tissue, as well as in stool samples for patients with adenomas and cancer diagnoses, compared to healthy controls (Kostic et al., 2013). Further animal studies demonstrated that *F. nucleatum* leads to an increased number of tumours in colorectal cancer mouse models and that the inflammation resulting from infection drives oncogenesis (Kostic et al., 2013). A molecular mechanism suggested for the role of *Fusobacteria* in oncogenesis is via the *Fusobacterium* adhesin A (FadA) adhesion molecule; FadA has been shown to bind to E-cadherin in order to invade epithelial cells, which in turn leads to the activation of a number of oncogenic pathways, including β-catenin signalling (Rubinstein et al., 2013). It has also been suggested that *Fusobacterium* spp. play a role in the development and progression of pancreatic and oesophageal cancer (Mitsuhashi et al., 2015; Yamamura et al., 2016).

Streptococcus gallolyticus has been also implicated in colorectal cancer for a long time and a recent study, using both cell culture and animal experiments, demonstrated that the bacterium promotes cell proliferation and tumour growth (Kumar et al., 2017).

1.3.1.3. Viral infections and cancer

1.3.1.3.1. Human papilloma virus (HPV) and cervical cancer

HPV is a sexually transmitted virus which has been associated with a number of conditions, including genital warts and cervical cancer. As reviewed by Schiffman et al. (2016), there are 13 HPV genotypes that have been linked to causing a large number of cervical cancers, as well as some oropharyngeal malignancies. Extensive care is taken for the prevention of cervical cancer caused by HPV, including regular screening and commercially available vaccines targeting the types of HPV most commonly associated with oncogenesis, most notably HPV16 and HPV18 (De Vincenzo et al., 2014).

1.3.1.3.2. Hepatitis C and hepatocellular carcinoma

Another example of a cancer driven by viral disease is hepatocellular carcinoma caused by hepatitis C infection. Unlike HPV, there are currently no vaccines developed against hepatitis C, but there is ongoing work for the development of antiviral agents which can prevent the damage caused by this viral infection. An extensive review on the topic by Manns et al. (2017).

1.3.2. *P. acnes* and prostatectomy samples

In 2005 it was reported that the predominant organism isolated from radical prostatectomy samples (at 35%) was *P. acnes*, and it was shown to be positively associated with the inflammation present in the tissue (Cohen et al., 2005). Possible reasons why the bacterium had not been isolated from the prostate earlier include *P. acnes*' resistance to lysozyme and the low number of bacteria present (Kamisango et al., 1982). Due to lysozyme resistance, the conventional methods for bacterial DNA extraction cannot be used in this case. The low bacterial numbers mean that Gram-staining of the tissue would be an inappropriate and non-specific method of detection. Furthermore, the specific requirements for *P. acnes* culture such as anaerobic environment and long incubation time (up to a week), are not routinely used. Finally, even if present, the organism is frequently dismissed as a contaminant.

Subsequent studies have focused on confirming the presence of the bacterium in prostate specimens. Using 16S rRNA, Alexeyev et al. (2006) demonstrated that *P. acnes* is the predominant microorganism isolated from BPH, and also showed that there is an association between the presence of *P. acnes* and subsequent prostate cancer diagnosis. The authors also concluded that the relative risk of prostate cancer for patients who tested positive for *P. acnes* is at levels similar to those with history of STIs or BPH (Lightfoot et al., 2004; Patel et al., 2005). A separate PCR-based study investigated the prevalence of different types of *P. acnes* in the male genitourinary tract in different age groups of healthy patients and in patients with prostate cancer: they identified *P. acnes* types IA, IB and II but found no association between the presence of different types of the bacterium in urine samples and the prostate biopsy results of patients (Shannon et al., 2006a). The presence of the bacterium was also demonstrated using fluorescent *in situ* hybridization, and *P. acnes* was seen both intracellularly and as extracellular biofilm-like aggregates, with the two forms differing in shape, size and organization (Alexeyev et al., 2007).

It is possible that the immune system may aid colonisation with *P. acnes* as the bacterium can use phagocytes as transport vectors (Drott et al., 2010). *P. acnes* can survive in macrophages, though the mechanism is not clear, and it differs from typical intracellular bacteria, as it does not cause the death of the host cells, it does not replicate

within the host cells, and it does not escape the host cells (Fischer et al., 2013; Nakamura et al., 2016).

1.3.3. *In vitro* investigation of *P. acnes* infection of the prostate

In vitro studies, using the human HPV-immortalised prostate epithelium cell line RWPE-1, demonstrated that *P. acnes* infection drives RWPE-1 cells to secrete vascular endothelial growth factor (VEGF), a number of cytokines (including IL-6, IL-8, TNF-α, etc.) and cyclcooxygenase-2 (COX-2, also known as prostaglandin-endoperoxide synthase 2 or PTGS2), all of which have been associated with prostate cancer progression (Drott et al., 2010; Fassi Fehri et al., 2011; Mak et al., 2012). VEGF is a signal protein which plays a role in angio- and vasculogenesis, and angiogenesis is one of the hallmarks of cancer as it enables the tumour to progress further and to become metastatic (Hanahan and Weinberg, 2011b). Both IL-6 and IL-8 affect the activity of VEGF. Via its influence on the production of VEGF, IL-6 may act as a driver of metastasis, and IL-8 has been shown to play a role in angiogenesis and prostate tumour progression (Cohen et al., 1996; McCarron et al., 2002). COX-2 is an enzyme involved in the synthesis of prostaglandins. It has been confirmed that the use of COX-2 inhibitors decreases the risk of a number of cancers, including skin and colorectal (Thun et al., 2002). It has been demonstrated that non-steroidal anti-inflammatory drugs (NSAIDs) may play a role in the prevention and treatment of cancer as *in vitro* studies have shown that on the cellular level NSAIDs inhibit proliferation and angiogenesis, and stimulate apoptosis and the immune system (Dannenberg et al., 2001). Additionally, *in vitro* studies have demonstrated that infection of prostate epithelial cells with *P. acnes* can also cause anchorage-independent growth (as demonstrated by soft-agar assays) and cell migration (Fassi Fehri et al., 2011).

1.3.4. Animal models

To date, there are two animal models of chronic infection of the prostate with *P. acnes*. A rat model of infection, where the animals were inoculated with live bacteria via an abdominal incision and sacrificed at day 5, week 3 or month 3 and 6. At 3 months viable *P. acnes* was still present in the dorso-lateral lobe of the prostate, together with clear signs of active inflammation (Olsson et al., 2012). However, the ventral lobes were clear of any sign of infection and live bacteria by the month 3 time point (Olsson et al., 2012).

A mouse model of chronic infection with a prostate-derived *P. acnes* strain has also been developed (Shinohara et al., 2013). Animals were inoculated with either live or heat-

killed *P. acnes* via transurethral catherization, and were sacrificed at day 2, week 1, 2 or 8. The resulting infection of the dorsal lobe of the prostate persisted for the duration of the experiment and was only seen if live bacteria were used (Shinohara et al., 2013). Both animal models of infection can be used to study the effect of chronic inflammation and its relationship to prostate disease, including BPH and prostate cancer.

It is worth noting that the murine prostate differs significantly from the human gland both histologically (e.g. rodent prostates have a higher epithelial-to-stroma ratio compared to human glands), and anatomically, as well as in that mice and rats do not develop spontaneous prostate cancers, unlike humans (Ittmann et al., 2013). Thus, rodent models of prostate *P. acnes* infection would not be an accurate representation of human prostate infection.

1.4. *Stratified Medicine*

With the development of high-throughput genome sequencing, other "-omic" technologies, completion of the human genome and the 1000 genome project, scientists have gained insight into predisposing factors or biomarkers for some diseases, as well as trends in response and lack of response to treatment in different subpopulations (Venter et al., 2001; Consortium, 2012). This approach, called stratified, personalized or precision medicine is now widely used in the treatment of a number of diseases, with the goal of stratifying patients into subgroups and finding the best possible treatment.

An example of stratification used in the field of oncology is breast cancer patients harbouring an overexpression of the HER2/neu receptor tyrosine kinase where treatment with trastuzumab (Herceptin® Genentech, US) proves a superior alternative to conventional treatment (Burstein, 2005). Another example of successful stratification has been seen in cystic fibrosis patients and depending on the cystic fibrosis transmembrane conductance regulator (CFTR) gene mutation present different treatment approaches are appropriate: in patients with the G551D mutation (about 5%) there is inadequate CFTR channel regulation, treatment which leads to dramatic improvement as it increases channel opening times (Ramsey et al., 2011; Brodlie et al., 2015). If the patients harbour a deletion leading to misfolding of the protein and decreased trafficking to the cell surface (F508del, seen in 85% of cases) a combination of lumacaftor and ivacaftor is more appropriate (Rehman et al., 2015; Brewington et al.,

2016). Contemporary approaches to antimicrobial therapy, based on identification and analysis of the resistance of the infecting organism, which in turn greatly increases chances of eradicating the infection, are also an example of stratified medicine.

There is a clinical need for development of better screening tests for prostate cancer that would lead to better diagnosis and the ability to predict outcome. There are currently three key issues which restrict the management of prostate cancer.

1. The widely used PSA test does not provide the necessary specificity and sensitivity, and leads to over-diagnosis and an increased number of unnecessary biopsies.
2. The only way to definitively diagnose and monitor prostate cancer progression is thorough biopsies.
3. The only way to analyse infection present in the prostate is once again via a biopsy or prostatectomy. However, if infection does play a role in oncogenesis, identification of the patients harbouring infection would offer a chance for antibiotic or other antimicrobial therapy as a preventative measure.

The idea of *P. acnes* infection as a modifiable risk factor for the development of prostate cancer presents it as an attractive target for the development of novel diagnostic tests which can identify the presence of the bacterium and could lead to the eradication of infection prior to oncogenesis.

1.5. *Hypothesis*

The involvement of *P. acnes* in prostate oncogenesis is strain-specific, with members of some phylogenetic types inducing a cancer-promoting immune response, while other types are passive bystanders or exhibit a cancer-protective role.

1.6. *Aims and objectives*

Aim 1 Genotypic analysis of prostate cancer-associated phylogenetic types of *P. acnes* (Chapter 3)

To perform MLST analysis on a number of available *P. acnes* prostate isolates.

Aim 2 Optimisation of *in vitro* infection model (Chapter 3)

To optimise the conditions for short and long-term *in vitro* infection models and to develop proof of concept experiments with cancer cell-lines, which will then be used in follow-up long-term experiments.

Aim 3 Investigation of the potential of *P. acnes* phylogenetic types to drive oncogenesis (Chapter 4)

To compare the molecular dysregulation of inflammatory and epithelial-mesenchymal transition genes caused by infection with different phylogenetic types of *P. acnes* in acute and chronic infections of human prostate epithelial cells. Additionally, to contrast bacterial and eukaryotic behaviour and select infection models to be used in follow-up experiments. Finally, to study the ability of *P. acnes* infection to induce anchorage-independent growth, migration and its potential to stimulate angiogenesis.

Aim 4 Analysis of prostate cancer-related genes following infection (Chapter 5)

Using a qPCR array to investigate the dysregulation in prostate cancer-related genes as a result of infection with different phylogenetic types of *P. acnes*, and to contrast the differences in expression patterns between the different infections studied.

The chapter addressing each aim is indicated in brackets.

Chapter 2:
General Materials and Methods

2

2.1. *Cell culture*

2.1.1. Cell culture and subculture

RWPE-1 (ATCC® CRL-11609™), a non-cancerous HPV-immortalised human prostate epithelium cell line, was cultured in keratinocyte serum-free medium (KSFM), supplemented with 0.05 mg/ml bovine pituitary extract and 5 ng/ml epidermal growth factor (EGF; Gibco, Life Technologies, UK) at 37°C in a 5% CO_2 humid environment. The cells were subcultured at a 1:5 ratio every 3 days. Upon reaching 80-90% confluence, the cells were washed with phosphate-buffered saline (PBS, 0.14M sodium chloride, 2.7 mM potassium chloride, 8.1 mM sodium phosphate dibasic, 1.5 mM potassium phosphate monobasic; Oxoid, UK) and then detached by treatment with 0.25% trypsin-EDTA (Gibco, Life Technologies, UK) and incubation at 37°C for 5 min. The trypsin was then neutralised with 10% (v/v) foetal bovine serum (FBS; Gibco, Life Technologies, UK) and the cell suspension was centrifuged for 5 min at 200 x g. The supernatant was removed, and the cell pellet was resuspended in PBS and centrifuged again for 5 min at 1000 rpm to remove any remaining trypsin and FBS. Finally, the PBS was aspirated, and the cells were resuspended in complete KSFM.

The prostate cancer cell lines PC-3 (ATCC® CRL-1435™) and 22Rv1 (ATCC® CRL-2505™) were cultured in RPMI-1640 medium (Gibco, Life Technologies, UK), supplemented with 10% (v/v) FBS (Gibco, Life Technologies, UK) at 37°C in a 5% CO_2 humid atmosphere. The PC-3 and 22Rv1 cell lines were subcultured every 3 days as follows: the medium was removed, and the cells were washed with PBS. They were then detached using 0.25% trypsin-EDTA (Gibco, Life Technologies, UK) and incubated at 37°C for 5 min. The trypsin was then neutralised with complete RPMI-1640 medium and the cell suspension was centrifuged at 200 x g for 5 min. The supernatant was aspirated, the cell pellet was resuspended in complete medium at ratio 1:3 for PC-3 and 1:5 for 22Rv1.

Human dermal microvascular endothelial cells (HDMEC, cell line HMEC-1, ATCC® CRL-3243™) were cultured in phenol red-free Medium 200 (Gibco, Life Technologies, UK), supplemented with 50x low growth serum supplements (LSGS; Gibco, Life Technologies, UK), with final concentrations after supplementation: 2% (v/v) FBS, 1 µg/ml hydrocortisone, 10 ng/ml human EGF, 3 ng/ml basic fibroblast growth factor, 10 µg/ml heparin. The flasks used for HDMEC culture were coated with 1% (w/v) gelatine (Sigma-Aldrich, UK) and incubated at 37°C overnight before use. The subculture protocol used

was the same as described above for PC-3 and 22Rv1 cell lines with the medium used being complete Medium 200.

The different cell lines were kindly provided by: RWPE-1 – Prof Lorraine Martin (Queen's University Belfast); PC-3 and 22Rv1 – Dr Caroline Conway and Philip Egan (Ulster University); HMEC-1 – Prof Christopher Mitchell and Naomi Todd (Ulster University). A summary of information relevant to the cell lines used in this thesis can be found in Table 2.1. The cell lines were validated by short tandem repeat (STR) analysis. STR typing was performed as follows: for 22Rv1, PC-3 and HDMEC-1 – prior to acquiring the cell lines; RWPE-1 was STR-typed before experiments were initiated. Mycoplasma screening was also performed at different stages during the project to confirm there was no contamination present.

2.1.2. Cell cryopreservation

For cryopreservation, the cells were detached as described in Section 2.1.1, and the resulting pellet was resuspended in freezing medium. The RWPE-1 cells were frozen in complete KSFM supplemented with 15% (v/v) FBS and 10% (v/v) dimethyl sulfoxide (DMSO; Sigma-Aldrich, UK). Complete RPMI-1640 with 10% (v/v) DMSO was used to freeze the PC-3 and 22Rv1 cell lines. FBS supplemented with 10% (v/v) DMSO was used for the HMEC-1 cell line. The cell suspensions for 22Rv1, PC-3 and RWPE-1 were prepared at 1.5 x 10^6 cells/ml, and 1 ml aliquots were stored at -80°C. For the HMEC-1 cell line, one third of an 80% confluent T75 flask was used.

2.1.3. Cell resuscitation

An aliquot of cells was thawed rapidly in a water bath for 2 mins and the contents of the cryovials were added to 4 ml of complete medium (KSFM for the RWPE-1 cell line; RPMI-1640 for PC-3 and 22Rv1; Medium 200 for HDMEC). The suspension was then centrifuged for 5 min at 200 x g to wash the cells. The supernatant was removed, and the cells were resuspended in fresh complete medium and seeded into a T25 flask. After an overnight incubation, the medium of the resuscitated cells was replaced with fresh complete medium to wash off any debris and remaining DMSO. The cells were then subcultured as described in Section 2.1.1.

Table 2.1. List of cell lines used

Cell line	Derivation	Medium (Supplier)	Supplements (Supplier)	Source
22Rv1 (ATCC® CRL-2505™)	Xenograft derived human prostate carcinoma epithelial cells	RPMI-1640 (Life Technologies, UK)	10% Foetal bovine serum (Life Technologies, UK)	Dr C. Conway* P. Egan*
HMEC-1 (ATCC® CRL-3243™)	Endothelial cells from human foreskin	Medium 200, phenol red-free (Life Technologies, UK)	Low serum growth supplements (Life Technologies, UK)	Prof C. Mitchell* N. Todd*
PC-3 (ATCC® CRL-1435™)	Prostate adenocarcinoma bone metastasis	RPMI-1640 (Life Technologies, UK)	10% Foetal bovine serum (Life Technologies, UK)	Dr C. Conway* P. Egan*
RWPE-1 (ATCC® CRL-11609™)	Human prostate epithelial cells from a histologically normal peripheral zone, immortalized with HPV-18	Keratinocyte serum-free medium (Life Technologies, UK)	0.05 mg/ml bovine pituitary extract 5 ng/ml epidermal growth factor (Life Technologies, UK)	Prof L. Martin+

** - Ulster University; + - Queen's University Belfast*

2.1.4. Cell viability counting

The trypan blue exclusion viability assay utilises the ability of live cells to not absorb the trypan blue dye, while it penetrates dead cells with damaged cell membranes. Trypan blue (Sigma-Aldrich, UK) viability counts were performed to calculate cell density. Equal volumes of trypan blue and cell suspension were added together and incubated at room temperature for 5 min. The suspension was then added to a haemocytometer (Immune Systems Ltd., UK) and cell counts were performed in 4 squares, with clear cells counted as viable and blue cells considered dead. The number of cells per ml was calculated by taking the average of the number of cells across all squares, which was then multiplied by the dilution factor 2 and the volume of the haemocytometer 10^4 with the result indicating the number of cells per ml of suspension.

$$^{\text{cells}}/_{\text{ml}} = \text{average number of cells} \times 2 \times 10^4$$

Percentage viability was calculated by dividing the number of viable cells by the total number of cells, and then multiplying by 100.

$$\%\ \text{viability} = \frac{\text{number of viable cells}}{\text{total number of cells}} \times 100$$

2.2. *Bacterial culture methods*

2.2.1. Routine bacterial culture

Different strains of *Propionibacterium acnes*, *Propionibacterium avidum* and *Propionibacterium granulosum* were used for the *in vitro* infection models and for multilocus sequence typing (MLST). A complete list of all strains used can be found in Table 2.2). The bacterial strains were routinely cultured on brain heart infusion (BHI) agar plates in boxes with anaerobic atmosphere generators (GenBox Anaerob, bioMerieux, France) for 5-7 days at 37°C. Additionally, for use in experiments, bacterial strains were cultured in BHI broth for 16-20 hours under anaerobic conditions at 37°C with mild agitation.

For optimization experiments a strain of *Staphylococcus epidermidis* (as described in Table 2.2) was used. *S. epidermidis* was cultured routinely on BHI agar overnight at 37°C. For experiments, BHI broth was inoculated and incubated at 37°C for 6 hours with mild agitation, until turbid.

Table 2.2. Bacterial strains used

Species	Strain	Referred to in this thesis as:	Phylogenetic type	Source	Comments on usage
P. acnes	00035 prostate	00035	IA_1	Prostate	Chapters 3, 4, 5
	00060R	00060R		Prostate	Chapter 3
	B2, 700-2010-0512	B2		Prostate	Chapter 3
	NCTC 737, also known as ATCC® 6919™	NCTC737		Acne, National Collection of Type Cultures	Chapters 3, 4, 5 Multiplex PCR control
	$24.1.A_1$	ST27*		Normal skin	Chapters 4, 5
	Pacn17	Pacn17	IA_2	Corneal scrape	Multiplex PCR control
	03E3900R	03R3900R	IB	Prostate	Chapter 3
	B3, 700-2010-0512	B3		Prostate	Chapters 3, 4, 5
	P6	P6		Prostate	-
	W1392	W1392		Dental	Multiplex PCR control
	PV66	PV66	IC	Acne	Multiplex PCR control
	NCTC 10390, also known as ACTC® 12930 ™	NCTC10390	II	National Collection of Type Cultures	Chapters 3, 4, 5 Multiplex PCR control
	Asn14	Asn14	III	Human disc material	Multiplex PCR control
	CFU2, L0076D	CFU2		Prostate	Chapters 3, 4, 5
P. avidum	pf771	*P. avidum*	-	Skin	Chapter 4
P. granulosum	PRP-18	*P. granulosum*	-	Skin	Chapters 4, 5
Staphylococcus epidermidis	NCTC 11047, also known as ATCC® 14990™	*S. epidermidis*	-	Nose	Chapter 6

* *Identified as ST27 using the "Aarhus" $MLST_9$ scheme. The strain belongs to ST4 using the "Belfast" $MLST_8$ method.*

All bacterial strains were kindly provided by Dr Andrew McDowell, except for P6, which was donated by Dr Holger Brüggemann

2.2.2. Bacterial counts

For bacterial counts the Miles Misra method was used (Miles et al., 1938). In brief, a 1:10 dilution series of broth cultures were prepared and 20 µl of each dilution were pipetted on the surface of an agar plate in triplicate. The plates were allowed to dry and were then incubated as described in Section 2.2.1. Following incubation, the colonies were counted at the dilution factor which showed clear, well defined colonies, and the mean of the three replicates was calculated. The average value of the triplicates was then multiplied by 50 (to give numbers per ml of broth) and by the dilution factor, resulting in colony-forming units (CFU)/ml.

$$\mathrm{CFU}/_{\mathrm{ml}} = \text{average number of colonies} \times 50 \times \text{dilution factor}$$

2.2.3. Gram staining

Gram staining (Gram Staining kit, Sigma-Aldrich, UK) was utilised to visualise bacteria under the microscope. Briefly, bacterial cells were heat-fixed on a glass microscope slide. The slide was subsequently flooded with Gram's crystal violet for 60 seconds, washed with water, and flooded again with Gram's iodine solution for 60 seconds. The slide was washed briefly with Gram's Decolourizer Solution, and was then washed with water and counterstained with Gram's safranin solution for a minute. Finally, the slide was briefly washed with water, air dried and examined under the microscope using Axio Imager.A2 with Zeiss EC Plan-NEUFLUAR 100x/1,30 oil immersion objective and AxioCam MRm with 1.0x magnification (Carl Zeiss Microscopy, GmbH, Germany).

2.3. *Co-culture methods*

2.3.1. Co-culture set-up

The RWPE-1 cell line was used for host response studies and was infected with different strains of *P. acnes* or *P. granulosum.* The RWPE-1 cells were counted as described in Section 2.1.1, and seeded at density of 100,000 cells/ml, and left overnight to attach. BHI broths were inoculated with strains of *P. acnes* or *P. granulosum*.

The following day, selected cell culture dishes were sacrificed to perform viability counts of the RWPE-1 cells. These counts were then used to calculate the number of bacteria needed to infect the prostate cells at a multiplicity of infection (MOI) 15:1, i.e. 15 bacterial cells per one prostate cell, following the method previously described by Drott

et al. (2010). The bacterial broths were incubated until they reached an optical density at 600 nm (OD_{600}) of 0.3.

The number of bacterial cells needed was determined by multiplying the total number of RWPE-1 cells in a cell culture dish by 15. Following, the volume of the bacterial suspension needed in µl per cell culture dish was calculated by dividing 1000 by the bacterial counts at OD_{600}, and then multiplying the result by the number of bacterial cells needed. The resulting volume was then taken from the broth culture, centrifuged at 10,000 rpm for 5 min and the BHI medium was removed. The bacteria were washed in PBS, centrifuged again at 10,000 rpm for 5 min, and the PBS was removed before resuspension of the bacteria in complete KSFM, prior to infecting the cells. The same amount of sterile complete KSFM was used for non-infected "mock" control RWPE-1 cells. Non-infected controls were used every time an experiment was set up.

2.3.2. Acute infections

Short-term or acute infection models were set up as described above (Section 2.3.1) and were defined as 24 to 72 hours in duration. In short term infections the cells were left undisturbed with no media changes, and at each time point (0h, 24h, 48h and 72h) epithelial cell counts and viability (Section 2.1.1), bacterial counts (Section 2.2.2), and RNA extraction (Section 2.4.2.1) were performed. In addition, a lactate dehydrogenase (LDH) assay (as described in Section 2.3.5) was used at each time point to determine the cytotoxic effect different strains have on the RWPE-1 cells. Intracellular bacteria were also counted at each time point (as outlined in Section 2.3.6). The conditioned medium from all acute experiments was stored at -80°C (Section 2.3.4).

2.3.3. Chronic infections

Long-term or chronic infection models were defined as 15 or 30 days in duration. The long-term infections were set up as described above (Section 2.3.1), and were split to 100,000 cells/ml every 5^{th} day. Their medium was replaced every 3^{rd} day post-split. Viability counts (Section 2.1.1) of the RWPE-1 cells were performed at every passage. At day 15 and day 30, conditioned medium was processed (Section 2.3.4) and, along with extracted RNA (Section 2.4.2.1), frozen at -80°C. DNA was also extracted at day 30 and stored at -20°C (outlined in Section 2.4.2.2). Finally, a soft agar assay to investigate cellular transformation (see Section 2.3.7) and a scratch assay for assessing cellular

migration (see Section 2.3.9) were set up, and immunostaining slides were also prepared (see Section 2.3.8).

2.3.4. Conditioned medium storage

The conditioned medium from the infection models was preserved for future downstream experiments. The medium was removed from the cells and three 1 ml aliquots were prepared. The aliquots were then centrifuged for 5 min at 10,000 rpm to pellet cells and bacteria. The supernatant was moved to a fresh tube and frozen at -80°C until further use.

2.3.5. Lactate dehydrogenase assay

The Pierce LDH Cytotoxicity assay (ThermoScientific, UK) was used to determine the cytotoxic effect of different *P. acnes* and *P. granulosum* strains on RWPE-1 cells. The colorimetric assay uses coupled enzymatic reactions to measure the amount of lactate dehydrogenase (LDH) released by damaged cells. The first reaction, the conversion of lactate to pyruvate, is catalysed by LDH via the reduction of NAD^+ to NADH. The NADH is then used in a second reaction, resulting in formazan formation, which produces colour that can be measured.

$$Lactate + NAD^+ \xrightarrow{\boldsymbol{LDH}} Pyruvate + NADH$$

$$NADH + tetrazolium\ salt \xrightarrow{\boldsymbol{Diaphorase}} NAD^+ + formazan$$

The assay was performed following the manufacturer's instructions. Briefly, 50 µl of reaction mixture was added to 50 µl of supernatant from different acute infection models. The samples were then incubated at room temperature for 30 min, and 50 µl of stop solution was added. The optical density was measured at 490 nm and 680 nm. Non-infected samples were used as spontaneous LDH release controls, and lysed cells were used as maximum LDH release controls. Percentage cytotoxicity was calculated using the formulas below:

$$\text{LDH activity} = \text{LDH at } 490\text{nm} - \text{LDH at } 680\text{nm}$$

$$\%\ \text{cytotoxicity} = \frac{\text{infected cells LDH activity} - \text{spontaneous LDH activity}}{\text{maximum LDH activity} - \text{spontaneous LDH activity}} \text{x}100$$

2.3.6. Intracellular bacterial counts

The RWPE-1 cells were seeded and infected at an MOI 15:1 as described in Section 2.3.1. At 24h, 48h and 72h intracellular bacterial counts were performed using a modification of the method described by Fischer et al. (2013), based on the monocytic cell line THP-1. The medium was removed from the cells, and they were washed twice with PBS. Fresh complete medium, supplemented with 0.4 mg/ml gentamycin (Gibco, Life Technologies, UK), 500 units/ml penicillin and 0.5 mg/ml streptomycin (Gibco, Life Technologies, UK), was added and the cells were incubated for 3 hours; following, the media was removed, and the cells were washed twice with PBS to remove any remaining antibiotics. Finally, a 20-minute treatment with 0.5% (w/v) saponin (Sigma-Aldrich, UK) solution was used to lyse the eukaryotic cells. Bacterial counts were performed as described in Section 2.2.2. Non-infected cells were used as controls for contamination. Additionally, cells treated with antibiotics but not lysed were used to determine whether all extracellular bacteria were eradicated following antibiotic treatment. If any growth was observed in the antibiotic controls, this number was subtracted of the intracellular counts of the corresponding strain.

2.3.7. Soft Agar assay

Soft agar assays were used to investigate anchorage independent growth and cellular transformation of the RWPE-1 cells following long-term infections. The two prostate cancer cell lines PC-3 and 22Rv1 were chosen as positive controls, and the non-infected RWPE-1 cell line as a negative control.

The soft agar assay consisted of two layers of agar. The bottom layer was prepared by melting 3% (w/v) UltraPure agarose (Invitrogen, UK) and adding it to complete medium (RPMI-1640 or KSFM, as appropriate for the cell line used) to a final concentration of 0.5% (w/v) agarose. The mixture was then aliquoted in 6-well plates, with 1.5 ml added per well, and left at room temperature to solidify. For the top layer, a cell suspension was prepared as described in Section 2.1, and the cells were counted as outlined in Section 2.1.1. A diluted suspension was then prepared at 7,500 cells/ml and molten 3% (w/v) agarose was added to a final concentration of 0.3% (w/v) agarose and a total of 10,000 cells/well. Erythromycin (Sigma-Aldrich, UK), at a final concentration 20 µg/ml was added to the cell/agarose mixture, to ensure no bacterial colonies were formed in the assay. As described above, 1.5 ml of the mixture were aliquoted on top of the

solidified layer of 0.5 % (w/v) agarose. The assays were briefly placed at 4°C to solidify and were then incubated at 37°C in a humid 5% CO_2 atmosphere for 14 days. Appropriate medium (100 µl) was added to each well every 3 days to prevent desiccation of the agar. The assay was stained by adding 100 µl of 10 mg/ml nitrotetrazolium blue chloride (Sigma-Aldrich, UK) per well and incubated overnight. Images were then taken at no magnification (Canon EF 50 mm f/1.2 USM objective, ChemiDoc-It^2 Imager, UVP, USA) and at x2 magnification using a PrimoVert inverted microscope (Primo Plan-ACHROMAT 4x/0.10 objective and AxioCam 105 colour with 0.5x magnification; Carl Zeiss Microscopy GmbH, Germany).

2.3.8. Immunofluorescence methods

2.3.8.1. Specimen preparation and immunostaining

The PathScan® Duplex IF kit (Cell Signalling, USA) was used for immunofluorescence investigation of whether the cells were undergoing epithelial-mesenchymal transition (EMT) after a chronic exposure to different *P. acnes* strains and *P. granulosum.* The kit contained PathScan® EMT duplex IF Kit Primary Antibody Cocktail, targeting E-cadherin and vimentin, and PathScan® Duplex IF Kit Detection Cocktail I secondary antibody mix targeting the E-cadherin and vimentin primary antibodies, labelled with fluorescent dyes AlexaFluor® 488 and AlexaFluor® 555, respectively.

At day 15 or day 30, the cells were harvested as described in Section 2.1 and a suspension was prepared at 100,000 cells/ml, 400 µl of which were added to a 35-mm Petri-dish (µ-Dish 35 mm, high, Ibidi, Germany). The cells were left to attach, and 1.6 ml of medium were added to the dishes. Alternatively, 700 µl of cell suspension were added if 4 well µ-slides (µ-Slide 4 Well, Ibidi, Germany) were used. The dishes were then incubated as described above until the cells reached confluence.

Once the cells had reached confluence, the medium was aspirated, and the cells were fixed for 15 min with 4% (v/v) formaldehyde diluted in warm PBS. The fixative was then aspirated, and the cells were washed 3 times with PBS. The specimen was blocked with blocking buffer (20% (v/v) FBS (Gibco, Life Technologies, UK), 5% (w/v) bovine serum albumin (BSA) (Sigma-Aldrich, UK), 0.05% (v/v) Triton X (Sigma-Aldrich, UK), 0.01% (v/v) Tween-20 (Sigma-Aldrich, UK) in PBS) for 60 min. The blocking buffer was removed from the cells and the Primary Antibody Cocktail, diluted 1:100 in blocking buffer, was added

to the sample and incubated at 4°C overnight. Post incubation, the cells were rinsed three times with PBS for 5 min, and PathScan Duplex IF Kit Detection Cocktail, diluted 1:100 in blocking buffer, was added and incubated for 90 minutes at room temperature in the dark. After another cycle of 3 washes in PBS for 5 min, the slides were counterstained with a drop of ProLong® Diamond Antifade Mountant with 4',6-diamidino-2-phenylindole, dihydrochloride (DAPI) (Life Technologies, UK), and incubated overnight at room temperature in the dark. The slides were then ready for imaging, and stored at 4°C in the dark until used. All experiments were performed in triplicate.

2.3.8.2. Acquisition and analysis

For each slide, 20 images were captured for each fluorescent dye and DAPI, using Axio Imager.A2 (Carl Zeiss Microscopy GmbH, Germany) with a Zeiss EC Plan-NEOFLUAR 40x/0.75 objective and AxioCam MRm with 1.0x magnification. The filters used for AlexaFluor® 488 and AlexaFluor® 555 were EGFP (enhanced green fluorescent protein; Filter 38; excitation 450-490 nm; emission 500-550 nm, Carl Zeiss Microscopy GmbH, Germany) and Rhodamine (Filter 20; excitation 540-552 nm; emission 575-640 nm, Carl Zeiss Microscopy GmbH, Germany), respectively. The exposure settings for each colour were optimised, so there were no overexposed sections and all signals were within the colour histogram, and were constant between slides and treatments.

The images were analysed using imageJ (Schneider et al., 2012). The DAPI staining was used to assess the number of nuclei in each slide. The orange and green channels were analysed separately following the same procedure. First, a threshold was selected to include all strong signal but remove any background fluorescence. The fluorescence was then quantified by measuring the integrated density (IntDen) on every image. Following, the IntDen was normalised by dividing by the number of nuclei in each image, resulting in the average signal per cell (NormIntDen). The NormIntDen was then averaged across all 20 images per biological replicate. The result for all three biological replicates was used for statistical analysis.

2.3.9. Scratch assay

At the end of a long-term infection, the cells were harvested as described in Section 2.1.1, and a 100,000 cells/ml suspension was prepared. The suspension was aliquoted in 12-well plates (ThermoFisher Scientific, UK) in triplicate, and were incubated until

100% confluence. The confluent monolayer was then scratched using a 200 µl pipette tip and a uniform wound was created. The medium was replaced in order to remove any debris, and the cells were incubated at 37°C in 5% CO_2 atmosphere. Images were taken every 24 hours, until the wound had healed, at 2x magnification using a PrimoVert inverted microscope (Carl Zeiss Microscopy GmbH, Germany) with a Prime Plan-ACHROMAT 4x/0,10 objective and AxioCam 105 colour with 0.5x magnification. The width of the wound at each time point was measured using ZEN 2.3 (Carl Zeiss Microscopy GmbH, Germany). An average for each biological replicate was calculated for every timepoint and the percentage closure was calculated by subtracting the distance measured at each time point from the initial T_0 distance, and the number was then divided by the T_0 measurement.

$$\%\ \text{closure} = \frac{\text{measurement at } T_0 - \text{measuremeant at time point}}{\text{measurement at } T_0}$$

2.3.10. MTT assay

The HDMEC cell line was seeded at $5x10^4$ cells/ml in a 96 well plate (Thermo Scientific, UK). The cells were left for 24h to attach. The medium was then removed, and the cells were treated with a serial dilution of conditioned medium from chronic infection models. Following, the cells were incubated for 48h at 37°C. A stock solution of 12 mM 3-(4,5-dimethylthiazol-2-yl)-2,5-diphenyltetrazolium bromide (MTT) (Sigma-Aldrich, UK) was added to each well, to a final concentration of 1.2 mM. The cells were then incubated for a further 3 hours. Metabolically active cells reduce the tetrazolium MTT salt to formazan crystals which can then be solubilised, resulting in a colour change. After the incubation, 100 µl of DMSO (Sigma-Aldrich, UK) solubilising solution was added and the plate was incubated at room temperature with mild agitation for 20 min. The colour change was measured at 570 nm using a microplate spectrophotometer (Epoch, BioTek Instruments, US).

$$MTT + NADH \xrightarrow{\boldsymbol{reduction\ in\ mitochondria}} NAD^+ + formazan$$

2.4. *Molecular methods*

2.4.1. Nucleic acid quantification

2.4.1.1. Nanodrop

Extracted short-term infection model RNA was quantified using a Nanodrop 1000 (Thermo Scientific, UK). Each sample was assessed in triplicate by adding 2 µl to the instrument. The elution buffer for each sample was used to calibrate the instrument prior to use.

2.4.1.2. Qubit assays

For chronic infection analysis, Qubit® RNA BR Assay kit (Thermo Scientific, UK) was used. Additionally, polymerase chain reaction (PCR) products for multilocus sequence typing (MLST) analysis were quantified using the Qubit® DNA HS assay kit. Briefly, 200 µl of working solution was prepared per reaction by diluting the Qubit® RNA/DNA reagent 1:200 in Qubit® RNA/DNA buffer. The samples were briefly vortexed and incubated for 2 mins. Two standards were used to calibrate the instrument by adding 10 µl of each standard to 190 µl of working solution (0 ng/µl low standard for both RNA and DNA kits; 100 ng/µl high standard for Qubit® RNA BR Assay; 10 ng/µl high standard for Qubit® DNA HS assay). For sample analysis, 2 µl of RNA/PCR product was added to 198 µl of working solution. The Qubit 3.0 fluorometer was then used to measure and calculate the nucleic acid concentration in the initial sample.

2.4.2. Eukaryotic analysis

2.4.2.1. RNA extraction

RNA was extracted using the RNeasy Plus Mini-Kit (QIAGEN, Germany), according to the manufacturer's instructions as follows: the cells were harvested as described in Section 2.1.1, pelleted and resuspended in 350 µl of buffer RLT Plus with 1% (v/v) β-mercaptoethanol (β-ME) (Sigma-Aldrich, UK). The cells were then homogenised by pulse vortexing for 30 seconds and were transferred to a genomic DNA eliminator tube and centrifuged for 30 s at 8000 x g. An equal volume of 70% (v/v) ethanol was added to the flowthrough and mixed. The sample was then transferred to an RNeasy column and centrifuged for 15s at 8000 x g. The membrane was then washed with 700 µl of Buffer RW1 and centrifuged for 15s at 8000 x g. The extraction was completed with two consecutive washes at 8000 x g with 500 µl of buffer RPE centrifuged for 15s and 2 min.

Finally, the RNA was eluted in 40 µl of RNase-free water by centrifuging for 1 min at 8000 x g. The extracted RNA was stored at -80°C until further use.

2.4.2.2. DNA extraction

Cells were harvested as described above and the pellet was resuspended to a final volume of 200 µl in PBS. QIAGEN's QIAamp DNA Mini Kit (QIAGEN, Germany) was used for DNA extraction following the manufacturer's protocol. Briefly, 20 µl proteinase K and 200 µl Buffer AL were added to the sample. The mixture was pulse-vortexed for 15 s and incubated for 10 min at 56°C before the addition of 200 µl of 100% ethanol with brief vortexing. The mixture was then applied to a QIAamp Mini Spin column and centrifuged at 6000 x g for 1 min. The filtrate was discarded, and the column was washed twice: first with 500 µl of buffer AW1 by centrifuging at 6000 x g for 1 min, and then with 500 µl of buffer AW2 and 3 min centrifugation at 20,000 x g. A drying step was used to remove any remaining ethanol from the column by an additional 1 min centrifugation at 20,000 x g. Finally, 100 µl of buffer AE (10 mM Tris-Cl; 0.5 mM EDTA; pH 9.0) were added to the column, and after 1 min incubation at room temperature, the DNA was collected by centrifuging at 6000 x g for 1 min. The extracted DNA was stored at -20°C until further use.

2.4.2.3. Complementary DNA synthesis

The Transcriptor First Strand complementary DNA (cDNA) Synthesis Kit (Roche, Switzerland) was used to produce 1 µg of cDNA from RNA, with a final concentration of 50 µg/ml. This would allow downstream analysis of gene expression using methods such as quantitative PCR (qPCR). The average of the three Nanodrop readings for each sample, or Qubit result, was used to calculate the amount of RNA in µl needed by dividing 1000 by the average RNA yield in ng/µl. The resulting volume of RNA was then topped up to 11 µl with UltraPure™ RNase free water (Invitrogen, Life Technologies, UK). cDNA synthesis was performed according to the manufacturer's protocol for each 20 µl reaction as follows: 11 µl of RNA and water, 2 µl of Random Hexamer Primers (600 pmol/µl), 4 µl of Transcriptor Reverse Transcriptase reaction buffer (5x conc.), 2 µl of Protector RNase Inhibitor (40 U/µl), deoxynucleotide (dNTP) mix (10 mM each), and 0.5 µl of Transcriptor Reverse Transcriptase (20 U/µl) were added (final concentrations of 60 µM, 1x 8 mM $MgCl_2$, 20 U, 1 mM each and 10 U, respectively). The reactions were then amplified in a thermocycler (Techne Prime, UK) for 10 min at 25°C, followed by 60

min at 50°C, and a final inactivation step at 85°C for 5 min. The reaction products were then stored at -20°C. Reactions with no reverse transcriptase (no-RT) reactions were used with every synthesis.

2.4.2.4. Quantitative polymerase chain reaction

2.4.2.4.1. Quantitative PCR protocol

Quantitative PCR was used to assess the differences in the expression in a range of genes. Probes master and primer-probe mixes (Roche, Switzerland) were used to set up qPCR reactions with 12.5 ng of cDNA used for most reactions, except for *IL6*, *TNF* and *CDH2* where 62.55 ng was used per reaction, as the second group of genes could not be detected at a lower concentration. Each reaction was prepared to a final volume of 10 µl using 5 µl LightCycler® 480 Probes Master (2x concentrate) (Roche, Switzerland), 1.5 µl of the primer-probe mix and 2.5 µl of cDNA. The reaction was run in a LightCycler® 480 (Roche, Switzerland) following the manufacturer's instructions. This consisted of a pre-incubation cycle of 10 min at 95°C, followed by 45 amplification cycles consisting of three steps, 95°C for 10 s, 60°C for 30 s, and 72°C for 1s; the program concluded with a cooling step of 30 s at 40°C. Cycle threshold (C_t values, also known as C_p values) were recorded and used to calculate fold-change in expression. If a C_p value was not detected, the value of 40 was used to calculate the ratio change. Each qPCR plate included negative (water) controls (to confirm there is no contaminating DNA in the reagents) and no-RT controls (to confirm that the cDNA reactions were successful and that there was no contaminating genomic DNA in the cDNA reactions).

2.4.2.4.2. qPCR assay efficiencies

To calculate the efficiency of each primer-TaqMan® probe mix (Roche, Switzerland), a serial dilution was prepared following the protocol described above (Section 2.4.2.4.1), and a standard curve was created for each gene. The efficiency was then calculated using $E\% = (10^{-1/slope}) \times 100$. The full list of genes can be found in Table 2.3.

2.4.2.4.3. Housekeeping gene selection

For the selection of the optimal housekeeping gene(s), cDNA prepared from short term infection models of infected and non-infected cells was used at different timepoints: T_0, 24h, 48h, and 72h. Each timepoint had three biological replicates for infected and mock

Table 2.3. List of Real-Time ready assays used

Gene	Assay ID	Full name	Function
ACTB	143636	Beta-actin	Housekeeping
CDH1	103920	E-cadherin	EMT
CDH2	137066	N-cadherin	EMT
GAPDH	141139	Glyceraldehyde 3-phosphate dehydrogenase	Housekeeping
HPRT1	145173	Hypoxanthine-guanine phosphoribosyltransferase	Housekeeping
IL1B	100950	Interleukin-1 beta	Inflammatory
IL6	144013	Interleukin-6	Inflammatory
IL8	103136	Interleukin-8	Inflammatory
SNAI1	144082	Snail family zing finger 1 (Snail)	EMT
SNAI2	147564	Snail family zing finger 2 (Slug)	EMT
TBP	101145	TATA-binding protein	Housekeeping
TGFB1	145593	Transforming growth factor beta	Inflammatory
TNF	103295	Tumour necrosis factor	Inflammatory
TWIST1	110770	Twist-related protein 1	EMT
VIM	112941	Vimentin	EMT

cells, and for housekeeping gene selection three technical replicates for each biological replicate were used. The genes investigated were *ACTB*, *GAPDH*, *HPRT*, and *TBP*, which are housekeeping genes previously used in the literature with the RWPE-1 cell line. Normfinder (https://moma.dk/normfinder-software) (MOMA, Aarhus University Hospital, Denmark), a statistical package specialising in the selection of the most stable housekeeping gene or a combination of housekeeping genes, based on a mathematical model of estimation of expression of variation, was then used (Andersen et al., 2004). The expression data for the housekeeping genes tested was separated into two groups (infected and non-infected) and the software then ranked the genes by a stability value, a combination of intragroup and intergroup variation, to provide a realistic assessment of the potential systematic error introduced by the different housekeeping genes in the dataset.

2.4.2.4.4. Ratio difference calculation

The ratio of differences in expression was calculated based on C_p values for the housekeeping gene and the gene of interest. The gene efficiencies (E) were used to more accurately represent the fold-change dysregulation. The formulas below were used to calculate ΔC_p for the target and housekeeping (reference) genes, and these two values were used to calculate the ratio change for each target gene.

$$\Delta C_{p_{target}} = C_{p_{control}} - C_{p_{treatment}}$$

$$\Delta C_{p_{reference}} = C_{p_{control}} - C_{p_{treatment}}$$

$$ratio = \frac{\left(E_{target}\right)^{\Delta C_{p_{target}}}}{\left(E_{reference}\right)^{\Delta C_{p_{reference}}}}$$

2.4.2.4.5. Human Prostate cancer qPCR array

2.4.2.4.5.1. cDNA synthesis

The RT^2 First Strand Kit (QIAGEN, Germany) was used to prepare cDNA for use in the Prostate cancer qPCR array. A total of 0.5 µg of RNA was added to 2 µl of Buffer GE, and the reaction volume was made up to 10 µl with PCR-grade water. After mixing, the sample was incubated at 42°C for 5 min in a thermocycler (Techne Prime, UK), followed by immediate incubation on ice for 1 min. Following, the remaining components of the reverse-transcription reaction were added: 4 µl of 5x reverse transcription buffer 3 (Buffer BC3), 1 µl of primer and external control mix (P2 control), 2 µl of reverse

transcription enzyme mix 3 (RE3) and 3 µl of RNase-free water to a total reaction volume of 20 µl. The samples were mixed and incubated at 42°C for 15 min and then for a further 5 min at 95°C (Techne Prime, UK). Once the incubation steps were competed, 91 µl of RNase-free water were added to each reaction and the tubes were then stored at -20°C until further use.

2.4.2.4.5.2. RT^2 Profiler PCR array

The RT^2 Profiler Human prostate cancer PCR array (QIAGEN, Germany) was used to assess the expression levels of 84 prostate cancer-related genes and to compare differences between cells infected for 15 days with different phylogenetic types of *P. acnes* and non-infected cells.

For each 96-well plate array 1350 µl 2x RT^2 SYBR Green Mastermix, 1248 µl RNase-free water and 102 µl cDNA synthesis reaction (prepared as described in Section 2.4.2.4.5.1) were mixed together and 25 µl of this mix were added to each well. The plates were then sealed and centrifuged at 1000 x g for 1 min at room temperature. Analysis was performed using LightCycler 480 (Roche, Switzerland) and a programme which included an initial activation cycle of 10 min at 95°C, followed by 45 cycles of 15 s at 95°C and 1 min at 60°C. The programme was concluded by performing a melt curve. C_p values were recorded and imported into the SABiosciences web based PCR Array data analysis software, version 3.5 (http://pcrdataanalysis.sabiosciences.com/pcr/arrayanalysis.php; QIAGEN, Germany).

2.4.3. Bacterial molecular methods

2.4.3.1. DNA extraction

A loop of bacteria was resuspended in 1 ml of PBS and then centrifuged for 5 min at 10,000 rpm. The supernatant was removed, the pellet was resuspended in 400 µl of UltraPure® nuclease-free water (Invitrogen, Life Technologies, UK) and the suspension was then boiled at 100°C for 10 min. Once cooled, the tubes were centrifuged for 5 min at 10,000 rpm. The supernatant containing the crude bacterial DNA preparation was moved to a fresh tube and stored at -20°C.Multiplex typing of *P. acnes*

A multiplex touchdown *P. acnes* typing scheme developed by Barnard et al. (2015) was used for the routine identification of the phylogenetic group of *P. acnes* strains used in experiments. Each reaction was prepared to a final concentration of 0.2 mM $MgCl_2$

(Invitrogen, Life Technologies, UK), 1x PCR buffer (Invitrogen, Life Technologies, UK), 0.2 mM dNTPs (Invitrogen, Life Technologies, UK), 0.8 U Platinum *Taq* polymerase (Invitrogen, Life Technologies, UK), and varying concentrations of primers as described in Table 2.4. To each reaction, 1 µl of crude bacterial DNA was added.

The reactions were then amplified with a four-stage programme in a thermocycler (Techne Prime, UK): an initial denaturation at 94°C for 1 min, followed by 30 cycles of 94°C for 1 min, and subsequent 14 cycles of 94°C for 30s, 66°C (with decrement of 0.3°C per cycle) for 30 s, and 72°C for 1 min. This was followed by 11 cycles of 94°C for 30 s, 62°C for 30 s and 72°C for 1 min. The programme concluded with a final extension step of 72°C for 10 min. The reaction products were analysed on a 1.5% (w/v) UltraPure® agarose (Invitrogen, Life Technologies, UK) stained with 1x GelRed (Cambridge Bioscience, UK).

Bacterial strains representing each major phylogroup were used as positive controls. NCTC737 was used as a control for type IA_1, Pacn17 for type IA_2, W1392 for type IB, PV66 for type IC, NCTC10390 for type II and Asn14 for type III, and PCR-grade water was used as a negative control.

2.4.3.1. Multilocus sequence typing

The multilocus sequence typing (MLST) scheme described previously by McDowell et al. (2013) was used for the phylogenetic analysis of a number of *P. acnes* prostate-derived isolates.

2.4.3.1.1. MLST PCR

Primers and PCR conditions for *aroE*, *atpD*, *camp2*, *gmk*, *guaA*, *lepA*, *sodA*, and *tly* were described previously (McDowell et al., 2011; McDowell et al., 2013). To summarise, each reaction containing 0.2 mM of each primer (primer list can be found in Table 2.5), 1x PCR buffer, 2 mM $MgCl_2$, 0.2 mM dNTPs, 1.25 U Taq polymerase, was made up to a final volume of 48 µl PCR-grade water and 2 µl of bacterial lysate DNA was added. The PCR conditions included an initial denaturation step of 94°C for 1 min, followed by 30 cycles of 94°C for 1 min, 56°C for 1 min and 72°C for 2 min, with a concluding extension step of 10 min at 72°C (Techne Prime, UK) (McDowell et al., 2013). The size of the PCR products was confirmed via 1.5% (w/v) UltraPure® agarose (Invitrogen, Life Technologies, UK) gel electrophoresis stained with 1x GelRed (Cambridge Bioscience, UK).

Table 2.4. Multiplex PCR primer sequences

Gene	Specificity	Primer	Sequence (5'-3')	Final concentration	Size (bp)
16S rRNA	All *P. acnes* strains	PArA-1	AAGCGTGAGTGACGGTAATGGGTA	0.2 mM	667
		PArA-2	CCACCATAACGTGCTGGCAACAGT		
ATPase	Types IA_1, IA_2, IC	PAHp-1	GCGTTGACCAAGTCCGCCGA	0.25 mM	494
		PAHp-2	GCAAATTCGCACCGCGGAGC		
sodA	Types IA_2, IB	PAHp-3	CGGAACCATCAACAAACTCGAA	0.6 mM	145
		PAHp-4	GAAGAACTCGTCAATCGCAGCA		
Toxin, Fic family	Type IC	PAHp-5	AGGGCGAGGTCCTCTTCTACCAGCG	0.1 mM	305
		PAHp-6	ACCCTCCAACTGCAACTCTCCGCCT		
atpD	Type II	PAHp-7	TCCATCTGGCCGAATACCAGG	0.15 mM	351
		PAHp-8	TCTTAACGCCGATCCCTCCAT		
recA	Type III	PAHp-9	GCGCCCTCAAGTTCTACTCA	0.25 mM	225
		PAHp-10	CGGATTTGGTGATAATGCCA		

Reference: Barnard et al. (2015)

Table 2.5. MLST PCR primer sequences

Gene	Function	Primer	Sequence (5'-3')	Size (bp)	Reference
aroE	Shikimate 5-dehydrogenase	aroE-F	ACCGATTAAGAGTGACTACC	1102	McDowell et al. (2013)
		aroE-R	ACTCCTCGGAAATCTCTACA		
atpD	ATP synthase beta chain	atpD-F	AATTACCCCCGAGACGAA	1261	McDowell et al. (2011)
		atpD-R	CGTGTTCTGGGACAGGAA		
camp2	Co-haemolytic factor	camp2-F	GTCGTAGCCATACACCACACG	1015	Valanne et al. (2005)
		camp2-R	GCACCGAGTGTTGATGTCAATTAGC		
gmk	Guanylate kinase	gmk-F	TAGCCATCCGGAGATCGT	444	McDowell et al. (2011)
		gmk-R	GCGCAACTGCGTGATCTA		
guaA	GMP synthase	guaA-F	TCGCCTTCATGGAACAAC	1384	
		guaA-R	CCATAAGTACGCCCGTCA		
lepA	GTP-binding protein	lepA-F	TCGCGCCCAGTACTTAGA	1218	
		lepA-R	CGGATTTCCACTCGATCA		
sodA	Superoxide dismutase	sodA-F	TGGAACTGCACCATGACA	488	
		sodA-R	GCTAACGACGTTCCACCA		
tly	Putative haemolysin gene	tly-F	CAGGACGTGATGGCAATGCGA	909	McDowell et al. (2005)
		tly-R	TCGTTCACAAGACCACAGTAGC		

2.4.3.1.2. PCR product purification

PCR products were purified using a QIAquick PCR Purification Kit (QIAGEN, Germany) following the manufacturer's protocol. Briefly, 5 volumes of buffer PB were added to 1 volume of PCR product. After mixing, the sample was applied to a QIAquick column and centrifuged for 45 s at 13,000 rpm. The column was then washed with 750 µl of buffer PE (10 mM Tris-HCl pH 7.5; 80% ethanol) and centrifuged as before. Finally, the sample was eluted in 50 µl of buffer EB (10 mM Tris-Cl, pH 8.5) and stored at -20°C until further use.

2.4.3.1.3. Sanger sequencing

Purified PCR products were quantified as described in Section 2.4.1.2 using the Qubit® DNA HS assay kit (Invitrogen, Life Technologies, UK), and were then diluted to 5 ng/µl for products of less than 1000 bp, and to 10 ng/ml for products over 1000 bp. The Sanger sequencing reactions using the BigDye™ Terminator v3.1 Cycle Sequencing Kit (Applied Biosystems, Thermo Fisher Scientific, USA) and capillary electrophoresis on an Applied Biosystems 3730xl 96-capillary DNA analyser were carried out by Eurofins Genomics (Ebersberg, Germany), using the sequencing primers described in Table 2.6.

2.4.3.1.4. Assignment of alleles and sequence types

After sequencing, the FASTA files for the forward and reverse read were combined to from the complete sequencing product. This complete sequence was then compared to the *P. acnes* MLST database of known alleles (http://pubmlst.org/pacnes/) hosted at the University of Oxford, UK (Jolley et al., 2004). The sequence type and clonal complex for each strain were then determined using their 8-gene allelic profile.

2.5. *Protein methods*

2.5.1. Protein extraction

Mammalian Protein Extraction Reagent (M-PER®) (Pierce Biotechnology, ThermoScientific, USA) was used to extract protein at day 30 of chronic infection models. The manufacturer's protocol was used, as follows: the cells were scraped into PBS, and centrifuged at 2,500 x g for 10 min. The supernatant was removed and 250 µl of M-PER were added to the sample. The mixture was gently shaken for 10 min, and cell debris were removed by centrifugation at 14,000 x g for 15 min. The supernatant, containing the extracted protein, was transferred into a fresh tube and stored at -80°C.

Table 2.6. MLST sequencing primers

Gene	Function	Primer	Sequence (5'-3')	Size (bp)	Reference
aroE	Shikimate 5-dehydrogenase	As PCR primers (Table 2.5)		424	McDowell et al. (2013)
atpD	ATP synthase beta chain	atpD-F	TAAGGGTCACGTCTGGAA	453	McDowell et al. (2011)
		atpD-R	ACATCGCGGAAGTACTCA		
camp2	Co-haemolytic factor	As PCR primers (Table 2.5)		804	Valanne et al. (2005)
gmk	Guanylate kinase	gmk-F	AGATCGTCGTTTCCAGGT	400	McDowell et al. (2011)
		gmk-R	ACAACGGCGTCAAATTC		
guaA	GMP synthase	guaA-F	GCGTTTGAAGACGTTGAG	493	
		guaA-R	GCTGGTCAGCATTGAGAC		
lepA	GTP-binding protein	lepA-F	GTCAAGGATGTCCGTCAA	452	
		lepA-R	GCAGGACTGAGAATGGTG		
sodA	Superoxide dismutase	sodA-F	ACAAGCACCACAACACCT	450	
		sodA-R	TAACGTAGTCGGCCTTGA		
tly	Putative haemolysin gene	As PCR primers (Table 2.5)		777	McDowell et al. (2005)

2.5.2. Enzyme-linked immunosorbent assay (ELISA)

ELISA 3,3',5,5'-Tetramethylbenzidine (TMB) development kits (PeproTech, US) were used to quantify the amount of IL-1β, IL-6, IL-8 and TNF-α in conditioned medium from acute and chronic infections. All steps were performed at room temperature. Nunc MaxiSorp™ 96-well plates (ThermoFisher Scientific, UK) were coated with 100 µl capture antibody and incubated overnight. The plates were then washed four times with 300 µl PBS-T (0.05% (v/v) Tween-20 (Sigma-Aldrich, UK) in PBS) per well, 300 µl blocking buffer (1% (w/v) BSA (Sigma-Aldrich, UK) in PBS) were added to each well and the plate was incubated for 1 hour. The plates were washed again as described above, 100 µl of standards and samples were added per well and the plates were incubated for 2 hours. After another wash, 100 µl of detection antibody were added per well and incubated for further 2 hours. The plates were washed again, 100 µl of streptavidin-horseradish peroxidase conjugate (S-HRP) were added to each well and were incubated for 30 min. Finally, after a wash, 100 µl of TMB (Sigma-Aldrich, UK) were added to each well and after 20 min incubation the reaction was stopped with 100 µl 1M HCl. The resulting colour change was measured using a spectrophotometer (Epoch, BioTek, US) at 450 nm with a correction wavelength at 620 nm.

2.6. *Statistical analysis*

All experiments were performed in triplicate and the data is represented as mean +/- standard error of the mean (SEM). Significance was determined using a two-tailed Student's t-test, unless otherwise stated, with $p < 0.05$ considered significant. Data analysis was performed using Microsoft Office Excel (Microsoft Office 365, version 1707, USA) or GraphPad Prism (Version 7, GraphPad Software Inc., USA).

Chapter 3:
Optimization of *in vitro* model of infection

3

3.1. *Introduction*

In vitro infection models allow the study of direct cellular response to infection. While the analysis is limited to a single eukaryotic cell type, they do provide the opportunity for basic investigation which can then be used in more complex models and can also identify potential biomarkers which can be further investigated in patients. In this chapter, preliminary experiments focused on the optimisation of the *in vitro* infection models used in this thesis, as well as experiments used for downstream analysis of dysregulation following acute and chronic infection. Additionally, a small investigation was undertaken into the phylogenetic types of *P. acnes* isolated from prostatectomy samples.

Multilocus sequence typing (MLST) is a molecular biology technique used for the phylogenetic typing of bacterial strains based on small differences in the sequences of multiple genes, usually housekeeping genes. Two MLST schemes have been developed for the typing of *P. acnes*. The first "Aarhus" $MLST_9$ scheme, developed by Lomholt and Kilian (2010), included 9 housekeeping genes and 2 putative virulence factors. The second "Belfast $MLST_8$ method, developed by McDowell et al. (2011), included seven genes, and was later updated to include six housekeeping genes and two putative virulence factors (McDowell et al., 2011; McDowell et al., 2012a). More recently, a single locus sequence typing scheme showing resolution similar to that of the previously established MLST schemes was also developed (Scholz et al., 2014). What all three schemes have in common is the agreement that *P. acnes* has six phylogroups: types IA_1, IA_2, IB, IC, II and III, despite each group referring to them using different nomenclature.

Previous studies have shown different phylotypes tend to be associated with different diseases. Type IB has been linked to medical device and soft tissue infections. Type III has been associated with spinal disk infections and the skin condition progressive macular hypomelanosis (McDowell et al., 2013; Barnard et al., 2016). A study of radical prostatectomy isolates of *P. acnes* showed that prostate isolates differ from those normally found on skin, as they were type IB and II, in contrast with type IA_1 which is a part of the skin microflora (Mak et al., 2013b).

There are multiple variants of infection models of prostate epithelial cells with *P. acnes* in literature, with the main difference being the multiplicity of infection (MOI) used.

Drott et al. (2010) selected an MOI of 16:1 in short term infections, while Fassi Fehri et al. (2011) and Mak et al. (2012) used MOI 50:1 for both acute and chronic infections. Finally, an infection model with primary prostate epithelial cells infected with MOI 100:1 for short-term infections and MOI 30:1 for long-term have also been used (Sayanjali et al., 2016).

P. acnes has demonstrated the ability to remain viable intracellularly in both prostate epithelial cells and in macrophages (Mak et al., 2012; Fischer et al., 2013). The methods to assess the intracellular presence of *P. acnes* used in literature vary, with the main differences being the antibiotics and the incubation times used. In the context of *P. acnes* and RWPE-1 cells, 2-hour incubation with 300 µg/ml penicillin/streptomycin, 3-hour incubation with 300 µg/ml gentamycin or 2 hours with 50 µM/ml tetracycline have been described (Mak et al., 2012; Fischer et al., 2013; Sayanjali et al., 2016). However, none of those studies indicated the use of negative controls, showing whether the antibiotics eradicate extracellular bacteria.

Further methods optimised in this chapter for analysis of cellular response and cellular transformation include soft agar assays, quantitative PCR (qPCR) and ELISA.

Soft agar colony formation assays are widely used to investigate cellular potential for anchorage-independent growth – a hallmark of cancer progression and contributing factor to metastasis (Borowicz et al., 2014). Previous studies appear to support *P. acnes*-driven cellular transformation by employing soft agar assays (Fassi Fehri et al., 2011).

There are two main approaches to analysing qPCR data. Absolute quantification is based on comparing the absolute concentrations of cDNA in each reaction, which are worked out by comparing to a standard curve. For relative quantification, a reference gene (also called a housekeeping gene) which is constitutively expressed is used to calculate the ratio change of a gene of interest. A good housekeeping gene should be stable between untreated and treated samples, and should not change with incubation times. Statistical packages for comparison of gene stability, such as Normfinder or geNorm, are available (Vandesompele et al., 2002; Andersen et al., 2004).

The colorimetric MTT assay, which investigates the production of formazan from 3-(4,5-dimethylthiazol-2-yl)-2,5-diphenyltetrazolium bromide (MTT) by viable cells was

selected as a cost-effective method of analysing cell proliferation, and thus angiogenic potential, of conditioned medium from long-term infection model experiments. However, the selection of optimal seeding for the HDMEC cells and the selection of appropriate controls is needed.

Sandwich ELISA assays for four inflammatory proteins were selected targeting the products of four inflammatory genes of interest, to quantify and corroborate any dysregulation seen in qPCR analysis. An illustration of the method can be seen in Figure 3.1.

The objectives of this chapter include MLST analysis of prostate *P. acnes* isolates and optimisation of short and long-term infection models, intracellular counts, soft-agar assay, qPCR assays, MTT assays and ELISA.

3.2. *Materials and Methods*

3.2.1. Bacterial culture

All bacterial strains were routinely cultured on brain heat infusion (BHI) agar, as per Section 2.2.1.

P. acnes strains 00035, ST27, NCTC737 (type IA_1), B3 (type IB), NCTC10390 (type II), CFU2 (type III), *P. avidum* and *P. granulosum* were grown to optical density at 600 nm (OD_{600}) 0.3 and counts were performed (following Section 2.2.2), as broth cultures with a known number of bacteria were needed to prepare the infection of eukaryotic cells with the appropriate inoculum to achieve the desired MOI.

Prostate isolates 00035, B2, 00060R (type IA_1), B3, 03R3900R (type IB) and CFU2 (type III) were cultured for MLST analysis. Further information about the origin of the strains can be found in Table 2.2.

3.2.2. Multiplex PCR and MLST analysis

Crude DNA extracts were prepared as outlined in Section 2.4.3.1. The phylogenetic type of the prostate isolates was analysed using the multiplex PCR typing scheme (Section 2.4.3.2). Following, reactions to be sent for sequencing were prepared as described in Section 2.4.3.1.3 and were then purified using a QIAquick PCR purification kit (Section

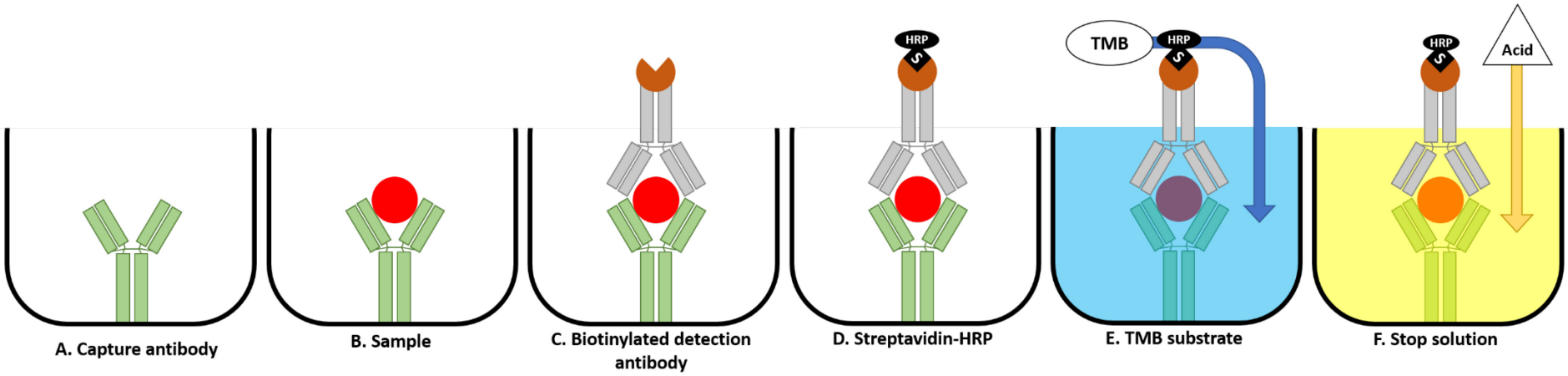

Figure 3.1. Sandwich ELISA method

In sandwich ELISA the plates are coated with a capture antibody (**A**). After a blocking step, samples are added and the target protein binds to the coating antibody. After a wash a secondary biotinylated antibody is added (**C**), binding the protein of interest in the well. Horseradish peroxidase (HRP)-labelled streptavidin is then added, forming a bond with the biotin in the detection antibody (**D**). A reaction substrate is added (3,3',5,5'-tetramethylbenzidine or TMB) which initiates the reaction and leads to the formation of a diamine, resulting in a colour change (**E**). Finally, the reaction is stopped by the addition of acid, which further oxidises the product, resulting in a yellow-coloured product which can be measured (**F**).

2.4.3.1.2) (Qiagen, Germany). The purified PCR products were quantified using Qubit® DS HS kit (Section 2.4.1.2), diluted as appropriate based on product size (5 ng/µl if < 1000 bp; 10 ng/µl if > 1000 bp) and sent for Sanger sequencing as described in section 2.4.3.1.3 (Eurofins Genomics, Ebersberg, Germany). MLST analysis was performed following Section 2.4.3.1.4.

3.2.3. Cell culture

RWPE-1, 22Rv1 and PC-3 cells were cultured as described in Section 2.1.1.

Prior to the setup of infection models, different seeding densities of the RWPE-1 cells were tested to select the optimal density, ensuring the cells remained viable for the duration of the co-culture experiments. The cells were seeded at 50,000 cells/ml, 100,000 cells/ml, 200,000 cells/ml and 300,000 cells/ml and then incubated for several days (3, 5, 7 or 14) with no media changes at 37°C in 5% CO_2 atmosphere. Viability counts were performed at each time point as described in Section 2.1.1.

Cells were infected as outlined in Section 2.3.1. Both MOI of 15:1 and 50:1 were tested, and infection models were maintained for 30 days as described in Section 2.3.3. To compare bacterial density between MOIs, bacterial counts were performed at days 10, 20 and 30.

3.2.4. Intracellular bacterial counts

Intracellular count experiments were set up in 12-well plates as described in Section 2.3.6 and incubated for 24, 48 and 72 hours to monitor the potential of *P. acnes* strains to become intracellular. At each time point, the medium was removed, the cells were washed twice with PBS and then treated with fresh complete medium supplemented with 300 µg/ml gentamycin (Gibco, Life Technologies, UK) only, a mixture of 50 units/ml penicillin and 50 µg/ml streptomycin (Gibco, Life Technologies, UK), or a combination of 400 µg/ml gentamycin, 50 units/ml penicillin and 50 µg/ml streptomycin for 3 hours to kill any extracellular bacteria. After two washes with PBS, aiming to remove of any residual antibiotics, the epithelial cells were lysed saponin (Sigma-Aldrich, UK) to a final concentration 0.5% (w/v), and bacterial counts were performed as described in Section 2.2.2. Bacterial counts were also performed after the 3-hour antibiotic incubation and prior to washes to assess whether any extracellular bacteria remained viable.

3.2.5. Soft agar assay

At day 15 of a long-term infection with the bacterial strain NCTC737, set-up as described in Section 2.3.1 and maintained as outlined in Section 2.3.3, cells were used to assess the need for antibiotic use in the preparation of soft agar assays. A modification of the commonly used methods was necessary as those protocols are targeted at cells cultured in medium readily available at 2x strength, such as RPMI-1640 (Borowicz et al., 2014). As this is not the case for keratinocyte serum-free medium (KSFM), a higher concentration of agarose was used to prevent the dilution of media, as described in Section 2.3.7. The bottom layer of the assay was prepared by mixing molten agarose (Invitrogen, Life Technologies, UK) with complete KSFM or RPMI-1640 to a final concentration 0.5% (w/v). The top layer was prepared by mixing molten agarose with a cell suspension at 7,500 cells/ml, to a final concentration 0.3% (w/v) agarose. Erythromycin (Sigma-Aldrich, UK) was added to the mixture, to a final concentration of 20 µg/ml. Wells with no antibiotic added were also prepared as controls.

The 22Rv1 cell line was used to assess whether antibiotics would influence the anchorage independent growth the cells demonstrate. The assay was prepared as described above, using RPMI-1640 with both treated and antibiotic-free wells.

The soft agar assays were incubated for 14 days at 37°C, 5% CO_2, and were kept hydrated by adding 100 µl of appropriate complete medium (KSFM or RPMI-1640) every 3 days. Nitrotetrazolium blue chloride (10 mg/ml, Sigma-Aldrich, UK) was used for staining by adding 100 µl to each well; the assays were imaged as described in Section 2.3.7.

3.2.6. RealTime Ready assays efficiency calculation

RNA extracted from the RWPE-1 cell line was used to calculate the efficiency of the RealTime ready primer-probe mixes (Roche, Switzerland). Following the protocol described in Section 2.4.2.3, cDNA was synthesised to a concentration of 50 ng/ml. A serial dilution of cDNA was prepared, and qPCR was performed as outlined in Section 2.4.2.4.1. To assess the primer-probe efficiency, a standard curve was plotted, and efficiency was calculated using the formula in Section 2.4.2.4.2.

3.2.7. Housekeeping gene selection

Housekeeping gene selection was performed as outlined in Section 2.4.2.4.3 using cDNA from a short-term infection model at time points T0, 24h, 48h and 72h. The genes were selected as they are commonly used in literature when studying gene dysregulation in prostate cancer (Ohl et al., 2005; Tsaur et al., 2013).

3.2.8. Gram staining

Gram staining to visualised bacteria was performed as described in Section 2.2.3.

3.2.9. MTT assay optimisation

HDMEC cells used for MTT assays were cultured in phenol red-free Medium 200 (Gibco, Life Technologies, UK), supplemented with low growth serum supplements (LSGS) (Gibco, Life Technologies, UK) as outlined in Section 2.1.1.

3.2.9.1. Infection models

Infection models using the RWPE-1 cell line (cultured in KSFM, supplemented with epidermal growth factor (EGF) and bovine pituitary extract, as described in Section 2.1.1), and a range of *P. acnes* strains were set up as outlined in Section 2.3.1. The chronic infections used for the optimisation of MTT assays in this chapter were sustained for 30 days.

The prostate cancer cell line PC-3 was cultured in RPMI-1640, supplemented with 10% foetal bovine serum (FBS), as seen in Section 2.1.1.

3.2.9.2. Conditioned medium processing

Medium from chronic infections was removed and three 1 ml aliquots were prepared, as outlined in Section 2.3.4. For experiments aimed at optimising the seeding density for the HDMEC cells, medium from the PC-3 cell line was used. For the remaining MTT assay-related optimization experiments, pooled conditioned medium from multiple chronic infections was used, as large volumes of medium were needed to provide consistency between testing conditions.

3.2.9.3. MTT assays

The HDMEC cells were detached using 0.25% trypsin-EDTA (Gibco, Life Technologies, UK), as described in Section 2.1.1, and were then counted using trypan blue (Sigma Aldrich, UK), following Section 2.1.1. The cells were initially seeded at a range of

densities (8 x 10^4, 5 x 10^4, 3 x 10^4, 2 x 10^4 and 1 x 10^4 cells/ml) to select the optimal seeding density to be used in following experiments.

Additionally, etoposide (Cayman Chemical Company, USA) concentrations of 2.5, 3.5 and 5 µM and 0.05% (w/v) saponin (Sigma-Aldrich, UK) were tested as negative controls, and cells grown in medium with 20% (v/v) FBS (Gibco, Life Technologies, UK) or in the presence of 25 ng/ml, 50 ng/ml or 100 ng/ml epidermal growth factor (EGF, Life Technologies, UK) were examined as potential positive proliferation controls.

Following incubation, the cells were treated with MTT (Sigma-Aldrich, UK) to a final concentration 1.2 mM, as described in Section 2.3.10, and incubated for 3 hours. The resulting formazan crystals were solubilised with the addition of 100 µl DMSO (Sigma-Aldrich, UK). After mixing, the absorbance was measured at 570 nm (Epoch, BioTek Instruments, USA).

3.2.9.4. Bacterial culture and MTT assay

A BHI broth was inoculated with *Staphylococcus epidermidis* (ATCC® 14990) and incubated at 37°C with mild agitation until the culture was turbid. A 1:10 serial dilution was performed and 100 µl of the neat sample and each dilution were added to a 96-well plate. Each well was then treated with MTT (Sigma-Aldrich, UK) to a final concentration of 1.2 mM MTT. The plate was incubated for an hour. Following, the produced formazan salt was solubilized with the addition of 100 µl DMSO (Sigma-Aldrich, UK) to each well. The plate was mixed briefly, and the absorbance was measured at 570 nm. (Epoch, BioTek Instruments, USA),

3.2.9.5. Statistical analysis

Statistical analysis was performed using a 2-tailed Student's t-test, comparing the different treatments to untreated controls.

3.2.10. ELISA

Sandwich ELISA assays were performed as outlined in Section 2.5.2 with the capture and detection antibodies described in Table 3.1. Additionally, for troubleshooting, available components from a Human IL-1 alpha/IL-1F2 ELISA (R&D Systems, US), using the buffers recommended by R&D with blocking buffer and reagent diluent being 1% (w/v) BSA in PBS, wash buffer consisting of 0.05% (v/v) Tween-20 in PBS, stop solution 2N H_2SO_4 and

antibody and streptavidin-HRP conjugate (S-HRP) dilutions as described in Table 3.2. Incubation times recommended did not differ between the two kits.

3.3. *Results*

3.3.1. Phylogenetic typing of prostate isolates

The multiplex PCR typing scheme was used to identify the phylogenetic type of all available prostate isolates. Figure 3.2.A shows the patterns observed, which correspond to type IA_1 for strains 00035, 00060R and B2; IB for strains B3 and 03R3900R; type II for CFU2. For each strain, eight MLST-PCR reactions were set up and the product size was checked as seen in Figure 3.2.B. The PCR products were then purified and sent for Sanger sequencing. The results from the sequencing were presented as chromatograms, an example of which can be found in Figure 3.2.C.

The six prostate isolates investigated showed 5 different allelic profiles, with the two type IB strains (B3 and 03R3900R) sharing the same alleles and thus sequence type (ST5). The type III strain CFU2 had an allelic profile matching ST33. The three type IA_1 strains belonged to three different sequence types, namely 00035 was ST122, 00060R was ST8 and B2 was ST1. The complete allelic profiles, sequence types and clonal complexes can be found in Table 3.3. A population snapshot of all *P. acnes* isolates available to date can be seen in Figure 3.3.

3.3.2. Strain selection for infection models

For the setup of acute and chronic infections, prostate isolates 00035, B3 and CFU2, representing distinct phylotypes were selected (types IA_1, IB and III, respectively). Due to the unavailability of a clinical prostate type II isolate (as type II is also commonly isolated from the prostate) reference strain NCTC10390 was used (Mak et al., 2013b). NCTC737, one of the most extensively studied *P. acnes* isolates, was used as a control. Additionally, strain ST27, named after the sequence type it belongs to according to the "Aarhus" $MLST_9$ scheme was also used as a control, as strains belonging to ST27 have been suggested as "skin health-associated" strains (Lomholt and Kilian, 2010). Finally, other *Propionibacteria* spp., *P. granulosum* and *P. avidum* were used due to their close relationship with *P. acnes* and the fact they have both also been isolated from the prostate (Mak et al., 2013b).

Table 3.1. Peprotech ELISA component concentrations

	Capture antibody	Concentration	Detection antibody	Concentration	Standard range	S-HRP
IL-1β ELISA	Mouse anti-human IL-1β	0.25 µg/ml	Biotinylated goat anti-human IL-1β	0.25 µg/ml	6 – 750 pg/ml	0.1 µg/ml
IL-6 ELISA	Rabbit anti-human IL-6	0.5 µg/ml	Biotinylated rabbit anti-human IL-6	0.1 µg/ml	8 – 2000 pg/ml	0.05 µg/ml
IL-8 ELISA	Rabbit anti-human IL-8	0.125 µg/ml	Biotinylated rabbit anti-human IL-8	0.25 µg/ml	1 – 150 pg/ml	0.05 µg/ml
TNF-α ELISA	Mouse anti-human TNF-α	1 µg/ml	Biotinylated rabbit anti-human TNF-α	0.05 µg/ml	16 – 2000 pg/ml	0.05 µg/ml

Table 3.2. R&D Systems IL-1β ELISA kit component concentration

	Capture antibody	Concentration	Detection antibody	Concentration	Standard range	S-HRP
IL-1β ELISA	Mouse anti-Human IL-1β	4 µg/ml	Biotinylated goat anti-human IL-1β	0.2 µg/ml	4 – 250 pg/ml	1:40 dilution

Table 3.3. MLST sequencing allelic profiles and ST results

Strain	Multiplex Phylotype	Allelic profile								ST	Clonal Complex
		aroE	*atpD*	*gmk*	*guaA*	*lepA*	*sodA*	*tly*	*camp2*		
00035	IA_1	1	1	1	3	1	13	1	1	122	CC1
00060R	IA_1	1	1	1	3	1	1	3	1	8	CC1
B2	IA_1	1	1	1	3	1	1	1	1	1	CC1
B3	IB	1	1	1	4	1	4	8	6	5	CC5
03R3900R	IB	1	1	1	4	1	4	8	6	5	CC5
CFU2	III	7	6	3	7	5	9	13	16	33	CC77

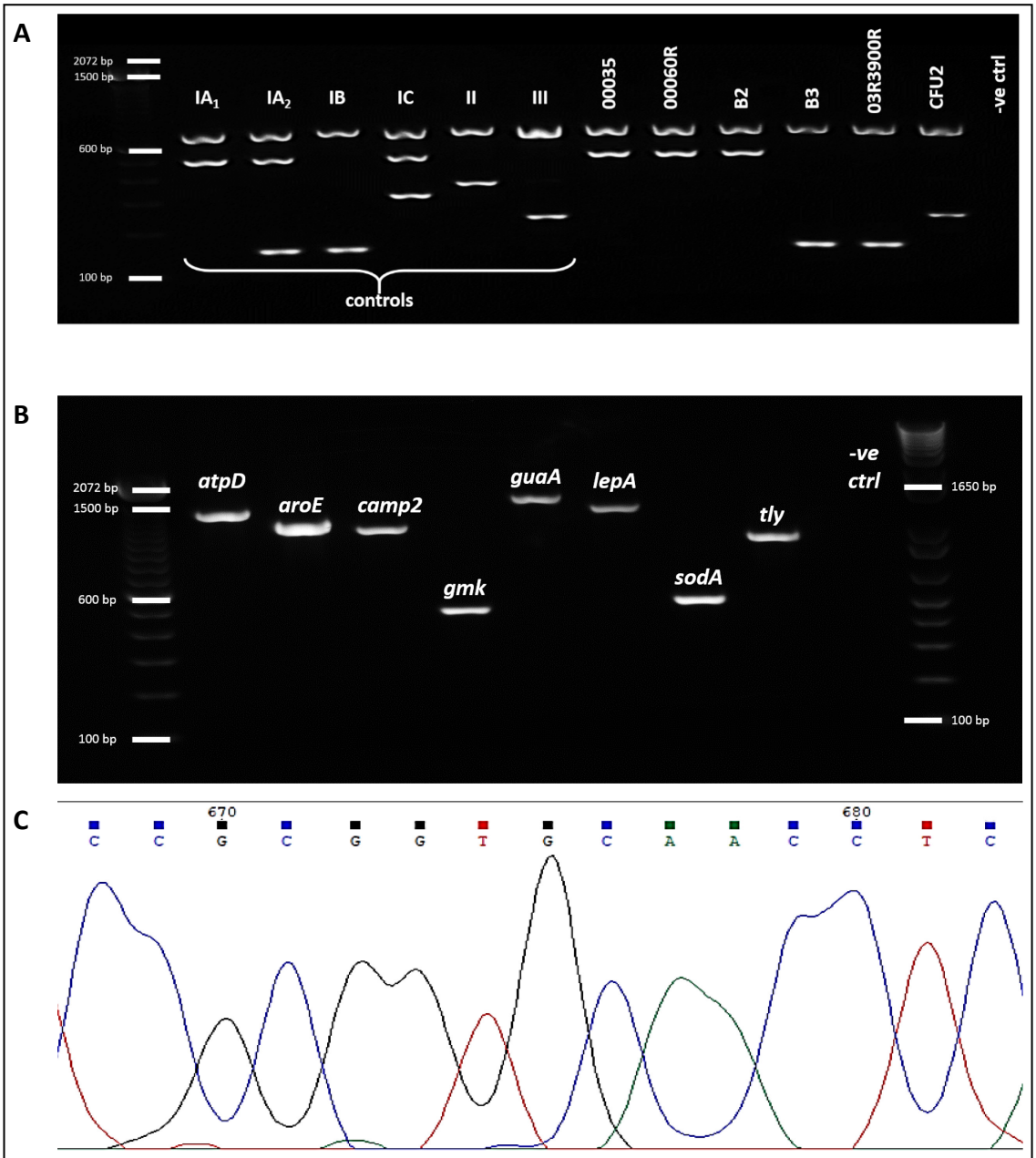

Figure 3.2. Phylogenetic typing of P. acnes strains.

A. Multiplex PCR results on a 1.5% (w/v) gel stained with GelRed. Strains of known phylogenetic type were used as positive controls, and a sample with no DNA was used as a negative control. The samples were assessed by comparing their band pattern with the controls. A 100 bp ladder (TrackIt™ 100 bp ladder, Invitorgen, UK) was used to assess band sizes.

B. MSLT analysis of strain B3. The band size and integrity for the 8 MLST genes were analysed in a 1% (w/v) agarose gel stained with GelRed. TrackIt™ 100 bp (left) and 1kb (right) ladders were used to assess band size (Invitrogen, UK) and a reaction with all primers but no DNA was used as a negative control.

C. A sample of the chromatogram read for sample B3, forward read of the *aroE* gene, between bases 668 and 682. Image captured using Chromas (Technelysium Pty Ltd, Australia).

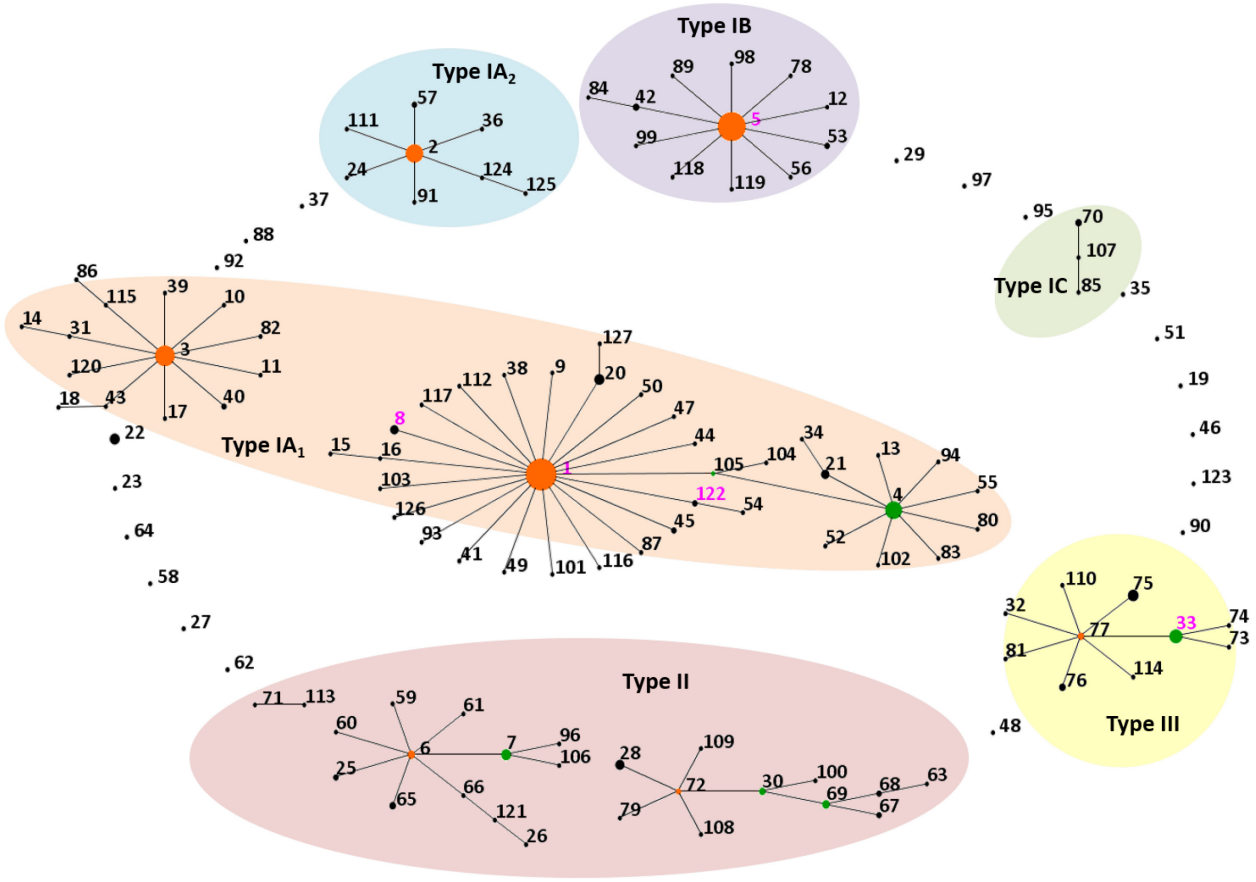

Figure 3.3. eBURST population snapshot of P. acnes

The current MLST database, containing 392 strains identified using the "Belfast" $MLST_9$ scheme described by McDowell et al. (2013), has a total of 9 clonal complexes (CC; within each CC the strains match 7 out of the 8 genes investigated) and 19 singletons. The frequency of each type is indicated by the size of the mark. The founding genotype of each CC is coloured in orange, and sub-founders are in green. The STs of prostate isolates analysed in this chapter are marked in magenta. Background colours were used to highlight the different phylogenetic types.

NB: Spacing between singletons and CCs does not signify the genetic difference between them.

3.3.3. Bacterial counts

In order to infect the eukaryotic cell line RWPE-1 with bacteria, broth cultures at known concentrations were needed. To determine the number of CFU/ml *P. acnes* strains and related *Propionibacterium* spp. were grown to OD_{600} 0.3 and bacterial counts were performed, with the results shown in Table 3.4.

For infection experiments, fresh broth cultures were prepared and incubated at 37°C for 16-20 hours anaerobically with mild agitation. As the bacterial concentration at OD_{600} 0.3 was known, broths were diluted to this optical density and the counts in Table 3.4 were used to calculate the amount of broth needed to inoculate the eukaryotic cells at the desired MOI.

3.3.4. Optimal seeding density

The optimal seeding density was determined by comparing the cell count and percentage viability of four different seeding densities over a period of two weeks with no media changes or passages of the cells. This was done to assess how long can the cells be left with no interference before a decrease in cell numbers and viability, as in infection models any media changes or passages would affect the MOI. Figure 3.4 shows the number of viable cells/ml and the overall cell viability determined using trypan blue exclusion test for cell viability.

The cells were seeded at 50,000, 100,000, 200,000 and 300,000 cells/ml. By day 3, all seeding densities had demonstrated increased cell numbers, with the cells seeded at 200,000 and 300,000 cells/ml reaching their peak numbers for the whole experiment and beginning to drop at the following time points. By day 5, the cells seeded at 100,000 cells/ml demonstrated the highest numbers. At day 7, the cells seeded at 300,000 cells/ml showed reduced numbers of cells, while the remaining seeding densities showed similar numbers of cells. By day 14, most of the cells in all experiments were no longer viable.

The viability of the cells in all experiments remained above 90% for the first 3 days. By day 5, the viability had started to decrease, with the cells seeded at 200,000 and 300,000 cells/ml showing viability of below 90% and below 80%, respectively, while the cells

Table 3.4. P. acnes strains counts at OD_{600} 0.3.

Strain	Phylotype	Counts at OD_{600} 0.3
ST27	IA_1	7.0×10^7 CFU/ml
NCTC 737		2.2×10^7 CFU/ml
00035		6.8×10^7 CFU/ml
B3	IB	1.4×10^8 CFU/ml
NCTC10390	II	1.7×10^8 CFU/ml
CFU2	III	6.0×10^7 CFU/ml
P. granulosum	-	1.2×10^8 CFU/ml
P. avidum	-	4.8×10^7 CFU/ml

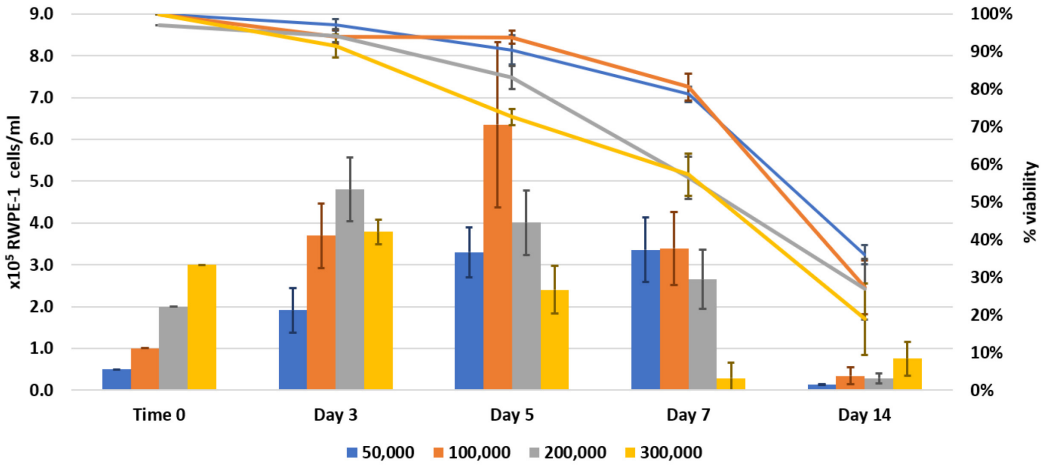

Figure 3.4. Optimisation of seeding density for infection models.
The RWPE-1 cell line was seeded (Time 0) at 50,000 (blue), 100,000 (orange), 200,000 (grey) and 300,000 (yellow) cells/ml and the cells were left undisturbed, with no media changes for up to 3, 5, 7 or 14 days. Trypan blue viability counts were performed at each time point. The number of viable cells (bars) and percentage viability (lines) are shown for each seeding density and time point. Each experiment had a minimum of three biological replicates and the data is presented as mean viable cells/ml (bars) and mean percentage viable cells (lines), +/- standard error. The bars at Time 0 represent the seeding density.

seeded at 100,000 and 200,000 remained above 90%. At day 7, cells seeded at the two lower denstities had viability of 80%, while the higher densities had about 60% viability. By day 14, the vibility values for all experiments were below 40%.

3.3.5. Multiplicity of infection

The bacterial counts were compared between MOI 15:1 and 50:1 with two different strains, NCTC737 and 00035. The counts, performed every ten days of the chronic infection model, showed that there was no statistically significant difference between the bacterial counts in the two MOIs at different time points (NCTC737: day 10, $p = 0.71$; day 20, $p = 0.49$; day 30, $p = 0.09$; 00035: day 10, $p = 0.17$; day 20, $p = 0.92$; day 30, $p = 0.58$) despite the inoculum being higher for the 50:1 replicates at the beginning of the experiments (Figure 3.5).

3.3.6. Intracellular bacterial counts

Different antibiotic concentrations were tested to establish the best way for intracellular count experiments to be conducted. However, in all combinations tested, viable bacteria remained in the negative controls. The antibiotic concentration which showed the lowest numbers of extracellular bacteria was 400 μg/ml gentamycin, 50 units/ml penicillin and 50 mg/ml streptomycin, following three-hour incubation. As a result of bacteria remaining viable despite the prolonged treatment with a mixture of antibiotics, for accurate assessment of the intracellular bacteria, the number of bacteria seen in the negative controls was subtracted from the intracellular counts. The number of extracellular bacteria remaining after this treatment can be seen in Table 3.5.

3.3.7. Antibiotics prevent the formation of bacterial colonies in soft agar

A soft agar assay was set-up following a 15-day infection of RWPE-1 cells with strain NCTC737 (type IA_1), aiming to assess the importance of the addition of antibiotics to the top layer of the assay. After 14-day incubation, the soft agar assay with no antibiotic added showed the formation of more than 30 colonies, while the assays with antibiotic had no visible colonies ($p = 0.0009$, Figure 3.6). A sample from a colony was taken and Gram-stained to reveal purple pleomorphic bacteria were forming the colonies (Figure 3.6.D).

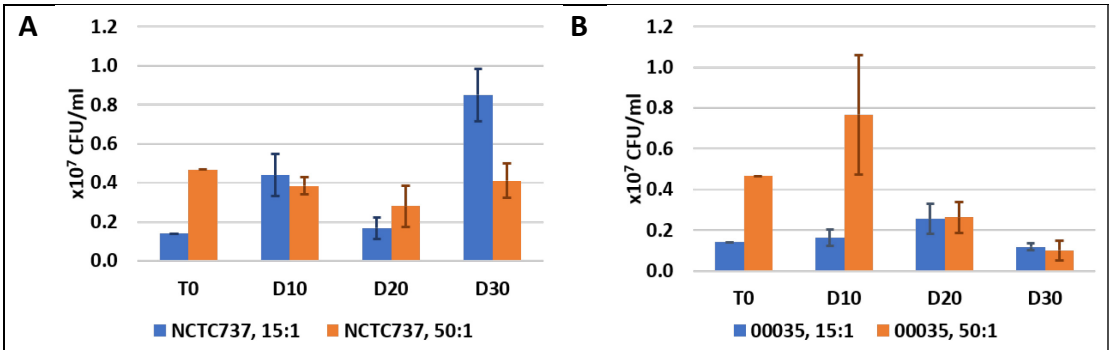

Figure 3.5. Comparison between MOI 15:1 and 50:1

Bacteria in the medium (in CFU/ml) at T0, D10, D20 and D30 in long term infection models infected with different MOI – 15:1 (blue), 50:1 (orange).

A. RWPE-1 cells infected with NCTC737. D10, p = 0.71; D20, p = 0.49; D30, p = 0.09

B. RWPE-1 cells infected with 00035. D10, p = 0.17; D20, p = 0.92; D30, p = 0.58

Data presented as mean of three biological replicated in CFU/ml +/- standard error

Table 3.5. Extracellular P. acnes counts following 3-hour antibiotic incubation

Strain	24h (CFU/ml)	48h (CFU/ml)	72 h (CFU/ml)
ST27	1,600	325	75
NCTC 737	1,600	475	325
00035	500	1,600	1,550
B3	225	150	200
NCTC 10390	275	100	-
CFU2	-	-	-
P. granulosum	75	200	75

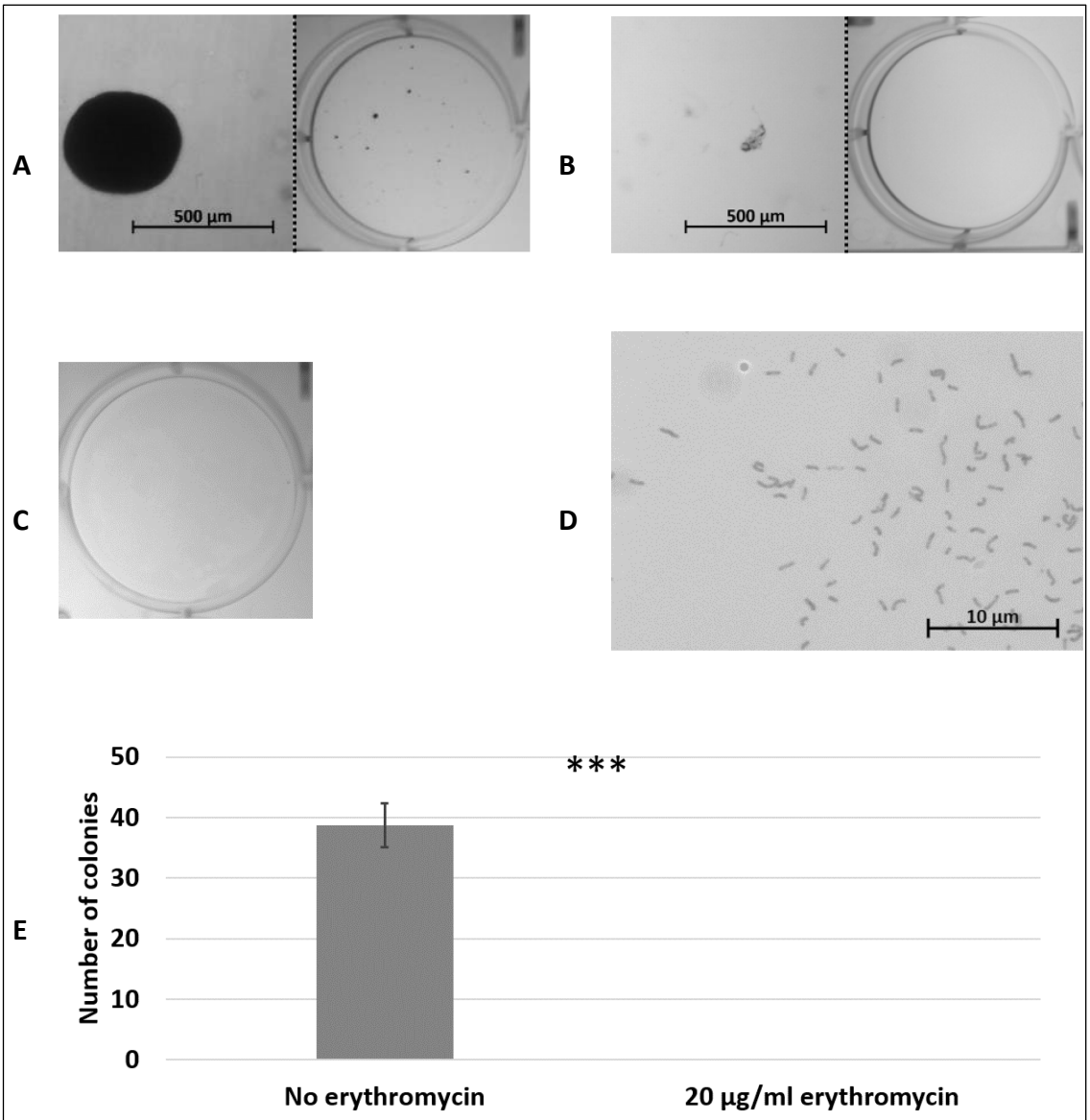

Figure 3.6. Soft agar assay optimisation with cells infected for 15 days with NCTC737 Soft agar colonies in assay with no erythromycin (**A**) and with 20 µg/ml erythromycin added (**B**), as seen under 2x magnification (left) and with no magnification (right) Soft agar colonies. **C.** No infection control with no magnification. **D.** Gram stain of colony from infected RWPE-1 cells not treated with erythromycin, 100x magnification. **E.** Summary of results, bars represent mean number of colonies between three replicates, +/- standard error; p = 0.0009.

3.3.8. Antibiotics decrease 22Rv1 cell line's ability to form colonies on soft agar

After 14 days incubation, the soft agar assay set up using the cancer cell line 22Rv1, treated with erythromycin and control wells, were assessed for colony formation. The control wells showed on average 333 colonies had formed, while the number of colonies in the treated wells averaged 181, showing a significant decrease in the anchorage-independent growth of the cells in the presence of erythromycin ($p = 0.0006$). Additionally, the colonies formed in the treated cells were of a noticeably smaller size (Figure 3.7).

3.3.9. Efficiency calculations

The efficiencies of all RealTime ready primer-probe mixes were assessed. The standard curves for the different groups of genes can be found in Figure 3.8 for housekeeping genes, Figure 3.9 for inflammatory genes and Figure 3.10 for epithelial-mesenchymal transition genes. The percentage efficiency (E) for each assay is calculated using the formula below, and a list of all efficiencies can be found in Table 3.6.

$$\mathrm{E} = \left(10^{-1/m} - 1\right) \times 100$$

All efficiencies calculated were within expected 100 +/- 10% range.

3.3.10. HPRT is the most stable housekeeping gene.

To perform the selection of the most stable housekeeping gene for use in future experiments, the investigated samples were separated into two groups based on infection status and tested with four possible housekeeping genes: *ACTB*, *GAPDH*, *HPRT*, and *TBP.*

When using the mean values of the two groups, the statistical package, based on a mathematical model estimating the variation of expression, returned *HPRT1* as the best housekeeping gene with a stability value of 0.167 (based on intergroup variation), compared to 0.550, 0.379 and 0.208 for *ACTB*, *GAPDH* and *TBP*, respectively (Figure 3.11). Intragroup variation was also assessed showing the difference within the non-infected (group 1) and infected (group 2) groups as follows: *ACTB*: 0.205 (group 1) and 5.355 (group 2), *GAPDH*: 0.680 (group 1) and 1.801 (group 2), *HPRT1*: 0.015 (group 1) and 0.181 (group 2), *TBP*: 0.383 (group 1) and 0.137 (group 2).

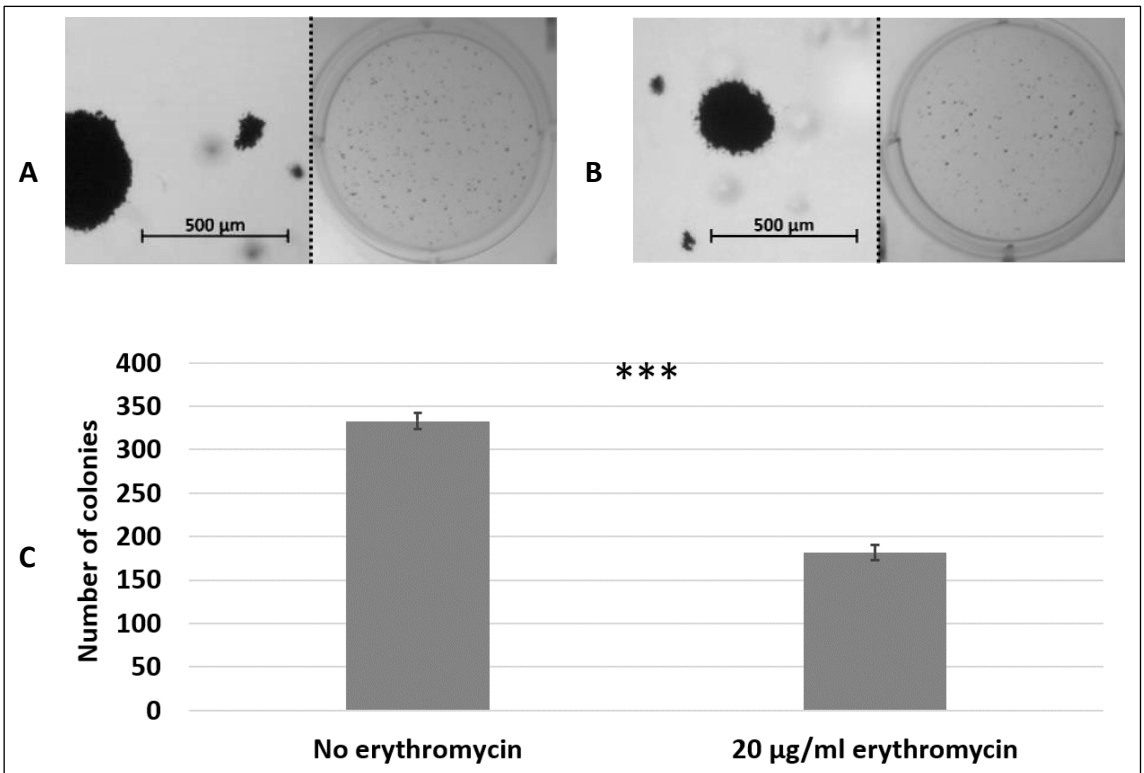

Figure 3.7. Soft agar assay optimisation with 22Rv1 cell line
Colonies in soft agar assay, with no erythromycin (**A**) and with 20 µg/ml erythromycin added (**B**), as seen under 2x magnification (left) and with no magnification (right).
C. Difference of the number of colonies seen between antibiotic-free and antibiotic-treated wells; bars represent the mean number of colonies between three replicates, +/ standard error; p = 0.0006

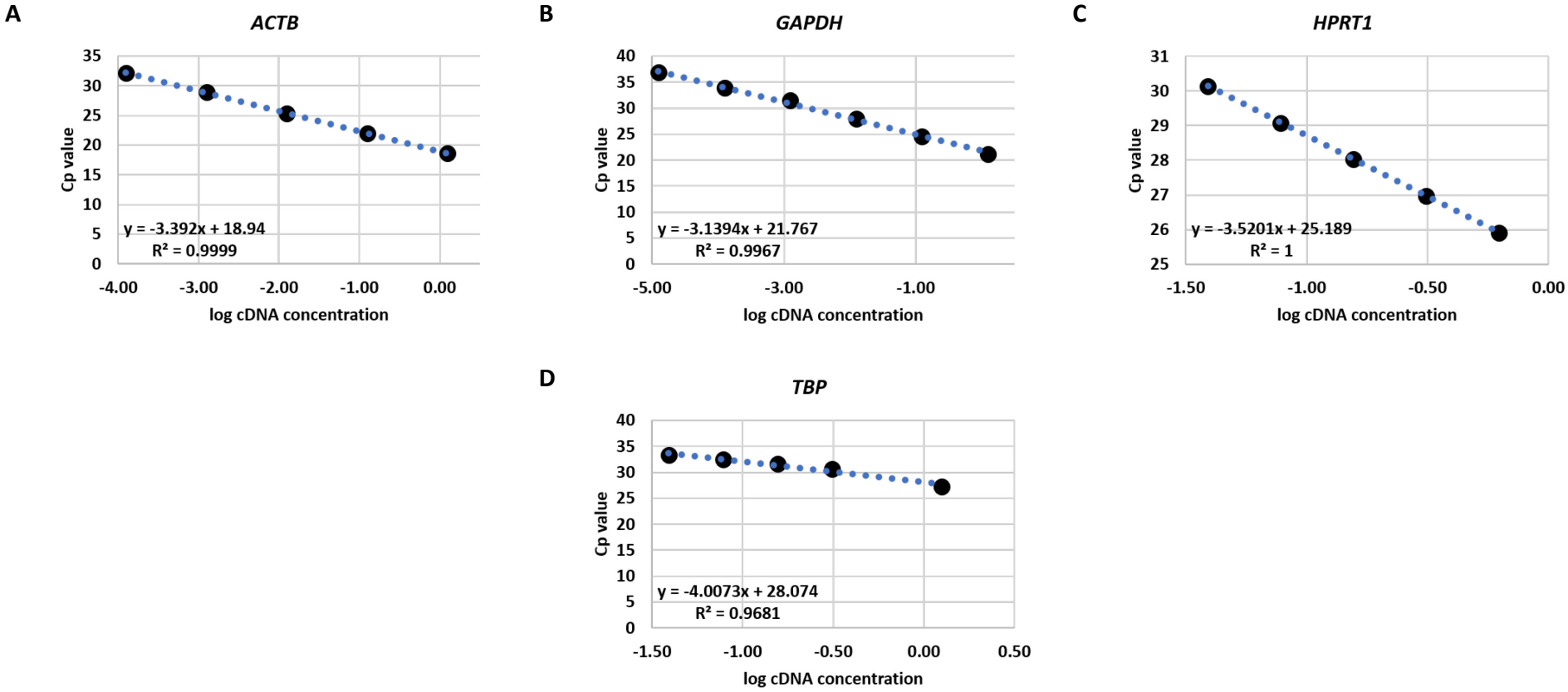

Figure 3.8. Standard curves for housekeeping genes

ACTB (**A**), *GAPDH* (**B**), *HPRT1* (**C**) and *TBP* (**D**). The data is presented as C_p value vs. $\log_{10}$ cDNA concentration were plotted and the slope value of each curve was used to calculate the probe efficiency. cDNA from untreated RWPE-1 cells was used to prepare serial dilutions and to produce the standard curves.

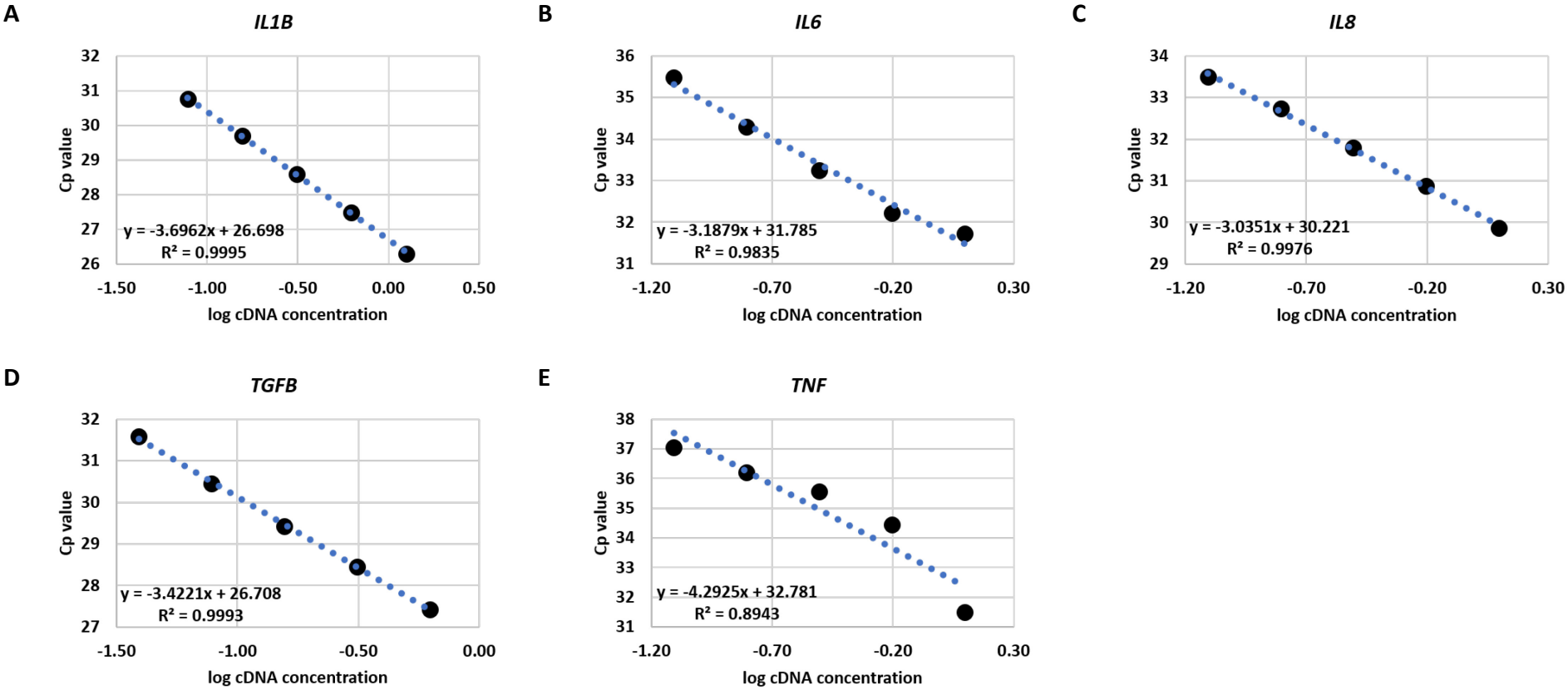

Figure 3.9. Standard curves for inflammatory genes

IL1B (**A**), *IL6* (**B**), *IL8* (**C**) *TGFB* (**D**)and *TNF* (**E**). The data is presented as C_p value vs. $\log_{10}$ cDNA concentration were plotted and the slope value of each curve was used to calculate the probe efficiency. cDNA from untreated RWPE-1 cells was used to prepare serial dilutions and to produce the standard curves.

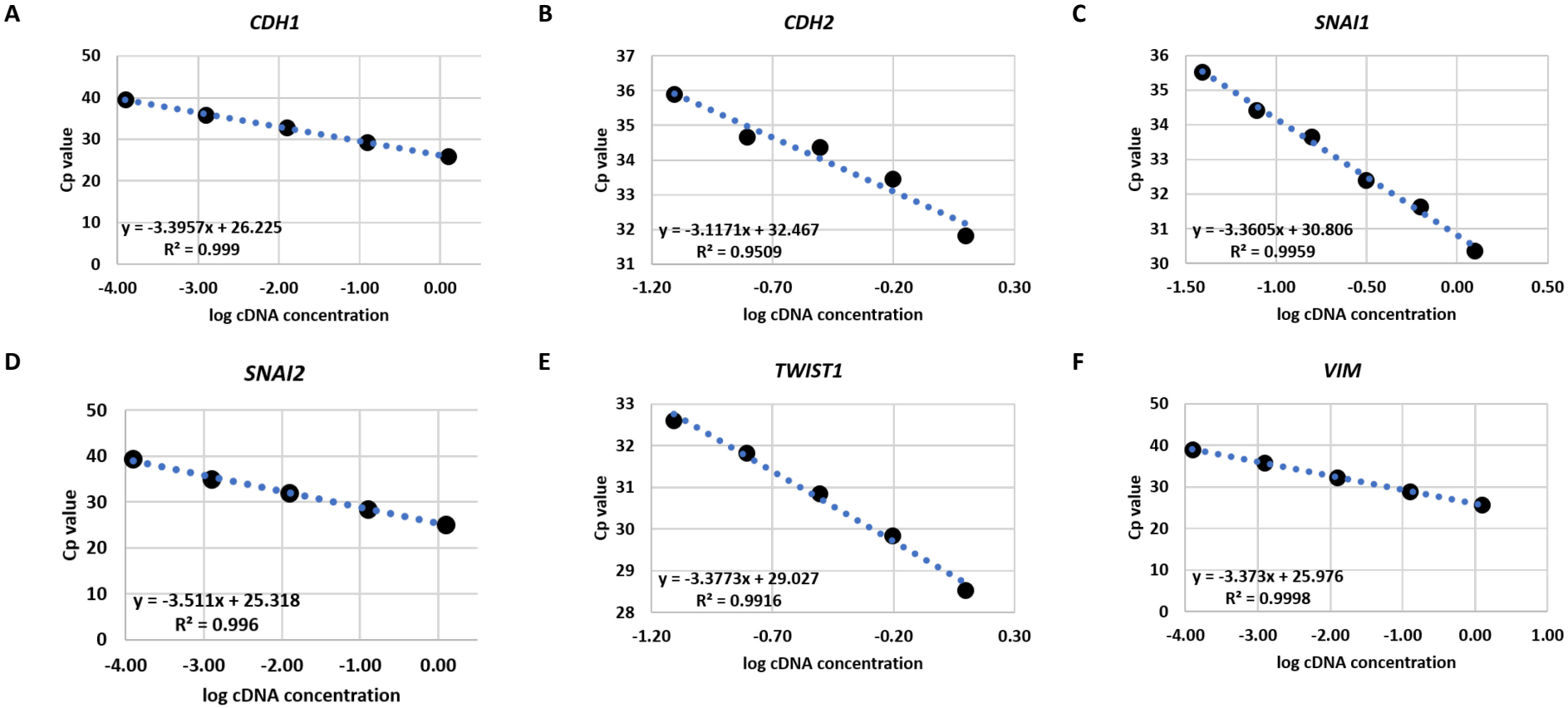

Figure 3.10. Standard curves for EMT genes

CDH1 (**A**), *CDH2* (**B**), *SNAI1* (**C**), *SNAI2* (**D**), *TWIST1* (**E**) and *VIM* (**F**). The data is presented as C_p value vs. $\log_{10}$ cDNA concentration were plotted and the slope value of each curve was used to calculate the probe efficiency. cDNA from untreated RWPE-1 cells was used to prepare serial dilutions and to produce the standard curves.

Table 3.6. Summary of probe efficiencies

Function	*Gene*	*Full name*	*Efficiency*
Housekeeping genes	*ACTB*	Beta-actin	97.2%
	GAPDH	Glyceraldehyde 3-phosphate dehydrogenase	103.8%
	HPRT1	Hypoxanthine-guanine phosphoribosyltransferase	92.3%
	TBP	TATA-binding protein	97.5%
Inflammatory genes	*IL1B*	Interleukin-1 beta	90.7%
	IL6	Interleukin-6	105.9%
	IL8	Interleukin-8	106.5%
	TGFB	Transforming growth factor beta	96.0%
	TNF	Tumour necrosis factor	101.2%
EMT genes	*CDH1*	E-cadherin	97.0%
	CDH2	N-cadherin	109.3%
	SNAI1	Snail family zing finger 1 (Snail)	98.4%
	SNAI2	Snail family zing finger 2 (Slug)	92.7%
	TWIST1	Twist-related protein 1	97.7%
	VIM	Vimentin	97.9%

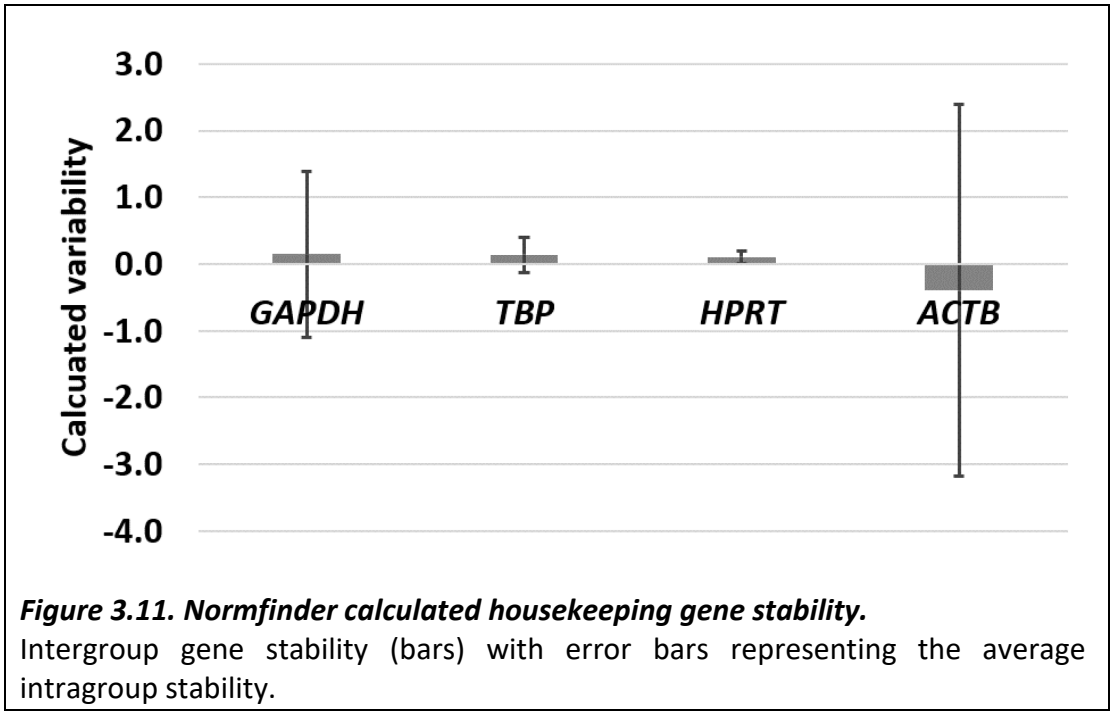

Figure 3.11. Normfinder calculated housekeeping gene stability.
Intergroup gene stability (bars) with error bars representing the average intragroup stability.

The best combination of genes suggested by the package was HPRT and TBP with a stability value of 0.173.

3.3.11. Bacteria can produce formazan from MTT

The MTT assay was used on a bacterial culture to confirm that bacteria can produce formazan from MTT. As seen in Figure 3.12, the absorbance reading decreased as the culture was diluted, with a mean absorbance reading at 570 nm of 1.5 for the neat bacterial broth, 0.6 for the 1:10 dilution and 0.1 for the 1:100 dilution. The sterile broth control had a reading of 0.06.

3.3.12. MTT assay seeding density optimisation

An initial experiment was set up with supernatant from the PC-3 cell lines. A serial dilution was performed, the cells were incubated overnight, and an MTT assay was used to assess the proliferation of the HDMEC cell line at different seeding densities.

The results showed that the amount of formazan produced following incubation with MTT was directly proportional to the seeding density, with the absorbance reading increasing with the number of cells (Figure 3.13). In all seeding densities tested, there was a significant decrease compared to untreated controls in the absorbance reading of cells treated with undiluted conditioned medium ($p < 0.001$ for cells seeded at 10,000 and 20,000 cells/ml; $p < 0.01$ for cells seeded at 30,000, 50,000 and 80,000 cells/ml).

Only the cells seeded at 20,000 cells/ml showed significant differences in absorbance in the dilution series compared to the untreated controls. A significant decrease ($p < 0.01$), was seen in the 1:5 dilution, and $p < 0.05$ in the 1:10, 1:50, 1:1,000 and 1:10,000 dilutions.

Based on these results, 50,000 cells/ml was selected as the seeding density to be used in further experiments.

3.3.13. MTT assay control selection

A range of controls were tested to select the optimal combination of positive and negative control for use in experiments. Incubation times of 24 and 72 hours were tested, with the data for 72-hour incubation seen in Figure 3.14.

As controls which increase the proliferation rate of the HDMEC cells line (positive controls) a range of EGF concentrations (25 ng/ml, 50 ng/ml and 100 ng/ml) and

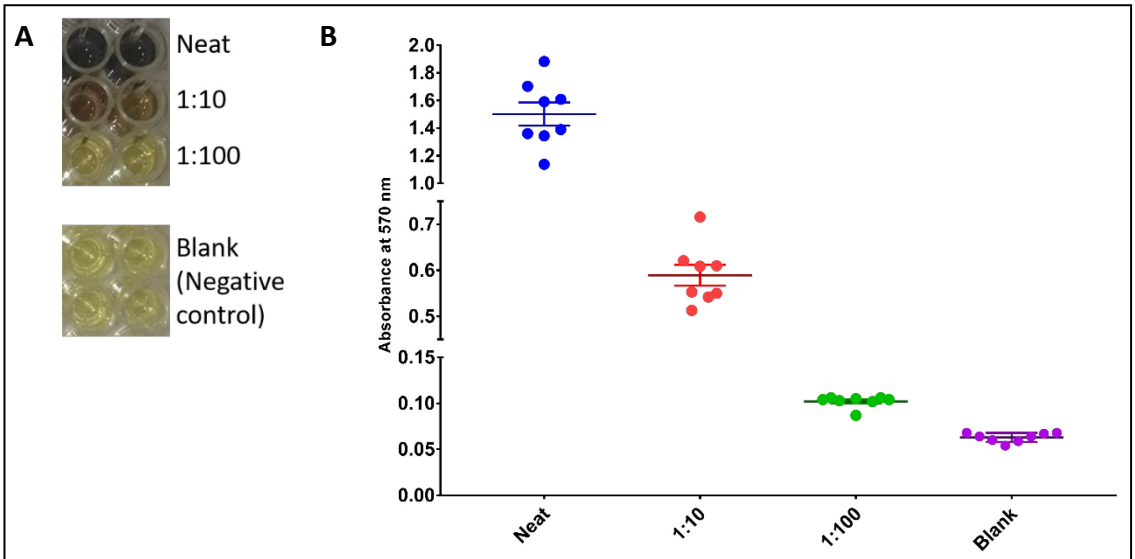

Figure 3.12. MTT assay used on bacterial culture

A. Image of *S. epidermidis* MTT assay with no magnification.

B. Absorbance measured at 570 nm. Data presented as mean of eight replicates +/- standard error; neat broth culture (blue), 1:10 dilution (red); 1:100 dilution (green), untreated BHI broth (purple).

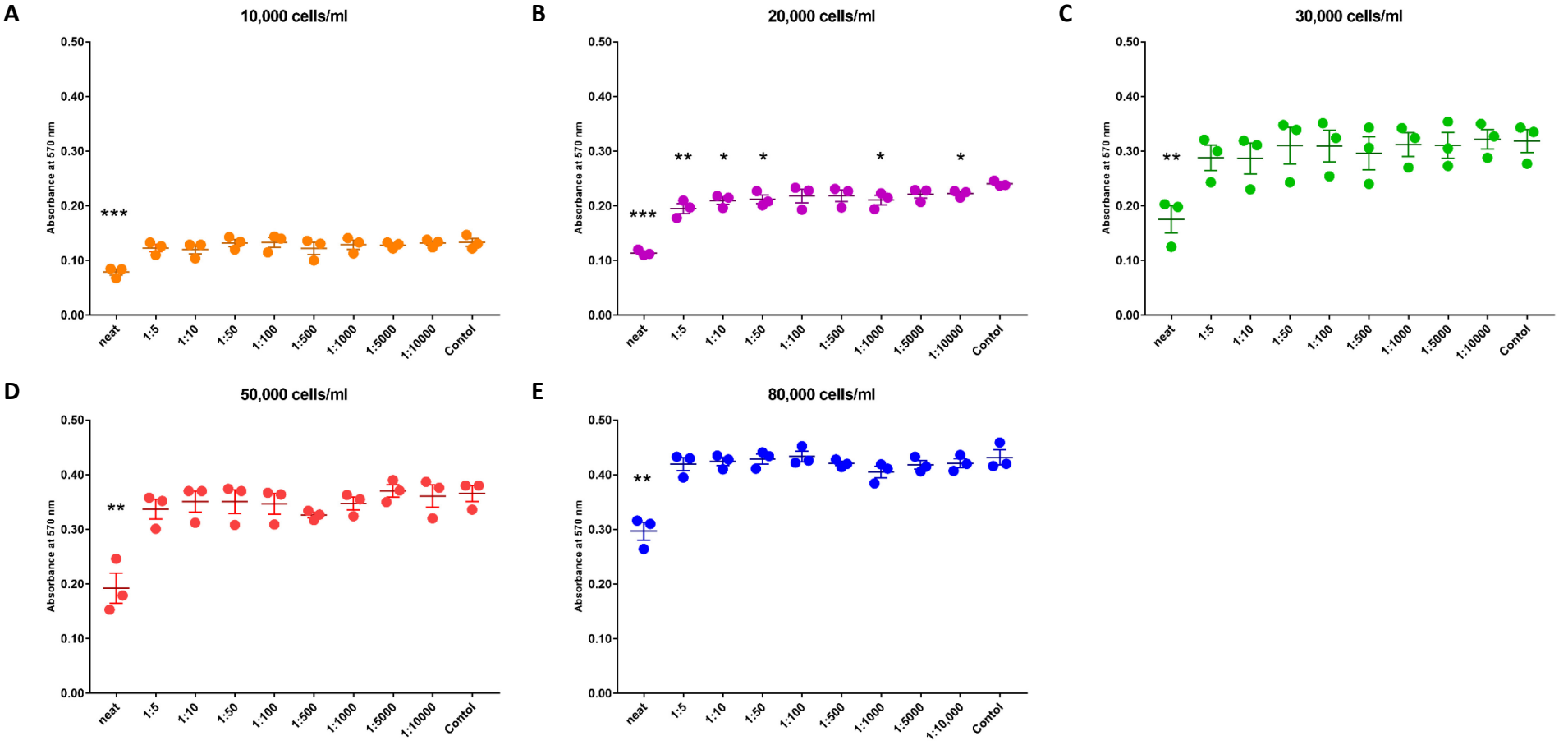

Figure 3.13. Seeding density optimisation

MTT assay (absorbance measured at 570 nm) assessing the effect of medium from the PC-3 on the HDMEC cell line, aiming to compare the differences in seeding density. Cells seeded at: **A.** 10,000 cells/ml; **B.** 20,000 cells/ml; **C.** 30,000 cells/ml; **D.** 50,000 cells/ml; **E.** 80,000 cells/ml. Data presented as mean of three replicates +/- standard error. Significance was calculated comparing to untreated control for each experiment, using a 2-tailed Student's t-test (* $p < 0.05$; ** $p < 0.01$; *** $p < 0.001$).

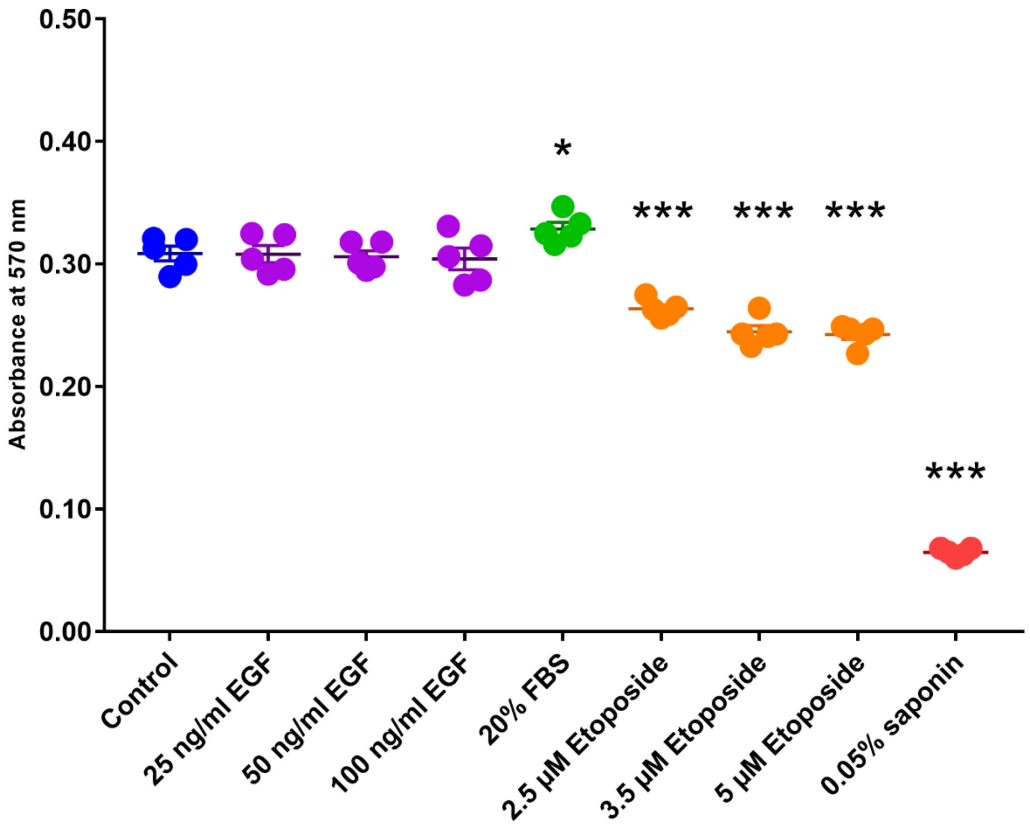

Figure 3.14. Selection of controls

Different positive controls (aiming increased proliferation rate) and negative controls (aiming decreased proliferation rate) were tested on the HDMEC cells. Untreated controls (blue) were used as comparison to calculate significance of the observed changes following a 72-hour incubation. Three concentrations of EGF (purple, 25 ng/ml, 50 ng/ml and 100 ng/ml) and complete Medium 200 + 20% FBS (green, $p = 0.037$) were investigated as potential positive controls. Three concentrations of etoposide (orange, 2.5 µM ($p = 0.0002$), 3.5 µM ($p < 0.0001$) and 5 µM ($p < 0.0001$)) and 0.05% (w/v) saponin (red, $p < 0.0001$) were possible choices for negative controls. Data is presented as mean of five replicates +/- standard error. Significance was calculated using a 2-tailed Student's t-test comparing each treatment to the untreated control.

complete Medium 200 with 18% (v/v) FBS (to a final FBS concentration of 20%) were trialled; concentrations of etoposide (2.5 µM, 3.5 µM, 5 µM) and 0.05% (w/v) saponin were tested as negative controls (controls which decrease proliferation of the HDMEC cells).

The only positive control that led to significant increase in MTT assay absorbance reading was complete Medium 200 with 20% FBS ($p < 0.05$). The EGF concentrations tested showed no significant difference in absorbance readings compared to the untreated control and showed no dose-dependent response.

All the potential negative controls tested showed significant decrease in absorbance readings ($p < 0.001$). A dose-dependent response was seen with etoposide treatment, with the optical density reading decreasing with increase of the drug concentration. Saponin treatment resulted in readings close to those of wells with just medium and no cells.

Based on these findings, 2.5 µM etoposide and Medium 200 + 20% FBS were selected as a negative and positive control, respectively.

3.3.14. MTT assay incubation time optimisation

To select the optimal incubation duration for the experiments, the HDMEC cells were seeded at 50,000 cells/ml and incubated in the presence of a serial dilution of pooled conditioned medium from chronic infections for 24, 48 and 72 hours. After each incubation an MTT assay was performed, and the results can be seen in Figure 3.15**.**

In all experiments a significant decrease ($p < 0.001$) in the absorbance reading was seen in all cells treated with undiluted conditioned medium. At 24 hours, a significant decrease in the absorbance readings compared to the untreated controls was observed in six of the dilutions tested, in addition to the decrease in the neat samples. A trendline showing an increase in absorbance as the dilution factor increased, was observed. In contrast, at 48 and 72 hours the change seen was an increase in the reading (four concentrations lead to significant increase at 48 hours and six at 72 hours). Additionally, when comparing the three timepoints, significant differences were seen in five of the concentrations tested between the 24-hour time points and both 48 and 72 hours (neat, 1:50, 1:100 (all $p < 0.001$) and 1:200 ($p < 0.05$) in both 48 and 72 hours, 1:500 ($p = 0.0076$)

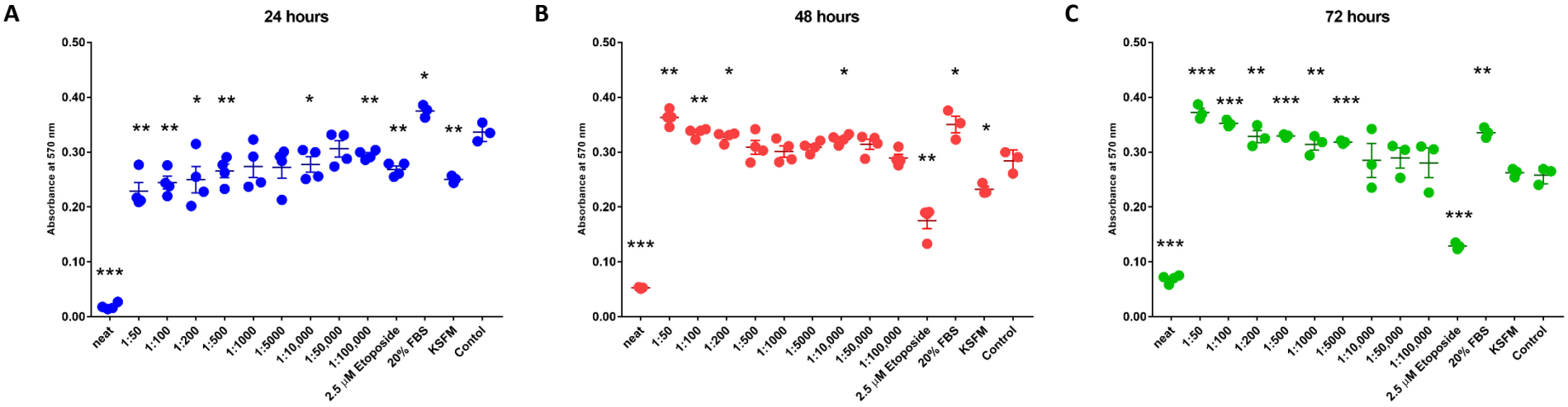

Figure 3.15. Incubation time selection

MTT assay (absorbance measured at 570 nm) assessing the effect of pooled conditioned medium from chronic infection of RWPE-1 cells on the HDMEC cell line, comparing the differences in incubation times. Cells seeded at 50,000 cells/ml and incubated for: **A.** 24 hours; **B.** 48 hours; **C.** 72 hours. Data presented as at least three replicates, +/- standard error. Significance was calculated by comparing to untreated control for each experiment.

at 72 hours only, and 1:10,000 ($p = 0.0206$) at 48 hours only). Furthermore, a significant difference was also seen in the untreated control measurements at 24 hours versus 48 and 72 hours ($p = 0.0271$ and $p < 0.0043$, respectively). Finally, a significant increase was observed in the optical density readings for neat ($p = 0.0144$) and 1:10 ($p = 0.0349$) samples comparing the 48 and 72-hour time points.

3.3.15. ELISA

Four ELISA kits were purchased to detect the amount of IL-1β, IL-6, IL-8 and TNF-α in conditioned medium following acute and chronic infection with a range of *P. acnes* phylogenetic strains and *P. granulosum* as a control.

Standard curves were prepared for each ELISA kit following the manufacturer's instructions, however, the values of the highest standards were significantly lower than expected, with the values remaining low in different repeats, and changes in experimental conditions such as incubation with agitation, incubation steps conducted at 25°C, and S-HRP and TMB steps incubated at 37°C and up to an hour for TMB (Figure 3.16 for representative standard curves).

As changes in the recommended protocol had no effect on the standard curve protocol, a trobleshooting experiment using components from an available R&D IL-1β ELISA kit were used to eastablish the reason the kits were not performing as expected. Different components of the Peprotech and R&D IL-1β kits were used to pinpoint the core of the issue (Figure 3.17).

In this troublshooting comparison experiment, the Peprotech IL-1β ELISA once again demonstrated lower than the expected absorbance values at 0.37 for the 750 pg/ml high standard (Figure 3.17.A). In contrast, the R&D ELISA showed a reading (absorbance at 450 nm with background at 620 nm subtracted) of 1.85 (Figure 3.17.B), which is in line with the predicated by the manufacturer value. When the R&D ELISA kit was used in combination with the buffers recommened by Peprotech, the values were even higher, at 3.04 absorbance reading for the top standard (Figure 3.17.C). The combination of R&D capture antibody with Peprotech standard and detection antibody showed an absorbance reading of 1.23 (Figure 3.17.D), while the reverse combination measured absorbance of 0.31 (Figure 3.17.E). Finally, when the Peprotech ELISA was used with the

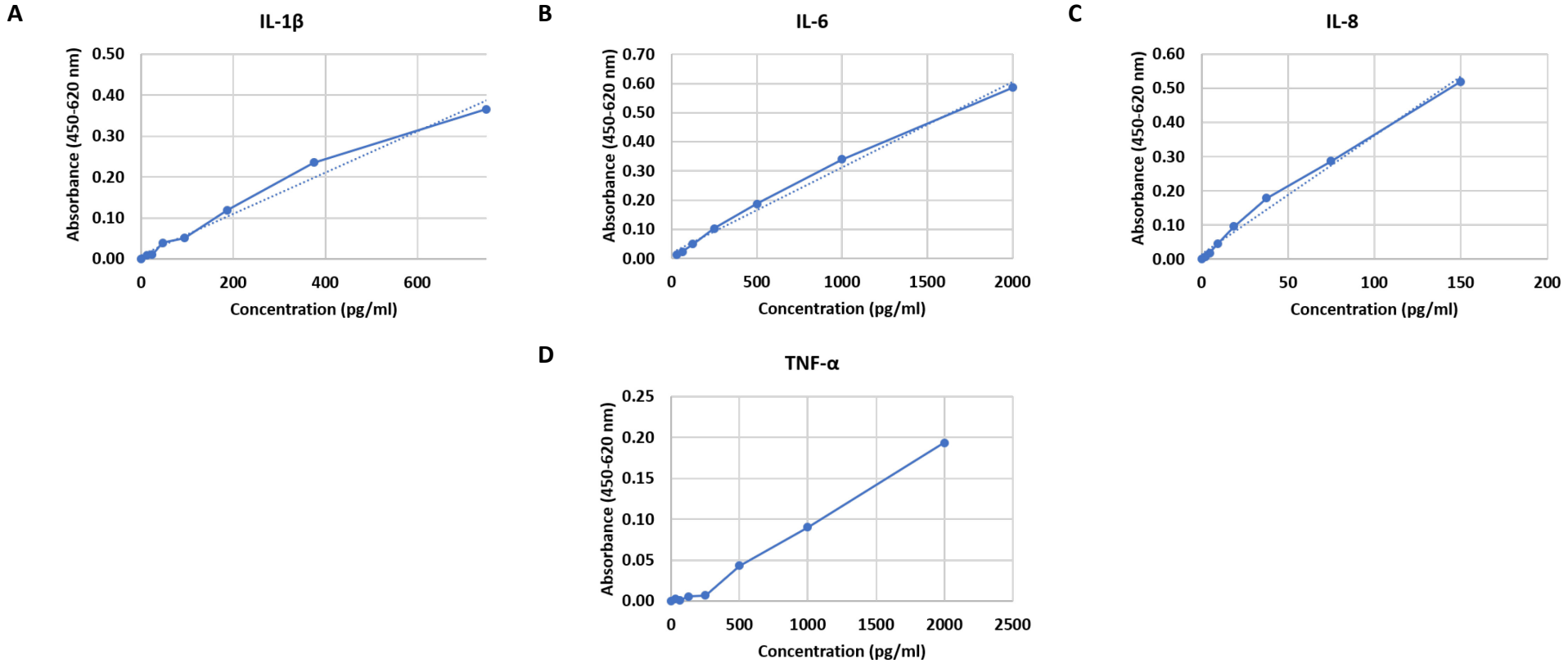

Figure 3.16. Standard curves for Peprotech ELISA kits

Standard curves for IL-1β (**A**), IL-6 (**B**), IL-8 (**C**) and TNF-α (**D**), demonstrating low absorbance of the highest standard when performed following the manufacturer's instructions.

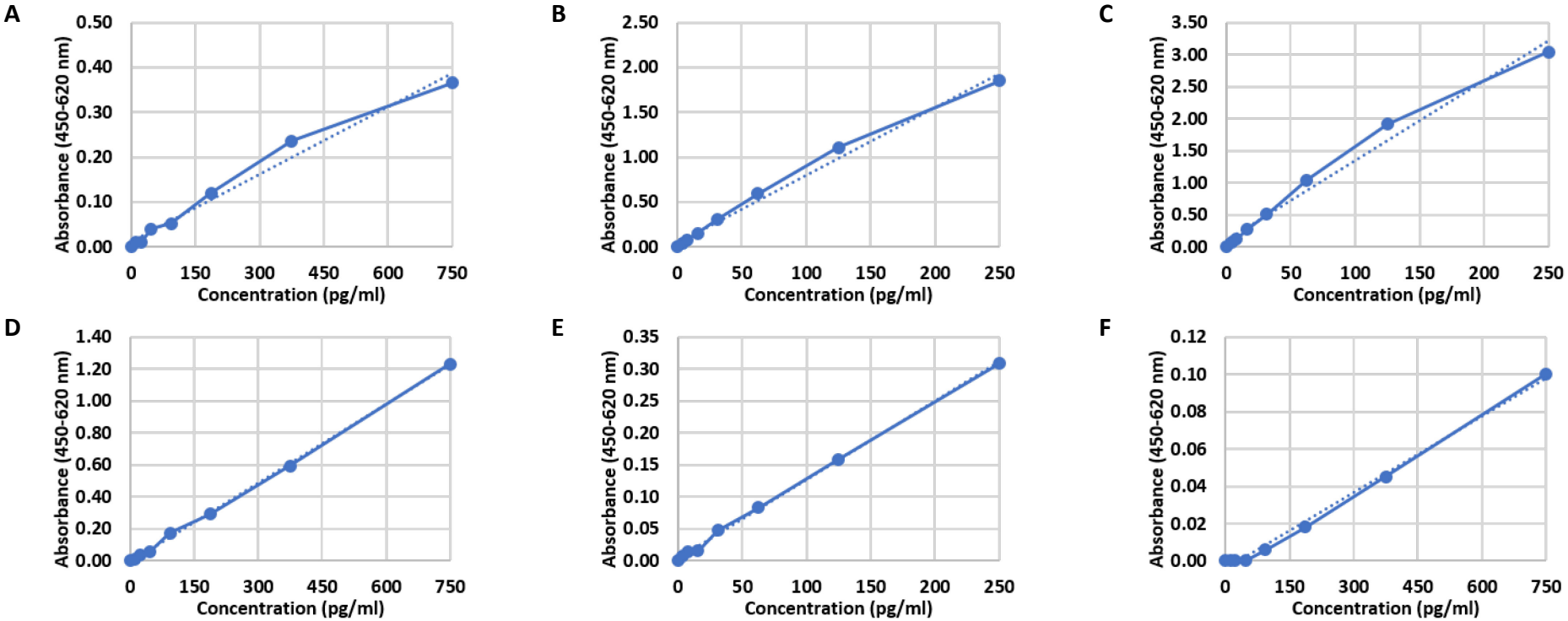

Figure 3.17. IL-1β ELISA troubleshooting

Standard curves were performed using a combination of Peprotech and R&D IL-1β ELISA kits, as follows:

A. Peprotech ELISA reagents;

B. R&D ELISA reagents;

C. R&D ELISA using Peprotech buffers (washing, blocking, diluent regent, S-HRP and TMB);

D. Peprotech blocking and capture antibody, followed by R&D standard, detection antibody, S-HPR and TMB;

E. R&D blocking and capture antibody, followed by Peprotech standard, detection antibody, S-HRP and TMB;

F. Peprotech ELISA using R&D buffers (washing, blocking, diluent reagent, S-HRP and TMB)

R&D buffers, the normalised absorbance readings for the highest standard were at 0.1 (Figure 3.17.F).

3.4. *Discussion*

Infection models of prostate epithelial cells with *P. acnes* have been previously used as a tool to investigate the potential role of *P. acnes* infection in oncogenesis (Drott et al., 2010; Fassi Fehri et al., 2011; Mak et al., 2012; Fischer et al., 2013; Sayanjali et al., 2016). Such infections shed light on the basic response of eukaryotic cells to infection with different *P. acnes* strains and can be used as stepping stones for future studies.

As we used the McDowell et al. (2012a) "Belfast" $MLST_8$ typing we are unable to compare our findings to some of the groups who have performed phylogenetic analysis of *P. acnes* prostate isolates, as different typing schemes utilise different genes sequences. It would be possible to perform *in silico* analysis of the published whole genome sequences available of *P. acnes* prostate isolates and elucidate their STs, however, this analysis was not performed due to time constraints. All comparisons in this Chapter are to an available database, containing STs of a collection of 372 isolates, compiled from a range of studies (McDowell et al., 2013).

The type IA_1 isolates in this study belong to three distinct STs. Strain 00035 is a part of ST1, which is the ST with the highest number of previously analysed strains, most of which have been linked to healthy skin or acne, but also a small proportion of the strains have been associated with corneal infections and endocarditis. The most widely used *P. acnes* control strain, NCTC737, also belongs to this ST. Strain 00060R belongs to ST8, with the members of this group being acne, skin or dental isolates (McDowell et al., 2013). The database does not contain any information about strains belonging to ST121 (as strain B2 used in this study) suggesting that isolates from this ST are rare.

The type IB strain from our study belongs to ST5, which includes skin and blood isolates but more importantly a large proportion of prostate cancer isolates (McDowell et al., 2013). Combining our isolates with the available database, members of ST5 comprise 33% of *P. acnes* prostate isolates discovered to date, with the remaining 67% being split between 6 distinct STs, highlighting the significance of ST5.

Finally, the type III isolate from our study (CFU2) belongs to ST33, which includes predominantly spinal disk isolates (McDowell et al., 2013).

Our findings suggest that the phylotypes of *P. acnes* isolated from cancerous prostate vary. Due to the small sample size, no solid conclusion can be made, however, there is a trend suggesting that phylogenetic type IB/ST5 strains are the ones most commonly associated with prostate cancer.

Trypan blue viability counts of the RWPE-1 cells were used to select the optimal seeding density. Both cells seeded at 50,000 and 100,000 cells/ml demonstrate good proliferation rates with increasing numbers up to day 5 and a high percentage of viable cells. The cells seeded at 100,000 cells/ml, however, demonstrated higher numbers and a marginally better viability at day 5 and were thus chosen as the optimal seeding density. The results from this experiment also suggest that the optimal seeding time point for any long-term infection would be day 5, before any loss in viable cells occurs.

As a variety of *P. acnes* MOIs have been tested in culture, to select the optimal MOI for infections, we compared bacterial numbers in chronic infections between cells infected at MOI 15:1 and MOI 50:1, with our results showing that as time progresses there is no statistically significant difference in bacterial concentration in the media using the different MOIs. As the medium is changed every 3rd day after passage, high number of the bacteria are washed off very early in the experiment, with the majority of remaining bacteria being either intracellular or attached to the cell surface. Based on the lack of significance in bacterial counts between MOIs, 15:1 was selected as the infection ratio to be used in future experiments, as it is closer to an *in vivo* situation where only small number of bacteria are found in epithelial and stromal cells (Alexeyev et al., 2007).

P. acnes has been shown to have the ability to become intracellular both in *in vitro* experiments and via fluorescent *in situ* hybridisation, using formalin-fixed, paraffin-embedded (FFPE) prostatectomy samples and needle biopsies (Alexeyev et al., 2007; Fischer et al., 2013). To assess the bacterium's ability to invade eukaryotic cells in culture, it is necessary to first remove all extracellular bacteria by treating the cells with antibiotics. However, with the different combinations tried in these experiments, there was still presence of extracellular bacteria. This could be due to insufficient incubation

time, though up to 4-hour incubation was trialled. Alternatively, any bacteria seen in the antibiotic control wells could be a result of eukaryotic death, thus the antibiotics would have not acted on the released bacteria for long enough to be effective. To achieve accurate numbers for the bacteria present intracellularly, any counts from the antibiotic control were subtracted from the intracellular counts in following experiments.

Our results demonstrated the importance of using antibiotics in soft agar assays using infected cells. When no antibiotics were used, colony formation was observed in soft agar assays prepared after a 15-day infection. Those colonies differed from colonies seen in assays set-up with cancer cell lines as they had rounder edges; this prompted further investigation which showed that the colonies were in fact bacterial colonies.

When antibiotics were used in a soft agar assay with a cancer cell line a significant decrease in the number of colonies formed was seen compared to untreated controls, indicating a decrease in the ability of cells to grow anchorage-independently. Studies have previously shown that antibiotics have the potential to affect cancer cell growth in culture by targeting the mitochondria (De Francesco et al., 2017). Such findings suggest the possible use of antibiotics as anti-cancer treatment but also highlight an issue with the wide-spread antibiotic use is tissue culture experiments, as they may have an effect results and cellular behaviour, especially in primary cells. As antibiotics affect eukaryotic cells on a metabolic level, it is likely that such activity is not limited to cancer cells.

Taken together these results show that use of antibiotics is necessary to eradicate any bacterial colonies; however, it can lead to a significant decrease in the observed number of colonies.

Quantitative-PCR is widely used for the investigation of transcript level changes. The efficiencies of all hydrolysis probe-primer mixes were analysed to confirm that they are within the expected range of 100% +/- 10%, which was the case.

Selecting the correct reference gene is vital for qPCR analysis. Housekeeping genes used are constitutively expressed genes which show no difference in expression between treated and control samples. It has been suggested that using more than one housekeeping gene increases the stability of the comparison. Our results showed that using a sole reference gene (*HPRT1*) has a greater stability value than using a

combination, thus only *HPRT1* was used for further analysis. This finding is in line with a previous study of 16 different reference genes, where *HPRT1* was shown to be the most stable (Ohl et al., 2005).

In order to optimise the MTT assays, five seeding densities of the HDMEC cells were examined and all showed an increase in the MTT assays absorbance reading directly proportional to seeding density. This result was expected as the higher the seeding density used, the more MTT is converted to formazan, resulting in the higher reading observed. The 50,000 cells/ml seeding density was selected, as the cells showed high readings but at the same time were not confluent, which would allow any treatment with conditioned medium to be continued for a number of days.

Two possible positive controls were trialled, a range of EGF concentrations and complete Medium 200, supplemented to a final concentration of 20% FBS.

EGF has been used in literature as a potential proliferation inducer at a range of concentrations, from 10 ng/ml to 100 ng/ml (Kato et al., 1998; Shao et al., 2008; Tomshine et al., 2009). The three dilutions used here showed no significant change in the HDMEC cell viability, following a 24 and 72-hour incubation, indicating that EGF is not a suitable positive control. Studies have suggested EGF is only effective at concentrations below 30 ng/ml and its pro-angiogenic effect is lost at higher concentrations (Shao et al., 2008). However, no difference was seen between the cells treated with 25 ng/ml and the untreated controls, or in comparison with the samples treated with higher levels of EGF. EGF was selected as a possible positive control for the MTT assays due to it being readily available, as it is one of the supplements added to KSFM used for culture of the RWPE-1 human prostate epithelial cells (together with BPE, as outlined in Section 2.1.1). EGF at a concentration of 25 ng/ml has also been used in a combination with VEGF as a proliferation control and VEGF is commonly used as a sole angiogenesis-inducer (Hussain et al., 2008; Wang et al., 2008b; Hwang et al., 2016). However, due to financial constraints, VEGF could not be used in the present study.

FBS contains a range of components including salts, vitamins, prostaglandins, hormones which can affect cell growth (Price and Gregory, 1982). It has long been observed that increasing the serum concentration in culture increases the growth rate of cells. The HDMEC cells are normally cultured in complete Medium 200 supplemented with LSGS

(which contains of 2% (v/v) FBS). However, supplementing the medium with FBS to a final concentration of 20% (v/v) lead to significantly increased proliferation compared to cells cultured in normal complete medium.

As the MTT experiments were only be used as a preliminary screen, the use of Medium 200 containing 20% (v/v) FBS was considered a sufficient positive proliferation control.

Two different treatments were also examined as potential negative controls: etoposide and saponin.

Etoposide is a commercially available anti-cancer drug, which works by targeting DNA topoisomerase type II during DNA-replication, thus inhibiting the re-ligation of DNA, causing DNA damage and inducing apoptosis in cancer cells (Pommier et al., 2010). A range of three concentrations used in literature were tested as potential anti-proliferation controls (2.5 µM, 3.5 µM and 5 µM) and all three showed significant decrease in MTT assay absorbance levels, making them suitable negative controls for future experiments (Panigrahy, 2010; Callaghan et al., 2016). The 2.5 µM etoposide concentration was selected, as its activity was significant even at the small dose used.

Finally, saponin at a concentration 0.05% (w/v) was also tested as a negative control, as it has been used previously in literature (at a higher concentration of 0.1%) as a negative proliferation control (Focaccetti et al., 2015). As expected, this treatment caused a significant decrease in the absorbance observed following MTT assay analysis, which is a result of the saponin lysing all cells. As no cells remain viable following this treatment, saponin was not selected as a negative control, and etoposide was used instead for analysis.

Experiments were also performed to select the optimal exposure time of the HDMEC cells to the conditioned medium. Cells were treated with a serial dilution of conditioned medium and incubated for 24, 48 and 72 hours. The results demonstrated that the length of incubation affected the results significantly. When the cells were only incubated for 24 hours, the trendline suggested that the conditioned medium had an inhibitory effect on proliferation which was lost as the medium was diluted. The opposite was observed when the cells were incubated with the same pooled conditioned medium but incubated for 48 and 72 hours. The trendline in both cases

started at the highest proliferation induction when treated with a 1:50 dilution and it slowly decreased as the conditioned medium was diluted.

The reverse trendline seen at 24 hours suggests that there may be an initial cytotoxic effect seen in the HDMEC cells when treated with the conditioned medium, which is overcome within 48 hours when the cells begin to show increased proliferation and is even more clear at 72 hours. Another observation of the importance of incubation time on proliferation of the HDMEC cells can be seen in the positive and negative controls between 48 and 72 hours. The significance in both increases with the longer incubation.

Taken together these findings point towards 72 hours being the optimal incubation time to be used in future experiments.

Another interesting observation made in the data at the optimisation stage was that in all cases there was a significant decrease in viability when the cells were treated with neat conditioned medium. While a drop in viability was seen when the HDMEC cells were treated with complete KSFM as a control, by the 72-hour time point such difference was lost and there was no significant difference between MTT assay absorbance in HDMEC cells cultured in complete Medium 200 versus those cultured in complete KSFM. The drop seen when cells were treated with neat conditioned medium is thus not due to the change of base medium but likely a result of the conditioned medium not having enough nutrients to sustain life in the endothelial cell line. Once the conditioned medium was diluted in fresh medium, the effect it has on the proliferation of the HDMEC cells can be seen.

An extensive troubleshooting investigation of the Peprotech ELISA kits demonstrated that the issue does not stem from the type of 96-well plate used and that the buffer composition or TMB does not interfere in the process, as when a different kit was used with the same plates and buffers it showed improved values. When a combination of Peprotech capture antibody was used with R&D standard and detection antibody, while lower than the advertised OD value of 2, the absorbance reading was still higher than that of the Peprotech kit alone, suggesting that the issue does not lie within the Peprotech capture antibody coating. When the alternative was tried, and the R&D capture antibody was combined with the Peprotech standard and detection antibody, the value of the high standard reading was 0.31, which is lower than expected even

when allowing for the difference in standard concentration. Additionally, S-HRP at the recommended concentration was tested directly with TMB to confirm that the reaction occurs. These findings suggest that the low and inconsistent absorbance readings observed with the Peprotech kit were related to the detection antibodies.

Due to the issues encountered, time limitations and financial constraints it was decided not to pursue the quantification of secreted inflammatory proteins further, and solely use gene dysregulation to analyse differences.

The combination of these initial optimisation experiments ensures a stringent and robust analysis of infection models in future experiments and the optimised gene efficiencies. The selection of a stable housekeeping gene allows for an accurate comparison in dysregulation levels following infection with different *P. acnes* phylotypes and species in the following chapter.

Chapter 4:
Acute and chronic models of infection

4

4.1. *Introduction*

The dysregulation of inflammatory and epithelial-mesenchymal transition (EMT) genes in acute and chronic infection models was investigated, to assess the differences in gene expression as a result of infection of human prostate epithelial cells (the RWPE-1 cell line) with a range of *P. acnes* phylotypes. Additionally, cellular and bacterial behaviour in the short and long-term infections was evaluated. The molecular findings were supplemented with soft agar assays, investigating anchorage-independent growth, scratch assays assessing migration, and immunocytochemistry was used to analyse the expression of EMT-related proteins.

4.1.1. Interleukin-1 beta

Interleukin-1 beta (IL-1β), a member of the IL-1 superfamily, is expressed as a precursor protein which becomes activated by caspase-1 (Dinarello, 1998). Caspase-1 itself also requires activation by the formation of the NACHT, LRR and PYD domains-containing protein 3 (NLRP3) inflammasome (Agostini et al., 2004). Alternatively, IL-1β can also be activated by neutrophilic enzymes, e.g. proteinase-3 and elastase (Dinarello, 2011). IL-1β has been linked to an increasing number of autoinflammatory diseases. These autoinflammatory diseases differ from autoimmune diseases in that they are periodic and linked with defects in innate immunity, rather than being progressive and linked to dysregulation of the adaptive immune response (Dinarello, 2011). Additionally, IL-1β has been shown to be involved in antibody production and the most commonly used adjuvant, aluminium hydroxide, initiates caspase-driven IL-1β activation (Marrack et al., 2009) (Summarised in Figure 4.1).

Both IL-1α and IL-1β can bind the IL-1 receptor type I (IL1RI) which summons co-receptors and adaptors, prior to signal initiation. The adaptor molecule that activates the IL1R is also a part of Toll-like receptor (TLR) activation (Barton and Medzhitov, 2003). The assembled receptor complex initiates a number of downstream pathways, including the nuclear factor-kappa B (NF-κB), mitogen-activated protein kinases/extracellular signal-regulated kinases (MAPK/ERK) and c-Jun N-terminal kinases (JNK) pathways.

In the context of prostate cancer, studies have shown that decreased expression of IL-1β is a feature seen in cancerous tissue but not in healthy or BPH samples (Ricote et al., 2004).

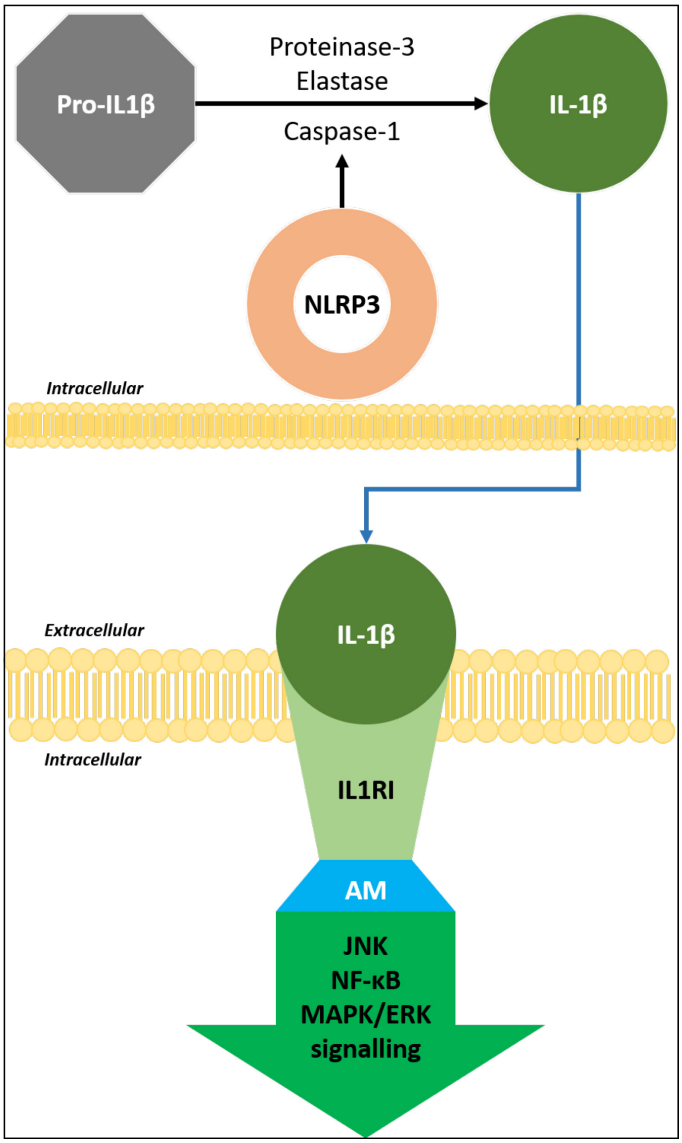

Figure 4.1. Overview of interleukin 1-beta (IL-1β) signalling

IL-1β is produced as a precursor protein (pro- IL-1β) which needs to be activated in order to become functional. The activation can be done by proteases (e.g. proteinase-3, elastase) or by cspase-1 (which is activated by the NLRP3 inflammasome). The functional IL-1β is then secreted and can bind interleukin receptor type I (IL1RI) which recruits adaptor molecules (AM), triggering a number of signalling pathways.

Legend: ERK – extracellular signal-regulated kinase; JNK – c-Jun N-terminal kinase; MAPK – mitogen-activated protein kinase; NF-κB – nuclear factor-kappa B; NLRP3 – NACHT, LRR and PYD domains-containing protein 3, inflammasome component

4.1.2. Interleukin-6

Interleukin-6 (IL-6) is a cytokine which belongs to the IL-6 type family. The IL-6 receptor (IL6R) consists of an α-subunit with no signalling functions, and a 130 kDa signal-mediating glycoprotein, also known as gp130 or IL-6Rβ (Taga et al., 1989). A soluble form of the receptor also exists (Lust et al., 1992). Activation of a number of pathways has been linked to IL-6 including Janus kinase/signal transducer and activator of transcription 3 (JAK/STAT3), NF-κB, MAPK/ERK and phosphatidylinositide 3-kinases/protein kinase B/mechanistic target of rapamycin (PI3K/AKT/mTOR) pathways. (Guschin et al., 1995). (Illustrated in Figure 4.2)

IL-6 is elevated in the serum of patients with metastatic prostate cancer and the levels correlate with prostate specific antigen (PSA) results (Adler et al., 1999). *In vitro* studies have also shown that IL-6 can activate the androgen receptor independently of its ligand and cause receptor activation in low androgen concentrations, which would be of importance in patients with advanced cancer and elevated IL-6 serum levels (Hobisch et al., 1998; Chen et al., 2000).

4.1.3. Interleukin-8

Interleukin-8 (IL-8), also known as chemokine C-X-C motif ligand 8 (CXCL8), is a chemokine produced by a variety of cells and it has a chemotactic activity on various inflammatory cell types. It can bind to two C-X-C motif chemokine receptors, CXCR1 and CXCR2. IL-8 dysregulation and abnormal IL-8 receptors are present in a number of tumours, including in prostate cancer (Veltri et al., 1999). Abnormal IL-8 activity in tumour sites has been linked to alterations in immune cells behaviour, regulation of angiogenesis, tumour growth and survival, and to promoting migration of cancer cells (Baggiolini et al., 1989; Strieter et al., 1995; Zlotnik and Yoshie, 2000; Strieter, 2002; Balkwill, 2003).

CXCL8 has been suggested as a promoter of androgen-independent growth and as a cause of increased proliferation of cancer cells, as it activates the PI3K/AKT/mTOR and MAPK/ERK pathways (Knall et al., 1997; MacManus et al., 2007). It has also been shown to upregulate CXCR7 (also known as ACKR3) which in turn induces cancer cell growth through epidermal growth factor receptor (EGFR) (Luppi et al., 2007). Accelerated prostate cancer progression can also be explained by common mutation is phosphatase and tensin homolog (PTEN) which leads to upregulation of IL-8 via hypoxia-inducible

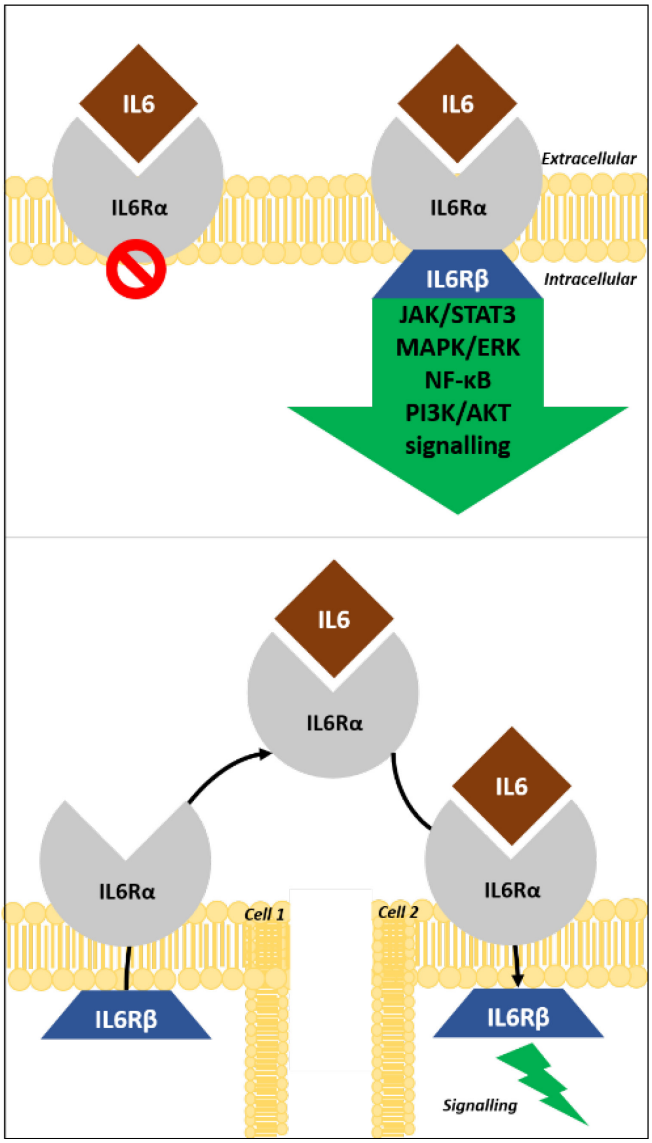

Figure 4.2. Overview of interleukin-6 (IL-6) signalling

IL-6 binds the ILR6α subunit of the IL-6 receptor, which is inactive until bound to the IL6Rβ-subunit (or gp130), initiating a range of signalling pathways. A soluble from of the receptor also exists with a soluble α-subunit which binds IL-6 and then guides it to the membrane bound gp130, initiating signalling. Adapted from Dayer and Choy (2010).

Legend: AKT – protein kinase B; ERK – extracellular signal-regulated kinase; JAK – Janus kinase; MAPK – mitogen-activated protein kinase; NF-κB – nuclear factor-kappa B; PI3K – phosphoinositide 3-kinase; STAT3 – Signal transducer and activator of transcription 3

factor-1 (HIF-1) and NF-κB (Maxwell et al., 2013; Armstrong et al., 2016). Elevated serum levels of CXCL8, together with prostate specific antigen (PSA) levels, can be used to differentiate benign prostatic hyperplasia (BPH) from prostate cancer (Veltri et al., 1999).

4.1.4. Transforming growth factor beta

Transforming growth factor beta (TGF-β) is one of the two members of the TGF family. It is expressed primarily by endothelial and neuronal cells, and it is involved in the regulation of cellular proliferation, differentiation, angiogenesis and wound healing (Pepper, 1997; Blobe et al., 2000). TGF-β either binds to type III receptors (which do not have a signalling function), and they transfer it to signalling receptors type II, or it binds type II receptors directly, which in turn recruit type I receptors (Wrana et al., 1994). Once bound, TGF-β activates the phosphorylation of a number of SMAD (a portmanteau of Sma (small body size) in *Caenorhabditis elegans* and MAD (mothers against decapentaplegia) in *Drosophila*) transcription factors. The activated SMADs are then translocated to the nucleus and are involved in transcriptional regulation (Nakao et al., 1997). TGF-β signalling is also involved in the MAPK/JNK, MAPK/ERK and PI3K/AKT/mTOR signalling pathways (Lee et al., 2007; Liu et al., 2012; Suwanabol et al., 2012). A visual representation of the TGF-β activation and signalling can be seen in Figure 4.3.

It has been established that TGF-β plays a direct role in cell cycle regulation by activating the production of cyclin-dependent kinase (Cdk) inhibitors, which leads to a downstream reaction resulting in cell cycle arrest in the G_1 phase (Ravitz and Wenner, 1997). Mutations in the receptors, SMADs or TGF-β itself, have been linked to cancer progression, as TGF-β can no longer inhibit proliferation or induce apoptosis; mutations in TGF-β receptor type II and SMAD4 have been linked to prostate cancer (Blobe et al., 2000). Increased levels of serum TGF-β1 have been found in prostate cancer patients (Ivanovic et al., 1995; Adler et al., 1999).

TGF-β signalling can act both as tumour suppressor and a tumour promoter (Muraoka-Cook et al., 2005). While TGF-β can induce apoptosis or inhibit proliferation thus inhibiting transformation, at later stages of cancer progression, TGF-β signalling can cause an increase in motility and invasiveness via the PIK3/AKT axis (Muraoka-Cook et al., 2005).

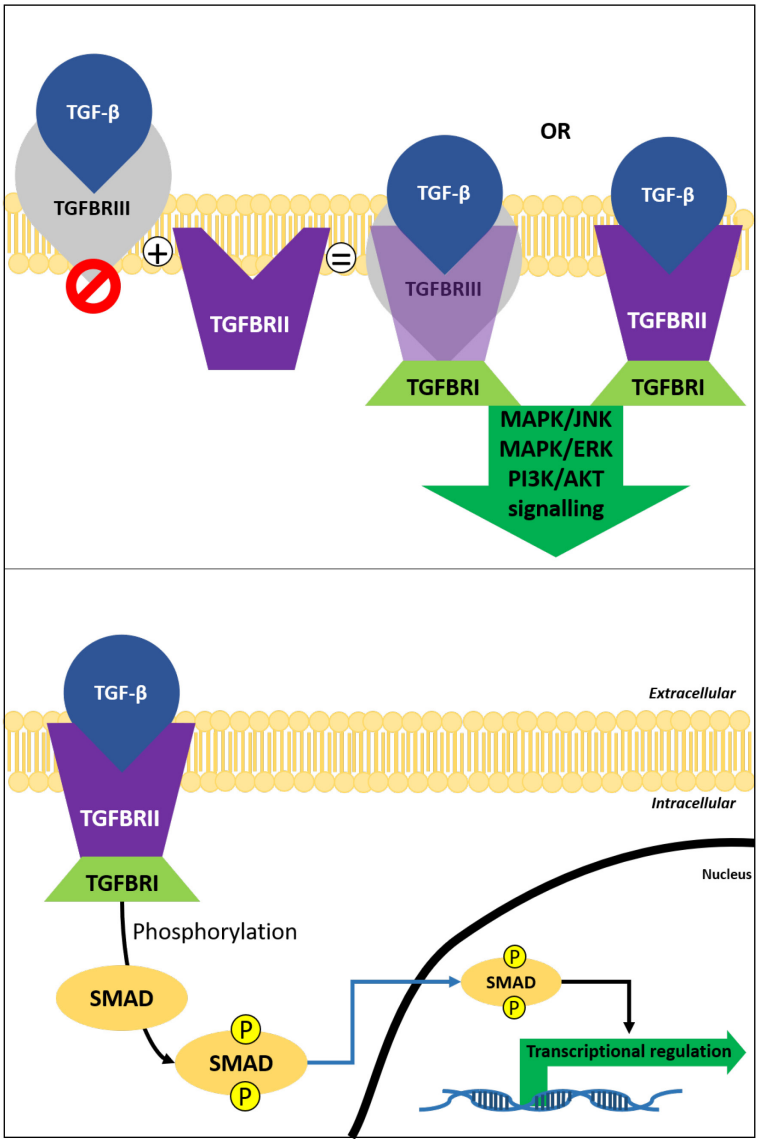

Figure 4.3. Overview of transforming growth factor-beta (TGF-β) signalling

TGF-β can initiate signalling one of two ways: it can bind the TGFB receptor type III (TGFBIII) which has no signalling capabilities and then interacts with TGFBII; alternatively, TGF-β can bind TGFBII directly. Following, TGFBI is recruited, which initiates multiple signalling pathways. A way of action for TGF-β is via phosphorylation of SMAD, which is then translocated to the nucleus, where it can regulate transcription. Adapted from Blobe et al. (2000).

Legend: AKT – protein kinase B; ERK – extracellular signal-regulated kinase; JNK – c-Jun N-terminal kinase; MAPK – mitogen-activated protein kinase; PI3K – phosphoinositide 3-kinase; SMAD – a portmanteau of Sma (small body size) in Caenorhabditis elegans *and MAD (mothers against decapentaplegia) in* Drosophila*;*

4.1.5. Tumour necrosis factor-alpha

Following its synthesis, tumour necrosis factor alpha (TNF-α) is present as a transmembrane protein, and it is not soluble until cleaved by TNF-α-converting enzyme (TACE, also called ADAM17) (Issuree et al., 2013). TNF-α can bind to TNF-receptors TNFR1 or TNFR2 with opposing results; TNFR1 is involved in programmed cell death initiation and inflammation, while TNFR2 mediates cellular survival and regeneration (Grell et al., 1995; Probert, 2015). Once it has interacted with TNF-α, the receptor signalling complexes activate intricate signalling pathways (Figure 4.4) (Brenner et al., 2015; Pasparakis and Vandenabeele, 2015). TNFR1 complex I and TNFR2 are linked to NF-κB and MAPK-signalling activation (plus AKT-pathway activation for TNFR2) and a positive outcome for the cell, while TNFR1 complexes IIa, IIb and III are linked to cell death through apoptosis (for the type II complexes) or necroptosis (for type III) (Micheau and Tschopp, 2003; Wang et al., 2008a; Aggarwal et al., 2012; Sun et al., 2012; Linkermann and Green, 2014; Brenner et al., 2015; Pasparakis and Vandenabeele, 2015).

When initially discovered, TNF was named after its ability to cause necrosis in tumour cells by inducing programmed cell death pathways (Carswell et al., 1975). It has also been linked to senescence and cytostatic effects (Sugarman et al., 1985; Braumuller et al., 2013). However, evidence suggests that TNF-α also has cancer promoting functions, for example by inducing mutations and inhibiting DNA-repair pathways, as well as driving proliferation and survival by inducing NF-κB and IL-6 production (Zhao et al., 2012; Elinav et al., 2013; Hu et al., 2014). Additionally, TNF-α can aid tumour cells in evading the immune system and can also promote EMT (Kalliolias and Ivashkiv, 2016).

4.1.6. Affected pathways

4.1.6.1. JAK-STAT3 signalling pathway

The signal transducer and activator of transcription (STAT) family of transcription factors includes a total of 7 members, split into two groups. The first group is activated by only a few cytokines and its primary functions include interferon-gamma (IFN-γ) signalling and T cell development (Siveen et al., 2014). The second group, which includes STAT1, STAT3 and STAT5, play a role in cell cycle progression and apoptosis, and are thus involved in oncogenesis (Subramaniam et al., 2013).

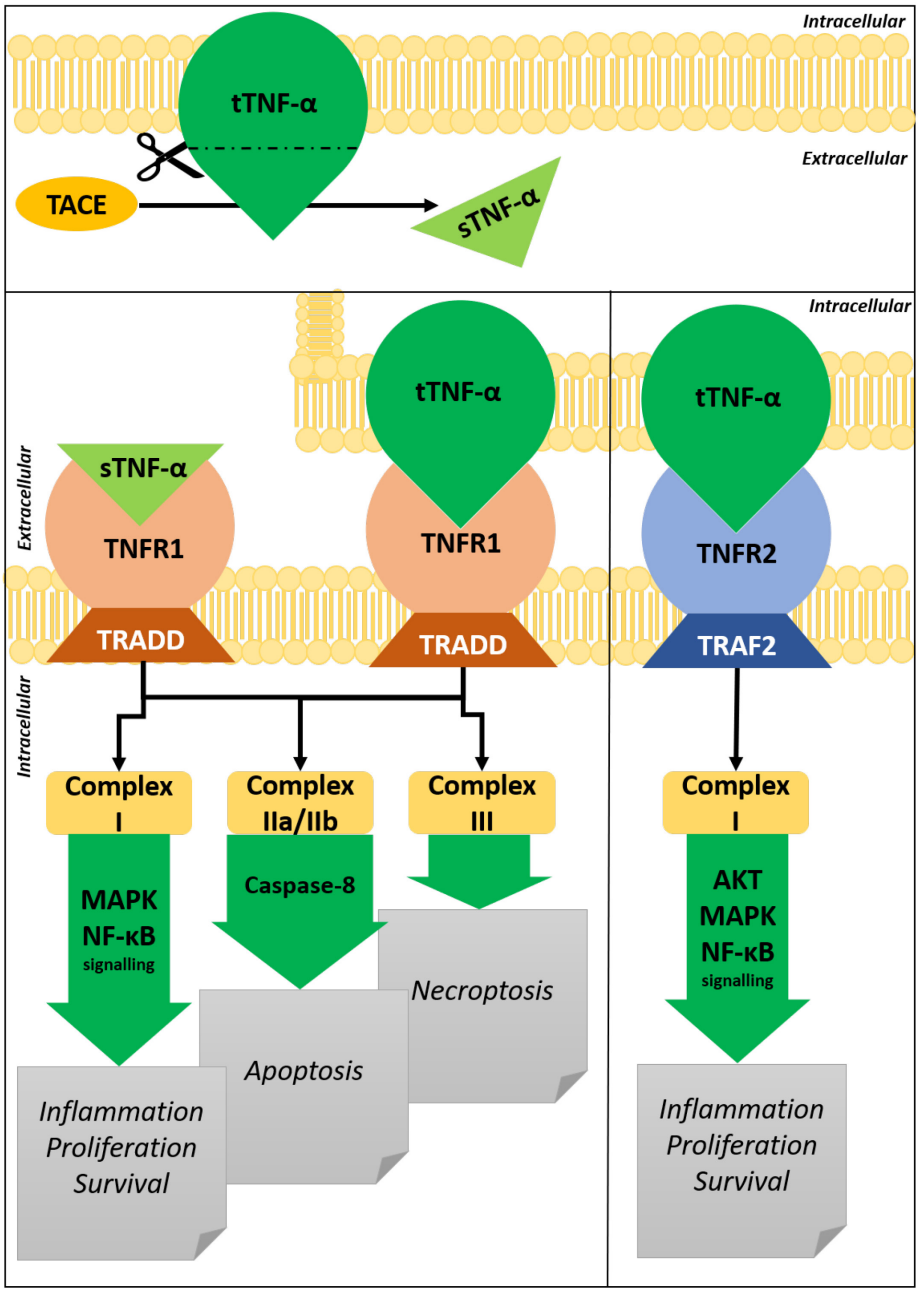

Figure 4.4. Overview of tumour necrosis-alpha (TNF-α) signalling

A. TNF-α exists as a transmembrane protein (tTNF) which can be solubilized (sTNF) if cleaved by TNF-α-converting enzyme (TACE).

B. TNF-α receptor 1 (TNFR1) can bind both soluble and membrane-bound TNF-α. Once the ligand is bound, and adaptor called TNFR1-associated death domain (TRADD) is recruited. This can then lead to the formation of a number of signalling complexes, initiating distinct signalling pathways, including proliferation and survival (type I), apoptosis (type II), necroptosis (type III). Additionally, membrane bound TNF-α can also interact with TNFR2, which recruits the TNFR-associated factor 2 (TRAF2) adaptor molecule, leading to the formation of complex type I and initiating signalling pathways involved in proliferation and survival. Adapted from Kalliolias and Ivashkiv (2016).

Legend: AKT – protein kinase B; MAPK – mitogen-activated protein kinase; NF-κB – nuclear factor-kappa B;

The Janus kinase (JAK)/STAT3 pathway can be activated by ligand-binding to either cytokine-specific receptors, G-coupled receptors or toll-like receptors (Rakoff-Nahoum and Medzhitov, 2009; Ritter and Hall, 2009; Jones et al., 2011). STAT3 can be activated by a variety of cytokines (including IL-6 and TNF-α), growth factors, carcinogens, and environmental stress (Park et al., 1996; Heinrich et al., 1998; Miscia et al., 2002; Carl et al., 2004; Chen et al., 2008a). The binding of a ligand to its receptor, for example IL-6, leads to the formation of a hexameric IL-6 receptor complex (formed by a IL-6Rβ homodimer, and two IL-6/IL-6Rα heterodimers) (Zhong et al., 1994; Catlett-Falcone et al., 1999; Heinrich et al., 2003). JAK is then activated and leads to the phosphorylation of IL-6Rβ, which in turn activates cytoplasmic STAT3 (Zhong et al., 1994; Catlett-Falcone et al., 1999; Heinrich et al., 2003). STAT3 forms dimers and is translocated to the nucleus, where it initiates a variety of processes (Chen et al., 2008a; Chen et al., 2008b; de Araújo et al., 2008; Weerasinghe et al., 2008). An overview of the pathway can be seen in Figure 4.5.

As STAT3 is a crossing point between signalling pathways linked to oncogenesis, it is considered an oncogene (Bromberg et al., 1999). In healthy cells, the process has a transient nature and is tightly regulated through negative feedback, while constitutive activation is seen in a wide range of cancerous cell lines (Sartor et al., 1997; Abdulghani et al., 2008; Masciocchi et al., 2011). This activation is a result of paracrine activation of STAT3 with growth factors and cytokines, or mutations in the negative-feedback proteins (Greenhalgh and Hilton, 2001).

Activated STAT3 can promote proliferation by directly affecting cell cycle regulation proteins, such as cyclin D1, which is involved in the transition between G_1 and S-phase (Kanda et al., 2004; Xiong et al., 2008; Bollrath et al., 2009; Jarnicki et al., 2010). The ability of STAT3 to aid survival through apoptosis-evasion has been demonstrated in multiple myeloma and colorectal cancer, where anti-apoptotic signals driven by constitutive STAT3-expression were seen (Yu and Jove, 2004; Xiong et al., 2008). A variety of cytokines and growth factors both induce STAT3 signalling and are produced as a result of its activation; if constitutive activation of STAT3 is present, this leads to a cancer-promoting inflammatory environment (Yu et al., 2009).

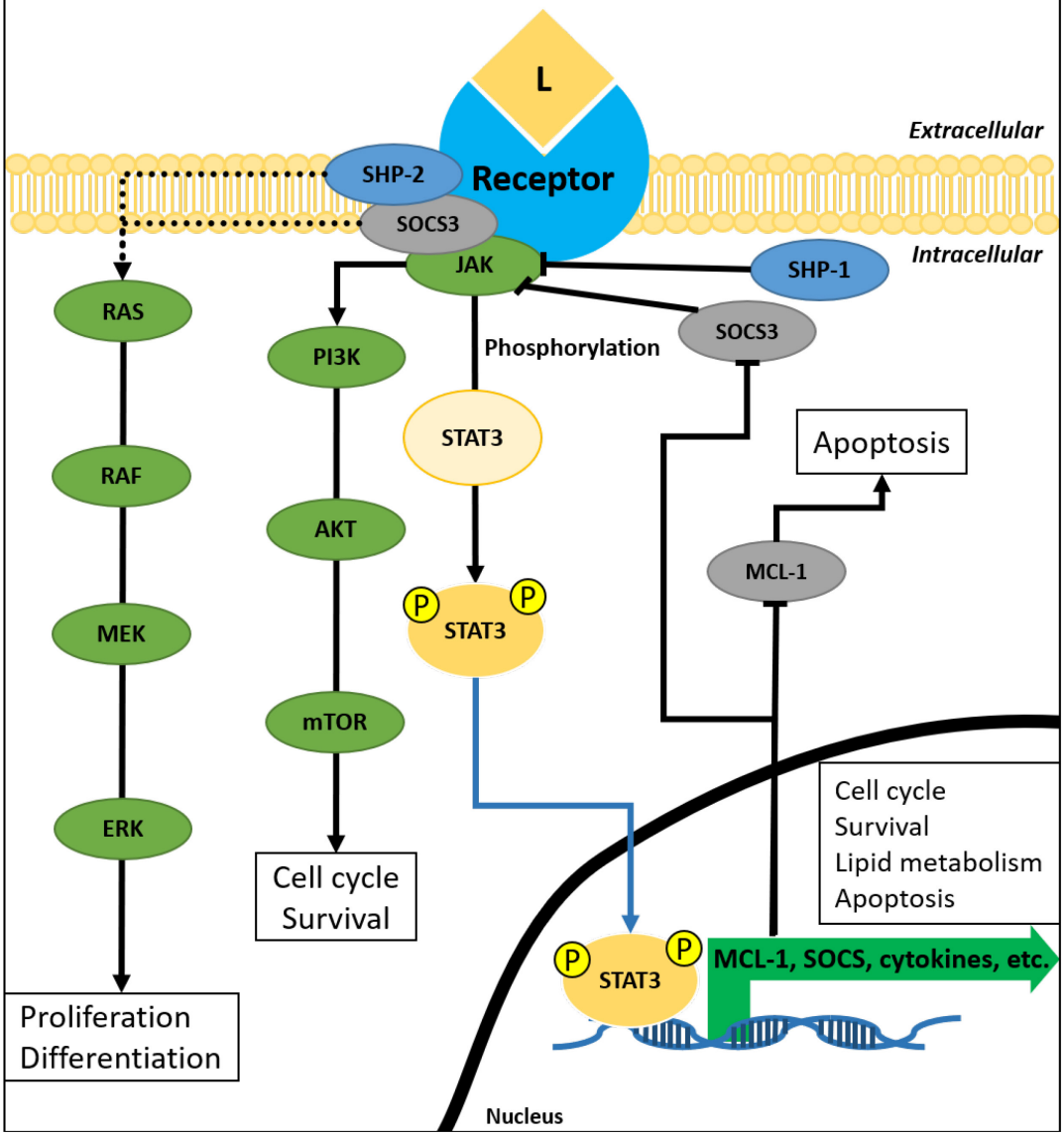

Figure 4.5. Overview of the JAK/STAT3 signalling pathway

The JAK/STAT pathway is key in the regulation of a number of different pathways involved in a range of processes, including the RAS/RAF/ERK pathway which can cause changes in proliferation and differentiation, the PI3K/AKT pathway which is involved in survival and cell cycle control. The phosphorylation of STAT3 by JAK leads to translocation of STAT3 to the nucleus where it is involved in the translational regulation of a range of genes, e.g. cytokines, *MCL1* which plays a role in apoptosis and *SOCS3* which is involved in a negative feedback loop of the JAK/STAT3 pathway.

*Legend: AKT – protein kinase B; ERK – extracellular signal-regulated kinase; JAK – Janus kinase; L – ligand; MCL-1 – myeloid cell leukaemia 1; MEK – mitogen-activated protein kinase kinase; mTOR – mammalian target of rapamycin; P – phosphorylation; PI3K – phosphoinositide 3-kinase; RAF – rapidly accelerated fibrosarcoma; RAS – **ra**t **s**arcoma protein; SHP-2 – protein-tyrosine phosphatase 1D; SOCS – Suppressor of cytokine signalling 3; STAT3 – Signal transducer and activator of transcription 3;*

Prostate cancer cell culture studies have shown that if treated with constitutively expressed STAT3, cells produce lower levels of E-cadherin, which in turn increases migration (Azare et al., 2007). STAT3 signalling is known to play a role in metastasis by activating multiple matrix metalloproteases (e.g. MMP-9 in breast cancer and MMP-1 in colorectal cancer) which are also involved in migration (Dechow et al., 2004; Tsareva et al., 2007). And finally, STAT3-activation is suspected to play a role in angiogenesis, by driving autocrine vascular endothelial growth factor (VEGF) activation (Schaefer et al., 2002).

4.1.6.2. Nuclear factor-kappa B pathway

Originally discovered as a nuclear factor which binds the kappa light-chain of immunoglobulins in B cells, NF-κB was later shown to be expressed by a wide range of cells (Sen and Baltimore, 1986; May and Ghosh, 1998). Currently, there are five known members of the NF-κB family: RelA, RelB, c-Rel, NF-κB1 (also called p105 due to its size; once processed becomes p50) and NF-κB2 (p100, becomes p52 post-processing), with the latter two being secreted as precursor proteins which undergo proteolysis before they can be activated (May and Ghosh, 1998). In normal cells, these factors form homo- or heterodimers which are bound to members of the IκB (inhibitors of NF-κB) family (Hoesel and Schmid, 2013). While bound to the inactivators, the ability of NF-κB to bind DNA and initiate transcription is inhibited, and its ability to translocate to the nucleus is decreased (Hoesel and Schmid, 2013).

For NF-κB to become active, it either needs to be released by the inhibitors or NF-κB1 needs to be proteolyzed by a series of reactions, including ubiquitination of the target regions, which is driven by phosphorylation via IκB kinases (IKKs) and NF-κB essential modulator (NEMO). A wide range of reactions can lead to the activations of those IKKs, including self-activation, MAP3K-family members, TGF-β-activating kinase 1 (Nakano et al., 1998; Ninomiya-Tsuji et al., 1999; Tan et al., 1999; Wu et al., 2000; Hayden and Ghosh, 2008; Schmid and Birbach, 2008).

There are two main NF-κB activation pathways. The canonical pathway can be triggered by stress (including physical, physiological or oxidative), TLRs, IL-1R, TNFRs, and ligands such as TNFα, lipopolysaccharides (LPS), IL-1β, as well as the MAPK/ERK pathway (Yeh et al., 2004; Perkins and Gilmore, 2006; Schmid and Birbach, 2008; Hoesel and Schmid, 2013). This in turn activates the IKK complex, namely IKKβ-driven phosphorylation

(Hoesel and Schmid, 2013). The alternative pathway or non-canonical pathway is activated by a range of receptors, including TNFR and it activates IKKα (Xiao et al., 2001). Further "atypical" pathways of activation also exist, e.g. genotoxic stress-driven NEMO-ubiquitination or epidermal growth factor receptor (EGFR) tyrosine related activation of NF-κB, as seen in ovarian cancer (Huang et al., 2003; Oeckinghaus and Ghosh, 2009; Alberti et al., 2012). Once the IKKs are active, IκBs are released and this allows NF-κB dimers to be shifted to the nucleus where they can recognize specific DNA sequences and bind them, leading to the possible activation of vast numbers of genes (Hoesel and Schmid, 2013). A summary of the canonical and alternative pathways can be found in Figure 4.6.

The inactivation of NF-κB-driven transcription is done mainly through a negative feedback loop, where NF-κB inhibitors are upregulated as a result of NF-κB activation; once synthesised, the inhibitors bind NF-κB and remove it to the cytosol (Klement et al., 1996; Pahl, 1999; Oeckinghaus and Ghosh, 2009). This feedback system is effective in the case of acute inflammation, where NF-κB levels are tightly controlled, but in cases of chronic inflammation, complete deactivation of NF-κB cannot be achieved, as it is overrun by activating stimuli (Hoesel and Schmid, 2013).

In the context of cancer, inflammation plays two contradictory roles. As a key player in tumour-immunosurveillance, NF-κB activation triggers a strong immune response, particularly involving cytotoxic cells, which neutralise any potential cancerous cells (Smyth et al., 2006; Disis, 2010). However, not all cancer cells can be identified, as some can escape the immune system, which seems to be more common in the presence of chronic inflammation, where constitutive moderate NF-κB levels are present (Dunn et al., 2004). Other than chronic infection which creates a cytokine-rich environment, NF-κB levels can be elevated due to mutation in the NF-κB pathway or mutations in genes which activate the signalling pathway (Ben-Neriah and Karin, 2011). Constitutive activation can then lead to pro-tumorigenic effects, for example by activating antiapoptotic genes, which aim to aid cells in resisting inflammation-related stress; it also leads to increased synthesis of multiple cytokines (IL-1β, IL-6, IL-8, TNF-α) and to the recruitment of leukocytes to the site, which release reactive oxygen species (ROS)

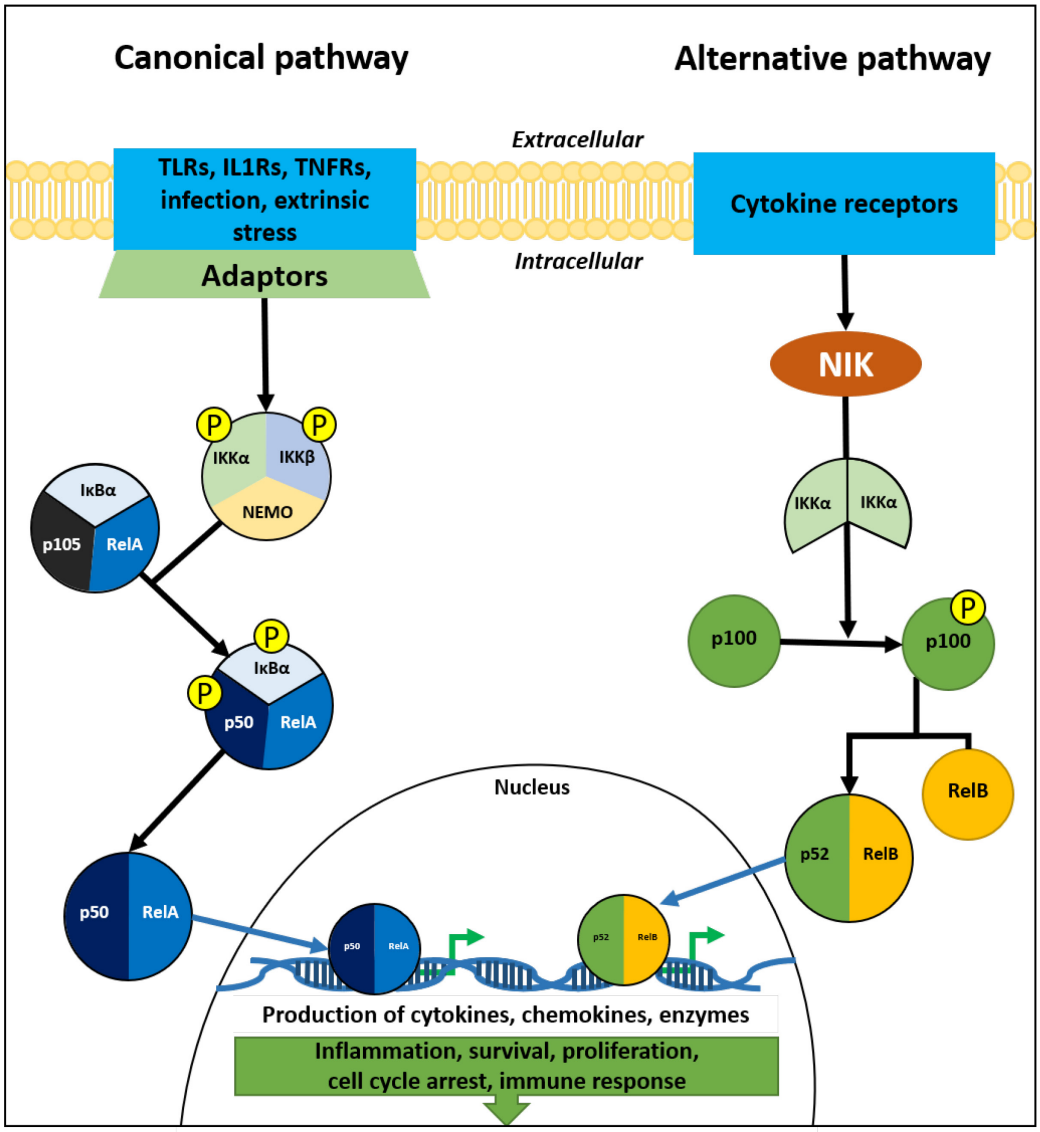

Figure 4.6.Overview of the NF-κB signalling pathway.

There are two pathways of nuclear factor-kappa B (NF-κB) activation. The **classical pathway** is activated by a range of receptors, including toll-like receptors (TLRs), tumour necrosis factor receptors (TNFRs), antigens and bacteria. Once activated the receptors recruit the necessary adaptor molecules with in turn activate the IKK complex (consisting of IKKα, IKKβ and NEMO). IKK in turn phosphorylates the IκBα, p105 and RelA complex, which leads to the degradation of IκBα and the processing of p105 to p50. The RelA/p50 dimer is then translocated to the nucleus, where it activates the transcription of a range of genes.

The **alternative pathway** involves the activation of an IKKα dimer by NF-κB-inducing kinase (NIK), which in turn phosphorylates p100. RelB then combines with the processed p100 to form a RelB/p52 complex which is translocated to the nucleus where it initiates transcription.

Legend: IκB – inhibitor of kappa-B; IKK – IκB kinase; IL1R – interleukin-1 receptor; NEMO – NF-kappa-B essential modulator; P – phosphorylation;

as a defence mechanism; these ROS can then cause DNA damage in cells and initiate oncogenesis (Liou and Storz, 2010). Furthermore, studies have shown the NF-κB aids EMT by altering expression of MMPs, and also has the potential to assist in the creation of blood supply to the tumour site by upregulation of receptors and angiogenic factors, such as VEGF (Yoshida et al., 1999; Huber et al., 2004).

Interestingly, in the case of hepatocellular carcinoma, the role of the NF-κB pathway differs depending on the original cause of cancer: in inflammation-related tumours NF-κB is seen as an anti-apoptotic pro-cancer factor, but it behaves as a tumour suppressor if the cause is chemical (Karin, 2009).

NF-κB has been shown to directly bind multiple transcription factors, including STAT3, SMAD3 and SMAD4 (Hoesel and Schmid, 2013). NF-κB and STAT3 work together on the regulation of anti-apoptotic and cell cycle-related genes, as well as on controlling cytokine production (Dauer et al., 2005; Yang et al., 2007). STAT3 has the potential to acetylate NF-κB and thus retaining it in the nucleus (Hoesel and Schmid, 2013); in an environment of constant stimulation (such as tumour microenvironment or chronic inflammation) this leads to increased synthesis of cytokines, which in turn activate STAT3, creating a cycle of constant activity of both STAT3 and NF-κB (Lee et al., 2009).

4.1.6.3. MAPK cascades

MAPK (mitogen-activated protein kinase) pathways consist of an intracellular signalling network involved in a variety of cellular processes, including proliferation, growth, stress response and apoptosis (Pimienta and Pascual, 2007; Raman et al., 2007; Shaul and Seger, 2007). Each cascade consists of three main kinases (MAPK kinase kinase or MAP3K, MAPK kinase or MAPKK, and MAPK), which act by sequential phosphorylation, leading to the activation of a target proteins by MAPK or accessory activators (Plotnikov et al., 2011). There are a number of MAPK-cascades identified: ERK1/2, JNK, and p38-MAPK, and an overview can be found in Figure 4.7.

The ERK1/2 cascade is activated by numerous extracellular signals via a wide range of receptors. In most cases, this cascade is activated by the Ras GTPase, which recruits MAP3K to the site, which leads to the activation of the induction cascade (Niault and Baccarini, 2010). Once activated, the ERK1/2 pathway is involved in the stimulation of a

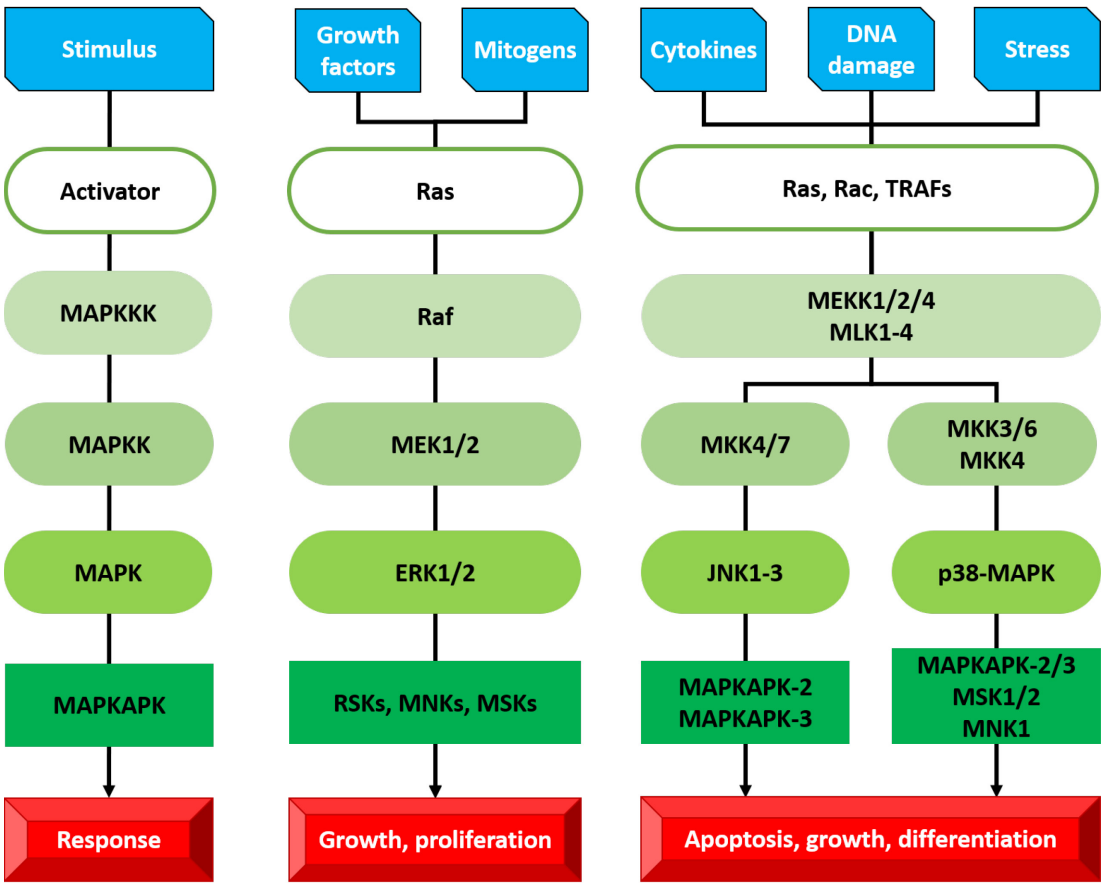

Figure 4.7. MAPK cascades overview.

The mitogen-activated protein kinase (MAPK) cascades include a range of different kinases which activate each other forming a kinase cascade. In general, a stimulus causes activation which initiates the MAPK-kinase kinase (MAPKKK), triggering a cascade of downstream phosphorylation/activation reactions which conclude with cellular response.

*Legend: JNK – c-Jun N-terminal kinase; MAPKAPK – MAPK-activated kinase; MAPKK – MAPK-kinase; MEK – MAPK/ERK kinase; MEKK – MEK-kinase; MKK – dual specificity MAPK; MLK – mixed lineage kinase; MNK – MAPK-interacting protein kinase; MSK – Mitogen and stress activated protein kinase; RAF – rapidly accelerated fibrosarcoma; RAS – **ra**t **s**arcoma protein; RSK – ribosomal s6 kinase; TRAF – tumour necrosis factor receptor associated factor;*

variety of pathways which regulate a broad range of cellular processes, including proliferation, survival, apoptosis (Yoon and Seger, 2006). If dysregulated, the pathway plays a role in more than 50% of cancers, and irregular activation of the pathway was seen with no mutations present in any of its components, indicating a role of the ERK1/2 cascade in oncogenesis induced by pathway activators (Dhillon et al., 2009; Montagut and Settleman, 2009).

The JNK pathway was thought to be solely involved in stress response, where the alternative name SAPK (stress-activated protein kinase) originated; it was later shown, that like all MAPKs, the JNK pathway is also activated by a wide range of stimuli (Davis, 1994; Johnson and Nakamura, 2007; Weston and Davis, 2007; Bogoyevitch et al., 2010). In this pathway, GTPases are activated, similarly to above, and lead to MAP3K activation, and the effects can be seen primarily in the nucleus where they are involved in transcription regulation of apoptosis, immune response, etc (Weston and Davis, 2007; Dhanasekaran and Reddy, 2008; Plotnikov et al., 2011). Involvement of JNK has been observed in multiple cancers, including upregulation of some members of the pathway in prostate cancer (Konishi et al., 2008; Wagner and Nebreda, 2009).

Through an alternative pathway, MAPK p38 aids in the activation of apoptosis, senescence, cell cycle progression and cellular survival (Sohn et al., 2007; Maruyama et al., 2009; Thornton and Rincon, 2009)

As a whole, the MAPK-related pathways are involved in regulation of transcription factors and transcription, chromatin remodelling, nuclear import, regulation of nuclear receptors (such as the androgen receptor) (Plotnikov et al., 2011).

4.1.6.4. Epithelial-mesenchymal transition

Epithelial and mesenchymal cells represent two main mammalian cell types. While epithelial cells form continual layers with cellular interactions, tight junctions at apical and lateral cells within the layers, polarised distribution of organelles within the cells and decreased motility, mesenchymal cells do not form layers and have loose or no interactions with other cells, lack polar organisation of their organelles and are motile, which in the context of cancer allows invasiveness (Martin-Belmonte and Perez-Moreno, 2012; Ullah et al., 2015). During EMT, some epithelial cells acquire mesenchymal properties; the opposite process, mesenchymal-epithelial transition (or MET), then

allows the cells to return to epithelial morphology and behaviour (reviewed in detail by Heerboth et al. (2015)).

While EMT plays a role in cancer, its primary function is seen during embryonic development, where it is involved in important milestones such as gastrulation and neural crest formation (Nakaya and Sheng, 2008; Theveneau and Mayor, 2012). EMT-like processes can also be induced by ERK in wound healing and by EGF after each menstrual cycle during post-ovulation ovarian epithelium surface repair (Ahmed et al., 2006; Arnoux et al., 2008). Despite the similarities in EMT during normal physiological processes and cancer, it is important to note that under normal circumstances EMT is tightly controlled; in the case of cancer-related EMT, the order of events is not regulated and may be a result in dysregulation of upstream EMT-inducing signalling pathways (Micalizzi et al., 2010).

One of the hallmarks of EMT is the loss of E-cadherin. E-cadherin (epithelial cadherin or CDH1) is an epithelial cell calcium-dependent cell-cell adhesion molecule. There is tight regulation on E-cadherin expression, and the *CDH1* gene is considered to be a tumour suppressor, as studies have shown loss of *CDH1* expression in a range of cancers; *in vitro* studies have demonstrated that re-expression of *CDH1* leads to decreased cancer aggressiveness, and germline mutations in the gene have been linked to hereditary cancers (Vleminckx et al., 1991; Guilford et al., 1998; Suriano et al., 2003).

In cancer, E-cadherin loss can be due to a mutation, silencing of expression through hypermethylation, abnormal post-translational modifications, proteolysis or a result of overexpression of E-cadherin suppressors, such as Snail and Slug; once E-cadherin levels are decreased, it leads to decreased cellular adhesion (due to loss of tight junctions and desmosomes) and increased motility (Berx et al., 1998; Larue and Bellacosa, 2005; Qin et al., 2005; Caldeira et al., 2006; Huang et al., 2012; Serrano-Gomez et al., 2016). When E-cadherin levels decrease, a “cadherin switch” occurs, and the levels of N-cadherin (neural cadherin or CDH2) increase, which leads to altered cell adhesion, loss of association with other epithelial cells and increased affinity for mesenchymal cells (Wheelock et al., 2008; Yilmaz and Christofori, 2009; Theveneau and Mayor, 2012). Furthermore, a change also occurs in cytoskeletal genes, such as the type III intermediate filament vimentin, which then causes vimentin-driven increase in cell motility if upregulated (Mendez et al., 2010; Huang et al., 2012). It has also been

suggested that in addition to its upregulation playing a role in cellular migration, vimentin may also aid bacterial invasion into the host cell (Mak et al., 2012). Another change occurring during EMT is the increased expression of MMPs, which further assist the loss of adhesion by targeting the extracellular domain of CDH1 (Nisticò et al., 2012).

Multiple transcription factor repressors are involved in the initiation of EMT, including Snail, Slug, Twist (Serrano-Gomez et al., 2016). These factors induce the expression of each other and work synergistically on target sites (Peinado et al., 2007). A brief summary of EMT can be found in Figure 4.8

Snail and Slug both repress epithelial genes by binding to E-box (enhancer-box) sequences on DNA. For example, Snail binding an E-box proximal to the *CDH1* promoter region leads to the recruitment of a wide range of factors and results in epigenetic repression of its expression (Batlle et al., 2000; Cano et al., 2000; Peinado et al., 2007; Xu et al., 2009). *SNAI1* and *SNAI2* expression can be activated by a range of pathways, including TGF-β and Wnt/β-catenin, depending on the physiological context; activated by MAPK-signalling, Snail can activate the synthesis of MMPs, while if driven by SMAD3-SMAD4 it can cause E-cadherin suppression (Jordà et al., 2005; Vincent et al., 2009). Inhibition of SNAI1 phosphorylation by Wnt/β-catenin, PI3K-AKT, and NF-κB signalling increases its stability (Yook et al., 2006; Wu et al., 2009).

Twist is a member of the basic helix-loop-helix (bHLH) family of transcription factors. It can drive the "cadherin switch" by downregulating E-cadherin (e.g. by E-box suppression, leading to changes in morphology, increased migration and upregulation of vimentin) and inducing *CDH2* expression in a process independent of Snail (Yang et al., 2004; Yang et al., 2008; Xu et al., 2009; Yang et al., 2010; Yang et al., 2012). *TWIST* expression can be induced by a range of signals, HIF-1α in hypoxia or β-catenin as a response to stress, both of which can lead to oncogenesis (Farge, 2003; Yang et al., 2008)

4.1.7. Angiogenesis

The ability of tumours to induce angiogenesis is one of the hallmarks of cancer and it is necessary for the progression of malignancy (Hanahan and Weinberg, 2011b). The generation of new blood vessels allows nutrients to reach the cancer cells. The new vessels can also be used as means to spread the tumour around the body during metastasis (Raymaekers et al., 2015). The creation of new blood vessels in the body can

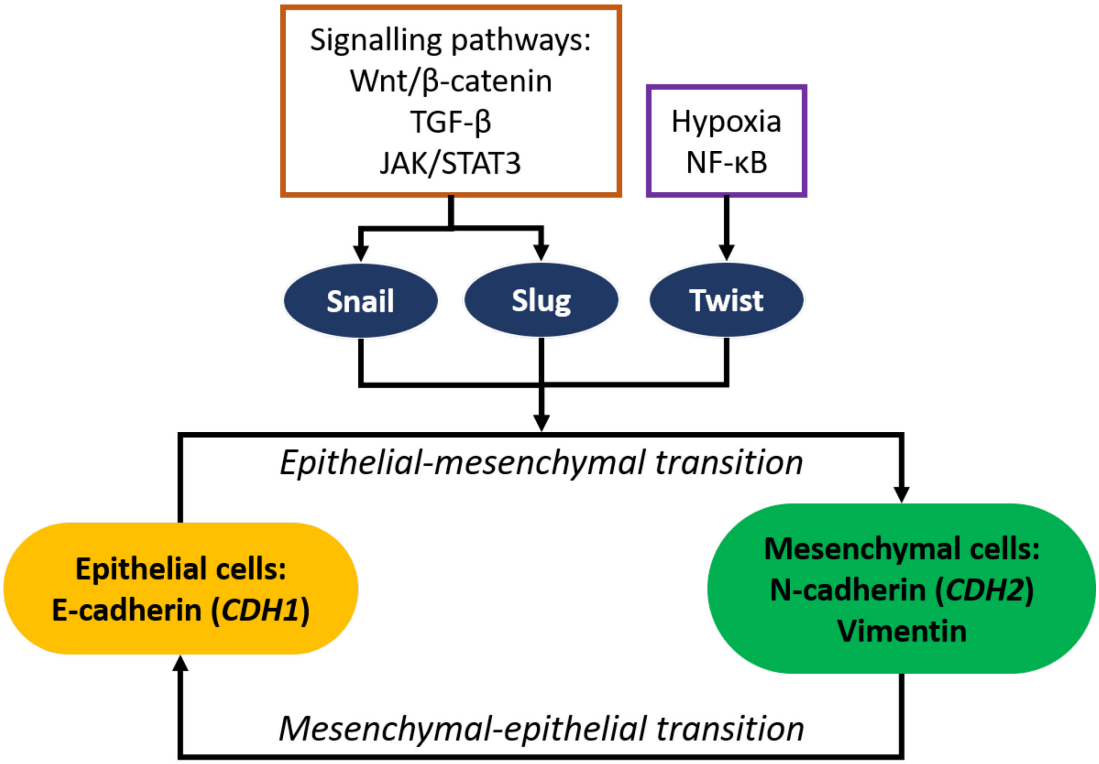

Figure 4.8. Summary of epithelial-mesenchymal transition

Epithelial cells normally express E-cadherin but when they undergo EMT that expression is lost and is replaced by increase in N-cadherin and vimentin. A number of signalling pathway, such as Wnt/β-catenin, TGF-β-signalling, JAK/STAT3 signalling can lead to an increase in Snail and Slug production which in turn can initiate EMT; similarly, hypoxia can increase the production of Twist which also has the ability to drive EMT.

Legend: JAK – Janus kinase; NF-κB – nuclear factor-kappa B; STAT3 – signal transducer and activator of transcription; TGF-β – transforming growth factor-beta;

be split into two categories. The *de novo* synthesis of blood vessels, seen mainly during development is called vasculogenesis; in contrast, if blood vessels originate from pre-existing blood vessels, the process is called angiogenesis (Vallée et al., 2017).

The main driver of angiogenesis is hypoxia, or the lack of adequate oxygen supply to highly proliferative cells (LaGory and Giaccia, 2016). Oxygen-sensitive prolyl hydroxylases are then activated in the hypoxic cell, and they hydroxylate hypoxia-inducible factor 1 subunit α (HIF-1α) (Bruick and McKnight, 2001). HIF-α can then form a dimer with the constitutively expressed HIF-1β subunit; the newly formed complex is translocated to the nucleus where it can initiate the transcription of a range of signalling pathways involved in immune response (both innate and adaptive immunity, with pathways including NF-κB, JAK-STAT3, etc.) and angiogenesis-inducing growth factors (Pugh and Ratcliffe, 2003; Ziello et al., 2007; Gorlach and Bonello, 2008; Demaria and Poli, 2012). The main angiogenesis promoting factor induced is VEGFA, however, placental growth factor (PlGF), fibroblast growth factors (FGF-1, FGF-2, FGF-7), EGF, insulin-like growth factor (IGF), platelet-derived growth factor (PDGF) and transforming growth factor β (TGF-β) also play a role (van Cruijsen et al., 2005; Lieu et al., 2011; Shibuya, 2011; Kim et al., 2012). An overview of the process can be seen in Figure 4.9.

Once VEGFA is released from the hypoxic cell, it interacts with its receptor, VEGFR2, located on the surface of endothelial cells (Abhinand et al., 2016). This leads to the differentiation of motile endothelial cells, called tip cells, which begin to break down the surrounding extracellular matrix and initiate the formation of vascular sprouts (De Palma et al., 2017). Additional factors, such as angopoietin-2 (ANGPT2) and delta ligand-like 4 (DLL4) are also necessary for the tight control of the process. In addition to hypoxia, some oncogenes can also initiate the process (Felcht et al., 2012). Thrombospondin-1 (TSP-1) acts as an inhibitor of the endothelial tip cells (Lawler, 2002).

Pericytes are accessory cells which are present in small blood vessels. Their main function is the regulation of survival and proliferation of endothelial cells, as well as inhibiting MMPs (Armulik et al., 2011).

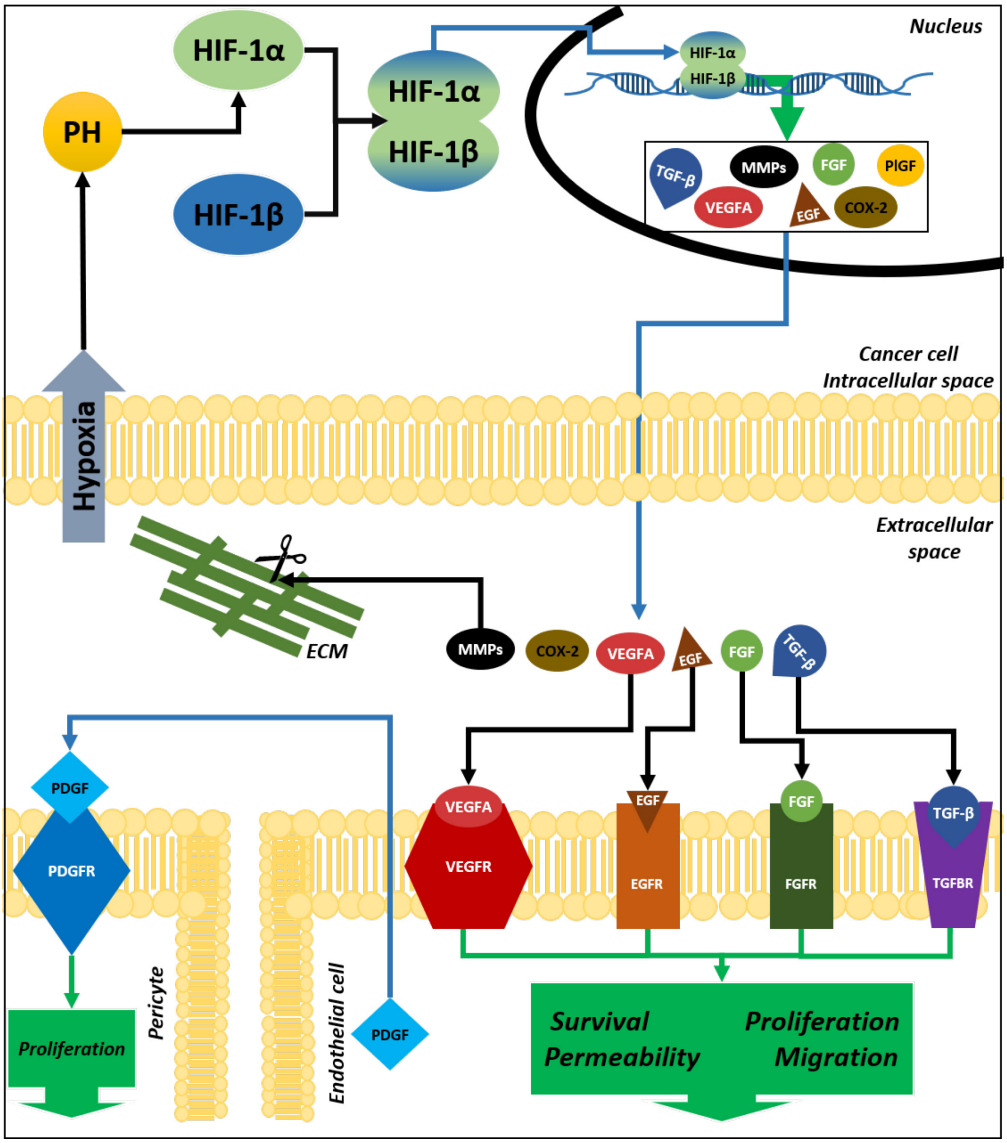

Figure 4.9. Hypoxia induced angiogenesis

Hypoxia activates prolyl hydroxylases (PH) which activate the α subunit of hypoxia inducing factor-1 (HIF-1α). HIF-1α then forms a dimer with HIF-1β, and the dimer is translocated to the nucleus where it induces the production of a range of molecules, including transforming growth factor beta (TGF-β), vascular endothelial growth factor A (VEGFA), matrix metalloproteinases (MMPs), epidermal growth factor (EGF), fibroblast growth factor (FGF), cyclooxygenase-2 (COX-2) and placental growth factor (PlGF). These molecules are then secreted by the hypoxic (cancer) cell. The MMPs can target the extracellular matrix (ECM) which allows endothelial tip cells to become motile. The remaining growth factors can interact with receptors on the surface of endothelial cells, initiating a range of processes, including survival, proliferation, migration. The signals also cause the production of platelet-derived growth factor (PDGF) by the endothelial cells which is secreted and can interact with pericytes, which are important for the formation and sustainability of the basal layer of small blood vessels.

Legend: EGFR – EGF receptor; FGFR – FGF receptor; PDGFR – PDGF receptor; TGFBR – TGF-β receptor; VEGFR – VEGF receptor;

4.1.7.1. Angiogenesis and cancer

Before progression to cancer, tumours originate as hyperplasia, which can then acquire mutations to become a carcinoma *in situ* (De Palma et al., 2017). What both these states have in common is that the basal layer of cells is intact, and the cancer cells cannot interact with the stromal cells. As a result, angiogenesis is rarely found in these two cancer-precursors. Once the cancer becomes invasive and escapes the basal layer it can then interact with the stroma, activating the so-called "angiogenic switch", i.e. initiating angiogenesis (Bergers and Benjamin, 2003). It is worth noting that blood vessel created within a tumour differ from healthy vessels. They are larger in size, with distorted morphology and increased branching; this results in issues with blood flow and can cause the vessels to leak (Huang et al., 2004; Baluk et al., 2005).

4.1.7.2. Angiogenesis and inflammation

Chronic inflammation and chronic infection also have the potential to induce angiogenesis. When the JAK/STAT3 pathway is activated, this causes an increase in the production of the pro-angiogenic factor VEGFA, and also leads to an increase in IL-6 levels, which drives further induction of the JAK/STAT3 pathway (Thomas et al., 2015).

Additionally, infection summons leukocytes to the site, including monocytes. When the monocytes follow the chemokine signalling and extravasate to the location where the signalling originates, they differentiate into macrophages (with the help of the macrophage colony-stimulating factor or M-CSF) (Bender et al., 2004). The tumour associated macrophages can then secrete a range of pro-angiogenic factors, including VEGFA, PlGF, VEGFC, as well as a number of cytokines which can summon more inflammatory cells to the site (Lewis et al., 2000; Baer et al., 2013). The macrophages can also initiate the Wnt/β-catenin signalling in the endothelial cells, thus activating the tip cells and initiating migration and sprout formation (Newman and Hughes, 2012).

Another key player in inflammation, cyclooxygenase-2 (COX-2), is commonly upregulated in cancer and precursor neoplasia, including prostate cancer and prostate intraepithelial neoplasia (Khor et al., 2007). COX-2 can also promote angiogenesis and cancer progression in general, as it can induce the production of MMP-2 and MMP-9 (which are involved in motility), VEGFA, FGF and PDGF (Fosslien, 2001; Albini et al., 2012; Liu et al., 2015). The inhibition of COX-2 can interfere with this upregulation, thus aspirin

and other nonsteroidal anti-inflammatory drugs have been suggested as possible anti-angiogenic preventative treatment (Sooriakumaran and Kaba, 2005).

Using molecular techniques, this chapter investigates the dysregulation of inflammatory and EMT-related genes, which have the potential to induce oncogenesis, in acute and chronic infection models with different phylotypes of *P. acnes* and *P. granulosum*, as a control strain. It also looks at cellular and bacterial behaviour in the different infection models, as well as anchorage-independent growth and migration of chronically infected cells. To investigate whether infection has the potential to cause increased endothelial cell proliferation rates, endothelial cells were treated with conditioned medium from a range of long-term infection models. This allowed for comparison of the angiogenic potential of different phylogenetic strains.

4.2. *Materials and Methods*

4.2.1. Cell and bacterial culture

RWPE-1 prostate epithelial cells were cultured as outlined in Section 2.1.1. *P. acnes* strains selected in Chapter 3, *P. avidum* and *P. granulosum* were routinely cultured as described in Section 2.2.1. Infection models were set up following the protocol outlined in Section 2.3.1, using multiplicity of infection (MOI) of 15:1, as optimised in Chapter 3 (Section 3.3.5). Acute infection models were defined as 24, 48 and 72 hours and were performed as seen in Section 2.3.2. Chronic infections lasted 15 or 30 days, and were maintained as described in Section 2.3.3.

Human dermal microvascular endothelial cells (HDMEC, HMEC-1 cell line) were routinely cultured in Medium 200 supplemented with low serum growth supplement (LSGS) as described in Section 2.1.1.

4.2.2. RWPE-1 cell viability counts and bacterial counts

Trypan blue viability counts were performed as described in Section 2.1.1 and bacterial counts were done using the Miles Misra counting method outlined in Section 2.2.2.

4.2.3. Intracellular bacterial counts

Intracellular bacterial counts were performed as described in Section 2.3.6, following optimisation steps outlined in Chapter 3, Section 3.3.6.

4.2.4. LDH assay

The Pierce lactate dehydrogenase (LDH) cytotoxicity assay (ThermoFisher Scientific, UK) was used to assess the cytotoxic effect different strains have on prostate epithelial cells following the manufacturer's protocol (summarised in Section 2.3.5).

4.2.5. Molecular methods

To analyse the molecular dysregulation in infected RWPE-1 cells, RNA was extracted using the RNeasy Plus Mini-Kit (QIAGEN, Germany) following manufacturer's protocol (see Section 2.4.2.1). RNA was quantified as described in Section 2.4.1.1 for short term infections using Nanodrop 1000 (ThermoScientific, UK) or following Section 2.4.1.2 for long-term infection using the Qubit® BR Assay kit (Invitrogen, UK). cDNA was synthesized as outlined in Section 2.4.2.3 and qPCR was performed following Section 2.4.2.4.1 using the reference gene *HPRT1*, as optimised in Chapter 3, Section 3.3.10. Ratio change was calculated using the formula shown in Section 2.4.2.4.3 and efficiencies from Table 3.6 in Chapter 3. Any change of more than 2-fold was considered significant.

4.2.6. Soft agar assays

Soft agar assays were used to assess anchorage independent growth of RWPE-1 cells following a long-term infection. The assays were prepared, stained and imaged following Section 2.3.7.

4.2.7. Immunofluorescence methods

Immunofluorescence staining using the PathScan® Duplex IF kit (Cell Signalling) and analysis were performed as described in Section 2.3.8.

4.2.8. Scratch assay

Scratch assays were used to assess cell migration. They were performed as outlined in Section 2.3.9 and imaged every 24 hours until the scratch had healed.

4.2.9. MTT assay

MTT assays were performed as described in Section 2.3.10. Briefly, the HDMEC cells were seeded at 50,000 cells/ml (5 x 10^4 cells/well), as optimised in Chapter 3 (Section 3.3.12) and were left overnight to attach. The medium was then replaced with a serial dilution of Day 30, long-term infection conditioned medium (and incubated for 72 hours (as optimised in Chapter 3, Section 3.3.14) at 37°C, 5% CO_2. The conditioned medium was diluted with complete Medium 200 and dilutions were selected based on the

amount of conditioned medium available (neat, 1:10, 1:50, 1:100, 1:200, 1:500, 1:1,000, 1:5,000, 1:10,000 and 1:100,000). As a positive proliferation control, the HDMEC cells were grown in complete Medium 200 containing 20% (v/v) FBS, and as a negative control, the cells were treated with etoposide to a final concentration of 2.5 µM (as optimised in Chapter 3, Section 3.3.13). MTT was added to each well to a final concentration of 1.2 mM and was incubated for 3 hours. The formed formazan was then solubilised with 100 µl DMSO, the plates were mixed and analysed at 570 nm (Epoch, BioTek Instruments, US). Student's t-test (2-tailed) was used to assess the effect treatment with conditioned medium from chronic infection models with a range of *P. acnes* strains had on the HDMEC cells in comparison to cells treated with conditioned medium from uninfected controls.

4.3. *Results*

4.3.1. Acute infection models

4.3.1.1. Cell counts and viability

Short term infections investigated bacterial and epithelial cell behaviour over a 72-hour period (Figure 4.10). Overall, in all short-term *P. acnes* and *P. granulosum* infections the number of cells/ml increased over time and the cells remained viable. There was no significant difference in the number of RWPE-1 cells/ml between infected and non-infected "mock" infection models at the 24-hour time point. Cells infected with ST27 and NCTC10390 displayed significantly lower number of cells/ml at 48 hours compared to untreated controls, although the significance was lost at 72 hours ($p = 0.0199$, Figure 4.10.C and $p = 0.0028$, Figure 4.10.E, left) and thus it is likely and experimental artefact, rather than a genuine result. Cells infected with NCTC737 and B3 showed counts significantly lower than untreated controls counts solely at 72 hours ($p = 0.0047$, Figure 4.10.B and $p < 0.0001$, Figure 4.10.D, left, respectively). In cells infected with *P. granulosum*, there was a significant difference in cells/ml at both 24 ($p = 0.0142$) and 48 hours ($p = 0.0231$) but the significance was lost by day 3 (Figure 4.10.G, left). In the case of *P. avidum* acute infection, there was no significant difference at 24 hours, but the cell numbers decreased significantly at 48 hours ($p = 0.0065$) and were undetectable by 72 hours ($p = 0.0015$, Figure 4.10, left).

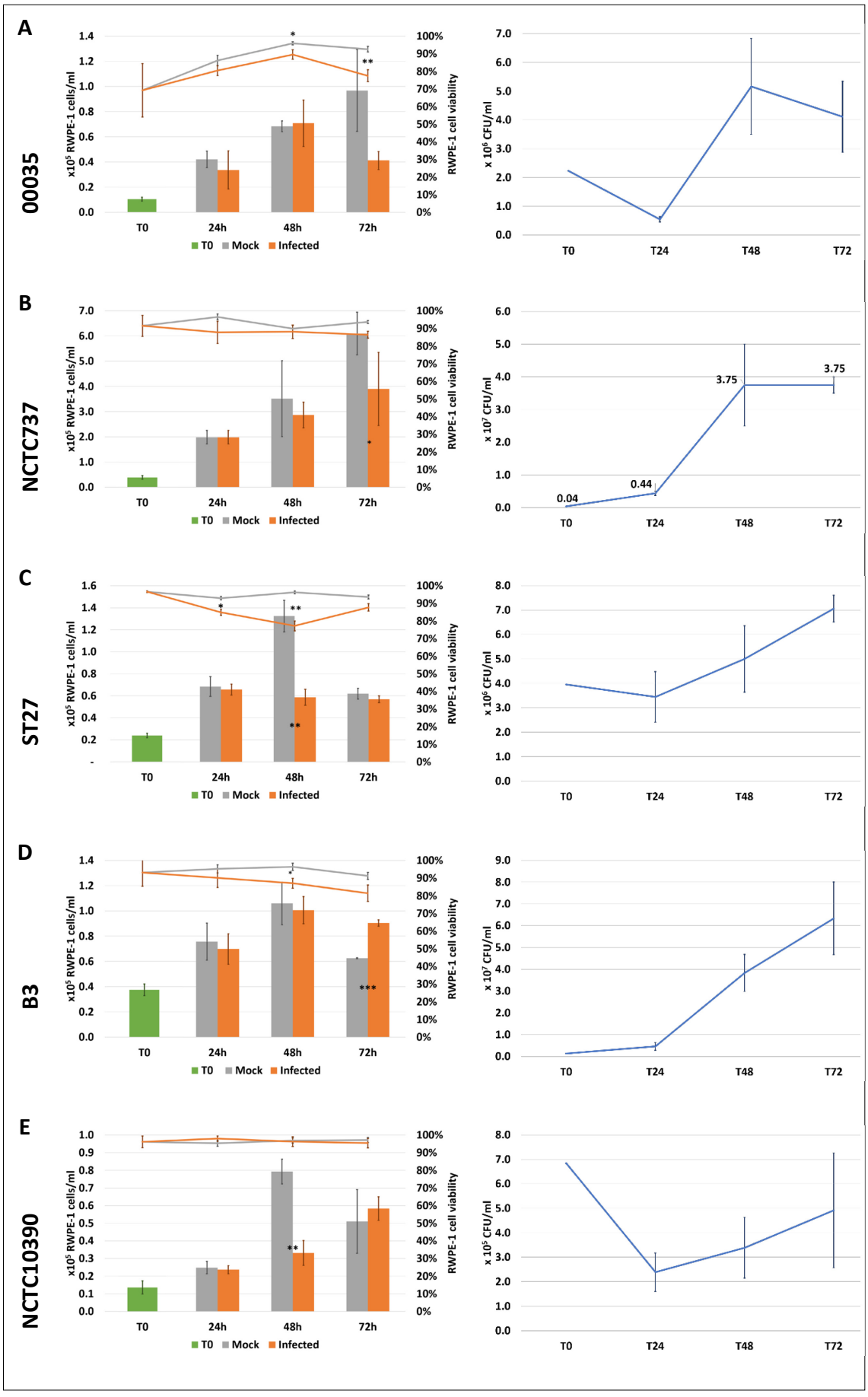
A
00035
x10⁵ RWPE-1 cells/ml
RWPE-1 cell viability
T0
24h
48h
72h
T0 Mock Infected
x 10⁶ CFU/ml
T0
T24
T48
T72
B
NCTC737
x10⁵ RWPE-1 cells/ml
RWPE-1 cell viability
T0 Mock Infected
x 10⁷ CFU/ml
3.75
3.75
0.44
0.04
C
ST27
x10⁵ RWPE-1 cells/ml
RWPE-1 cell viability
T0 Mock Infected
x 10⁶ CFU/ml
D
B3
x10⁵ RWPE-1 cells/ml
RWPE-1 cell viability
T0 Mock Infected
x 10⁷ CFU/ml
E
NCTC10390
x10⁵ RWPE-1 cells/ml
RWPE-1 cell viability
T0 Mock Infected
x 10⁵ CFU/ml

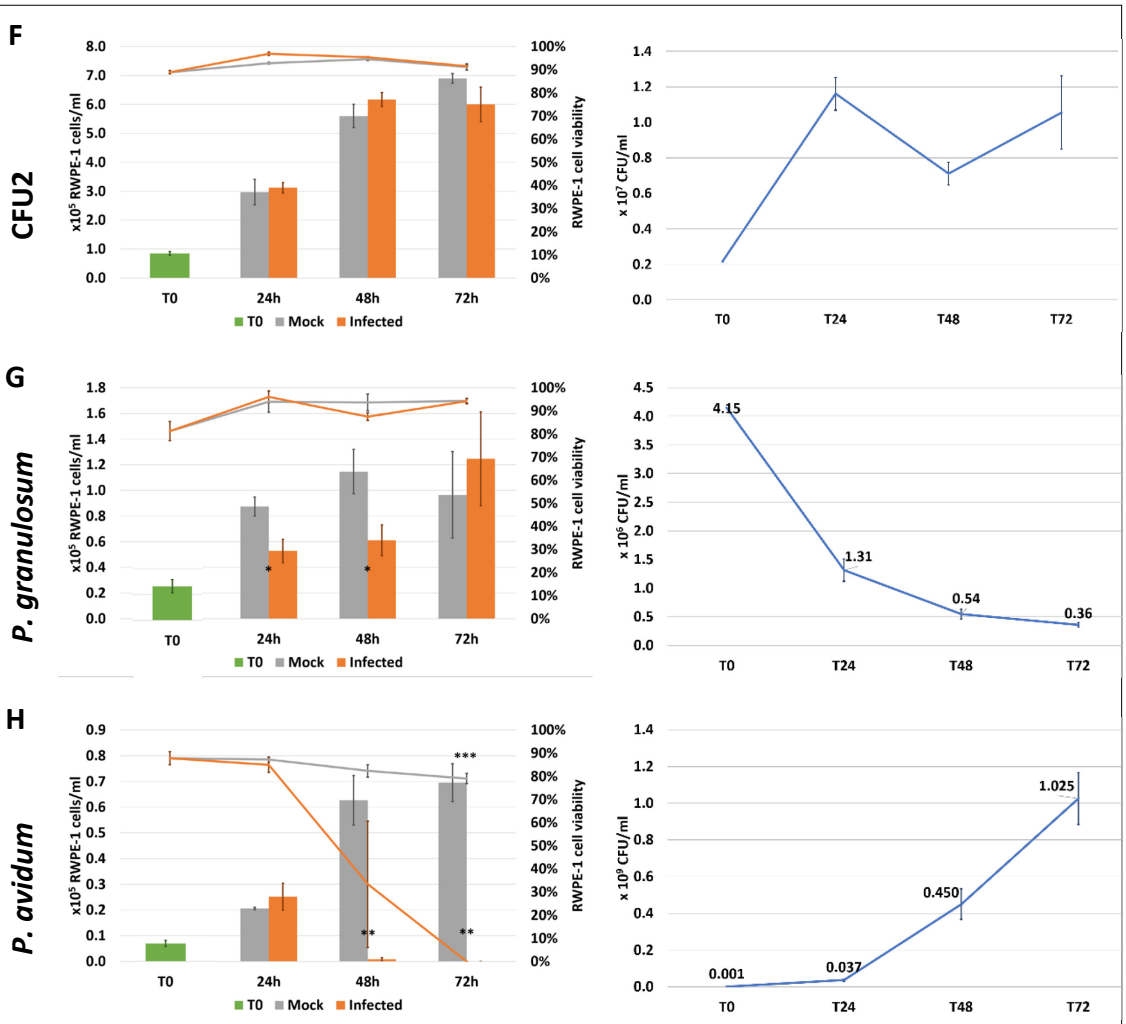

Figure 4.10. RWPE-1 cell counts and viability (left) and bacterial counts (right) in short-term infections

Left: RWPE-1 cell count (bars) and viability count (lines) values representing uninfected ("mock"; grey) and infected cells (orange). Right: bacterial counts. Change in the counts presented for each infection model at T0, 24, 48 and 72 hours. Data presented as mean of three biological replicates, +/- standard error. * $p < 0.05$; ** $p < 0.01$; *** $p < 0.001$.

A. 00035; **B.** NCTC737; **C.** ST27; **D.** B3; **E.** NCTC10390; **F.** CFU2; **G.** *P. granulosum*; **H.** *P. avidum*.

The values for T0 (green) represent counts prior to infection, used to calculate the amount of bacterial suspension needed to achieve MOI 15:1, and are thus the same between infection models and "mock" controls.

In cells infected with NCTC10390, CFU2 and *P. granulosum*, there was no significant difference in cell viability for the duration of the experiment (Figure 4.10.E., Figure 4.10.F and Figure 4.10.G, left). Cells infected with ST27 had significantly lower viability at time points 24 and 48 hours ($p = 0.0285$ and $p = 0.0061$, respectively), but the values did not significantly differ at 72 hours, although they were still lower for infected cells (Figure 4.10.C, left). Cells infected with 00035 also displayed viability lower than "mock" infections, which became significant at 48 hours ($p = 0.034$) and remained significant at day 3 ($p = 0.005$; Figure 4.10.A, left). In the *P. avidum* infection model, there was a rapid decrease in viability and there were no viable cells at the 72-hour time point (Figure 4.10.H, left).

4.3.1.2. Bacterial counts

The decrease in viability in the *P. avidum* infection model directly correlated with the rapid increase of bacterial counts in the infection model, increasing from 3.7×10^7 CFU/ml at 24 hours to 1×10^9 CFU/ml at day 3 (Figure 4.10.H, right). The counts for NCTC10390 underwent a rapid decrease at the 24-hour time point compared to the initial inoculum, however, the counts then began to rise slowly, reaching 5×10^5 CFU/ml at 72 hours (Figure 4.10.E, right). Both 00035 and ST27 demonstrated an initial decline, which was more prominent in 00035, and then increased slowly overtime to 4×10^6 and 7×10^6 CFU/ml, respectively (Figure 4.10.A and Figure 4.10.C, right). NCTC737 and B3 both increased steadily for the duration of the experiment with values at 72 hours of 3.8×10^7 and 6.2×10^7 CFU/ml, respectively (Figure 4.10.B and Figure 4.10.D, right). CFU2 demonstrated an initial increase, followed by a small dip in numbers at 48 hours and a further increase at 72 hours; however, due to the size of the error bars these numbers can be interpreted as an initial increase, followed by a plateau (Figure 4.10.F.). In contrast with the *P. acnes* strains and *P. avidum*, *P. granulosum* showed a decline in numbers overtime, with counts at 72 hours more than 10-fold lower than the initial inoculum (Figure 4.10.G, right).

4.3.1.3. LDH assay

The cytotoxicity of each strain was measured using a colorimetric LDH assay. Most strains were not shown to be cytotoxic, with levels below 4% (Figure 4.11). Strain 00035 showed an initially relatively high cytotoxicity of 8.7%, which decreased overtime, while

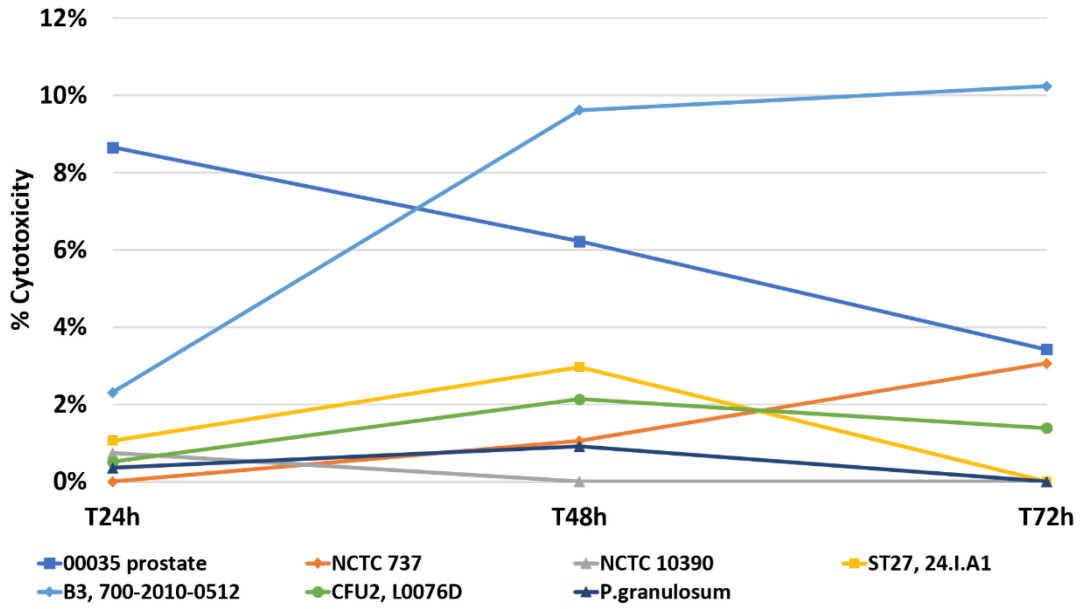

Figure 4.11. Strain cytotoxicity seen in acute infection models

The cytotoxic effect different strains of *P.* acnes and *P. granulosum* have on RWEP-1 prostate epithelial cells in acute infection models was assessed using an LDH assay and presented as percentage (%) cytotoxicity for each time point. The data is represented as mean value of three biological replicates.

If the calculated value was a negative number, the % cytotoxicity was presented as 0% (seen in strain NCTC10390 and *P. granulosum*)

the opposite was seen with strain B3 which was more cytotoxic the longer the cells were exposed to it (2.3% at 24 hours, 9.6% of 48 hours and 10.2% at 72 hours). The remaining strains showed negligible changes in cytotoxicity, and remained below 4% for the duration of the experiment.

4.3.1.4. Intracellular bacterial counts

Bacterial counts were performed on lysed RWPE-1 cells following an incubation in antibiotic, aiming the eradication of any extracellular bacteria. These counts were performed to investigate the ability of different *P. acnes* strains and *P. granulosum* to become intracellular in human prostate epithelial cells. While the absolute counts for the different strains varied at each time point, there was no statistical significance between time points. The strain with the highest intracellular counts was 00035 at 8 x 10^4 CFU/ml (Figure 4.12). ST27, NCTC737 and B3 also displayed the ability to survive intracellularly with numbers above 2 x 10^4 for the duration of the experiment. NCTC10390, CFU2 and *P. granulosum* had intracellular counts lower than 00035 and ST27, with NCTC10390, having the lowest counts at 2-3 x 10^3 CFU/ml.

4.3.1.5. qPCR analysis of inflammatory and EMT-related genes

The dysregulation of a number of prostate cancer-related inflammatory genes, as well as genes linked with EMT was assessed using qPCR. Any fold-changes of less than 2-fold increase or -2-fold decrease were regarded as insignificant. Complete figures for the individual results for all genes and all infection models can be found in Appendix B.

Strain 00035 induced an acute immune response, causing significant increase in the expression of *IL6*, *IL8* and *TNF*; the levels of *IL8* and *TNF* were highest at 24 hours and gradually decreased overtime. An induction of *IL1B* was also present, with a peak spike of 5-fold increase at 48h. A similar pattern was seen in *SNAI1* with a 10-fold increase also at 48 hours, while *SNAI2* showed significant downregulation at 72 hours. *CDH2* demonstrated an initial upregulation of 10-fold with values decreasing gradually over the time course of the experiment.

The skin health-associated strain ST27 caused a significant increase in all inflammatory genes with values rising over time, and only *TGFB* showing significance solely at 72 hours. ST27 also induced trends towards increasing *CDH2*, *SNAI1*, *SNAI2* and *TWIST*,

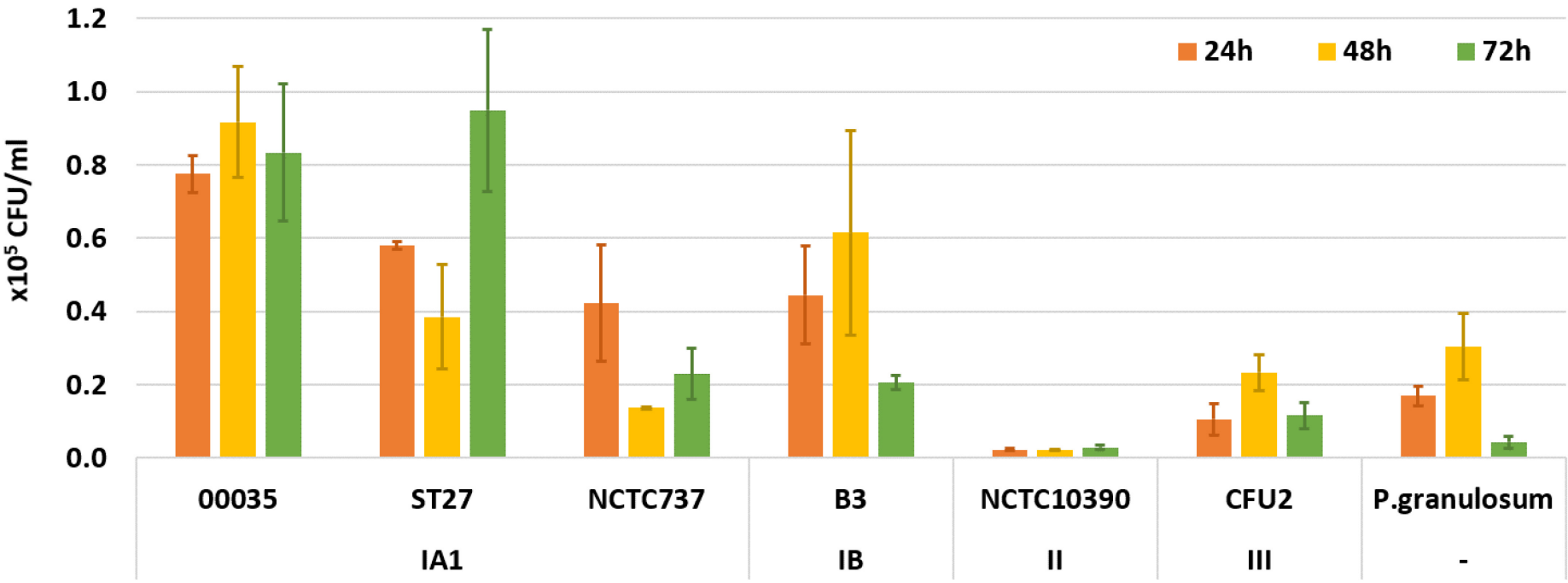

Figure 4.12. Intracellular counts in acute infection models

Intracellular counts of *P. acnes* strains and *P. granulosum* in RWPE-1 cells at 24h, 48h and 72h post-infection. Values are presented as mean of three replicates with any viable extracellular bacteria subtracted. The data is presented as mean of three biological replicates, +/- standard error.

however, significance was only seen with *CDH2* at 24 hours (4.3-fold increase), *SNAI1* at 48 hours (3.5-fold increase) and *CDH2*, *SNAI1* and *VIM* at 72 hours (14.5-fold, 6.3-fold and 4.7-fold upregulation, respectively).

With the reference strain NCTC737, a significant upregulation in *IL6*, *TNF* and *TGFB* was observed, as well as a steady increase in *SNAI1* for the duration of the experiment.

The type IB strain, B3, displayed significantly upregulated *IL6*, *IL8* and *TNF*, with an increase seen at 24h, followed by a steady decrease. *IL1B* was also upregulated, reaching a peak at 48h, however, its values were lower than the above-mentioned cytokines. Out of the EMT genes investigated, only *SNAI1* showed any noteworthy change of 10-fold upregulation at 48 hours.

Strain NCTC1090 also induced *IL6* and *TNF*, with *TNF* peaking at 24 hours and decreasing thereafter. Significant downregulation was seen in *IL1B* at 24 hours and in *SNAI2* at 72 hours.

Infection with the type III strain CFU2, led to a mild increase in *TNF* and *IL6* levels, and a decrease in the expression of most other genes, including *TGFB* and *IL8* (-10.5-fold and -3.4-fold decrease in expression, respectively).

Finally, *P. granulosum*-infected cells expressed higher levels of all inflammatory genes (excluding *TGFB*) compared to untreated controls. In the inflammatory genes levels, a clear increase was seen overtime for *IL1B, IL6, IL8*, and there were no statistically significant changes in the expression of the investigated genes with the exception of *SNAI1 with* -2.6-fold decrease of at 72 hours.

Comparing the gene dysregulation between strains, at 24 hours the cells infected with 00035 had the highest upregulation of *IL6, IL8* and TNF, with expression of these genes also being increased by ST27, B3 and *P. granulosum*. NCTC737 and NCTC10390 also led to an increase in *IL6* and *TNF*. NCTC737 also caused the highest upregulation (20.6-fold) of *TGFB* at this timepoint, while CFU2 caused significant downregulation of *TGFB* (-10.5-fold). *IL1B* expression was poorly affected by infection at 24 hours, with the only strain showing significant dysregulation being a 5-fold decrease caused by NCTC10390. Summary of the inflammatory gene dysregulation can be found in Figure 4.13.A, and Figure 4.13.B shows the dysregulation of EMT genes.

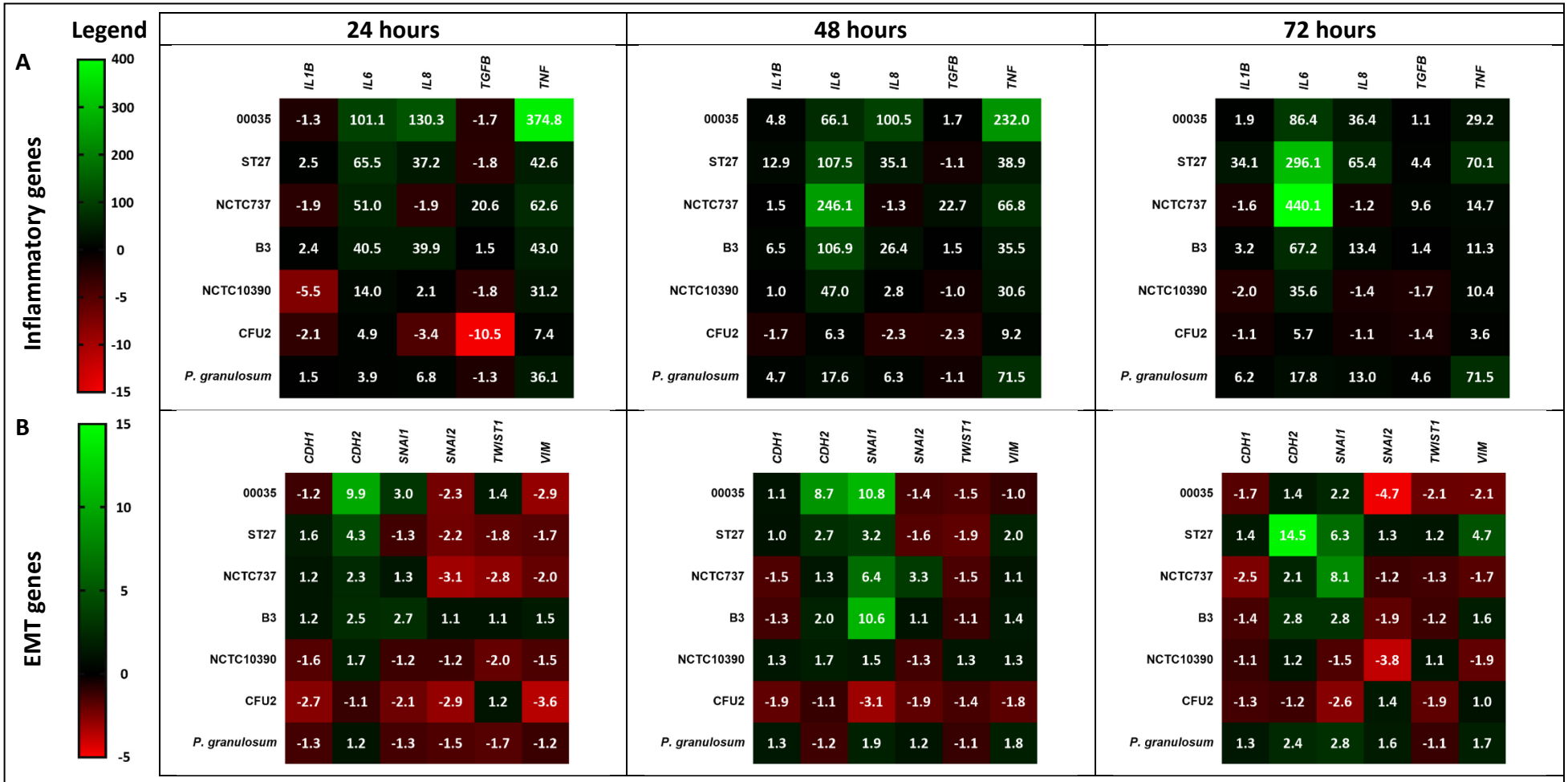

Figure 4.13. Gene dysregulation in short-term infection models

Gene dysregulation in RWPE-1 cells infected with different strains of *P. acnes* and *P. granulosum.* The data is presented as mean fold change of three biological replicates and is normalised to non-infected controls using HPRT as a housekeeping gene. **A.** Inflammatory genes; **B.** Epithelial-mesenchymal transition genes

At 48 hours, strains 00035, ST27 and B3 once again led to significant upregulation of *IL6*, *IL8* and *TNF*, while strains NCTC737, NCTC10390 and *P. granulosum* only caused significant upregulation of *IL6* and *IL8.* CFU2 infected cells also displayed upregulation of *IL6* and *TNF* but at levels lower compared to the other strains tested. *IL1B* was upregulated in cells infected with 00035, ST27, B3 and *P. granulosum*, and no significant downregulation was seen at this time point. *TGFB* expression was only affected by two strains: NCTC737 infection led to a 22.7-fold upregulation, while CFU2 caused a mildly significant downregulation at -2.3-fold.

By day 3, NCTC737 had caused a 440-fold increase in the expression of *IL6* compared to uninfected controls; an almost 300-fold increase was also observed in cells infected with ST27.

Overall, *IL6* was significantly upregulated in infections with all strains, with expression levels ranging between 5.7-fold and 440-fold. *TNF* exhibited high expression levels in all infection models with highest fold-change seen in ST27 and *P. granulosum* (70-fold and 71.2-fold increase, respectively), and the lowest of 3.6-fold in cells infected with CFU2. *IL1B* levels were affected by *ST27* (34-fold increase)*, P. granulosum* (6.2-fold increase) and B3 (3.2-fold increase) and no downregulation was seen. *IL8* expression was increased by infection with 00035, ST27, B3 and *P. granulosum*, and increased expression of *TGFB* was seen in infection models with ST27*,* NCTC737 and *P. granulosum.* At the 72-hour time point, only two infection models showed significant upregulation of all 5 inflammatory genes tested (ST27 and *P. granulosum*), while no significant downregulation in expression was seen.

At 24 hours, dysregulation of the EMT genes investigated was within +/- 3-fold difference for most genes and strains. Exception to this was *CDH2* cells infected with 00035 and ST27, where the observed upregulation was 10-fold and 4.3-fold, respectively. *SNAI1* also showed a mild increase in expression in the 00035 and B3 infection models, with fold change of 3-fold and 2.7-fold, respectively. *SNAI2* was downregulated 3.1-fold in cells infected with NCTC737, and *VIM* expression was decreased 3.6-fold in the CFU2 infection model. Figure 4.13.B presents heatmaps of the gene dysregulation observed.

The 48-hours timepoint uncovered significant upregulation of the expression of *SNAI1* in 00035, ST27, NCTC737, and B3-infected cells (10.8-fold, 3.2-fold, 6.4-fold, and 10.6-fold, respectively) and downregulated -3.1-fold in the CFU2 infection model. Changes were also seen in the expression of *CDH2* in cells infected with 00035 and ST27, as well as in *SNAI2* in the NCTC737 infection model.

At 72 hours, significant upregulation in *CDH2* was only seen in the ST27 infection model (14.5-fold). *SNAI1* had significantly increased expression in cells infected with ST27, NCTC737, B3 and *P. granulosum* (6.3-fold, 8.1-fold, 2.8-fold and 2.8-fold, respectively). *VIM* also showed an increase with ST27 treatment (4.7-fold). Finally, downregulation in *SNAI2* was seen in the presence of 00035 (-4.7-fold) and NCTC10390 (-3.8-fold). *SNAI1* was downregulated in cells infected with CFU2, and *CDH1* expression was significantly decreased in the NCTC737 infection model

4.3.2. Chronic infection model

4.3.2.1. Cell counts and viability

Trypan blue viability counts were performed at every passage point in all long-term infection models for the duration of the experiment. The RWPE-1 cells remained viable in all chronic infection models, for the 30 days of the experiments. The NCTC10390 infection models was only continued for 15 days due to time constraints. Overall, there was no significant difference in cell numbers between infected and non-infected cells (Figure 4.14.D, Figure 4.14.E and Figure 4.14.F, left). Where significance was seen, it was only in one (Figure 4.14.C, left, D20, $p = 0.0476$ and Figure 4.14.G, left, D20, $p = 0.0057$) or two time points (Figure 4.14.A, left, D20, $p = 0.0254$ and D25, $p = 0.0017$ and Figure 4.14.B, D10, $p = 0.001$ and D30, $p = 0.0422$) but the significance was lost in following counts. The viability counts also showed no significant difference between “moc”k and infected cells, and again, if any significance was seen it was lost by the following time point (Figure 4.14).

4.3.2.2. Bacterial counts

Bacterial counts in the media were assessed in all chronic infection models at every passage time point. There were two trends seen in bacterial numbers. Strains 00035, NCTC737 and B3 demonstrated the ability to remain viable in the long-term infection

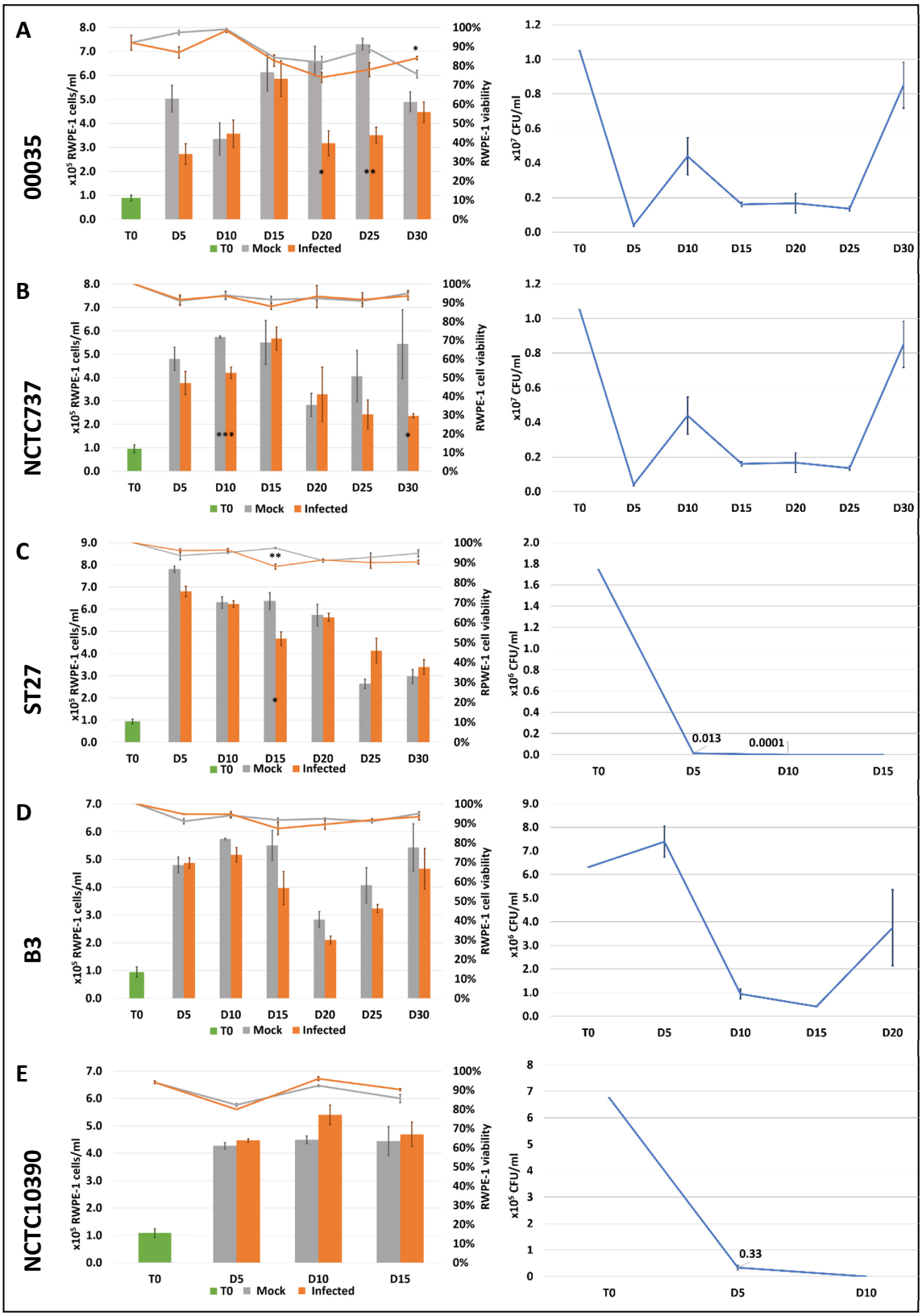
A
00035
x10⁵ RWPE-1 cells/ml
RWPE-1 viability
T0 Mock Infected
x10⁷ CFU/ml
B
NCTC737
x10⁵ RWPE-1 cells/ml
RWPE-1 cell viability
T0 Mock Infected
x10⁷ CFU/ml
C
ST27
x10⁵ RWPE-1 cells/ml
RPWE-1 cell viability
T0 Mock Infected
x10⁶ CFU/ml
0.013
0.0001
D
B3
x10⁵ RWPE-1 cells/ml
RWPE-1 cell viability
T0 Mock Infected
x10⁶ CFU/ml
E
NCTC10390
x10⁵ RWPE-1 cells/ml
RWPE-1 viability
T0 Mock Infected
x10⁵ CFU/ml
0.33

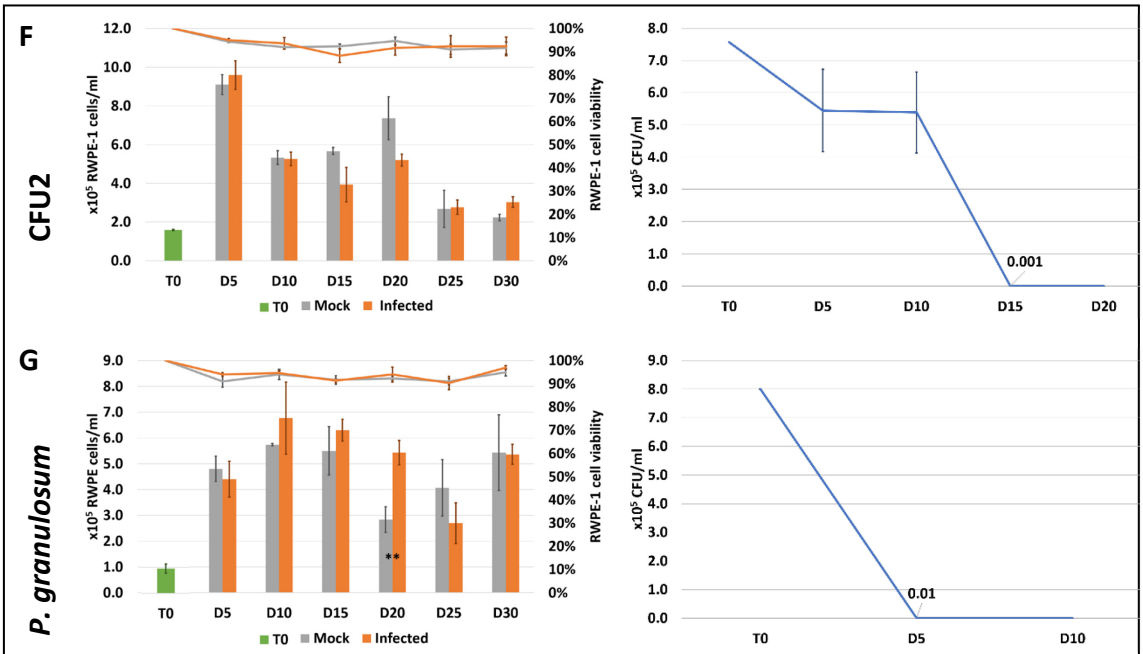

Figure 4.14. RWPE-1 cell counts and viability (left) and bacterial counts (right) in long-term infections

Left: RWPE-1 cell count (bars) and viability count (lines) values representing uninfected "mock" (grey) and infected cells (orange). Right: bacterial counts. Change in the counts presented for each infection model at T0, day 5 (D5), day 10 (D10), day 15 (D15), day 20 (D20), day 25 (D25) and day (30). Data presented as mean values of three biological replicates, +/- standard error. * $p < 0.05$; ** $p < 0.01$; *** $p < 0.001$

A. 00035; **B.** NCTC737; **C.** ST27; **D**. B3; **E.** NCTC10390; **F.** CFU2; **G.** *P. granulosum*

The values for T0 (green) represent counts prior to infection, used to calculate the amount of bacterial suspension needed to achieve MOI 15:1, and are thus the same between infection models and "mock" controls.

models, meaning the RWPE-1 cells remained challenged with bacteria for the duration of the experiment (Figure 4.14.A, Figure 4.14.B and Figure 4.14.D, right). In contrast, bacterial counts in infection models ST27, NCTC10390, CFU2 and *P. granulosum*, showed a rapid decrease, with bacteria being undetectable by day 10 in the NCTC10390 and P. granulosum infection models (Figure 4.14.E and Figure 4.14.G, right), by day 15 in the case of ST27 (Figure 4.14.C) and by day 20 in the CFU2 infection model (Figure 4.14.F, right).

4.3.2.3. qPCR

Real-time qPCR analysis was performed to investigate the dysregulation of inflammatory and EMT-related genes at day 15 and day 30 of chronic infections (Figure 4.15). Complete figures for the individual results for all genes and all infection models can be found in Appendix C.

Strain 00035 caused significant increase in expression of all inflammatory genes investigated at day 15, namely increase in *IL1B*, *IL6*, *IL8*, *TGFB* and *TNF* with 13.8-fold, 9.7-fold, 8.5-fold, 13.2-fold and 2.6-fold, respectively. Three of these genes were still upregulated at day 30 – *IL6* (6.7-fold), *IL8* (9.8-fold), and *TNF* (20.5-fold).

The ST27 infection showed a mild upregulation of *IL1B*, *IL6* and *IL8* at day 15 with fold change of 3.1-fold, 3-fold and 3.4-fold, respectively; only a 2.2-fold increase in *IL6* expression was seen in this infection at day 30.

NCTC737 showed significant dysregulation in all genes tested at the day 15 time point with downregulation seen in *TNF*, and increase seen in the rest of the genes. By day 30, the downregulation of *TNF* was lost, however, the rest of the genes remained upregulated.

The B3-infections showed a mild upregulation of *IL6, IL8* and *TGFB* (4.1-fold, 2.3-fold and 3.6-fold, respectively) and a downregulation of *TNF* (-2.2-fold) at day 15, and an upregulation of all inflammatory genes at day 30 (ranging between 3.1-fold and 7.7-fold).

Cells infected with NCTC10390 were only sustained for 15 days, and thus dysregulation information is only available for this time point, showing significant increase in *IL1B, IL8* and *TGFB* with 5.5-fold, 2.2-fold and 3-fold change, respectively.

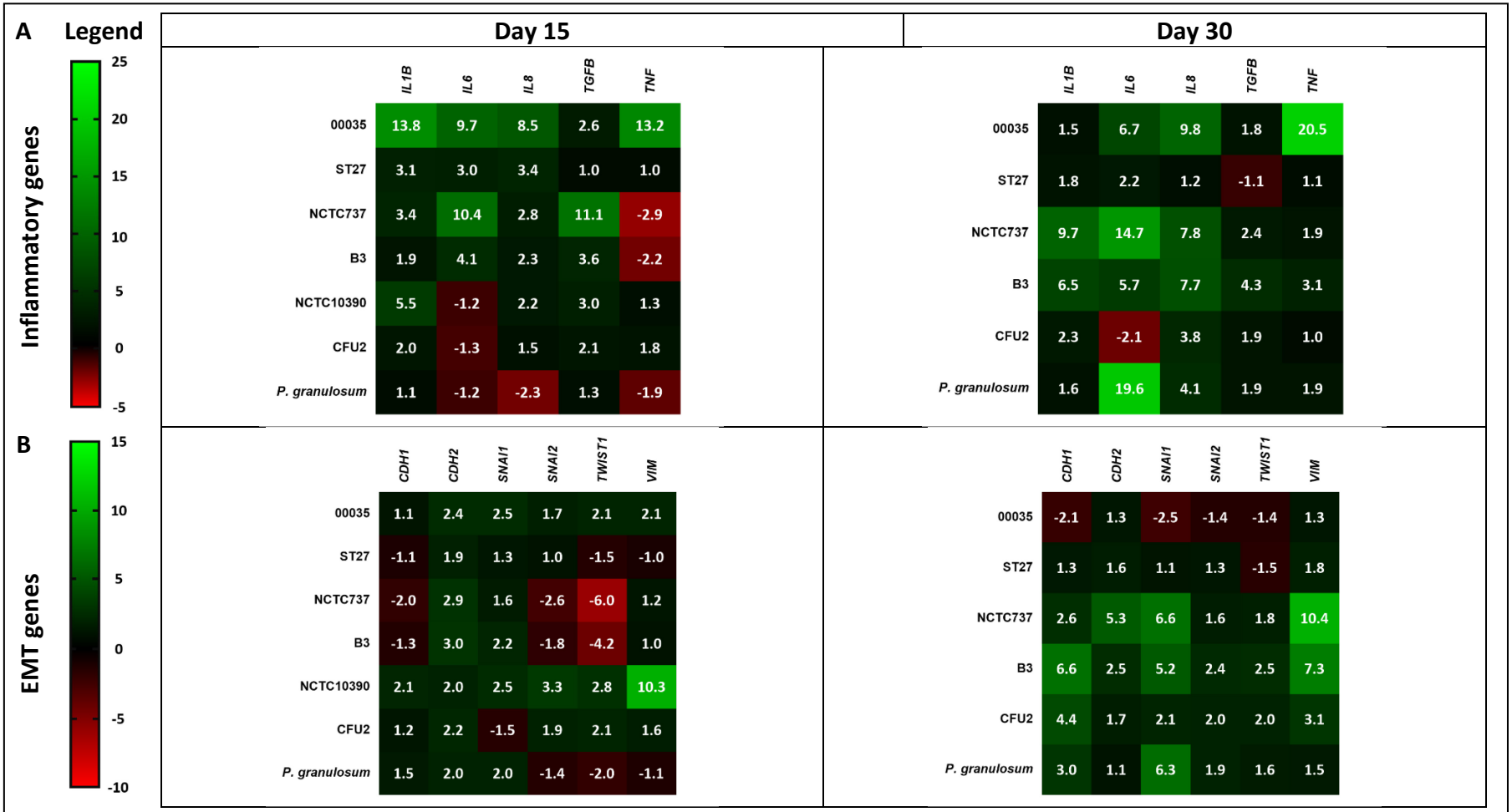

Figure 4.15. Gene dysregulation in long-term infection models.

Gene dysregulation in RWPE-1 cells infected with different strains of *P. acnes* and *P. granulosum.* The data is presented as mean fold change of three biological replicates and is normalised to non-infected controls using HPRT as a housekeeping gene. **A.** Inflammatory genes; **B.** Epithelial-mesenchymal transition genes.

Infections with CFU2 demonstrated only a significant change in the expression of *IL1B* (2-fold increase) at day 15. At day 30 this infection model demonstrated an increase in *IL1B* and *IL8* (2.3-fold and 3.8-fold, respectively) and a marginal decrease of *IL6* expression (-2.1-fold).

The *P. granulosum* infection models only showed dysregulation of *IL8* (-2.3-fold decrease) at day 15, and significant increase of *IL6* and *IL8* (19.6-fold and 4.1-fold) at day 30.

Only a few EMT genes were dysregulated in the infection models investigated. No significant changes were seen in cells infected with ST27 for the duration of the experiment.

RWPE-1 cells infected with 00035 showed upregulation of below 2.5-fold for *CDH2*, *TWIST* and *VIM* at day 15, and downregulation of -2.1-fold and -2.5-fold for *CDH1* and *SNAI1*, respectively.

NCTC737-infected cells, demonstrated a decrease in the expression of *CDH1* (-2-fold), *SNAI2* (-2.6-fold) and *TWIST1* (-6-fold) and a 2.9-fold increase for *CDH2* at day 15; at day 30 this infection model showed increase in *CDH1*, *CDH2*, *SNAI1* and *VIM* (2.6-fold, 5.3-fold, 6.6-fold and 10.4-fold respectively).

In the B3 infection model, 3-fold upregulation of *CDH2* and 2.2-fold upregulation of *SNAI1* were seen at day 15, together with a -4.2-fold decrease in *TWIST1* expression. At day 30 an increase was seen in all genes investigated, ranging between 2.4 and 7.3-fold.

The NCTC10390 infection model was only investigated at the day 15 time point. All EMT genes tested were upregulated, with values ranging between 2-fold and 10.3-fold.

At day 15 the CFU2 model showed a mild upregulation in two genes with fold increase of 2.2 and 2.1 for *CDH2* and *TWIST*, respectively. At day 30, this infection model showed increased expression levels of *CDH1* (4.4-fold), *SNAI1* (2.1-fold), *SNAI2* (2-fold), *TWIST* (2-fold) and *VIM* (3.1-fold).

Finally, *P. granulosum*-infected cells had significant dysregulation of 2-fold in three genes: an increase in *CDH2* and *SNAI1*, and a decrease in *TWIST*. A significant upregulation was seen in *CDH1* (3-fold) and *SNAI1* (6.3-fold) at day 30 (Figure 4.15.B).

4.3.2.4. Soft agar assay

Soft agar assays were used to assess whether infection leads to anchorage-independent growth. Soft agar assays were performed at day 15 or day 30 post-infection with different strains.

No colonies were formed following most of the infections. Strains tested following a 15-day infection included ST27, B3, NCTC10390 and CFU2 (Figure 4.16). Additionally, cells infected with 00035, NCTC737, ST27, B3, CFU2 and *P. granulosum* were also investigated for anchorage-independent growth following a 30-day infection (Figure 4.17). Only cells infected with 00035 for 30 days formed colonies in the soft agar. An average number of 7 colonies were formed per experimental well in all three biological replicates (Figure 4.17.G and Figure 4.17.H).

4.3.2.5. Immunofluorescence analysis

A commercially available immunostaining kit was used to investigate any changes in the expression of E-cadherin and vimentin in cells, following a long-term infection of 15 or 30 days.

In cells infected with B3 for 15 days there was a statistically significant increase in E-cadherin expression ($p = 0.012$). There were no significant changes in E-cadherin levels in cells infected with ST27, NCTC10390 or CFU2 at this time point. A change of protein expression was also seen in vimentin levels; a decrease in the cells infected with ST27 and an increase in the NCTC10390 infection models at the day 15 timepoint with p-values $p = 0.033$ and $p = 0.022$, respectively (**Error! Reference source not found.**).

There was no significant difference in the expression of E-cadherin and vimentin in the 30-day infection models compared to untreated controls (Figure 4.19 and Figure 4.20).

4.3.2.6. Scratch assays

Scratch assays were used to assess differences in cell migration between untreated controls and infected RWPE-1 cells. Cells treated with mitomycin were used as controls in a subset of experiments to demonstrate that any wound closure is due to migration and not proliferation.

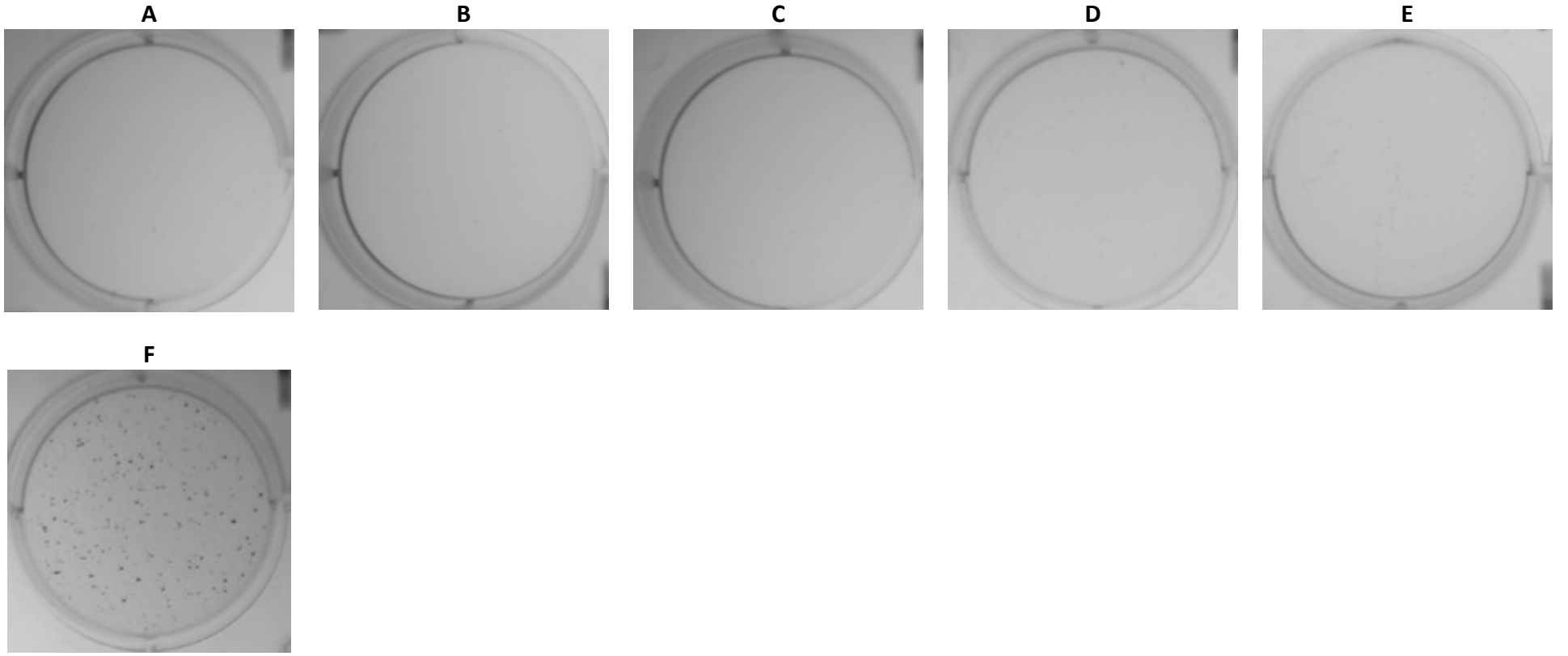

Figure 4.16. Soft agar assays after 15-day infections.

No magnification images of soft agar assays set up with RWPE-1 cell following a 15-day long-term infection, showing that no colonies were formed following infection with the strains listed below, i.e. the cell have not acquired anchorage-independent growth.

A. Not infected; **B.** ST27; **C.** B3; **D.** NCTC10390; **E.** CFU2; **F.** Positive control, showing colonies formed by the 22Rv1 prostate cancer cell line.

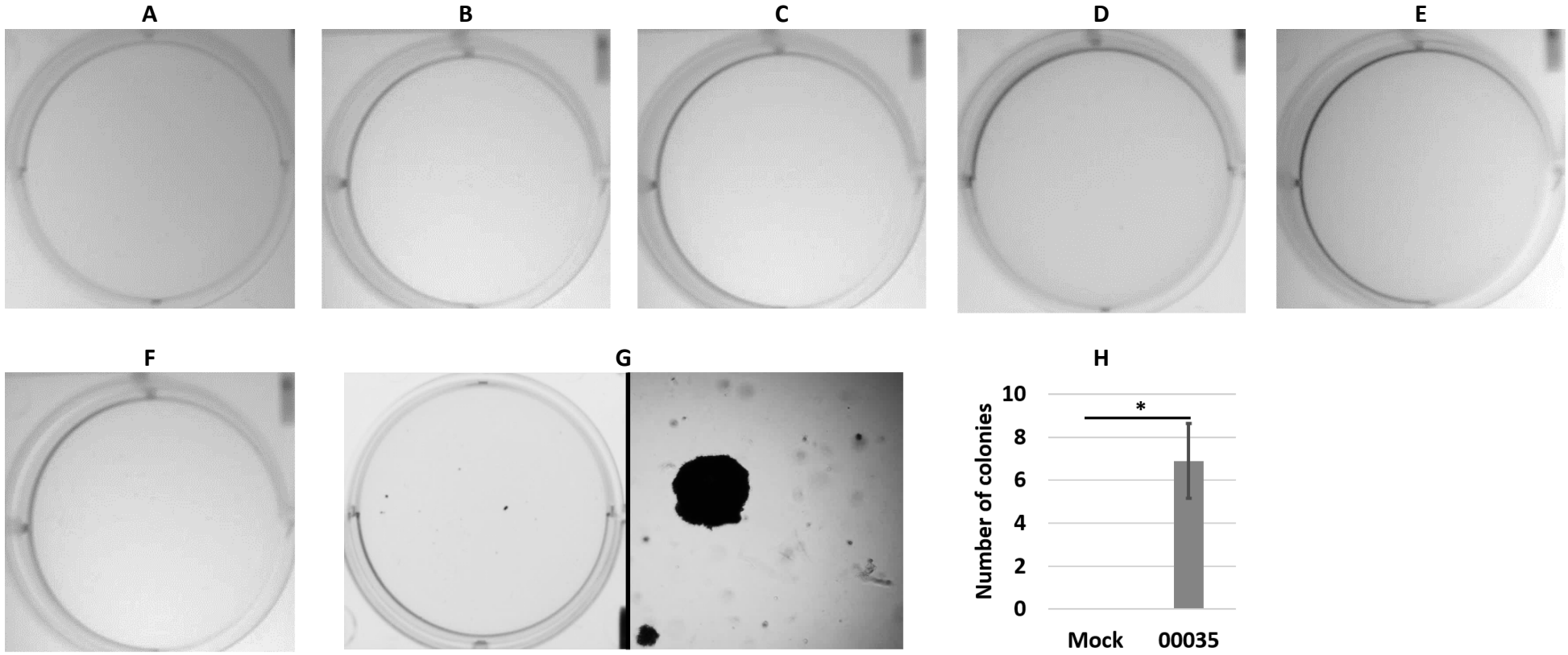

Figure 4.17. Soft agar assays after 30-day infections.

No magnification images of soft agar assays set up with RWPE-1 cell following a 30-day long-term infection, showing that no colonies were formed in infection models following infection with the strains A-F, i.e. the cell have not acquired anchorage-independent growth.

A. Not infected; **B.** NCTC737; **C.** ST27; **D.** B3; **E.** CFU2; **F.** *P. granulosum*; **G.** 00035 (left – no magnification; right – x2 magnification); **H.** Number of colonies in 00035 infected cells vs not infected "mock" cells. Data presented as mean number of three biological replicates, +/- SEM. * $p < 0.05$

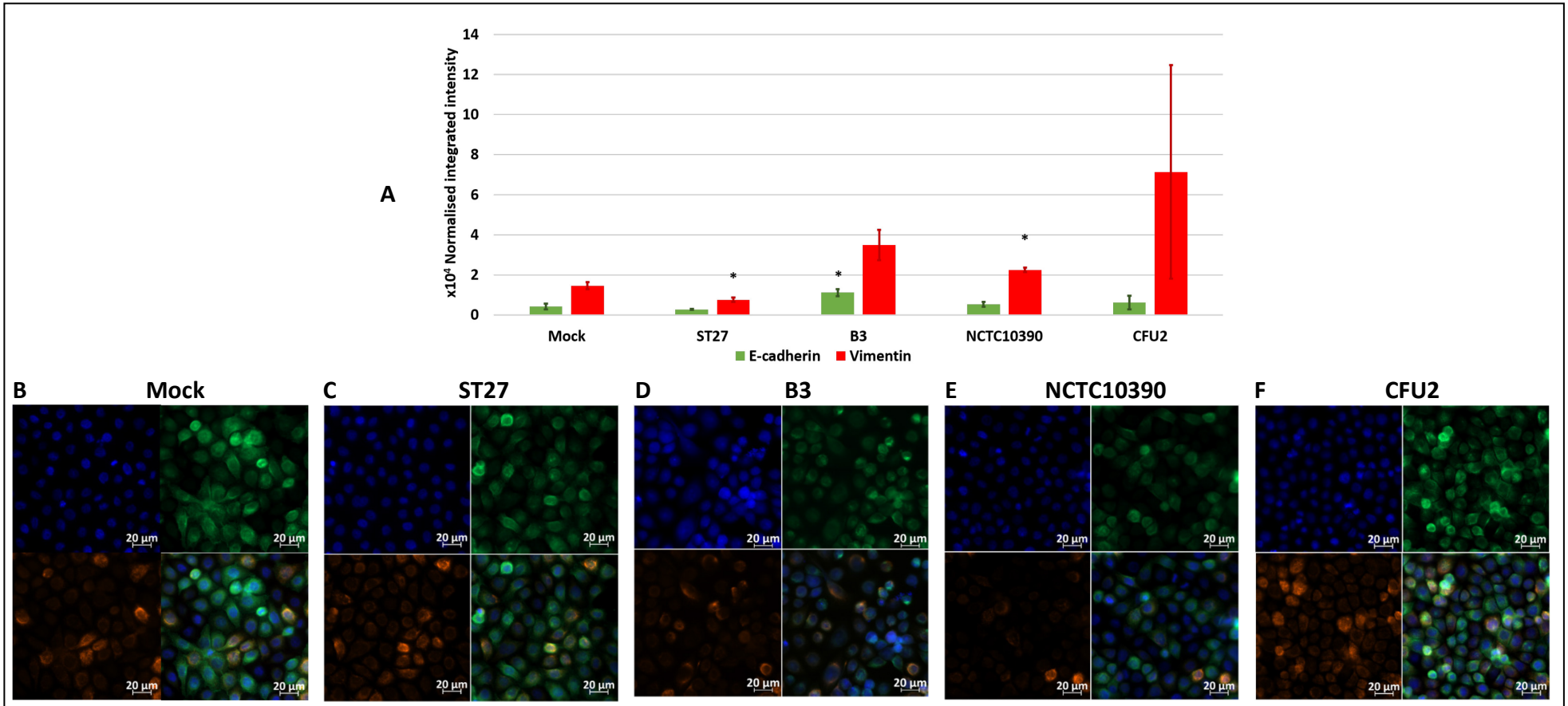

Figure 4.18. Quantified immunofluorescence of E-cadherin and vimentin following a 15-day infection

RWPE-1 cells infected with strains of *P. acnes* for 15 days were used for immunofluorescence analysis of E-cadherin (green) and vimentin (red) protein expression. **A.** Mean normalised integrated density for different infection models. The data is presented as mean of three biological replicates, +/- SEM. * p = 0.05; **B-F.** Representative images acquired under x40 magnification, with staining for E-cadherin (green) and vimentin (orange), and counterstained nuclei (DAPI, blue).

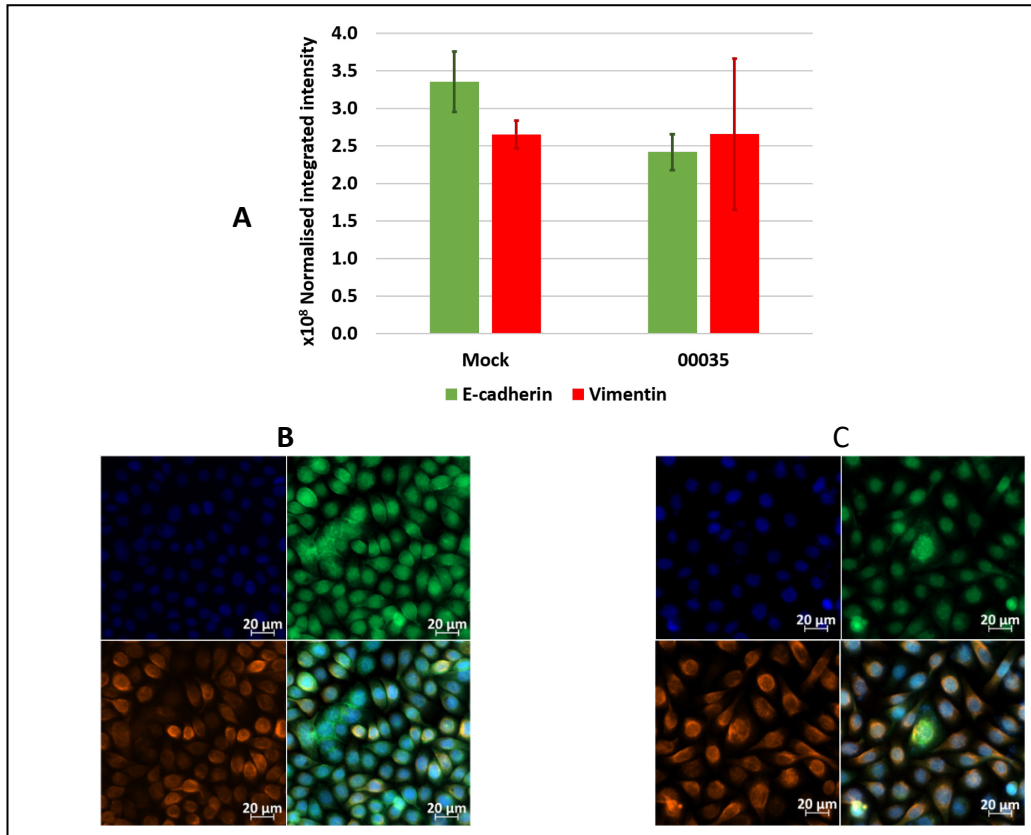

Figure 4.19. Quantified immunofluorescence of E-cadherin and vimentin following a 30-day infection

RWPE-1 cells infected with *P. acnes* strain 00035 for 30 days were used for immunofluorescence analysis of E-cadherin (green) and vimentin (red) protein expression. **A.** Mean normalised integrated density. The data is presented as mean of three biological replicates, +/- SEM. **B-C.** Representative images acquired under x40 magnification, with staining for E-cadherin (green) and vimentin (orange), and counterstained nuclei (DAPI, blue).

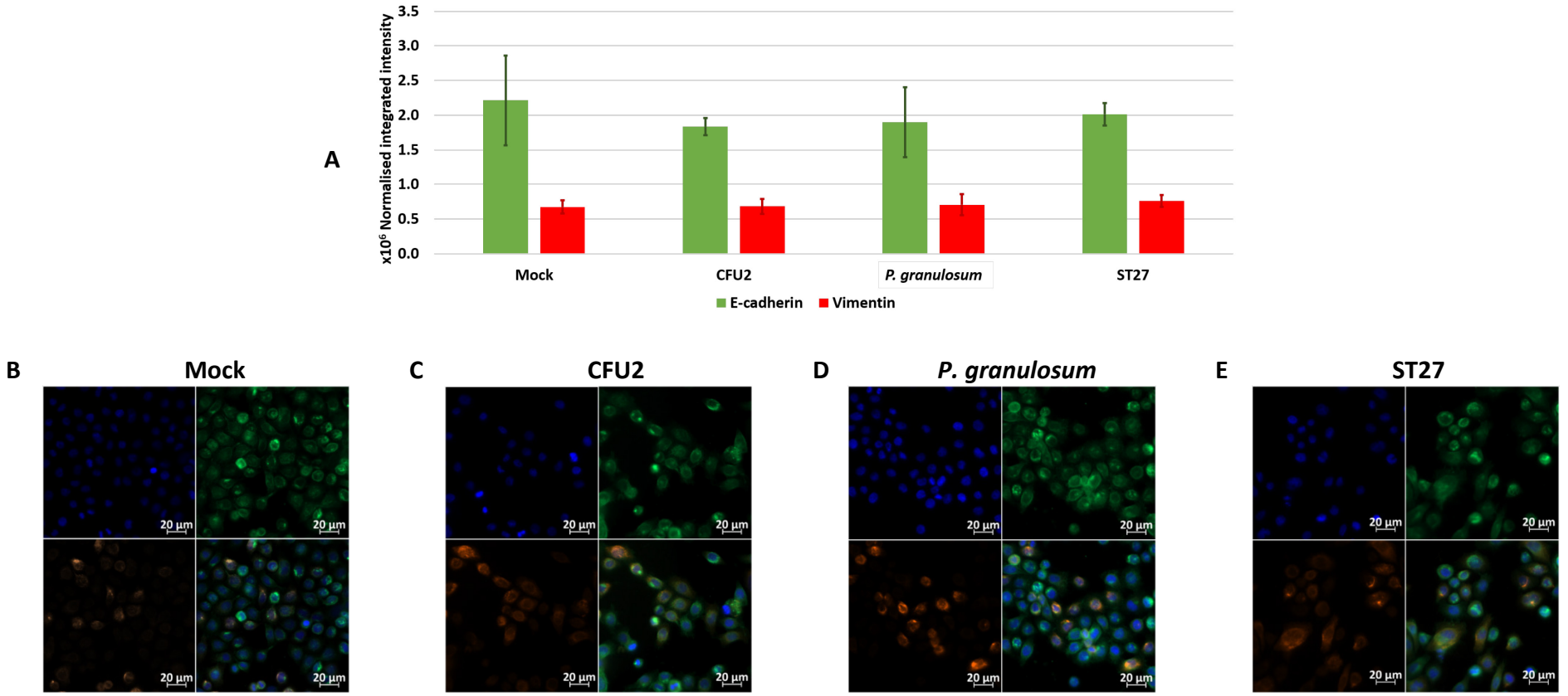

Figure 4.20. Quantified immunofluorescence of E-cadherin and vimentin following a 30-day infection

RWPE-1 cells infected with *P. granulosum* and strains of *P. acnes* for 30 days were used for immunofluorescence analysis of E-cadherin (green) and vimentin (red) protein expression. **A.** Mean normalised integrated density for different infection models. The data is presented as mean of three biological replicates, +/- SEM. **B-E.** Representative images acquired under x40 magnification, with staining for E-cadherin (green) and vimentin (orange), and counterstained nuclei (DAPI, blue).

In the scratch assays prepared with cells following 15-day infection, there was no significant difference in wound closure rates at 24 and 48 hours post-scratch between uninfected and cells infected with B3, NCTC10390 and CFU2 (Figure 4.21). In cells treated with mitomycin, there was a significant decrease of the wound closure rate.

Following a 30-day infection with 00035, the RWPE-1 cells did not show difference in wound closure rate compared to untreated controls (Figure 4.22.A). Similarly, there was no significant difference between mock infections and cells infected with ST27 or B3 (Figure 4.22.C and Figure 4.22.D). Cells infected with NCTC737 showed higher wound closure rate compared to untreated controls at each timepoint ($p = 0.0094$ at 24 hours and $p = 0.0028$ at 48h, Figure 4.22.B). Finally, the cells infected with CFU2 and *P. granulosum*, exhibited significantly higher scratch healing rate at 48 hours ($p = 0.034$ Figure 4.22.E and $p = 0.032$, Figure 4.22.F, respectively).

4.3.2.7. MTT assays

MTT assays were used to assess whether treatment of HDMEC cells with conditioned medium from long-term infection models (maintained for 30 days) with a range of phylogenetic strains has any effect on the proliferation of endothelial cells. To better compare each treatment, the absorbance reading as normalised to the untreated control in each experiment. The value was then used to calculate the percentage change compared to the untreated control. Cells treated with medium from “mock” infections (i.e. non-infected RWPE-1 cells) were used as a comparator and the statistical analysis assessed the difference between the response to different infections and non-infected RWPE-1 cells. Figure 4.23 presents comparison between the MTT results for HDMEC cells treated with medium from non-infected cells and different infection models.

In most cases, there was no significant difference in the MTT assay results between cells treated with conditioned medium from infection models and medium from “mock” controls. An exception was seen when conditioned medium from the NCTC737 infection model was used, which caused a significant decrease in optical density readings at dilutions 1:500 ($p = 0.03$) and 1:1000 ($p = 0.03$).

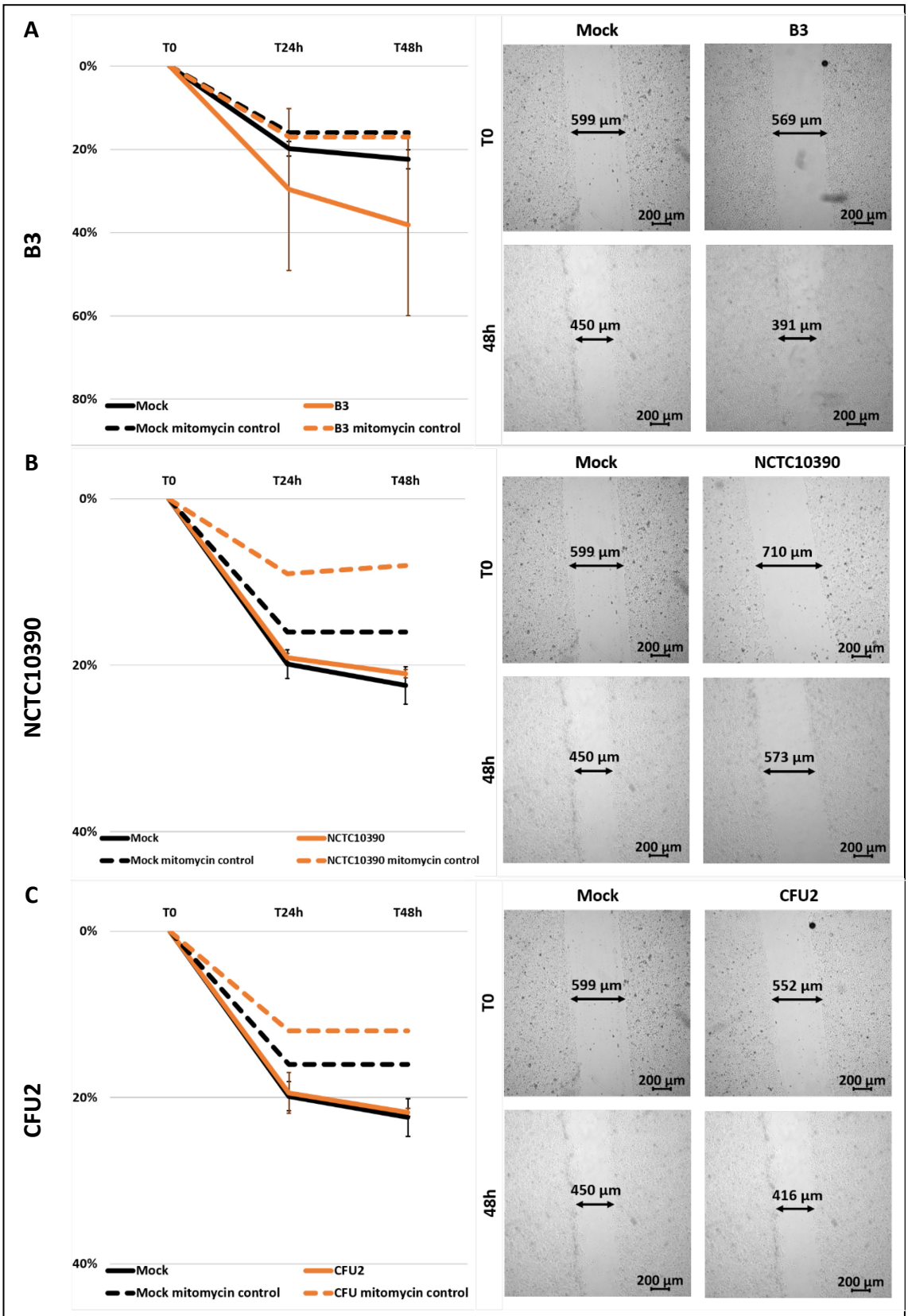

Figure 4.21. Scratch assays following 15-day chronic infection

Scratch assays were performed on RWPE-1 cells following a chronic 15-day infection. Data is shown as mean percentage wound closure of three biological replicates +/- SEM, with "mock" (black) and infected cells (orange). Dotted lines represent mitomycin C treated controls. Images (representative images shown on the right) were taken at x2 magnification, with the mean scratch size at T0 and 48 hours indicated. **A.** B3; **B.** NCTC10390; **C.** CFU2.

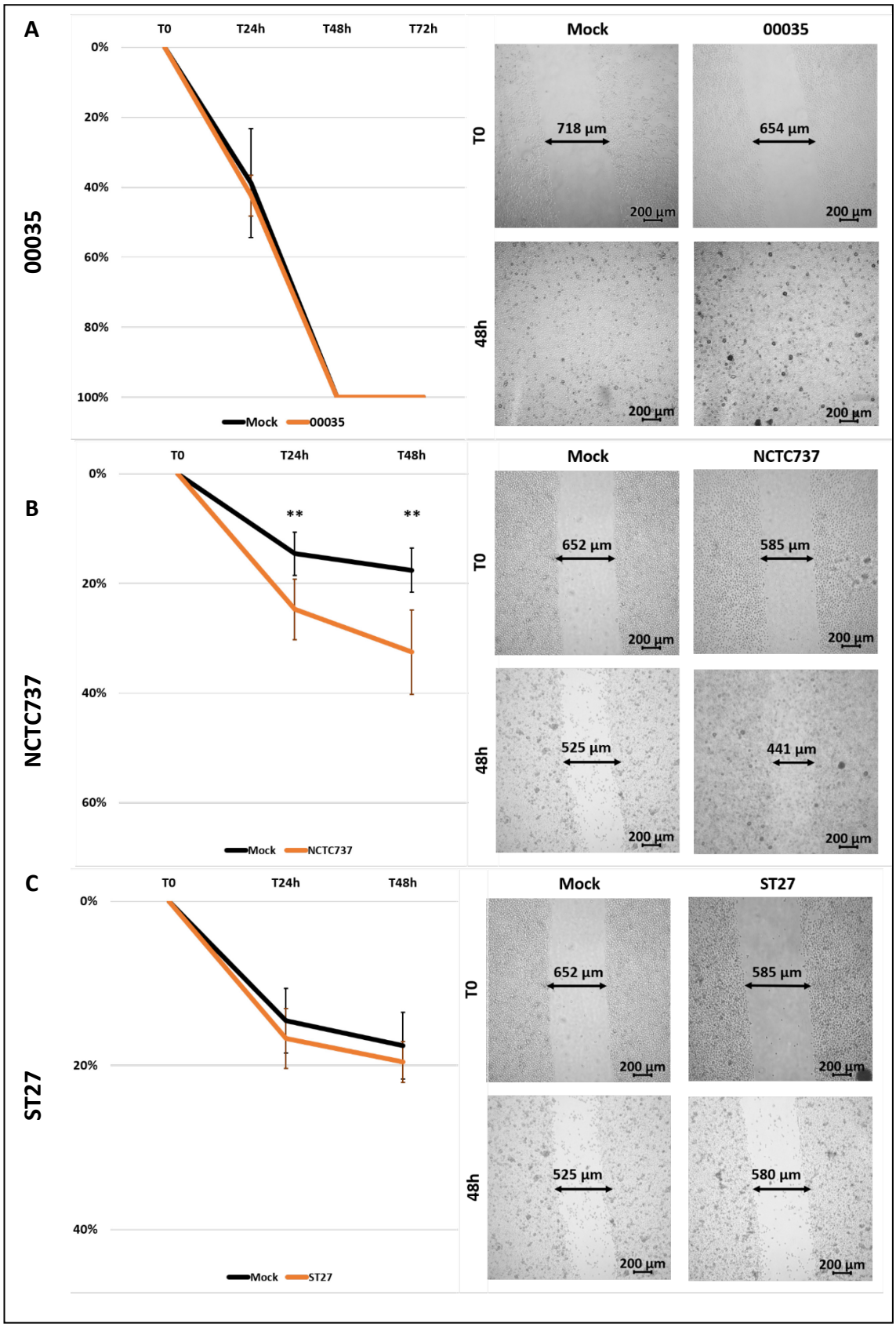
A
00035
T0
T24h
T48h
T72h
0%
20%
40%
60%
80%
100%
Mock
00035
Mock
00035
T0
718 µm
654 µm
200 µm
48h
200 µm
B
NCTC737
T0
T24h
T48h
0%
20%
40%
60%
**
**
Mock
NCTC737
Mock
NCTC737
T0
652 µm
585 µm
48h
525 µm
441 µm
C
ST27
T0
T24h
T48h
0%
20%
40%
Mock
ST27
Mock
ST27
T0
652 µm
585 µm
48h
525 µm
580 µm

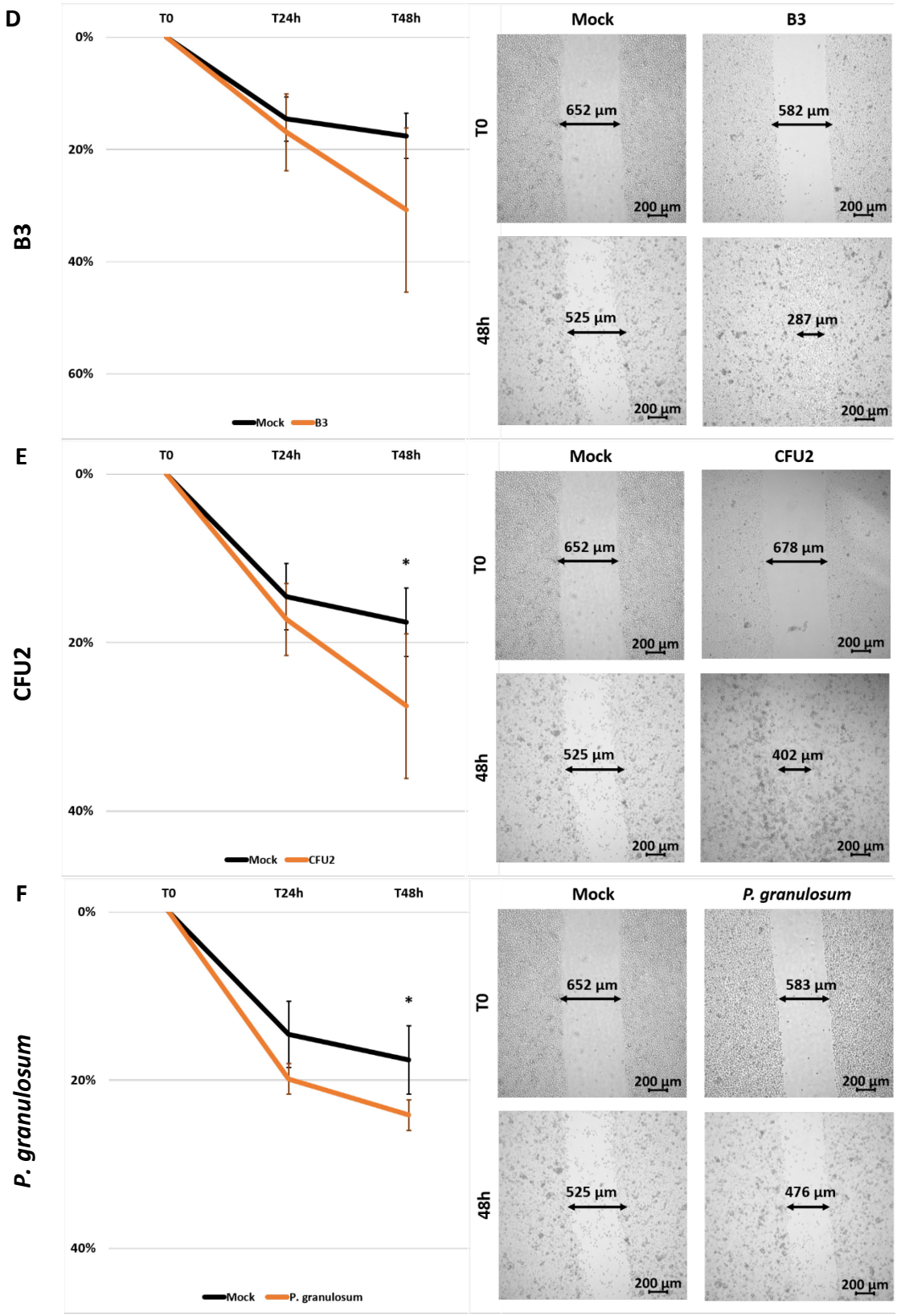

Figure 4.22. Scratch assays following 30-day chronic infection

Scratch assays were performed on RWPE-1 cells following a chronic 30-day infection. Data is shown as mean percentage wound closure of three biological replicates +/- SEM, with "mock" (black) and infected cells (orange); * p = 0.05; ** p = 0.01. Images (representative images shown on the right) were taken at x2 magnification, with the mean scratch size at T0 and 48 hours indicated.

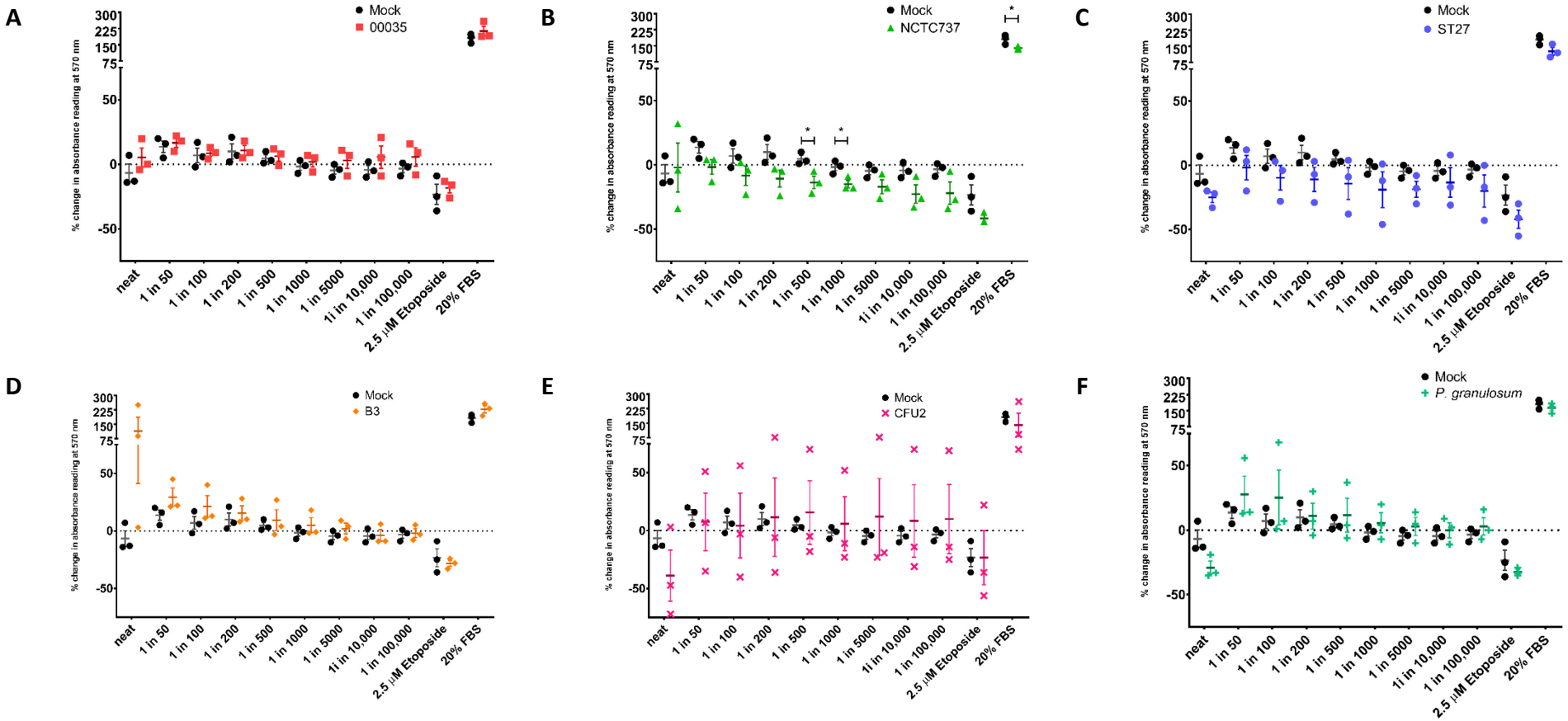

Figure 4.23. MTT assay of HDMEC cells treated with conditioned medium.

MTT assay (absorbance measured at 570 nm) assessing the effect conditioned medium from chronic infection of RWPE-1 prostate epithelial cells with different phylotypes of *P acnes* has on the proliferation of the endothelial cell line HDMEC. Conditioned medium used: **A.** 00035 (red); **B.** NCTC737 (green); **C.** ST27 (blue); **D.** B3 (orange); **E.** CFU2 (pink); **F.** *P. granulosum* (turquoise). The data is presented as mean of three biological replicates +/- standard error. Significance was calculated in comparison to cell treated with conditioned medium from uninfected RWPE-1 cells (black), using a 2-tailed Student's t-test. (* $p < 0.05$)

4.4. *Discussion*

The focus of the initial stages of this study was to evaluate eukaryotic and bacterial behaviour in the infection model optimised in Chapter 3. To investigate the numbers and viability of the RWPE-1 prostate cells in the infection model, the inexpensive trypan blue exclusion assay was used, which allowed the monitoring of cell viability at each passage with no loss of cells. The cell counts were also used to ensure that mock and infected cells are seeded at 100,000 cells/ml at every passage, rather than using a 1:5 ratio, as done in previous studies (Drott et al., 2010). Seeding the cells at their optimal density at each timepoint allowed limiting the stress on the RWPE-1 cells as a result of them being split too sparsely or too densely. For example, if infection with a strain increases proliferation rates, by the time the cells are split, these cells are likely to have reached confluence. In contrast, if a strain has a negative impact on proliferation or if it leads to cell death, the number of viable cells would be lower compared to the example above. Thus, splitting both at a set ratio would not be adequate to accommodate the difference in viable cell numbers and would result in differences which may have a severe effect on behaviour.

Our results showed that prostate epithelial cells remain viable following infection with *P. acnes* strains representing all phylogenetic types related to prostate cancer. The phylogenetic types IA_2 and IC were not investigated, as there have been no links found between these two lineages and patient prostate tissue samples. *P. granulosum* and *P. avidum* strains were tested as controls, as the organisms are closely related with *P. acnes*. While the cells survived both acute and chronic infections with *P. granulosum, P. avidum* infection led to cell death 48 hours post-infection in the short-term models and a long-term infection was thus not trialled, leaving *P. granulosum* as the sole non-*P. acnes* control.

With both short term and long-term infections, statistical significance was rarely seen in viable cell numbers or cell viability between controls and infected cells; if such a significance was seen it was a single occurrence and did not represent a trend with infected cells being less viable or demonstrating higher numbers, suggesting the optimal growth conditions were present for all infected cells.

Bacterial numbers, however, showed two clear and consistent trends, especially in the long-term infections. The first group consisted of bacterial strains that remained viable in the 5% CO_2 tissue culture environment, namely the type IA_1 strains 00035 and NCTC737, the type IB stain B3. The second group was formed by strains that did not remain viable in the infections and their numbers in the cell culture medium decreased over time; strains in this group included the type IA_1 ST27, type II strain NCTC10390 and type III strain CFU2. *P. granulosum* was also a part of the second group with the notable difference that its numbers had started decreasing at each time point of the short-term infection, as well as the long-term. These differences in bacterial survival might be a result of the type I strain being more aerotolerant than types II and III.

An investigation of the cytotoxic effect different strains of *P. acnes* and *P. granulosum* had on the RWPE-1 showed that only two of the 6 strains tested caused more than 5% cytotoxicity; 00035 cytotoxicity decreased as the experiment progressed indicating the relatively high percentage cytotoxicity was a result of an initial shock to which the cells slowly became accustomed as infection progressed and the cytotoxicity of type B increased overtime, with the increasing bacterial numbers being a possible explanation here.

The ability of *P. acnes* to survive intracellularly in a range of cells, including macrophages (THP-1 cell line) and RWPE-1 cells, has been demonstrated previously (Mak et al., 2012; Fischer et al., 2013). It has also been shown that *P. acnes* is present in patient prostate tissue samples both in the cells and as an extracellular biofilm-like aggregate (Alexeyev et al., 2007). Here we compared the ability of representatives of the different prostate-related phylogenetic types of *P. acnes* to remain viable intracellularly in short-term infections. Overall, the type I strains investigated (both IA_1 and IB) showed higher intracellular numbers compared with types II and III. The type II strain, NCTC10390, demonstrated significantly lower numbers compared with all other strains investigated and they did not increase with prolonged exposure, suggesting that type II strains may not possess the ability to invade epithelial cells.

The role inflammation plays in oncogenesis, especially prostate cancer, has been widely studied. In the case of prostate cancer, lesions are often associated with inflammatory cells, including macrophages and neutrophils, which are suspected of further driving oncogenesis, for example by causing reactive oxygen species-driven DNA damage

(Babior, 2000). Cytokines and chemokines play the main role in recruiting these leukocytes to the site of the developing tumour. Thus, inflammatory gene dysregulation is important at the start of the oncogenic process. The dysregulation of prostate cancer-related inflammatory genes (*IL1B*, *IL6*, *IL8*, *TNF* and *TGFB*) was investigated in both acute and chronic infections (Adler et al., 1999; Veltri et al., 1999; Blobe et al., 2000; Ricote et al., 2004; Tse et al., 2012). Although there are conflicting findings in the literature, the consensus is that prostate cancer is linked to upregulation of *IL6*, *IL8*, *TNF* and *TGFB* expression, and downregulation in *IL1B* (Ivanovic et al., 1995; Hobisch et al., 1998; Veltri et al., 1999; Ricote et al., 2004; Tse et al., 2012). All those inflammatory genes are involved in complex signalling pathways that, if dysregulated, have the potential to drive oncogenesis.

The protein levels of IL-6 and IL-8 have previously been investigated in similar *in vitro* infection models and the result of those studies match our findings: both cytokines are upregulated in response to acute infection with *P. acnes* (Drott et al., 2010; Fassi Fehri et al., 2011). The expected upregulation of *IL6* and *TNF* levels was observed in all acute infections, while *IL8* was upregulated in most acute infections. The upregulation of IL-6 and IL-8 can have downstream effects on the NF-κB and PI3K/Akt pathways. The anticipated downregulation in *IL1B* was only noted in the case of NCTC10390-infection at 24 hours in the acute infections; *TGFB* upregulation did not occur in the initial 48 hours of infection but was observed in 3 of the tested strains at 72 hours. These results suggest that the potential for infection-driven oncogenesis is present at the early stages of infection through some of the prostate cancer-linked pathways in published literature, e.g. NF-κB, PI3K/Akt, JAK/STAT3.

The number of significantly dysregulated genes in chronic infections is reduced, as is the fold-increase. Nevertheless, significant upregulation is seen in at least one of the inflammatory genes of interest both at day 15 and day 30 in all of the infections. The notable examples are 00035-infected cells which show upregulation of all inflammatory genes at day 15, and B3 which leads to upregulation of all inflammatory genes tested at day 30. These data, once again, confirm that the potential for oncogenesis as a result of infection is present.

To have a clearer understanding of the role of inflammatory gene dysregulation in prostate epithelial cells and its potential role in oncogenesis, its effect on inflammatory

cells needs to be studied. In the controlled environment of tissue culture experiments, the interactions between different cell types is difficult to study; however, co-culture experiments (infected prostate epithelial cells and leukocytes) or treating immune cells with conditioned medium from infected prostate epithelial cells would give insight on the behaviour of the inflammatory cells in the context on *P. acnes* infection, especially as most of the cytokines studied directly affect inflammatory cells.

EMT-related genes are considered a marker of cellular transformation. The genes whose expression is investigated here (*CDH1*, *CDH2*, *SNAI1*, *SNAI2*, *TWIST* and *VIM*) are all interconnected. The overall expression changes in short term infections show rapid changes in expression between time points with no clear trends in expression dysregulation. EMT gene expression changes are also seen in the chronic infection models, however, the expression patterns do not match what would be expected if the cells were undergoing EMT. For example, while the B3 infection model day 30 demonstrated significant increase in *SNAI1*, a significant increase is also seen in *CDH1* expression, a gene whose expression is suppressed by Snail.

Previous studies using RWPE-1 infected cells to investigate the effect of *P. acnes* infection have demonstrated that vimentin plays an enabling role in *P. acnes* cell invasion into host cells (Mak et al., 2012). While our results do not show a link between high intracellular counts and increased VIM expression in acute infections or at day 15 of chronic infections, it is possible that the baseline expression of vimentin is sufficient to aid the invasion of some strains. However, at day 30 both NCTC737 and B3-infected cells demonstrated increased vimentin expression which was paired with the high levels of bacteria in the medium, suggesting the possibility of bacteria-driven vimentin-overexpression, aiming an increase in the ability of *P. acnes* to invade epithelial cells.

A hallmark of EMT is the so called “cadherin switch”, or the downregulation of E-cadherin and the upregulation of N-cadherin (encoded by *CDH1* and *CDH2*, respectively) (Wheelock et al., 2008). E-cadherin is a calcium-dependent adhesion molecule and while its production is not limited to epithelial cells, changes in *CDH1* expression are a useful tool for detecting the transition of epithelial cells to mesenchymal (Carvell et al., 2007; Zeisberg, 2009). As the adhesion molecule is lost in epithelial cells, the cells can acquire increased motility; E-cadherin also interacts with a number of pathways, including Wnt via β-catenin, which further contributes to the cells’ invasiveness (Jiang et al., 2007). As

the infection models used here are comprised solely of epithelial, E-cadherin is a marker suitable for detection of EMT.

In the acute infection models, this pattern is seen on several occasions, but it is not consistently present between timepoints. Of exceptional interest is the *CDH1*/*CDH2* expression at day 30 in the 00035 infection, where the "cadherin switch" is seen, despite the small dysregulation levels (-2.1-fold for E-cadherin and 1.3-fold for N-cadherin). These results, together with 00035 at day 30 being the only infection model which formed colonies in soft agar assays, indicate that 00035 has the potential to drive cellular transformation. Quantifying the immunofluorescence of E-cadherin in the 00035 infection models also supports a decrease of CDH1 on the protein level, although the immunofluorescence results were not statistically significant. Despite the data suggesting cellular transformation, the cells infected with 00035 showed no increased migration compared to untreated cells. The likely explanation is that further mutations are necessary for the cells to acquire increased motility (Simpson et al., 2008). In addition to the EMT changes seen, the observed increase in *IL6*, *IL8* and *TNF* expression in this infection model at both day 15 and day 30, are consistent with what is observed in prostate cancer.

With all remaining infections, the results of soft agar assay experiments showed no colony formation. This could either mean that the cells have not acquired anchorage-independent growth, or that the antibiotic used in the assay has suppressed the formation of colonies, as demonstrated in Chapter 3 (Section 3.3.7). Additionally, it could be possible that challenging the prostate epithelial cells with bacteria for 4 weeks is insufficient time to cause cellular transformation. The results of qPCR analysis of mRNA levels and immunostaining analysis of protein expression for some infections are somewhat conflicting. A simple explanation for the differences is that the immunostaining experiments are performed 3-4 days after the mRNA extractions used for qPCR analysis, thus the values for protein and mRNA are not related to cells in the same passage or at the same growth stage.

Immunostaining was used to identify the presence and quantify E-cadherin and vimentin expression levels at the protein level. The method used allowed the easy comparison of expression between different infection models and comparison to untreated cells by looking at the overall fluorescence associated with each gene. An alternative method

for analysis of the immunostaining images would be to identify cells expressing E-cadherin and vimentin and analyse them separately. This would clarify whether the increase or decrease in fluorescence was due to an overall change in expression of the proteins across all cells, or whether it was due to subpopulations of cells having significantly higher expression than others. However, due to time constraints this analysis was not performed, and a more general approach was used.

Further studies using immunofluorescence, identifying cells harbouring intracellular infection and interrogating their specific EMT gene expression compared to infection-free cells would clarify the role of infection in oncogenesis: whether it is the infected cells that undergo transformation or if surrounding cells change as a result of signalling from the infected cells.

Scratch assays were performed to assess cell migration following a long-term infection. Studies have found that there are at least 66 different genes involved in cell migration, thus the gene expression assessed in this study is insufficient to make conclusions about the cause of any migration seen (Simpson et al., 2008). Significantly increased cell migration relative to untreated controls can be seen in cells infected for 15 days with B3, and in 30-day infections with NCTC737, CFU2 and *P. granulosum.* A correlation between increased levels of the EMT marker vimentin and increased migration was observed following a 30-day infection with NCTC7373 and B3. It is worth noting, that where a mitomycin control was used the migration of both infected and uninfected cells differed significantly from that of mitomycin-treated control cells, suggesting that increased wound closure rate could be a result of increased migration or increased proliferation. Due to time constraints, not all experiments were repeated in the presence of a mitomycin control, thus comparisons between infected and not infected cells can only be interpreted as trends and not definitive results.

As the creation of blood supply to a tumour is a crucial step in cancer progression, it is important to investigate whether infection of the prostate could drive angiogenesis and thus enable cancer development and future metastasis.

The MTT assay was used here to assess whether proliferation rates are increased or decreased as a result of treatment with conditioned medium from chronically infected cells. However, the MTT assay is not a proliferation assay but measures the reduction of

MTT to formazan, which is only done by metabolically active cells. It was selected for these initial investigations as it is cost effective and would allow the screening of a range of different strains, permitting the unrestricted use of replicates. Any conclusions about increased or decreased proliferation rates were made by comparing the absorbance readings of treated to untreated cells and assuming that the change in absorbance is a result of change in proliferation and not due to differences in metabolism. Further experiments using proliferation assays, such as the BrdU assay, can be used to confirm the results observed here.

A limitation of the assay is that the reduction of MTT to formazan is done mainly by the mitochondria, and as mitochondria and bacteria share many similarities, the conversion can also be done in bacterial cells. During processing of the conditioned medium a centrifugation step is taken to pellet any bacteria in the medium, however, this does not guarantee the removal of all bacterial cells. The filter-sterilisation of conditioned medium was also not possible, as it could remove secreted protein and growth factors (filtering is not recommended for complete KSFM) and could thus alter the results of the experiment. Antibiotics were also not used as the HDMEC cells were cultured routinely in antibiotic-free medium and are sensitive to changes in the medium composition, thus the addition of antibiotics could also affect the results from the experiments. However, as a rather long incubation time of 72 hours was selected, if bacteria were present, they would cause the medium to become cloudy and when the MTT was added they would cause a rapid colour change, which would be easy to distinguish from non-contaminated wells.

The dilutions of conditioned medium that could be used for experiments were limited by the amount of conditioned medium stored, thus dilutions such as 1:2, 1:5 and 1:10 were not possible. The selected dilutions spanned over five orders of magnitude, thus allowing the investigation of the effect of minute amounts of conditioned medium have on the endothelial cells.

The role of *P. acnes* infection of the prostate in angiogenesis has not previously been investigated. Overall, the results here do not show statistically significant difference in MTT assay results between HDMEC cells treated with medium from 30-day chronic infections, compared to uninfected controls. The exception is seen in cells treated with medium from the type IA_1 NCTC737 (dilutions 1:500 and 1:1,000). The likely reason for

the lack of observed dysregulation is that the infected prostate cells alone do no not produce enough growth factors to induce a change in the behaviour of the HDMEC cells.

It is worth noting that in the context of tumour-associated angiogenesis, the immune cells summoned to the location of the forming tumour also play an important role in angiogenesis in the area, as they also release a number of pro-angiogenic factors (Stockmann et al., 2014; Mortara et al., 2017). Thus, the examination here, focusing solely on the epithelial cells, does provide information about only a portion of the potential pro-angiogenic signals in cancer.

A future experiment could investigate what effect conditioned medium from immune cells infected with *P. acnes*, has on angiogenesis (for example the monocytic cell line THP-1), as it would provide additional insight of the role of *P. acnes* in angiogenesis in the context of prostate cancer.

The findings from the experiments in this chapter were used to select strains for infection models whose gene dysregulation will be further investigated in Chapter 5, using qPCR arrays with 84 prostate cancer-specific genes. Day 15 was selected as the time point for further analysis as bacterial numbers for most strains are undetectable past this point. Prostate isolates 00035, B3 and CFU2, representing three different phylogenetic types were selected for qPCR array analysis. Both NCTC737 and 00035 are type IA_1 strain and show significant gene dysregulation in both short and long-term infections, and while NCTC737 shows a trend towards migration induction, the 00035 strain was chosen for further analysis as it is a prostate-derived isolate and it is the only strain showing colony formation in soft agar and downregulation in *CDH1* expression in chronic infections. B3, a type IB isolate, and CFU2, were selected as they are both prostate isolates and both infections are still challenged with bacteria at day 15; additionally, the B3 infection model shows a trend towards increased cellular migration as a result of infection.

The results from this study present data supporting the role of some strains of *P. acnes* in prostate oncogenesis and highlight the strain-specific differences in immune response and gene dysregulation as a whole.

Chapter 5:

Molecular dysregulation of prostate cancer-related genes in chronically infected cells

5

5.1. *Introduction*

In this chapter, the QIAGEN Profiler Prostate Cancer qPCR array was used to detect dysregulation of prostate cancer-related genes. The array consists of 84 genes which have been shown to play a role in prostate cancer, 5 housekeeping genes and 7 controls. The 84 genes tested are involved in different pathways affecting cancer progression, including the phosphoinositide 3-kinase/protein kinase B (PI3K/AKT) and the androgen signalling pathways, apoptosis, cell cycle control, fatty acid synthesis, and metastasis. Two further groups exist within the selection. First is the group of transcription factors, which regulate the expression of a range of genes; the second group consists of genes which are dysregulated in prostate cancer by promoter methylation. Finally, a number of genes are included in the array as they are known to be up- or downregulated in prostate cancer.

5.1.1. Phosphoinositide 3-kinase/protein kinase B signalling

The PI3K/AKT signalling pathway has been linked to the progression of a number of the hallmarks of cancer, including survival, motility and cell cycle control, angiogenesis, as well as recruitment of inflammatory cells (Beagle and Fruman, 2011; Hanahan and Weinberg, 2011a; Soler et al., 2013; Hirsch et al., 2014). It can be activated by a range of receptors, e.g. B cell and T cell receptors, cytokine receptors, tyrosine kinase receptors and G-protein coupled receptors, all of which lead to the activation of PI3K and the subsequent production of phosphatidylinositol (3,4,5)-trisphosphate (PIP_3) (Aman et al., 1998; Genot et al., 2000; Wegiel et al., 2008; Lemmon and Schlessinger, 2010; Law et al., 2016). PIP_3 can then activate phosphoinositide-dependent protein kinase-1 (PDK1) and also partially activate AKT; once phosphorylated by mechanistic target of rapamycin (mTOR) complex 2 (mTROC2), AKT gains full enzymatic activity (Alessi et al., 1996; Yang et al., 2015). An overview of the pathway can be seen in Figure 5.1.

AKT is a serine-threonine protein kinase and has three isoforms, with similar structure and once activated, it phosphorylates a wide range of downstream processes, including cell cycle progression, proliferation, and EMT (Scheid and Woodgett, 2001; Vivanco and Sawyers, 2002; Manning and Cantley, 2007). AKT can also be activated by other members of the PI3K kinase family (e.g. DNA-dependent protein kinase or DNA-PK),

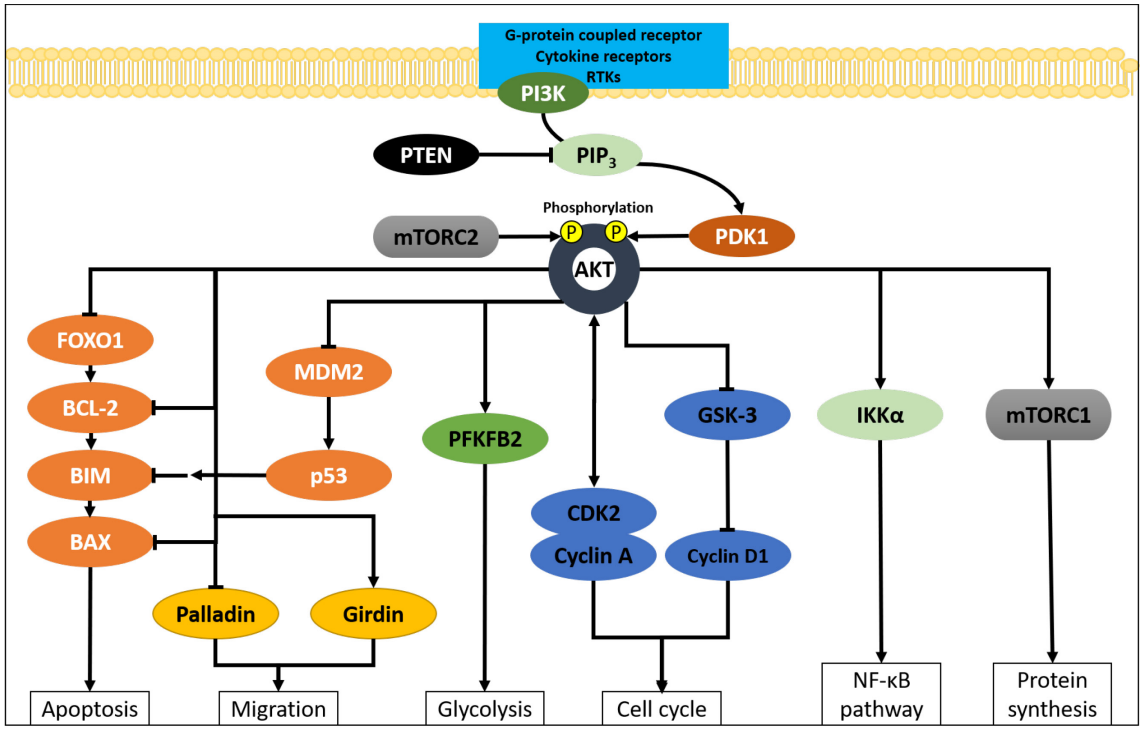

Figure 5.1. Overview of PI3K/AKT signalling

The phosphoinositide 3-kinase/protein kinase B signalling (PI3K/AKT) signalling pathway is a complex network of processes involved in cellular regulation. By inhibiting proteins involved in apoptosis, such as FOXO1 or BCL-2, the pathway can have a direct effect on outcome for the cell. The pathway can also induce Girdin and inhibit Palladin, both of which play a role in migration. PI3K/AKT signalling can also influence glycolysis via PFKB2. Cell cycle proteins such as CDK2, cyclins A and D1 and also under its influence thus altering cell cycle progression. The nuclear factor-kappa B (NF-κB) pathway can be affected by PI3K/Akt by induction of IKKα. Activation of the mTROC2 complex can cause alterations in protein synthesis.

Legend: BAX – BCL-2-associated X protein; BCL-2 – B-cell lymphoma 2; BIM – BCL-2-like protein; CDK2 – Cyclin-dependent kinase; FOXO1 – Forkhead box protein O1; GSK-3 – glycogen synthase kinase 3; IKKα – inhibitor of kappa B kinase; MDM2 – mouse double minute 2; mTORC – mechanistic target of rapamycin complex; p53 – protein 53; PDK1 – 3-phosphoinositide dependent protein kinase-1; PFKFB2 – 6-phosphofructo-2-kinase/fructose-2,6-biphosphatase; PIP_3 – phosphatidylinositol (3, 4, 5)-triphosphate; PTEN – phosphatase and tensin homolog; RTK – receptor tyrosine kinase;

while phosphatase and tensin homolog (PTEN) can act as its inhibitor by dephosphorylating PIP_3 (Maehama and Dixon, 1998; Stronach et al., 2011). AKT's involvement in different pathway is mediated by its interactions with various molecules. By direct inhibition of forkhead box "O" (FOXO) or inhibition of B-cell lymphoma 2 (Bcl-2) family proteins, AKT is involved in apoptosis (Datta et al., 1997; Brunet et al., 1999). By phosphorylating and degrading inhibitor of κB (IκB), AKT initiates the NF-κB signalling pathway (Bai et al., 2009). Loss of at least one PTEN allele is seen in 60% of prostate cancers and complete loss of PTEN has been linked to disease progression and androgen-independent growth (Phin et al., 2013).

Activation of AKT leads to downregulation of E-cadherin expression and produced E-cadherin protein to be contained within perinuclear organelles, thus stimulating EMT; AKT also induces the production of matrix metalloproteinases (MMPs) and can aid cell invasion (Kim et al., 2001; Park et al., 2001; Grille et al., 2003). AKT has been suggested as an oncogene and its activation is seen in various cancers, including prostate cancer (Staal, 1987; Bellacosa et al., 1995; Nakatani et al., 1999; Sun et al., 2001).

mTOR is involved in cellular growth and proliferation and it acts as a response to stress and mitogenic signals (Wullschleger et al., 2006). It belongs to the class IV PI3K superfamily, and it forms two complexes, mTORC1 and mTORC2 (Sabatini, 2006; Wullschleger et al., 2006). The most notable consequence of mTOR activation by AKT is the effect it has on protein signalling, thus having the ability to provide cancers cell with enhanced protein synthesis if dysregulated (Hay and Sonenberg, 2004).

In the context of prostate cancer, the PI3K/AKT pathway may have mutations that cause its dysregulation; loss of function of the tumour suppressor PTEN has also been reported (Cairns et al., 1997; Sun et al., 2009). Additionally, IL-6 driven constitutive activation of the PI3K/ AKT-signalling pathway causes upregulation of cyclin A (encoded by *CCNA1*), which promotes oncogenesis and cancer progression (Wegiel et al., 2008).

5.1.2. Androgen receptor signalling

The androgen receptor (AR) is a transcription factor which is involved in the transcriptional activation of a range of processes in the cell. The main way of activating the AR is described in the Introduction of this thesis (Section 1.1.2.5.4.4.1, Figure 1.4) and includes binding to dihydrotestosterone (DHT), dimerization of the receptor and

translocation of the nucleus (Lonergan and Tindall, 2011). Alternatively, AR-signalling can be initiated either by IL-6 activation which then drives Janus kinase/Signal transducer and activator of transcription (JAK/STAT3) and RAS-signalling leading to AR activation or by activation of receptor tyrosine kinases (e.g. epidermal growth factor (EGF) activating the EGF receptor (EGFR), insulin-growth factor 1 (IGF-1) binding the insulin receptor, vascular endothelial growth factor (VEGF) binding to the VEGF receptor (VEGFR)), which can also lead to activation of the PI3K/AKT pathway.

5.1.3. Apoptosis

Apoptosis, also referred to as programmed cell death, is initiated when the cell receives lethal stimuli, either intrinsic (such as signals for DNA damage, or metabolic stress) or extrinsic (from neighbouring cells, e.g. cytokines, IGF-1, EGF) (Ichim and Tait, 2016). When apoptosis is initiated, the nucleus condenses and the cell shrinks; the membrane begins to form blebs which mature into apoptotic bodies and the DNA is fragmented (Figure 5.2). The remnants of the cell are then engulfed by phagocytes. Different caspases (members of the **c**ysteine-**asp**artic acid prote**ase** family) play a key role in the regulation of the process. The complex process of apoptosis and its role in carcinogenesis is reviewed in detail by Turner et al. (2014). Here, we will only highlight the role of the genes investigated in this chapter.

The apoptotic pathway leads to the activation of a number of initiator caspases which in turn stimulate downstream executioner caspases (including caspase-3) and it has been shown that decreased expression of the precursor-caspase-3 or activated caspase-3 decreases sensitivity to apoptosis signalling in prostate cancer and thus aids cancer progression (Rodríguez-Berriguete et al., 2015).

The B-cell CLL/lymphoma 2 (BCL-2) is a key regulator of apoptosis which has been shown to be dysregulated in a range of malignancies (Asmarinah et al., 2014; Seong et al., 2015). In normal cells, BCL-2 has an anti-apoptotic activity as it inhibits the release of the caspase-activating cytochrome C from mitochondria. In cancer, upregulation of BCL-2 allows cells to avoid apoptosis (Yang et al., 1997a; Placzek et al., 2010). In prostate cancer, this increase in expression is likely a result of the activation of the PI3K/NF-κB cascade (Catz and Johnson, 2003).

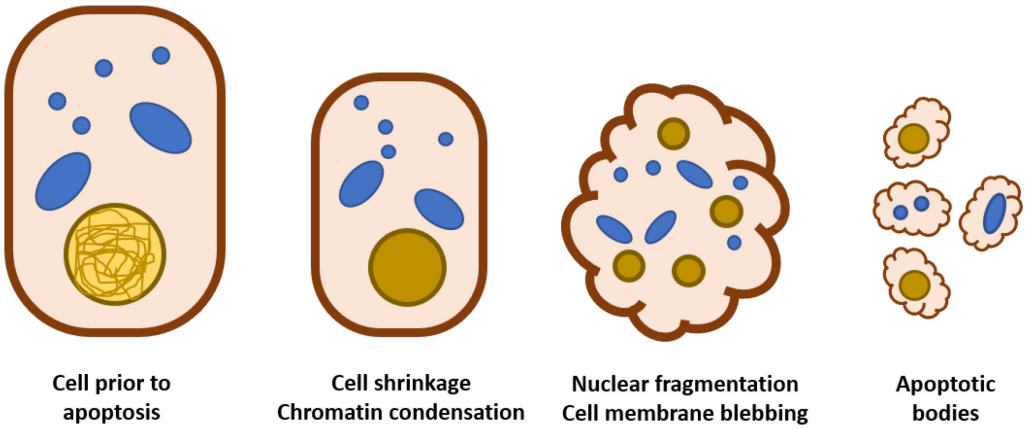

Figure 5.2. Overview of apoptosis

Once the cell receives apoptotic signals it begins to shrink and the chromatin in its nucleus condenses. This is followed by fragmentation of the nucleus and the development of cell membrane blebs. This leads to the formation of apoptotic bodies which are phagocytosed by the immune cells.

The main function of the tumour suppressor gene p53 is to prevent cells with DNA-damage from proliferating, thus preventing oncogenesis; loss of functional protein means this tight control of damage prevention is lost (Zilfou and Lowe, 2009). In healthy cells, DNA damage or cellular stress is detected by p53, and it can activate programmed cell death by inducing p53-regulated apoptosis-inducing protein 1 (p53AIP1) to enter the mitochondria, thus disturbing the mitochondrial membrane. Additionally, ubiquitinated p53 can inhibit the antiapoptotic activity of BCL-2 (Matsuda et al., 2002; Amaral et al., 2010). Studies in cellular models of prostate cancer have shown that loss of functional p53 leads to resistance to chemo- and radiotherapy, as the cells can proceed through the cell cycle despite treatment (Chappell et al., 2012).

Death domain-associated protein (or DAXX) is involved in apoptosis and the regulation of autophagy, and has been shown to be upregulated in prostate cancer (Yang et al., 1997b; Puto et al., 2015). Another inducer of the apoptosis cascade is tumour-necrosis factor (TNF)-related apoptosis-inducing ligand (or TRAIL) and its binding to decoy receptors, with the TNF-receptor superfamily 10D (encoded by *TNFRSF10D*) being investigated by the qPCR array.

A brief overview of the process can be found in Figure 5.3.

5.1.4. Cell cycle

The cell cycle is a series of processes a cell undergoes in order to divide and produce two daughter cells.

Once division is initiated the cell enters the interphase state which consists of three stages G_1, S and G_2 (Figure 5.4.A). The Gap/Growth 1 (G_1) phase is initiated by mitogens and the phase involves accumulation of nutrients and organelles for the upcoming cellular division (Massague, 2004). During the G_1 phase the cell must progress through the cell division restriction point. Until this point the retinoblastoma (Rb) tumour suppressor protein is hypophosphorylated (Figure 5.4.B). If no issues are detected by p53, this tumour suppressor allows the cell cycle to progress and leads to the activation of two main protein complexes cyclin E-cyclin dependent kinase 2 (CDK2) and cyclin D-CDK4/6 and cyclin E-CDK2 which leads to the hyperphosphorylation of Rb and inhibits its suppression of transcription, i.e. it allows S-phase gene transcription to proceed

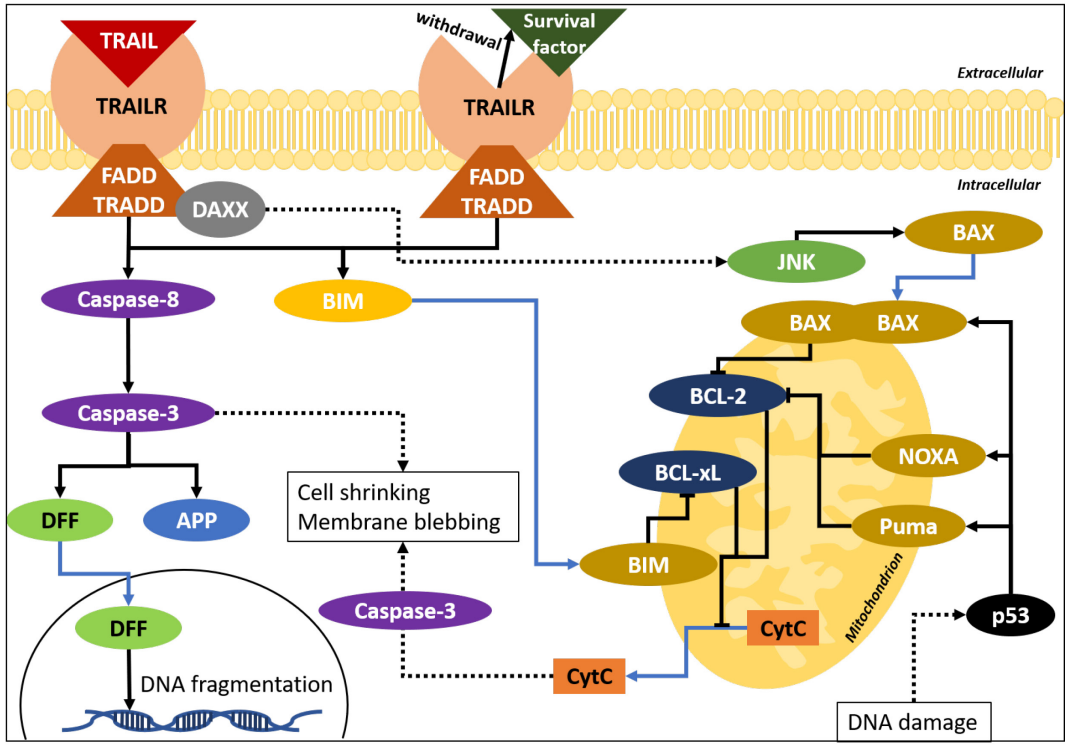

Figure 5.3. Overview of the apoptosis pathway

Signalling via TNF-related apoptosis-inducing ligand (TRAIL) leads to the recruitment of Fas-associated protein with death domain (FADD) and tumour necrosis factor receptor type 1-associated DEATH domain (TRADD) which initiate downstream signalling. The activation of the activator caspase 8 is followed by the formation of functional executioner caspase 3 which can cause DNA fragmentation and can indirectly initiate apoptosis. Death domain-associated protein (DAXX) and the withdrawal of survival signalling lead to the translocation of BCL-2-associated protein X (BAX) and BCL-2-like protein 11 (BIM) to the mitochondria which inhibit the anti-apoptotic B-cell lymphoma 2 (BCL-2) and B-cell lymphoma-extra large (BCL-xL). If active, BCL- and BCL-xL inhibit the release of cytochrome C (Cyt C) from the mitochondria. DNA damage, for example, activated Puma, NOXA and BAX, which inhibit BCL-2 and BCL-xL, the inactivation of cytochrome C release. Cytochrome C can also indirectly activate apoptosis.

Legend: APP – amyloid precursor protein; DFF – DNA fragmentation factor; JNK – c-Jun N-terminal kinase; p53 – protein 53; TRAILR – TRAIL receptor;

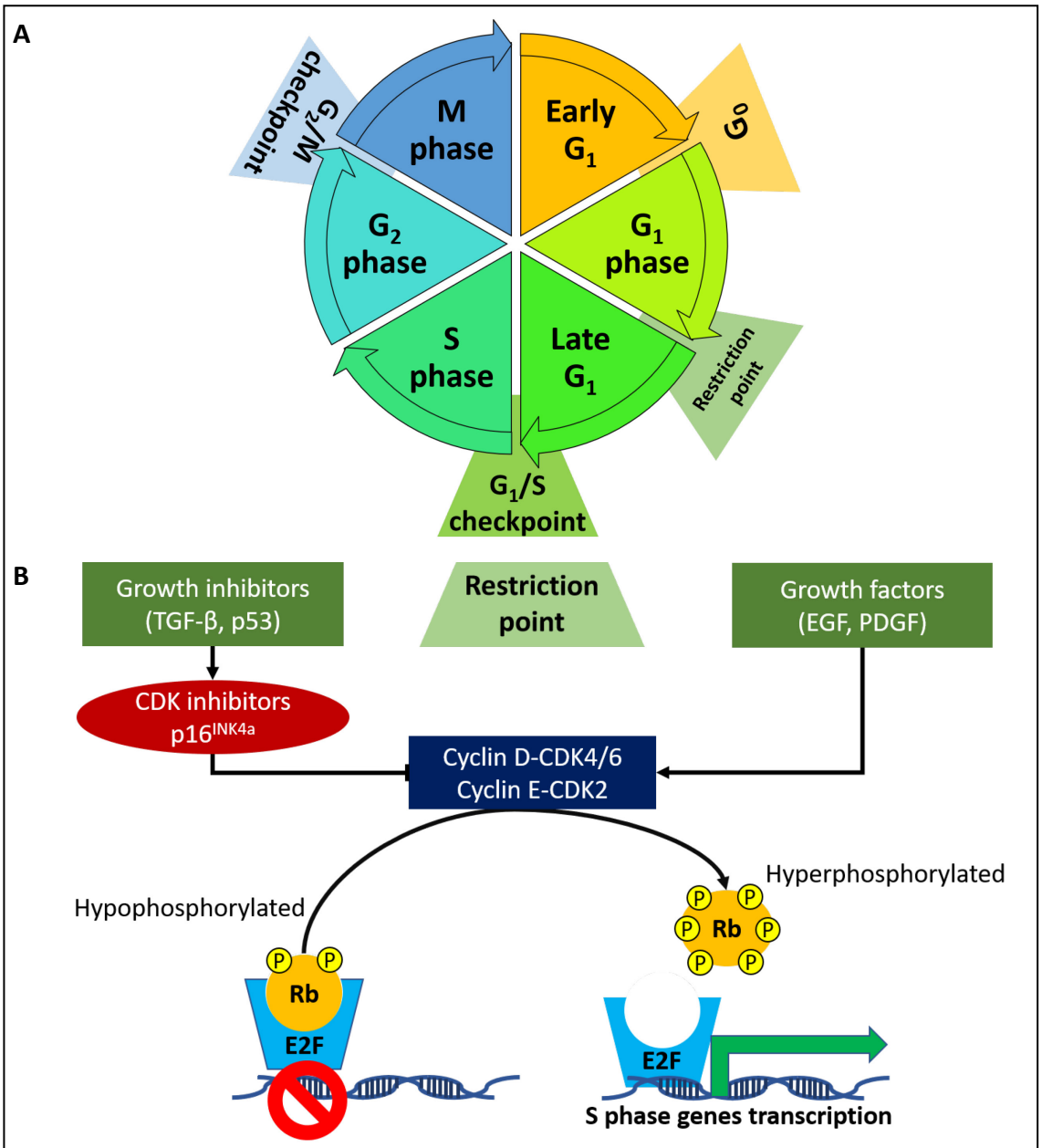

Figure 5.4. Cell cycle overview

A. Cell cycle progression. The cell cycle consists of Gap/Growth phase (either G_1 phase which prepares the cell for division, or G_0 phase of arrested development), the synthesis phase (S phase), G_2 phase preparing proteins necessary for the division and mitosis (M-phase; cell division).

B. Restriction point of the cell cycle. The restriction point is controlled by activating (e.g. growth factors) and inhibiting signalling, which affect the formation of cyclin D-CDK4/6 and cyclin E-CDK2 complexes which hyperphosphorylate retinoblastoma protein (Rb). This leads to the release of E2F, initiating transcription. If Rb is not phosphorylated, it remains bound to E2F, inhibiting transcription.

Legend: *CDK – cyclin-dependent kinase; E2F – E2 factor; EGF – epidermal growth factor p16^{INK4a} – cyclin-dependent kinase inhibitor 2A; p53 – protein 53; PDGF – platelet-derived growth factor; TGF-β – transforming growth factor-beta;*

(Giacinti and Giordano, 2006). If any issues are detected at this G_1/S checkpoint the cell may enter the G_0 phase (resting state) or apoptosis may be initiated. The resting state of the cell can be either reversible (called quiescence which occurs when insufficient nutrients are available, and the cell cannot proceed with division or when DNA damage is discovered and proceed until the issue is repaired) or irreversible (differentiation or senescent) (Linke et al., 1996).

When the cell proceeds to the S-phase (or synthesis phase) it undergoes replication and as a result at the end of the S-phase chromosomes are duplicated (Takeda and Dutta, 2005). Once the S-phase is complete, the cell enters a second growth-phase (G_2) when it produces proteins necessary for undergoing mitosis and proceeds through the G_2/M checkpoint where any damaged DNA is detected and repaired; if DNA damage remains unrepaired then it could have fatal consequences for the newly divided cell, or it can lead to oncogenesis (Otto and Sicinski, 2017).

The final stage of the cell cycle is mitosis (or the M-phase) where the cell divides. An illustration of the process can be found in Figure 5.5. Mitosis begins with the prophase where the DNA is condensed into chromosomes, continues with loss of nuclear structure and arrangement of the chromosomes along the metaphase plane. The cell then undergoes the anaphase, where the two daughter chromosomes are pulled apart by the kinetochore microtubules. Finally, the cells enter the telophase, where the nucleus is once again formed, and a cleavage furrow leads to the separation of the two new daughter cells (cytokinesis).

Loss of heterozygosity or loss of function mutations in either p53 or Rb, which play a role in the tight regulation of the process, can drive uncontrolled cell division and progression of the cell cycle even if DNA damage is present (Demidenko et al., 2005). Furthermore, abnormal expression of cyclins (e.g. cyclin A and cyclin E) and CDKs (including CDK4), as well as CDK-inhibitors, such as p16 (also known as cyclin-dependent kinase inhibitor 2A (CDKN2A) or $p16^{Ink4A}$), may lead to cell cycle progression despite p53 stop signals (Opitz et al., 2001). Downregulation of $p16^{Ink4A}$ has been shown to be an indicator of metastatic prostate cancer (Chakravarti et al., 2007).

Caveolin-1 and 2 (encoded by *CAV1* and *CAV2*, respectively) are membrane proteins normally expressed as a heterocomplex. It has been suggested that a loss of CAV1 in

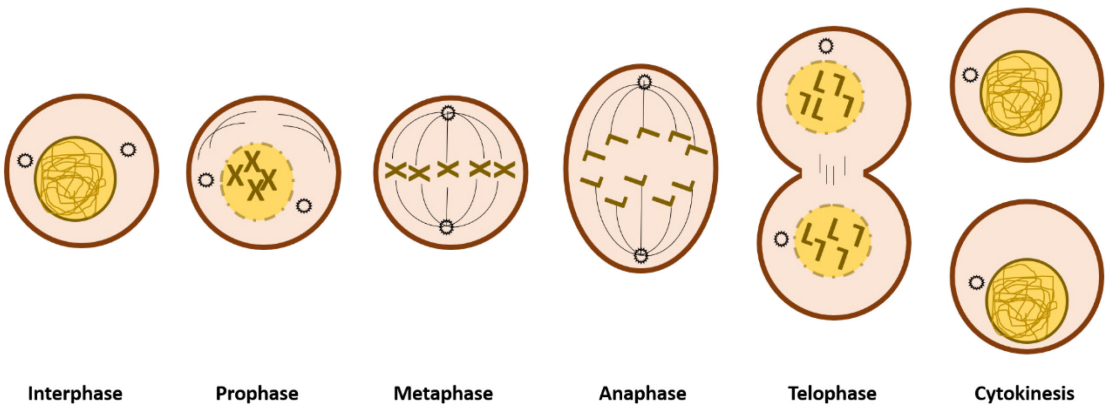

Figure 5.5. Mitosis

Cellular division has six distinct stages. The interphase includes the Gap/Growth 1 (G_1), synthesis (S) and G_2 phases, during the cell prepares for division. It also includes a restriction point and two checkpoints, ensuring that only healthy cells proceed through division. During the prophase, chromatin condenses to from chromosomes and the nucleus is lost. The metaphase includes the arrangement of the chromosomes along the metaphase plane. During the anaphase the sister chromatids are pulled apart towards the opposite ends of the cell. The telophase includes the re-formation of the nuclear membrane surrounding the two newly formed nuclei, and this is followed by cytokinesis, where the two daughter cells are separated.

stromal cells drives prostate cancer metastasis, while other studies have demonstrated that increased plasma levels of both CAV1 and CAV2 are associated with aggressive prostate tumours (Chakravarti et al., 2007; Sugie et al., 2015).

5.1.5. Fatty acid synthesis

As healthy prostate cells require citrate as part of the prostatic fluid secretions, they mainly produce energy using glycolysis; however, when cells become cancerous they require larger energy supplies and thus switch to the more energy-efficient Krebs cycle (the citric acid cycle) (Costello and Franklin, 2000). This contrasts what happens in other cells where there is a switch from efficient to energy-inefficient metabolism if they undergo oncogenesis. When the newly-cancerous prostate cells do switch to utilising the Krebs cycle for energy the citric acid that would be secreted in a healthy cell, turns into building blocks for the synthesis of fatty acids. As a result, studies have shown that genes involved in fatty acid and cholesterol biosynthesis are altered in prostate cancer, including acetyl-CoA carboxylase alpha (ACACA), fatty acid synthase (FASN*)*, 3-hydroxy-3-methylglutaryl-CoA reductase (HMGCR), AMP-activated protein kinase (AMPK, encoded by *PRKAB1*), sterol regulatory element-binding protein 1 (SREBF1) (Heemers et al., 2001; Van de Sande et al., 2005; Hager et al., 2006; Beckers et al., 2007; Kim et al., 2014).

ACACA is involved in the conversion of acetyl-CoA to malonyl-CoA which is the first step of the *de novo* fatty acid synthesis pathway in the cells. This process is ATP-dependent and is the rate-limiting step for the pathway. The next step in the synthesis of long chain fatty acids in catalysed by the homodimer fatty acid synthase (FASN) which has three enzymatic domains, and converts acetyl-CoA and malonyl-CoA to palmitate (a 16-carbon long chain fatty acid) in the presence of reduced nicotinamide adenine dinucleotide (NADH). A separate pathway, also utilising acetyl-CoA leads to the synthesis of cholesterol (with cholesterol being a building block of steroid hormones such as androgens), with a key regulator being HMGCR (which is in turn transcriptionally controlled by SREBF and by AMPK-phosphorylation, targeting it at the protein level) (Wu et al., 2014). An overview can be seen in Figure 5.6.

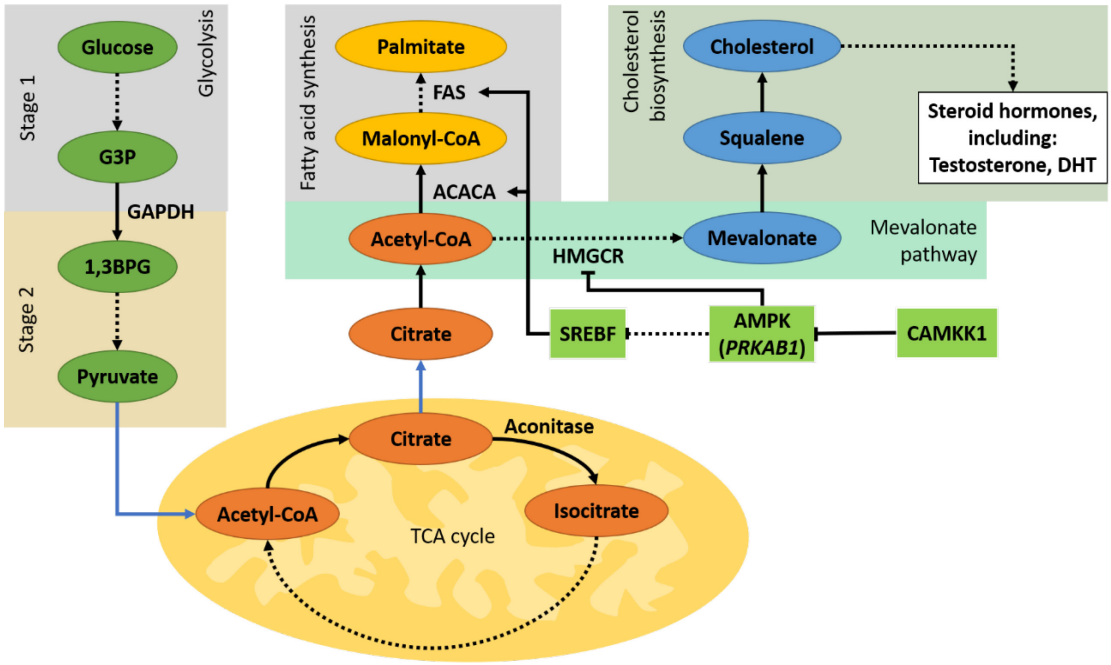

Figure 5.6. Glycolysis and fatty acid synthesis

Glycolysis is the breakdown of glucose to produce pyruvate and energy. The process has two stages: Stage 1 where energy is invested concluding with the formation of two 3-carbon molecules (glyceraldehyde 3-phosphate, G3P) from a 6-carbon precursor. Stage 2 is initiated by the conversion of G3P to 1,3-bisphosphoglycerate (1,3BPG) by glyceraldehyde phosphate dehydrogenase (GAPDH). The reaction concludes with the formation of pyruvate, which is converted to acetyl-CoA and is translocated to the mitochondria where in initiates the tricarboxylic acid cycle (TCA or Krebs cycle). In the first step of the TCA acetyl-CoA is converted to citrate. The citrate is then converted to isocitrate by the enzyme aconitase; however, in prostate cells this reaction is inhibited by the high concentration of accumulated zinc ions.

In addition to being a key component of the TCA cycle, citrate can be translocated to the cytoplasm, where it can be reverted to acetyl-CoA, which can have multiple fates. Acetyl-CoA can be used for *de-novo* fatty acid synthesis, by being converted to Malonyl-CoA by acetyl-CoA carboxylase-alpha (ACACA), and then can be used to synthesise palmitate via the activity of the enzymatic complex fatty acid synthase (FAS, encoded by *FASN*). Both FAS and ACACA can be stimulated by sterol regulatory element-binding factor 1 (SREBF). Alternatively, acetyl-CoA can initiate the Mevalonate pathway, where it can be converted to mevalonate by 3-hydroxy-3-methylglutaryl-CoA reductase (HMGCR). AMP-activated protein kinase (AMPK) can act as a direct or indirect inhibitor for HMGCR and SREBF, respectively. Additionally, AMPK activity can be inhibited by calcium/calmodium-dependent protein kinase kinase 1 (CAMKK1).

The newly synthesised mevalonate can then enter the cholesterol biosynthesis pathway, where it can be converted to squalene and then cholesterol, which has a number of functions, including the formation of steroid hormones (including testosterone and dihydrotestosterone (DHT), which are of interest in the context of prostate cancer).

5.1.6. Wnt/β-catenin pathway

The Wnt/β-catenin pathway is key both in development and in sustaining homeostasis, damage repair and growth in adult life (Alonso and Fuchs, 2003; Pinto and Clevers, 2005; Malhotra and Kincade, 2009; Nemeth et al., 2009; Beers and Morrisey, 2011; Monga, 2011; Whyte et al., 2012). It is also commonly dysregulated in a range of cancers, and it plays a role in genetic instability, apoptosis, cellular migration (Alberici and Fodde, 2006; Pećina-Šlaus, 2010; Rawson et al., 2011; Hoffmeyer et al., 2012; Frisch et al., 2013; Webster and Weeraratna, 2013). The pathway's dysregulation in cancer can be a result of activation of pathway components which promote tumour progression; alternatively, it could be due to mutations or loss of function of genes which normally suppress it (Polakis, 2012). An example of the involvement of the Wnt/β-catenin pathway in cancer can be seen in colorectal cancer with a mutation in the adenomatous polyposis coli (APC) tumour suppressor gene, which is a known negative regulator of β-catenin activity; loss of both alleles of APC leads to loss of regulation of β-catenin functions and also causes chromosomal instability (Lengauer et al., 1998; Polakis, 2007). The APC tumour suppressor gene can also mediate the activity of β-catenin which in turn has the potential to affect the production of cyclin D1; incapacitated APC would not inhibit the activity of β-catenin, leading to increased cyclin D1 production and the potential for the cell to undergoes uncontrolled proliferation (Shtutman et al., 1999). APC also forms complexes with other proteins which plays a key role in apoptosis induction if high levels of DNA damage are present during the cell cycle (Jaiswal and Narayan, 2008).

The Wnt/β-catenin pathway can be involved in oncogenesis by aberrant activity of pathway ligands, epigenetically silenced antagonists of the pathway (which is seen in many cancers, including prostate cancer) or through β-catenin-independent signalling (Rhee et al., 2002; Wong et al., 2002; Milovanovic et al., 2004; Kikuchi and Yamamoto, 2008; Kypta and Waxman, 2012). An overview of Wnt/β-catenin signalling can be seen in Figure 5.7.

A more direct example of how the pathway may be involved in oncogenesis, especially EMT, is that one of the transcription factors activated by the pathway is Slug (encoded by *SNAI2*), which can induce EMT; additionally, the pathway also inhibits the degradation of Snail (encoded by *SNAI1*) (Conacci-Sorrell et al., 2003; Yook et al., 2005).

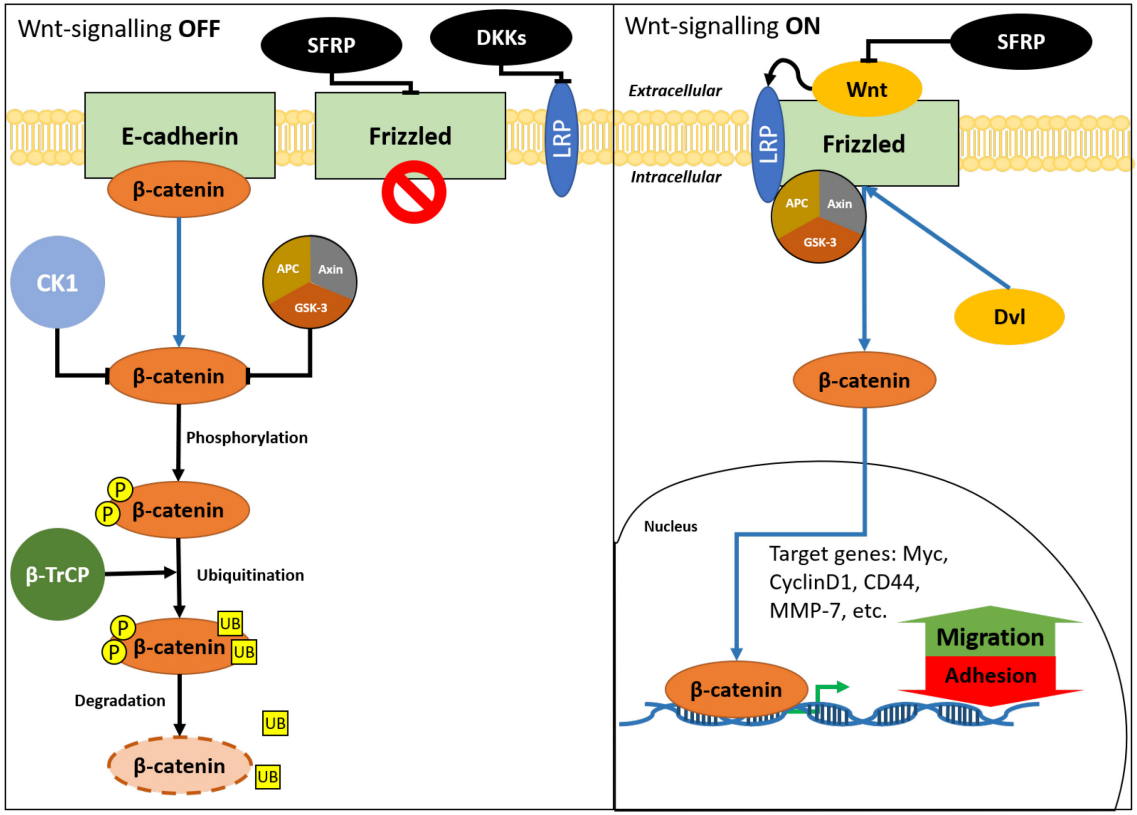

Figure 5.7. Wnt/β-catenin signalling pathway

If the Wnt/β-catenin pathway is not activated β-catenin is translocated to the cytoplasm where it is inactivated by phosphorylation (P, by CK1 and the APC/Axin/GSK-3 complex) and ubiquitination (UB), leading to its degradation. If the signalling is activated, Dishevelled (Dvl) binds the APC/Axin/GSK-3 complex, preventing it from initiating the degradation of β-catenin. Thus, β-catenin is translocated to the nucleus where it can initiate the transcription of a range of target genes, leading to decreased adhesion and increase migration.

Legend: APC – adenomatous polyposis coli; β-TrCP – F-box/WD repeat-containing protein 1A; CK1 – casein kinase 1; DKK – Dickkopf related proteins; GSK-3 – glycogen synthase kinase 3; LRP – lipoprotein receptor-related protein; MMP – matrix metalloproteinase; SFRP – secreted frizzled-related protein;

5.1.7. Metastasis

Metastasis is a complex process which allows cancer cells to travel to distant sites in the body and to form secondary tumours in distinct organs, for example prostate cancer most commonly metastasizes to the bone. To become metastatic, the cancer cells need to undergo EMT (which is discussed in more detail Chapter 4, Section 4.1.6.4) and to gain the ability to invade the surrounding areas. The cancerous cells can then enter the blood stream (intravasation) and travel around the body. If the cancer cells escape the blood stream (extravasation) at a different location they can undergo mesenchymal-epithelial transition (MET) and form distant metastasis.(Quail and Joyce, 2013).

One of the key players in metastasis is E-cadherin (encoded by *CDH1*), as its loss is vital for cells to undergo EMT. Tissue inhibitors of metalloproteases (TIMPs) have been shown to play a role in the dysregulation of the switch of cadherins (from E-cadherin to N-cadherin in EMT), e.g. TIMP1 downregulates E-cadherin, while TIMP2 has an opposing effect and loss of TIMP3 has been linked to E-cadherin and β-catenin-signalling dysregulation (Hojilla et al., 2007; Bourboulia et al., 2013; D'Angelo et al., 2014). Other genes involved in metastatic cancer whose dysregulation is assessed in this chapter include cyclic AMP-responsive element-binding protein (CREB1), Myc-associated factor X (MAX), N-myc downregulated gene family member 3 (NDRG3*).*

Phosphorylated CREB1 has been shown to be upregulated in prostate cancer and bone metastases, and is absent in benign prostate samples, indicating a role for CREB1 in metastasis and cancer progression (Wu et al., 2007).

Myc is a transcription factor which has low level of expression in healthy cells; its production is tightly controlled and can be activated by a number of pathways (including the Wnt/β-catenin and JAK/STAT3 pathways); a known inhibitor of Myc is TGF-β-signalling (Bromberg et al., 1999). To become an active transcription factor Myc forms a heterodimer with MAX and together they can bind enhancer boxes (E-boxes) and initiate the transcription of a range of genes (Eilers and Eisenman, 2008). Examples of genes controlled by Myc include upregulation of cyclin D and cyclin E (which are involved in the tight control of cell cycle progression), BCL-2 (which plays a role as a regulator of apoptosis) and fatty acid synthase, as well as downregulation in a range of genes, e.g. cell cycle inhibitors (Perez-Roger et al., 1999; Beier et al., 2000; Eischen et al., 2001; Gartel et al., 2001; Seoane et al., 2001; Dang, 2013). NDRG, another target of the MYC-

MAX complex, is a protein involved in proliferation, growth and differentiation (Shimono et al., 1999; Zhang et al., 2008).

5.1.8. Promoter methylation

The field of epigenetics focuses on investigating phenotypic changes which are not a result of DNA alterations and it plays an important role in the normal functionality of cells, for example in differentiated cells; it does, play a role in disease, and specifically cancer (Jones and Laird, 1999; Jones and Takai, 2001; Egger et al., 2004). One form of epigenetic modification is the methylation of the cysteine residue of the so-called CpG islands (clusters of CpG sequences in the genome, usually in close proximity to gene promoter regions) (Bird, 1986). Studies discovered that constitutively expressed genes lack such methylation, while if the same genes were methylated their expression was lost (Bird, 1986).

Bacteria have the ability to affect DNA methylation. Examples include *Fusobacterium* sp. accelerating DNA methylation in a subgroup of ulcerative colitis-related genes (Tahara et al.). Additionally, *H. pylori* has been shown to play a role in aberrant CpG island methylation of gastric cells and the methylation observed has been linked to gastric cancer (Maekita et al., 2006; Matsusaka et al., 2014).

In cancer, methylation can play a role in two ways. First, hypomethylation of genes which would normally have suppressed expression may lead to the activation of oncogenes which drive cancer progression (Chen et al., 1998). Alternatively, hypermethylation of promoters can lead to loss of expression of tumour suppressor genes, for example *CDH1*.

A number of genes have been shown to be epigenetically modified in prostate cancer, including *CDH1*, *CAV1, APC, RASSF1A, CRBP1, TIMP3* (Cui et al., 2001; Li et al., 2001; Jeronimo et al., 2004).

5.2. *Materials and methods*

5.2.1. RNA extraction and quantification

RNA was extracted as described in Section 2.4.2.1 using the RNeasy Plus Mini-Kit (QIAGEN, Germany) following the manufacturer's protocol, and was quantified using the Qubit® RNA BR Assay kit (ThermoScientific, UK) as outlined in Section 2.4.1.2.

5.2.2. cDNA synthesis

For cDNA synthesis, the recommended RT^2 First Strand Kit (QIAGEN, Germany) was used as detailed in Section 2.4.2.4.5.1. The infection models used for cDNA synthesis and the following qPCR array analysis were 00035, B3 and CFU2 at day 15, selected based on the Chapter 4 findings.

5.2.3. RT^2 Profiler Human Prostate Cancer PCR array

The qPCR arrays were prepared as described in Section 2.4.2.4.5.2, mixing 1350 µl 2x RT^2 SYBR Green Mastermix (QIAGEN, Germany), with the cDNA synthesised in Section 5.2.2 and water. Each qPCR array consisted of 84 prostate cancer related genes, 5 housekeeping genes, 1 genomic DNA control, 3 reverse-transcription (RT) controls and 3 positive PCR controls (PC). The 5 housekeeping genes (*ACTB*, *B2M*, *GAPDH*, *HPRT1* and *RLPL0*) were used by the analysis software to select the most stable gene or a combination of genes. The genomic DNA control was used in the place of a standard no-RT control, and it targeted a non-coding DNA region was selected as a target of the assay. The cDNA kit was preloaded with a synthetic mRNA sequence with a poly-A tail which was transcribed along with the sample mRNA. This RT-control was used to determine the efficiency of the reverse transcription and was used as a comparator between different samples. Finally, the PC wells contained a small amount of DNA and primers, which were used as a control between qPCR arrays, and should not differ between plates. For analysis, the recommended threshold of 35 cycles was used, thus excluding any Cp values above 35.

Table 5.1 presents a list of all genes included in the array (including housekeeping genes and controls), and the signalling pathways they are involved in; it also includes genes not involved in pathways but with promoters known to be methylated in prostate cancer and genes known to be up- or downregulated in prostate cancer.

Out of the 84 genes included in the array, in the context of prostate cancer 59 are linked to at least one signalling pathway, while the remaining 25 are either known to have methylated promoters or to be up/down regulated.

Table 5.1. List of genes included in the qPCR array and their main functions

Gene	Accession number	Full name	Function									
			1	2	3	4	5	6	7	8	9	UD
IGF1	NM_000618	Insulin-like growth factor 1 (somatomedin C)	+	+	+	+						**D**
PTEN	NM_000314	Phosphatase and tensin homolog	+	+	+	+						
TIMP2	NM_003255	Tissue inhibitor of metalloproteinases 2	+	+	+					+		
NFKB1	NM_003998	Nuclear factor of kappa light polypeptide gene enhancer in B-cells 1	+	+	+						+	
GNRH1	NM_000825	Gonadotropin-releasing hormone 1 (luteinizing-releasing hormone)	+	+	+							
IL6	NM_000600	Interleukin 6	+	+	+							
TIMP3	NM_000362	Tissue inhibitor of metalloproteinases 3	+	+	+							
EGFR	NM_005228	Epidermal growth factor receptor	+	+		+						
CCND1	NM_053056	Cyclin D1	+	+		+						
AR	NM_000044	Androgen receptor	+	+						+	+	
FOXO1	NM_002015	Forkhead box O1	+	+							+	
VEGFA	NM_003376	Vascular endothelial growth factor A	+	+								
CDKN2A	NM_000077	Cyclin-dependent kinase inhibitor 2A (melanoma, p16, inhibits CDK4)	+		+	+				+	+	
TP53	NM_000546	Tumour protein p53	+		+	+					+	
BCL2	NM_000633	B-cell CLL/lymphoma 2	+		+	+						
MAPK1	NM_002745	Mitogen-activated protein kinase 1	+		+							
CCND2	NM_001759	Cyclin D2	+			+						**D**
CDH1	NM_004360	Cadherin 1, type 1, E-cadherin (epithelial)	+							+		
DAXX	NM_001350	Death-domain associated protein	+								+	
PDPK1	NM_002613	3-phosphoinositide dependent protein kinase-1	+									**U**
AKT1	NM_005163	Protein kinase B	+									
CAV1	NM_001753	Caveolin 1, caveolae protein, 22kDa		+						+		
TNFRSF10D	NM_003840	Tumour necrosis factor receptor superfamily, member 10d, decoy with truncated death domain		+						+		

Gene	Accession number	Full name	Function									
			1	2	3	4	5	6	7	8	9	UD
NRIP1	NM_003489	Nuclear receptor interacting protein 1		+							+	
TGFB1I1	NM_015927	Transforming growth factor beta 1 induced transcript 1		+								
CASP3	NM_004346	Caspase 3, apoptosis-related cysteine peptidase			+	+						
ETV1	NM_004956	Ets variant 1			+						+	**U**
APC	NM_000038	Adenomatous polyposis coli				+				+		
CCNA1	NM_003914	Cyclin A1				+				+		
PTGS2	NM_000963	Prostaglandin-endoperoxide synthase 2 (prostaglandin G/H synthase and cyclooxygenase)				+				+		
PPP2R1B	NM_002716	Protein phosphatase 2, regulatory subunit A, beta				+						**D**
CAV2	NM_001233	Caveolin 2				+						
PTGS1	NM_000962	Prostaglandin-endoperoxide synthase 1 (prostaglandin G/H synthase and cyclooxygenase)				+						
SREBF1	NM_004176	Sterol regulatory element binding transcription factor 1					+				+	
ACACA	NM_198834	Acetyl-CoA carboxylase alpha					+					
CAMKK1	NM_032294	Calcium/calmodulin-dependent protein kinase kinase 1, alpha					+					
FASN	NM_004104	Fatty acid synthase					+					
HMGCR	NM_000859	3-hydroxy-3-methylglutaryl-CoA reductase					+					
PRKAB1	NM_006253	Protein kinase, AMP-activated, beta 1 non-catalytic subunit					+					
STK11	NM_000455	Serine/threonine kinase 11					+					
CREB1	NM_004379	CAMP responsive element binding protein 1						+			+	
MAX	NM_002382	MYC associated factor X						+			+	
KLHL13	NM_033495	Kelch-like 13 (Drosophila)						+				
NDRG3	NM_022477	NDRG family member 3						+				
PES1	NM_014303	Pescadillo homolog 1, containing BRCT domain (zebrafish)						+				
SCAF11	NM_004719	SR-related CTD-associated factor 11						+				

Gene	Accession number	Full name	Function									
			1	2	3	4	5	6	7	8	9	UD
SEPT7	NM_001788	Septin 7						+				
MKI67	NM_002417	Antigen identified by monoclonal antibody Ki-67							+			
TMPRSS2	NM_005656	Transmembrane protease, serine 2							+			
MSX1	NM_002448	Msh homeobox 1								+	+	
RARB	NM_000965	Retinoic acid receptor, beta								+	+	
SFRP1	NM_003012	Secreted frizzled-related protein 1								+		**D**
SLC5A8	NM_145913	Solute carrier family 5 (iodide transporter), member 8								+		**D**
ARNTL	NM_001178	Aryl hydrocarbon receptor nuclear translocator-like								+		**U**
DKK3	NM_015881	Dickkopf homolog 3 (*Xenopus laevis*)								+		
DLC1	NM_006094	Deleted in liver cancer 1								+		
EDNRB	NM_000115	Endothelin receptor type B								+		
GPX3	NM_002084	Glutathione peroxidase 3 (plasma)								+		
GSTP1	NM_000852	Glutathione S-transferase pi 1								+		
MGMT	NM_002412	O-6-methylguanine-DNA methyltransferase								+		
PDLIM4	NM_003687	PDZ and LIM domain 4								+		
RASSF1	NM_007182	Ras association (RalGDS/AF-6) domain family member 1								+		
ZNF185	NM_007150	Zinc finger protein 185 (LIM domain)								+		
RBM39	NM_004902	RNA binding motif protein 39									+	**U**
SOX4	NM_003107	SRY (sex determining region Y)-box 4									+	**U**
SUPT7L	NM_014860	Suppressor of Ty 7 (*S. cerevisiae*)-like									+	**U**
EGR3	NM_004430	Early growth response 3									+	
ERG	NM_182918	V-ets erythroblastosis virus E26 oncogene homolog (avian)									+	
NKX3-1	NM_006167	NK3 homeobox 1									+	
SHBG	NM_001040	Sex hormone-binding globulin									+	
CLN3	NM_000086	Ceroid-lipofuscinosis, neuronal 3										**D**

Gene	Accession number	Full name	Function									
			1	2	3	4	5	6	7	8	9	UD
GCA	NM_012198	Grancalcin, EF-hand calcium binding protein										**D**
LGALS4	NM_006149	Lectin, galactoside-binding, soluble, 4										**D**
LOXL1	NM_005576	Lysyl oxidase-like 1										**D**
TFPI2	NM_006528	Tissue factor pathway inhibitor 2										**D**
USP5	NM_003481	Ubiquitin specific peptidase 5 (isopeptidase T)										**D**
CAMSAP1	NM_015447	Calmodulin regulated spectrin-associated protein 1										**U**
DDX11	NM_004399	DEAD/H (Asp-Glu-Ala-Asp/His) box polypeptide 11										**U**
ECT2	NM_018098	Epithelial cell transforming sequence 2 oncogene										**U**
HAL	NM_002108	Histidine ammonia-lyase										**U**
IGFBP5	NM_000599	Insulin-like growth factor binding protein 5										**U**
KLK3	NM_001648	Kallikrein-related peptidase 3										**U**
MTO1	NM_012123	Mitochondrial translation optimization 1 homolog (*S. cerevisiae*)										**U**
SOCS3	NM_003955	Suppressor of cytokine signalling 3										**U**
ACTB	NM_001101	Actin, beta	Housekeeping genes									
B2M	NM_004048	Beta-2-microglobulin										
GAPDH	NM_002046	Glyceraldehyde-3-phosphate dehydrogenase										
HPRT1	NM_000194	Hypoxanthine phosphoribosyltransferase 1										
RPLP0	NM_001002	Ribosomal protein, large, P0										
PPC	SA_00103	Positive PCR Control	Controls									
RTC	SA_00104	Reverse Transcription Control										
HGDC	SA_00105	Human Genomic DNA Contamination Control										

Function *indicated what role the different genes have in prostate cancer: 1. AKT and PI3K signalling pathway; 2. Androgen receptor signalling; 3. Apoptosis; 4. Cell cycle; 5. Fatty acid synthesis; 6. Metastasis; 7. Other prostate cancer-related genes; 8. Genes in methylated promoters in prostate cancer; 9. Transcription factor;* ***UD*** *indicates whether a gene is up or down regulated in prostate cancer;*

5.2.4. Data analysis

The qPCR array data was analysed using the SABiosciences RT^2 Profiler PCR Array Data Analysis software (http://pcrdataanalysis.sabiosciences.com/pcr/arrayanalysis.php), version 3.5. Once the data was uploaded, the software prompted the selection of a housekeeping gene to be used, based on a list of calculated most stable options. The data was then normalized, using the selected control gene and the $\Delta\Delta C_T$ method was used for further analysis (Livak and Schmittgen, 2001). Briefly, the raw data was normalized to the housekeeping gene by subtracting the C_T value for housekeeping gene from the C_T value of the gene of interest. The mean value of all housekeeping genes is used, if multiple genes are selected).

$$\Delta C_T = C_{T\ (gene\ of\ interest)} - C_{T\ (housekeeping\ gene)}$$

Following, the mean ΔC_T value for all biological replicates was calculated; the mean ΔC_T was then used to calculate the $\Delta\Delta C_T$ by subtracting the ΔC_T of the control group from the ΔC_T of the test group.

$$\Delta\Delta C_T = \Delta C_T\ (test\ group) - \Delta C_T\ (control\ group)$$

Finally, the fold-change (FC) difference was calculated by converting the $\Delta\Delta C_T$ to a linear scale from a $\log_2$ scale using the equation below:

$$\mathrm{FC} = 2^{(-\Delta\Delta C_T)}$$

Once calculated, the fold-change values represented the difference in expression between control and test groups, with values higher than 1 representing upregulation and values lower than 1 – downregulation. A better visual representation of this information is referred to as “fold-regulation” where all fold-change values lower than 1 are presented as negative inverse fold-change, i.e. -1 is divided by the fold-change, resulting in a negative value. For example, a fold-change of 0.2 would be presented as a fold-regulation of -5.

The data was represented using scatter plots and volcano plots. The scatter plots compared the normalised expression for all genes in each infection model to the uninfected controls. Each scatter plot has a single solid trendline indicating a baseline, where no difference was observed between the two treatments, and two dashed lines, indicating change of more than 2-fold increase and 2-fold decrease. Volcano plots were

used to present fold-dysregulation versus p-value. Each graph has a single black horizontal line, representing a threshold p-value p = 0.05. Additionally, three vertical lines can be seen. A single thick grey line indicating a baseline fold-change of 1, and two thin grey lines surrounding it, marking fold-deregulation in expression of more than -2-fold downregulation or more than 2-fold upregulation.

The statistical significance of the dysregulation observed was assessed using Student's t-test, comparing each infection model to untreated controls.

5.3. *Results*

5.3.1. qPCR array housekeeping gene selection

Out of the 5 housekeeping genes used in the qPCR array the software detected *HPRT1* as the most stable gene with values showing standard deviation between groups of 0.111, with mean C_T values for each group seen in Table 5.2.

5.3.2. qPCR array data

All control samples passed the respective assessments, meaning that the data was comparable between all arrays, there was no differences in how effective the cDNA synthesis was between different cDNA reactions and there was no genomic DNA contamination in the samples.

Fold regulation and p-values were calculated for all of the genes in the qPCR array and for each infection model tested. Three biological replicates were used for each infection model investigated. The gene dysregulation was assessed as statistically significant change based on 2-fold change of fold regulation combined with p-values $p < 0.05$. If only one of the criteria was present, then the change was considered a trend.

In the 00035 infection model a total of 56 genes showed signs of dysregulation compared to untreated controls, with 44 upregulated genes and 12 downregulated genes; 64% (36 genes) of the dysregulated genes showed statistically significant change, while 36% were only showing a trend (one gene had a statistically significant difference between mock and infected samples but the dysregulation was not greater than 2-fold

Table 5.2. Housekeeping gene selection for qPCR array analysis (C_T values)

Gene	Mocks			00035			B3			CFU2		
	M1	**M2**	**M3**	**I1**	**I2**	**3**	**I1**	**I2**	**3**	**I1**	**I2**	**3**
HPRT1	25.8	25.7	26.2	25.8	26.1	25.7	25.8	25.6	25.7	26.1	26.1	25.9
Mean	25.90			25.88			25.71			26.03		

and 19 genes had fold-regulation of more than 2-fold upregulation or -2-fold downregulation with $p > 0.05$). Table 5.3 presents the fold regulation and p-values for this infection model, while Figure 5.8 represents scatter and volcano plots. Gene ontology and STRING analyses can be found in Appendix D Figure 1. Out of the statistically significantly dysregulated genes, 13 were associated with methylated promoter regions in prostate cancer, 9 are transcription factors involved in the control of numerous processes, 7 are involved in the PI3K/AKT signalling pathway. Androgen receptor signalling and apoptosis involved 6 of the genes investigated, 5 of the genes participate in cell cycle control, and two have been linked to prostate cancer metastasis. Some genes are involved in more than one of the signalling pathways listed above, as seen in Table 5.1.

Cells infected with the type IB strain B3 had 9 genes with increased expression and 3 with decreased (a total of 12 genes). Out of these genes, only one was significantly dysregulated (*TFPI2* with 3.5-fold upregulation, $p = 0.0002$); additionally, only one gene showed a fold-regulation change greater than 2 but no significance (*SOCS3*, 2.5-fold increase, $p = 0.12$). The remaining 10 genes showed p-values $p > 0.05$, but fold-change in the -2-fold decrease to 2-fold increase range. Results for this infection model can be seen in Table 5.4 and scatter and volcano plots in Figure 5.9. Gene ontology and STRING analyses can be found in Appendix D Figure 2.

The third set of infection models investigated were cells infected with the type III strain CFU2. These arrays showed dysregulation in 59 genes, 57 of which were upregulated and 2 downregulated (only one of which, *ETV1*, showed statistical significance with 4.29-fold decrease and $p = 0.0002$). Significant dysregulation was seen in 23 genes (39%) and only p-value significance was seen in 36 genes (61%). The results for the CFU2 infection model can be found in Table 5.5; scatter and volcano plots can be seen in Figure 5.10. Gene ontology and STRING analyses can be found in Appendix D Figure 3. Out of the 23 genes showing significant changes in expression, 6 either have methylated promoters in the context of prostate cancer or are known transcription factors. There are 5 dysregulated genes in this infection model that play a role in both PI3K/AKT signalling and the androgen receptor signalling (namely *FOXO1*, *GNRH1*, *TIMP2*, *TIMP3*, and *VEGFA*). Out of the apoptosis-related genes investigated, 4 are dysregulated in this

Table 5.3. qPCR array results for the 00035 infection model

Gene	Fold regulation	p-value	Role in prostate cancer									
			1	2	3	4	5	6	7	8	9	UD
IL6	1811.96	0.0000	+	+	+							
SOCS3	42.13	0.0031										U
GPX3	41.07	0.0000								+		
TNFRSF10D	27.16	0.0031		+						+		
TMPRSS2	18.42	0.0000							+			
PTGS2	14.62	0.0000				+				+		
SFRP1	12.76	0.0004								+		D
B2M	10.85	0.0004	Housekeeping gene									
LGALS4	9.19	0.0001										D
TFPI2	8.96	0.0000										D
EGR3	8.71	0.0018									+	
CCNA1	8.55	0.0058				+				+		
SOX4	6.06	0.0007									+	U
DKK3	5.88	0.0001								+		
NKX3-1	5.15	0.0043									+	
IGFBP5	4.94	0.0001										U
LOXL1	4.89	0.0001										D
DLC1	4.88	0.0046								+		
GNRH1	4.51	0.0124	+	+	+							
MSX1	3.83	0.0010								+	+	
VEGFA	3.77	0.0003	+	+								
RASSF1	3.34	0.0057								+		
BCL2	3.21	0.0186	+		+	+						
TIMP2	2.73	0.0005	+	+	+					+		
DDX11	2.68	0.0212										U
CCND1	2.57	0.0053	+	+		+						
SUPT7L	2.30	0.0010									+	U
ARNTL	2.26	0.0015								+		U
HMGCR	2.20	0.0013					+					
RBM39	2.08	0.0040									+	U
GSTP1	1.56	0.0016								+		
SEPT	1.73	0.0045						+				
MAPK1	1.62	0.0079	+		+							
CAV1	1.84	0.0100		+						+		
FOXO1	1.51	0.0161	+	+							+	
CASP3	1.53	0.0173			+	+						
PDPK1	1.35	0.0223	+									U
CLN3	1.69	0.0245										D
PES1	1.95	0.0266						+				
PPP2R1B	1.21	0.0283				+						D
GCA	1.36	0.0339										D
EGFR	1.37	0.0419	+	+		+						

Gene	Fold regulation	p-value	Role in prostate cancer									
			1	2	3	4	5	6	7	8	9	UD
HAL	1.76	0.0459										U
ACTB	1.26	0.0462	Housekeeping gene									
PDLIM4	-11.60	0.0033								+		
ETV1	-8.40	0.0001			+						+	U
CCND2	-3.10	0.0012	+			+						D
GAPDH	-2.77	0.0092	Housekeeping gene									
TIMP3	-2.39	0.0013	+	+	+							
PTGS1	-2.27	0.0222										
ERG	-2.21	0.2790									+	
RPLP0	-1.74	0.0041	Housekeeping gene									
MGMT	-1.86	0.0108								+		
CDH1	-1.59	0.0156	+							+		
KLHL13	-1.86	0.0200						+				
NDRG3	-1.67	0.0228						+				
FASN	1.71	0.0895					+					
SHBG	1.44	0.2908									+	
CAMSAP1	1.41	0.0808										U
NFKB1	1.38	0.0530	+	+	+						+	
MAX	1.22	0.1713						+			+	
CAV2	1.21	0.0596				+						
APC	1.18	0.1162				+				+		
SCAF11	1.16	0.2588						+				
PRKAB1	1.15	0.3233					+					
TGFB1I1	1.11	0.6894		+								
IGF1	1.10	0.4953	+	+	+	+						D
DAXX	1.06	0.7154	+								+	
PTEN	1.02	0.8460	+	+	+	+						
HPRT1	1.00	-	Housekeeping gene									
SREBF1	1.00	0.9054					+				+	
ACACA	-1.00	0.9885					+					
AR	-1.01	0.8874	+	+						+	+	
SLC5A8	-1.01	0.8874								+		D
EDNRB	-1.01	0.8874								+		
NRIP1	-1.05	0.7961		+							+	
KLK3	-1.06	0.6492										U
ECT2	-1.06	0.5336										U
CDKN2A	-1.08	0.2504	+		+	+				+	+	
CAMKK1	-1.12	0.5185					+					
MTO1	-1.15	0.2078										U
CREB1	-1.16	0.0907						+			+	
USP5	-1.25	0.3491										D
AKT1	-1.29	0.2835	+									
ZNF185	-1.33	0.0672								+		

Gene	Fold regulation	p-value	Role in prostate cancer									
			1	2	3	4	5	6	7	8	9	UD
RARB	-1.46	0.2100								+	+	
STK11	-1.54	0.1933					+					
TP53	-1.56	0.0539	+		+	+					+	
MKI67	-1.82	0.1645							+			

Role in prostate cancer *indicates which pathways the genes are involved in: 1. PI3K/AKT signalling pathway; 2. Androgen receptor signalling; 3. Apoptosis; 4. Cell cycle; 5. Fatty acid synthesis; 6. Metastasis; 7. Other prostate cancer-related genes; 8. Genes in methylated promoters in prostate cancer; 9. Transcription factor;* ***UD*** *indicates whether a gene is up or down regulated in prostate cancer;*

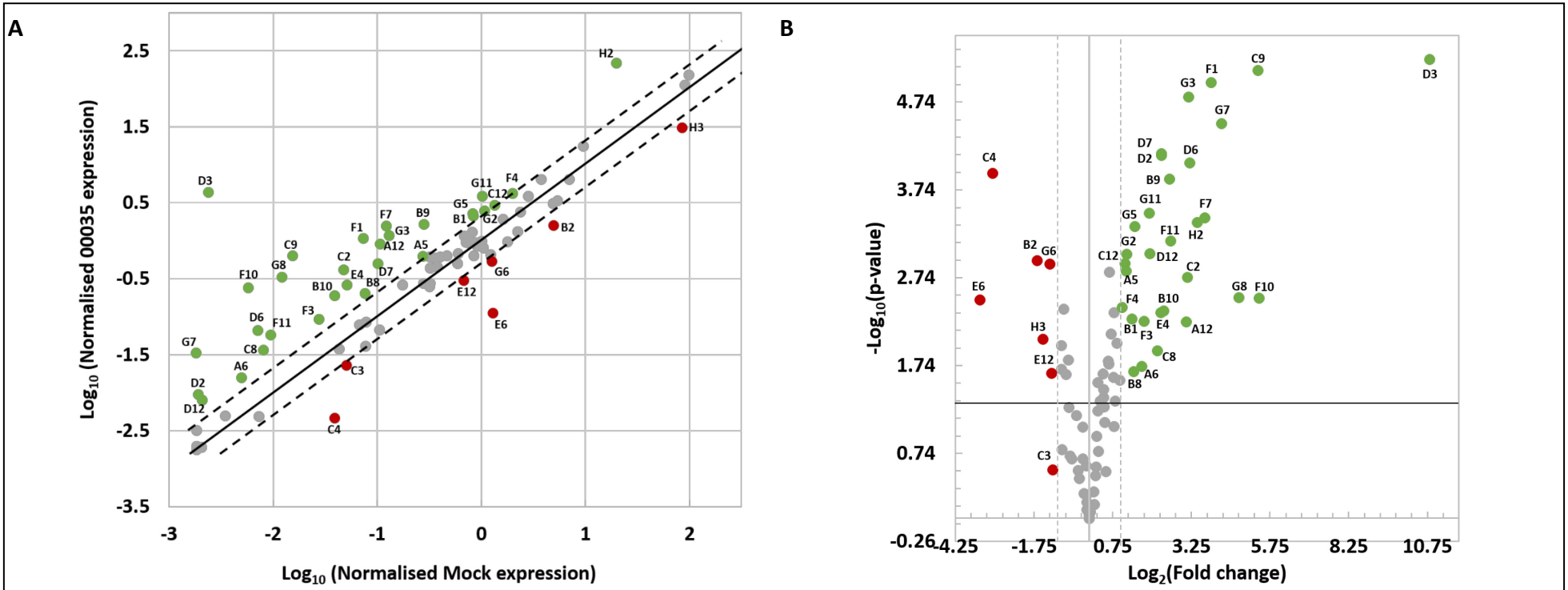

Figure 5.8. 00035 infection model qPCR array results.

A. Scatter plot with values dysregulated more than +/- 2-fold shown in colour; upregulated (green), downregulated (red). The thick black line indicates no fold change, and the two dashed lines mark +/- 2-fold dysregulation.

B. Volcano plots of fold change versus p-value. Values dysregulated more than +/- 2-fold shown in colour. Black horizontal line indicates p = 0.05; upregulated genes (green), downregulated genes (red). The solid grey line indicated no fold change, and the two dashed grey lines mark +/- 2-fold dysregulation.

Legend: A5 – *ARNTL;* A6 – *BCL2;* A12 – *CCNA1;* B1 – *CCND1;* B2 – *CCND2;* B8 – *DDX11;* B9 – *DKK3;* B10 – *DLC1;* C2 – *EGR3;* C3 – *ERG;* C4 – *ETV1;* C8 – *GNRH1;*C9 – *GPX3;* C12 – *HMGCR;* D2 – *IGFBP5;* D3 – *IL6;* D6 – *LGALS4;* D7 – *LOXL1;* D12 – *MSX1;* E4 – *NKX3-1;* E6 – *PDLIM4;* E12 – *PTGS1;* F1 – *PTGS2;* F3 – *RASSF1;*F4 – *RBM39;* F7 – *SFRP1;* F10 – *SOCS3;* F11 – *SOX4;* G2 – *SUPT7L;* G3 – *TFPI2;* G5 – *TIMP2;* G6 – *TIMP3;* G7 – *TMPRSS2;* G8 – *TNFRSF10D;* G11 – *VEGFA;*H2 – *B2M;* H3 – *GAPDH;*

Table 5.4. qPCR array results for the B3 infection model

Gene	Fold regulation	p-value	Role in prostate cancer									
			1	2	3	4	5	6	7	8	9	UD
TFPI2	3.53	0.0002										D
SOCS3	2.49	0.1200										U
ETV1	1.97	0.0004			+						+	U
B2M	1.47	0.0008	Housekeeping gene									
NKX3-1	1.76	0.0022									+	
DLC1	1.44	0.0053								+		
ARNTL	1.40	0.0057								+		U
TIMP2	1.31	0.0282	+	+	+					+		
IL6	1.81	0.0327	+	+	+							
TIMP3	-1.60	0.0124	+	+	+							
FOXO1	-1.46	0.0474	+	+							+	
CAV1	-1.16	0.0490		+						+		
LGALS4	1.68	0.1698										D
PTGS2	1.55	0.1335				+				+		
SOX4	1.52	0.239									+	U
BCL2	1.48	0.1772	+		+	+						
VEGFA	1.46	0.0695	+	+								
GPX3	1.38	0.2295								+		
CCND1	1.36	0.0511	+	+		+						
DDX11	1.34	0.3634										U
TNFRSF10D	1.32	0.576		+						+		
GNRH1	1.30	0.0836	+	+	+							
CCNA1	1.25	0.1023				+				+		
PES1	1.25	0.3404						+				
NRIP1	1.24	0.054		+							+	
CCND2	1.23	0.1077	+			+						D
TGFB1I1	1.23	0.4035		+								
NFKB1	1.22	0.1106	+	+	+						+	
LOXL1	1.22	0.3398										D
USP5	1.22	0.5144										D
FASN	1.21	0.5573					+					
SHBG	1.19	0.6497									+	
RASSF1	1.19	0.6591								+		
CAMSAP1	1.18	0.4205										U
DAXX	1.16	0.3201	+								+	
PDPK1	1.12	0.1913	+									U
RBM39	1.12	0.5765									+	U
MKI67	1.12	0.9317							+			
CDKN2A	1.11	0.1412	+		+	+				+	+	
CAMKK1	1.11	0.6345					+					
STK11	1.11	0.7425					+					
GSTP1	1.10	0.0947								+		

Gene	Fold regulation	p-value	Role in prostate cancer									
			1	2	3	4	5	6	7	8	9	UD
MTO1	1.09	0.5013										U
GCA	1.08	0.3115										D
SUPT7L	1.08	0.6284									+	U
GAPDH	1.08	0.6943	Housekeeping gene									
PRKAB1	1.07	0.5955					+					
CLN3	1.07	0.8123										D
ACACA	1.06	0.6596					+					
SREBF1	1.05	0.8791					+				+	
AKT1	1.03	0.9094	+									
CASP3	1.02	0.8471			+	+						
SCAF11	1.01	0.9869						+				
HPRT1	1.00	-	Housekeeping gene									
APC	-1	0.9722				+				+		
PPP2R1B	-1	0.9735				+						D
SEPT7	-1.01	0.8963						+				
CAV2	-1.01	0.9489				+						
MAPK1	-1.02	0.8889	+		+							
MSX1	-1.02	0.902								+	+	
HMGCR	-1.03	0.7852					+					
IGF1	-1.03	0.8308	+	+	+	+						D
RPLP0	-1.04	0.6227	Housekeeping gene									
MGMT	-1.04	0.6343								+		
ACTB	-1.05	0.5821	Housekeeping gene									
CDH1	-1.05	0.6917	+							+		
DKK3	-1.05	0.6971								+		
PTEN	-1.07	0.3873	+	+	+	+						
MAX	-1.07	0.5794						+			+	
ECT2	-1.08	0.5213										U
TP53	-1.09	0.3631	+		+	+					+	
SFRP1	-1.09	0.6054								+		D
ZNF185	-1.1	0.5285								+		
PDLIM4	-1.11	0.4994								+		
CREB1	-1.12	0.1473						+			+	
HAL	-1.12	0.3615										U
AR	-1.14	0.2943	+	+						+	+	
SLC5A8	-1.14	0.2943								+		D
EDNRB	-1.14	0.2943								+		
TMPRSS2	-1.14	0.2943							+			
PTGS1	-1.18	0.2801				+						
RARB	-1.18	0.5158								+	+	
IGFBP5	-1.19	0.1244										U
EGFR	-1.19	0.3488	+	+		+						
NDRG3	-1.2	0.2005						+				

Gene	Fold regulation	p-value	Role in prostate cancer									
			1	2	3	4	5	6	7	8	9	UD
KLK3	-1.21	0.2212										U
EGR3	-1.21	0.578									+	
KLHL13	-1.3	0.1973						+				
ERG	-1.95	0.3507									+	

Role in prostate cancer *indicates which pathways the genes are involved in: 1. PI3K/AKT signalling pathway; 2. Androgen receptor signalling; 3. Apoptosis; 4. Cell cycle; 5. Fatty acid synthesis; 6. Metastasis; 7. Other prostate cancer-related genes; 8. Genes in methylated promoters in prostate cancer; 9. Transcription factor;* ***UD*** *indicates whether a gene is up or down regulated in prostate cancer;*

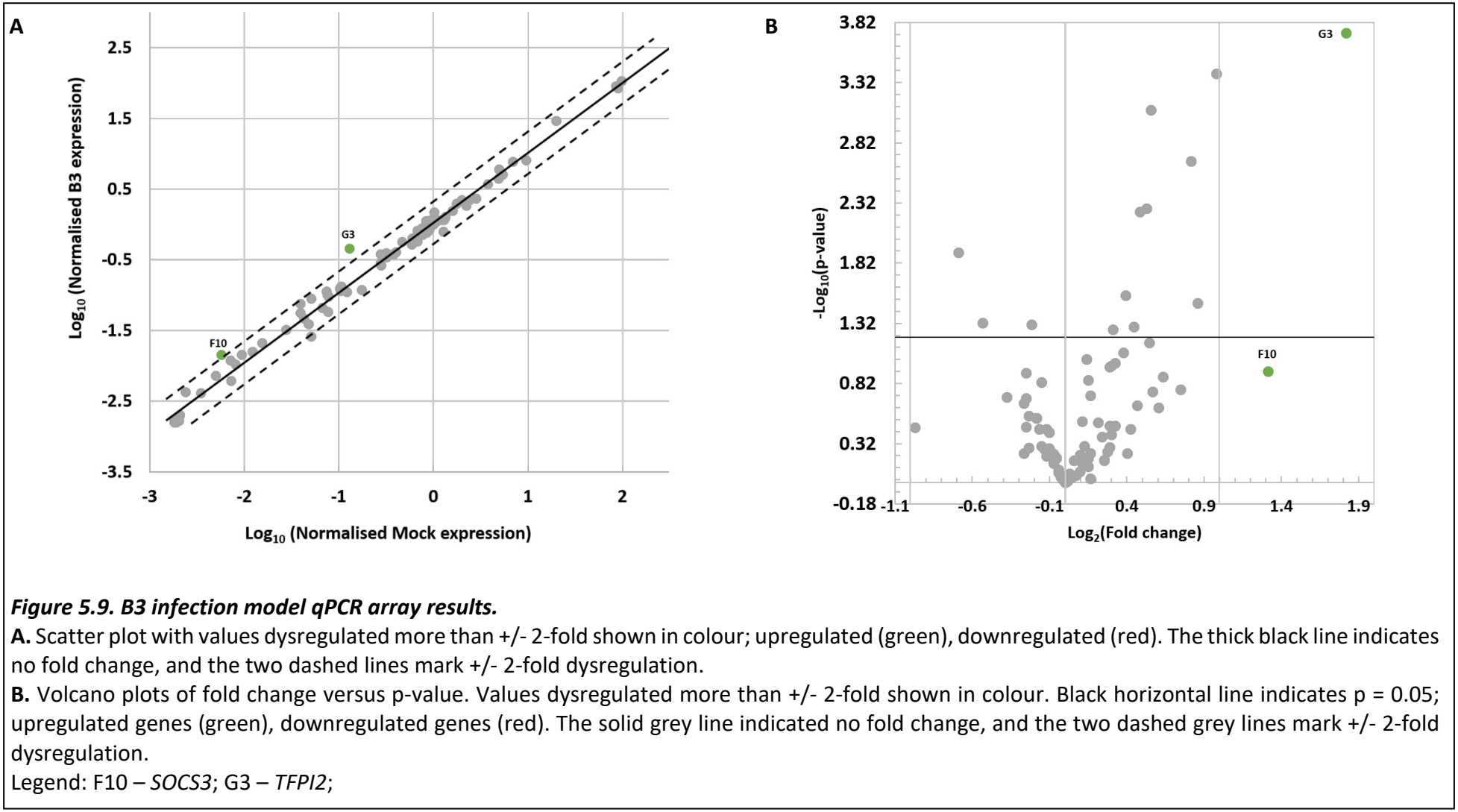

Figure 5.9. B3 infection model qPCR array results.

A. Scatter plot with values dysregulated more than +/- 2-fold shown in colour; upregulated (green), downregulated (red). The thick black line indicates no fold change, and the two dashed lines mark +/- 2-fold dysregulation.

B. Volcano plots of fold change versus p-value. Values dysregulated more than +/- 2-fold shown in colour. Black horizontal line indicates p = 0.05; upregulated genes (green), downregulated genes (red). The solid grey line indicated no fold change, and the two dashed grey lines mark +/- 2-fold dysregulation.

Legend: F10 – *SOCS3*; G3 – *TFPI2*;

Table 5.5. qPCR array results for the CFU2 infection model

Gene	Fold regulation	p-value	Role in prostate cancer									
			1	2	3	4	5	6	7	8	9	UD
IGFBP5	10.08	0.0059										U
LGALS4	3.43	0.0119										D
GPX3	3.08	0.0007								+		
CAMKK1	3.07	0.0010					+					
SOX4	3.07	0.0010									+	U
DDX11	3.02	0.0024										U
RBM39	3.02	0.0006									+	U
FOXO1	2.57	0.0015	+	+							+	
RASSF1	2.56	0.0143								+		
EGR3	2.52	0.0050									+	
TIMP2	2.43	0.0081	+	+	+					+		
FASN	2.36	0.0066					+					
CLN3	2.28	0.0025										D
GNRH1	2.26	0.0004	+	+	+							
ZNF185	2.23	0.0033								+		
PTGS1	2.19	0.0047				+						
PDLIM4	2.12	0.0033								+		
MKI67	2.10	0.0460							+			
VEGFA	2.08	0.0043	+	+								
SREBF1	2.07	0.0343					+				+	
DLC1	2.04	0.0005								+		
TIMP3	2.02	0.0015	+	+	+							
B2M	1.49	0.0008	Housekeeping gene									
PTEN	1.72	0.0010	+	+	+	+						
ARNTL	1.94	0.0014								+		U
CAV1	1.62	0.0016		+						+		
MAX	1.72	0.0024						+			+	
MAPK1	1.54	0.0032	+		+							
HMGCR	1.83	0.0036					+					
CREB1	1.43	0.0038						+			+	
GCA	1.62	0.0043										D
SUPT7L	1.75	0.0046									+	U
SFRP1	1.78	0.0064								+		D
PPP2R1B	1.48	0.0064				+						D
DAXX	1.70	0.0069	+								+	
CAV2	1.64	0.0079				+						
NRIP1	1.50	0.0079		+							+	
PDPK1	1.72	0.0081	+									U
CDH1	1.58	0.0116	+							+		
DKK3	1.88	0.0119								+		
APC	1.67	0.0129				+				+		
CCND1	1.49	0.0130	+	+		+						

Gene	Fold regulation	p-value	Role in prostate cancer									
			1	2	3	4	5	6	7	8	9	UD
ACACA	1.71	**0.0137**					+					
SCAF11	1.54	**0.0145**						+				
LOXL1	1.88	**0.0147**										D
NDRG3	1.47	**0.0166**						+				
KLHL13	1.42	**0.0176**						+				
SEPT7	1.44	**0.0191**						+				
CAMSAP1	1.74	**0.0205**										U
GSTP1	1.27	**0.0217**								+		
EGFR	1.44	**0.0225**	+	+		+						
USP5	1.92	**0.0247**										D
CASP3	1.32	**0.0275**			+	+						
BCL2	1.95	**0.0355**	+		+	+						
NFKB1	1.38	**0.0399**	+	+	+						+	
ECT2	1.30	**0.0431**										U
HAL	1.78	**0.0463**										U
ETV1	**-4.29**	**0.0002**			+						+	U
CDKN2A	-1.24	**0.0277**	+		+	+				+	+	
TMPRSS2	1.78	0.1346							+			
TGFB1I1	1.59	0.0716		+								
STK11	1.59	0.1194					+					
SOCS3	1.52	0.6729										U
AKT1	1.50	0.0696	+									
RARB	1.47	0.1572								+	+	
PES1	1.41	0.1147						+				
SHBG	1.39	0.3689									+	
ACTB	1.38	0.0521	Housekeeping gene									
TNFRSF10D	1.38	0.5153		+						+		
NKX3-1	1.23	0.0936									+	
PTGS2	1.12	0.3279				+				+		
KLK3	1.10	0.3987										U
MTO1	1.09	0.4084										U
AR	1.09	0.4969	+	+						+	+	
IGF1	1.09	0.4969	+	+	+	+						D
EDNRB	1.09	0.4969								+		
SLC5A8	1.09	0.4969								+		D
MGMT	1.07	0.6460								+		
PRKAB1	1.04	0.7647					+					
TP53	1.03	0.7311	+		+	+					+	
RPLP0	1.02	0.8422	Housekeeping gene									
HPRT1	1.00	-	Housekeeping gene									
CCND2	-1.01	0.8673	+			+						D
GAPDH	-1.01	0.8764	Housekeeping gene									
MSX1	-1.02	0.8698								+	+	

Gene	Fold regulation	p-value	Role in prostate cancer									
			1	2	3	4	5	6	7	8	9	UD
TFPI2	-1.09	0.2544										D
CCNA1	-1.16	0.1663				+				+		
IL6	-1.20	0.4211	+	+	+							
ERG	-1.34	0.4980									+	

Role in prostate cancer *indicates which pathways the genes are involved in: 1. PI3K/AKT signalling pathway; 2. Androgen receptor signalling; 3. Apoptosis; 4. Cell cycle; 5. Fatty acid synthesis; 6. Metastasis; 7. Other prostate cancer-related genes; 8. Genes in methylated promoters in prostate cancer; 9. Transcription factor;* ***UD*** *indicates whether a gene is up or down regulated in prostate cancer;*

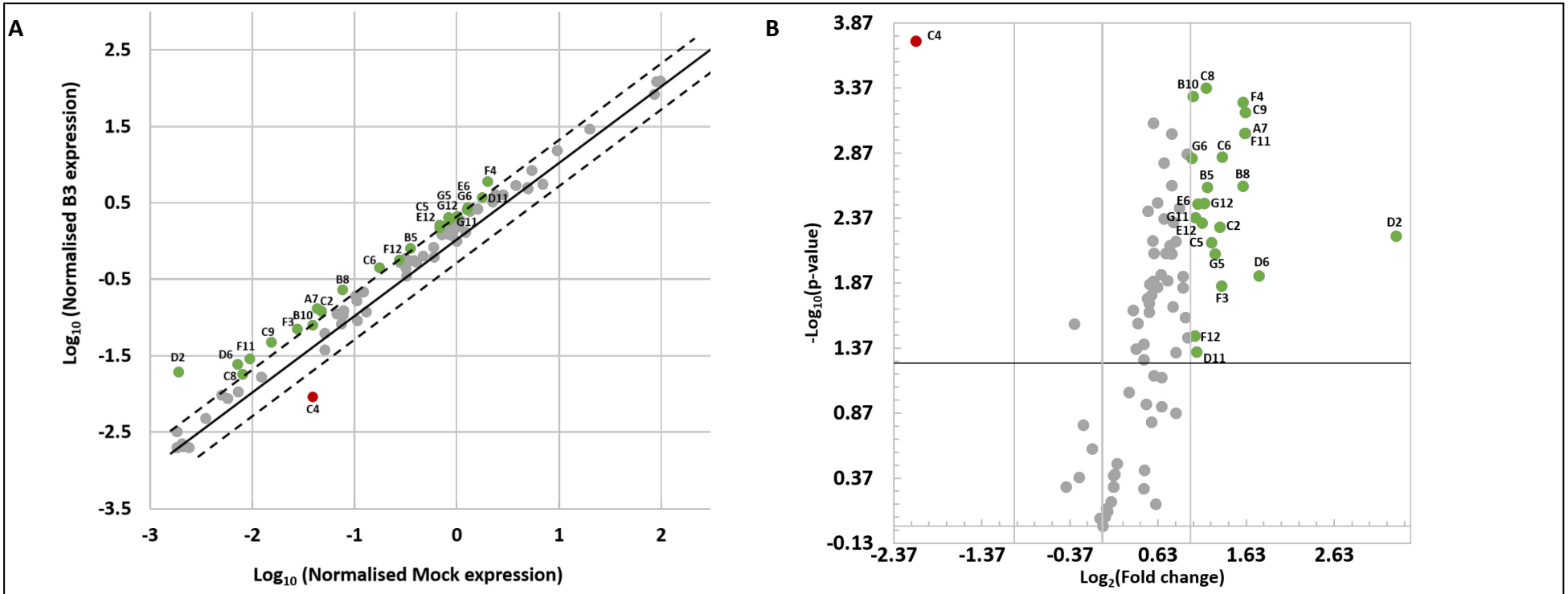

Figure 5.10. CFU2 infection model qPCR array results.

A. Scatter plot with values dysregulated more than +/- 2-fold shown in colour; upregulated (green), downregulated (red). The thick black line indicates no fold change, and the two dashed lines mark +/- 2-fold dysregulation.

B. Volcano plots of fold change versus p-value. Values dysregulated more than +/- 2-fold shown in colour. Black horizontal line indicates p = 0.05; upregulated genes (green), downregulated genes (red). The solid grey line indicated no fold change, and the two dashed grey lines mark +/- 2-fold dysregulation.

Legend: A7 – *CAMKK1*; B5 – *CLN3*; B8 – *DDX11*; B10 – *DLC1*; C2 – *EGR3*; C4 – *ETV1*; C5 – *FASN*; C6 – *FOXO1*; C8 – *GNRH1*; C9 – *GPX3*; D2 – *IGFBP5*; D6 – *LGALS4*; D11 – *MKI67*; E6 – *PDLIM4*; E12 – *PTGS1*; F3 – *RASSF1*; F4 – *RBM39*; F11 – *SOX4*; F12 – *SREBF1*; G5 – *TIMP2*; G6 – *TIMP3*; G11 – *VEGFA*; G12 – *ZNF185*;

infection model. Fatty acid synthesis-related genes show significant upregulation only in 3 genes; only one gene involved in the cell cycle (*SREBF1*, 2.07-fold increase and p = 0.0343) is affected as a result of infection.

5.4. *Discussion*

The results presented in this chapter confirm that the response of prostate epithelial cells to infection differ depending on the *P. acnes* strain which is used to challenge them.

5.4.1. Housekeeping genes

The housekeeping gene selection algorithm used by the QIAGEN software selected *HPRT1* as the most stable housekeeping gene out of the 5 options available, which is in line with our findings from Chapter 3 using the Normfinder software (Section 3.3.10). What is interesting is that the 00035 infection model demonstrated statistically significant dysregulation in two of the housekeeping genes B2M and GAPDH (10.85-fold upregulation, with p = 0.0004 and -2.77-fold downregulation, p = 0.0092) which highlights the importance of careful selection of stable housekeeping genes.

Beta-2-microglobulin (B2M), is one of the components of class I major histocompatibility complex (MHC). It has been shown to be upregulated in prostate cancer, as it has androgen receptor (AR)-dependent expression (Mink et al., 2010). Cell culture experiments suggest that B2M expression has a higher specificity as a prognostic marker for AR activity than PSA (Gross et al., 2007). GAPDH is a key regulator of glycolysis, but it has also been shown to be affected by a number of factors dysregulated in cancer (Zhang et al., 2015). For example, hypoxia-driven increase in GAPDH can lead to activation of the PI3K/AKT signalling pathway, causing increased cellular proliferation (Zhang et al., 2015). Other studies have shown that GAPDH expression is indirectly controlled by p53, however, the mechanism is unclear (Chen et al., 1999).

Despite the fact that both genes have been described in the literature as dysregulated in cancer progression, they have both been included as potential housekeeping control in the qPCR array, highlighting a limitation of the use of pre-designed commercially available arrays.

5.4.2. B3 infection model

The cells infected with B3 only showed significant dysregulation of only two genes, suppressor of cytokine signalling 3 (*SOCS3*) and tissue factor pathway inhibitor 2 (*TFPI2*).

While the *SOCS3* gene is associated with promoter methylation and is silenced in roughly 40% of prostate cancers, the results from this infection model contradict those previous findings (Pierconti et al., 2011). As the members of the SOCS family are involved in the control of IL-6, JAK/STAT3, ERK/MAPK, PI3K/AKT, NF-κB signalling, it is not surprising that there is an increase it its levels, albeit non-significant (Larsen and Ropke, 2002; Rui et al., 2002; Park et al., 2003; Wang et al., 2005). The second gene upregulated in the B3 infection model is *TFPI2*. *TFPI2* is normally downregulated in cancer and *in vitro* experiments have shown that if levels of *TFPI2* are increased the tumour becomes less aggressive (Konduri et al., 2001).

As neither of the genes dysregulated in this infection model are involved in the progression of cancer, and due to the low number of dysregulated prostate cancer-related genes, infection with the type IB strain B3 seems to be an unlikely cause of oncogenesis. This contradicts previous findings where a type IB strain (prostate isolate P6) was shown to drive cancer-related changes in the RWPE-1 cell line (Fassi Fehri et al., 2011; Mak et al., 2012). The difference in the results observed is likely due to the difference in sequence type of the IB strains used, as with strain B3 being identified as ST5 (Chapter 3, Section 3.3.1) and strain P6 belonging to ST119 (Mak et al., 2013a).

5.4.3. 00035 and CFU2 infection models

Unlike the B3 infection model, both cells infected with 00035 (type IA1) and cells infected with CFU2 (type III) demonstrated dysregulation of multiple genes, 36 and 23, respectively, showed both more than 2-fold dysregulation and p-value $p > 0.05$.

5.4.3.1. PI3K/AKT signalling and apoptosis

Out of all pathways investigated by the qPCR array, the PI3K/AKT pathway had the highest number of dysregulated genes in both infections (6 genes in the 00035 models, and 5 in cells infected with CFU2), four of which were common between the two infection models.

The PI3K/AKT pathway has the power to inhibit *BCL2*, which plays a key role in apoptosis, and is upregulated in the 00035 infection model (3.21-fold increase, $p = 0.0186$); this suggests that the increased level of Bcl-2-driven inhibition could make cells resist apoptosis, even if death signals are received. Furthermore, studies have shown that *BCL2* upregulation is necessary for cells to progress to androgen-independent growth,

suggesting that infection with this strain could lead to castration resistance (Cory et al., 2003; Lin et al., 2007). In contrast, the cells infected with CFU2 demonstrated high expression of *FOXO1* (2.57-fold, p = 0.0015) which is a promoter of apoptosis and increased levels of *FOXO1* have been shown to decrease AR-driven cell proliferation, implying that CFU2 infection opposes androgen resistance. (Ma et al., 2009). These findings highlight the difference in the effect different phylogenetic types have on prostate epithelial cells and support the potential role of infection in the development of treatment-resistant cancer. They also support the hypothesis that some strains have the potential to drive oncogenesis (strain 00035), while other have a cancer-protective role (strain CFU2).

TRAIL (encoded by *TNFRSF10*) plays a role in death signalling and apoptosis activation and is significantly upregulated in the 00035 infection model (27.15-fold, p = 0.0026). TRAIL expression can be activated through a number of pathways and genes, including NF-κB signalling, STAT3 signalling, *FOXO1*, cytokines and infection, with the latter being the most likely reason for its upregulation in this case (Allen and El-Deiry, 2012).

Another gene dysregulated in the 00035 infection that has normal expression in the CFU2 model is *IL6*. The explanation for the difference here is most likely due to the significantly higher number of bacteria still present in the medium at this time point (as seen in Chapter 4, Section 4.3.2.2), which initiate cytokine signalling pathways, aimed at the eradication of the infection by the immune system, which cannot be achieved in the closed system of an infection model. A similar reason is also likely behind the upregulation of TRAIL.

TIMP2 and *TIMP3* are both dysregulated in the two infections. *TIMP2* is upregulated in both infection models (2.73-fold, p = 0.0005 in 00035 and 2.46-fold, p = 0.0081 in CFU2-infected cell). *TIMP2* has been shown to be downregulated in prostate cancer which contradicts the findings here, though the exact mechanism of its involvement in cancer is not clear (Bratland et al., 2003). With *TIMP3*, a difference in expression is seen between the two infections – a significant increase in cells infected with CFU2 (2.02-fold, p = 0.0015) and a decrease in 00035 infection models (-2.39-fold, p = 0.0013). The latter results are in line with findings in prostate cancer studies which have shown that the *TIMP3* promoter region is usually methylated (97% of cases) and thus the gene expression is downregulated (Jeronimo et al., 2004). However, further analysis is needed

to confirm the downregulation here is a result of an epigenetic change. Conversely, the upregulation in the CFU2 models again hints towards this model exhibiting some cancer-protective gene dysregulation, as increase of TIMP3 has been linked to increase in apoptosis and improved susceptibility to treatment (Jeronimo et al., 2004).

MMPs are the primary target of TIMPs and are a family of 28 endopeptidases which have been implicated in cancer progression, angiogenesis and EMT. The different MMPs and their functions have been reviewed in detail by Kessenbrock et al. (2010). As no information is available for the expression of MMPs which are targeted by the TIMPs investigated by the qPCR, it is difficult to interpret the significance of their upregulation. Further experiments, aiming to quantify the protein levels of the different TIMPs and the MMPs they target would give insight into the importance of the molecular dysregulation observed here.

Both infections have a statistically significant increase in *VEGFA* (3.77-fold upregulation, $p = 0.0003$ in 00035-infected cells and 2.08-fold, $p = 0.0043$ in CFU2 infections) which is a known promoter of angiogenesis as it acts specifically on endothelial cells, leading to increased proliferation, survival and migration (Hoeben et al., 2004).

Overall, the gene dysregulation in this pathway points towards apoptosis resistance and androgen-independent growth in the 00035 infection, findings consistent with prostate cancer. In contrast, cells infected with CFU2 demonstrate increased apoptosis and androgen-dependence.

5.4.3.2. Cell cycle-related genes

Another gene which is dysregulated in both infection models is E26 transformation specific (ETS) translocation variant 1 (*ETV1*, -8.4-fold, $p = 0.0001$ and -4.29-fold, $p = 0.0002$ in 00035 and CFU2 infections, respectively), which has been shown to work in concert with the AR (Baena et al., 2013). It is worth noting that the RWPE-1 cell line used in this study requires stimulation with androgen to express the AR and is thus not a suitable model to investigate this interaction. Studies have shown that in prostate cancer the *ETV1* gene is commonly translocated and is under the influence of *TMPRSS2*; the downregulation of ETV1 combined with the high level of expression of *TMPRSS2* (18.42-fold increase, $p < 0.0001$) in the 00035 infection model strongly suggest that no such translocation has yet occurred (Tomlins et al., 2005). Another member of the ETS

transcription factor family is ETS-related gene (ERG), which similarly to ETV1, has been shown to be translocated, thus forming a complex with *TMPRSS2* (Tomlins et al., 2005). Similarly to ETV1, ERG shows a trend in expression towards a decrease in infected cells, as the downregulation is not significant (-2.21-fold, p = 0.27) once again suggesting that no translocation has occurred.

Cyclins A, D1, and D2 are all dysregulated in the 00035 infection model (8.55-fold increase, p = 0.0058; 2.57-fold increase, p = 0.0053; -3.1-fold decrease and p = 0.0012, respectively). Cyclin A1, one of the regulators of the cell cycle is significantly upregulated, which could be a result of IL-6-driven activation of the PI3K/AKT and ERK signalling pathways (Wegiel et al., 2008). This increase can lead to dysregulation of the cell cycle and promote uncontrolled cell division but cyclin A1 has also been shown to cause expression of *VEGFA*, which would allow angiogenesis and enhance cancer progression (Wegiel et al., 2005). The dysregulation of cyclins D1 (upregulated) and cyclin D2 (downregulated) are in agreement with the expectation for prostate cancer; increased *CCND1* expression is suggested to have a role in androgen-independent growth and metastasis, and decrease in *CCND2* transcription is also linked to metastatic growth (Drobnjak et al., 2000; Chen et al., 2017).

The dysregulation seen in the cell cycle-related genes also point towards cancer-like dysregulation in the 00035 infection models with dysregulation suggesting uncontrolled division, androgen-independence and metastasis.

5.4.3.3. Wnt/β-catenin signalling pathway

Two genes involved in the suppression of Wnt/β-catenin signalling are upregulated in both 00035 and CFU2-infected cells (secreted frizzled-related protein 1 (*SFRP1*), which acts as an inhibitor of Frizzled, and Dickkopf-related protein (*DKK*), which inhibits the Frizzled-associated lipoprotein receptor-related protein, or LRP). The upregulation of the two inhibitors suggest that infected cells do not have increased migration and decreased adhesion resulting from β-catenin signalling. Additionally, the upregulation seen in the infection models of β-catenin targets, e.g. *CCND1*, is also not a result of activation of this signalling pathway. Both *SFRP* and *DKK* have methylation in their promoter regions in prostate cancer, and are thus downregulated, allowing the progression of Wnt/β-catenin signalling (Lodygin et al., 2005; Garcia-Tobilla et al., 2016).

Expression of both prostaglandin G/H synthase 1 (*PTGS1*) and *PTGS2* is under the influence of the Wnt/β-catenin signalling pathways and both genes are dysregulated in the infection models. *PTGS1* (also known as cyclooxygenase 1 or COX-1) is downregulated in the 00035 infection and upregulated in the CFU2-infection (-2.27-fold and $p = 0.0222$, and 2.19-fold and $p = 0.0047$, respectively). COX-1 a has primarily housekeeping function being responsible for the normal functioning of the cell and the dysregulation seen here is most likely due to the stress resulting from infection. COX-2 in only dysregulated in the 00035 infection model, where a 14.62-fold increase is seen ($p < 0.0001$); this increase is likely a result of cytokine signalling activated by the ongoing infection. High levels of COX-2 are suspected to play a role in promoting tumorigenesis by helping the cells to resist apoptosis in the earlier stages of cancer progression and driving angiogenesis at the later stages (Tsujii and DuBois, 1995; Gallo et al., 2001).

The dysregulation seen in COX-2 further supports a role of 00035 infection in apoptosis evasion.

5.4.3.4. Fatty acid synthesis and related pathways

A total of five genes involved in fatty acid and cholesterol biosynthesis are dysregulated in the CFU2 infection models, with *HMGCR* also having increased expression in cells infected with 00035. Additionally, *GAPDH*, involved in glycolysis is also dysregulated in 00035 infections. Due to the low number of fatty acid synthesis pathway members dysregulated in the cells infected with 00035, no conclusions of the significance can be made.

In contrast, in the CFU2 infection model, the dysregulated genes are related in function and may influence each other's activity. FAS (encoded by *FASN*, with 2.36-fold upregulation, $p = 0.0066$) is the key enzyme in *de novo* fatty acid synthesis and is commonly upregulated in prostate cancer (Flavin et al., 2010). An upregulation is also seen in the FAS activator SREBP (encoded by *SREBPF1*); 2.07-fold, $p = 0.0343$). An upstream increase in expression of *CAMKK1* (3.07-fold increase, $p = 0.000954$), which acts as an inhibitor for AMPK, which is in turn normally downregulates the production of SREBP. There is an increase in *CAMKK1* expression, AMPK-inhibition of SREBP1 is not seen, and an expected increase in FAS is observed. Additionally, SREBP-induced increase is also seen in ACACA, which acts as a limiting step in *de novo* fatty acid synthesis, indicating that the cells are dedicated to the process. As AMPK inhibition is not present,

a trend towards increased expression (1.83-fold, p = 0.00356) is seen in HMGCR, the enzyme controlling the conversion of acetyl-CoA to mevalonate, the rate limiting step of the mevalonate pathway and cholesterol biosynthesis (products of which are steroid hormones, including testosterone and DHT) (Murtola et al., 2012).

Taken together these findings suggest an induction of the fatty acid synthesis pathway by infection with strain CFU2, which is line with prostate cancer behaviour but as no other dysregulation pointing towards cancer-like behaviour in this infection model, this increase in fatty acid synthesis and its related pathways is likely a metabolic switch aiming lipogenesis as means of storing energy (Wu et al., 2014).

5.4.3.5. Promoter methylation

Promoter methylation plays an important role in silencing gene transcription, especially in cancer. Out of the dysregulated genes in the array following infection with the type IB and type III strains there are a total of 11 genes that have methylated promoters in prostate cancer, 9 are dysregulated in the 00035 infection and 6 in the cells infected with CFU2. Only one of those genes, *PDLIM4* shows decrease in expression levels (00035-infection model, -11.6-fold downregulation, p = 000033), which would be the expected outcome if the promoter had become hypermethylated; methylation of the *PDLIM4* gene has been suggested as a molecular biomarker for prostate oncogenesis (Vanaja et al., 2006). However, further analysis is necessary to confirm that the downregulation is as a result of epigenetic changes.

5.4.3.6. Transcription factors and other prostate cancer-related genes

A number of transcription factors commonly involved in prostate cancer are also included in the array, with 6 transcription factors having no functions related to the pathways outlined above being included, making the analysis of the significance of their upregulation difficult.

The homeobox protein NKX3.1 is a known tumour suppressor in prostate cancer and the disease is commonly associated with loss of heterozygosity of the *NKX3.1* gene (Sakr et al., 1994; Suzuki et al., 1995; Vocke et al., 1996). Dysregulation of the *NKX3.1* gene is seen in the 00035 infection model, namely an increase of 5.15-fold (p = 0.0043). However, the PCR array does not provide information whether both alleles of the genes are present and functional.

Another transcription factor investigated is Aryl hydrocarbon receptor nuclear translocator-like protein 1 (*ARNTL*), also known as BMAL1, which forms an E-box-binding complex with circadian locomotor output cycles kaput (CLOCK) and plays a central role in circadian rhythm maintenance (Jung et al., 2003). Downregulation of CLOCK and increase in ARNTL have been linked to prostate cancer, and melatonin has been suggested as a regulator of this dysregulation and a potential management agent for the disease (Otalora et al., 2008; Jung-Hynes et al., 2010; Savvidis and Koutsilieris, 2012).

Upregulated in both infections is *GNRH1* (4.51-fold, p = 0.0124 and 2.26-fold, p = 0.0004, for 00035 and CFU2 infection, respectively), encoding GnRH, the gonadotropin releasing hormone. *In vitro* models of prostate cancer (PC-3, LNCaP, DU145) have previously been shown to produce GNRH transcripts and it was suggested that they play an autocrine role in cells, though clarity is needed on any such mechanism (Bahk et al., 1998)

Another gene that is not involved in the pathways outlined here is *CLN3*, also called battenin, which is involved in lysosomal function and mutations in *CLN3* have been linked to the neurodegenerative disorder Batten disease (Cotman and Staropoli, 2012). Overexpression of the *CLN3* gene has been observed in a range of cancers cell lines, as well as in breast tumour specimens and it is upregulated in the CFU2-infection model (2.28-fold, p = 0.002481); it has been suggested as a possible drug target, as its silencing was shown to inhibit ovarian cancer progression and induce apoptosis. (Rylova et al., 2002; Makoukji et al., 2015; Mao et al., 2015). However, its exact involvement in cancer progression is unclear

5.4.4. Summary

The study was limited to only investigating 3 sets of infection models and a set of 3 untreated controls due to financial constraints. It would, however, have been interesting to see what the dysregulation pattern of a prostate isolate of the phylogenetic type II would be, as well as the health associated strain ST27. Additionally, investigation of the dysregulation following longer infection (e.g. 30 days) would cause further dysregulation.

A limitation of the method used here is the design of the array. Firstly, the genes selected are not all related to specific pathways, making it challenging to analyse the data accurately, as very few of the genes react directly with each other within the pathways

included. An additional challenge to the analysis is that the array is not specifically designed for cell culture experiment analysis, but it is prepared in such a way, so it could work with patient samples, an example here being the inclusion of GNRH, which acts on the pituitary gland to stimulate the production of luteinising hormone (LH) and follicle stimulating hormone (FSH), and significance in the prostate alone is unclear.

The findings of this chapter confirm that different phylogenetic types of *P. acnes* induce different response in the prostate epithelial cells, and also suggest that the type IA_1 strain 00035 is pro-oncogenic, as the dysregulation seen in the PI3K/AKT signalling pathway, apoptosis, cell cycle and Wnt/β-catenin-related genes all suggest 00035 infection causes the prostate epithelial cells to exhibit cancer-like behaviour. In contrast, the CFU2 type III infection model, while also showing dysregulation, appears to be more cancer protective, as most of the dysregulation seen in the CFU2 infection model aims to combat oncogenesis.

Chapter 6:
General Discussion

6

6.1. *Overview*

A wide range of studies have investigated the potential role of inflammation in the development of prostate cancer (extensively reviewed by Sfanos and De Marzo (2012)), with multiple observations supporting the part inflammation plays in oncogenesis. Multifocal inflammation is seen in the prostate gland in men of all ages, as demonstrated by autopsy studies (8% of teenagers, 28% of men aged 20-39, and 60% in men in aged between 40 and 59); the presence of inflammation with no evidence of prostate cancer suggests that the inflammation is not a result of immune response to a developing cancer (Boström, 1971). Possible causes of the inflammation seen within the prostate include infection, reactive oxygen species, or autoimmune disease.

There is a long history of conflicting studies regarding the variety and prevalence of organisms which comprise the prostate microflora, with some studies suggesting that the gland is sterile (Hochreiter et al., 2000; Lee et al., 2003). As culturing techniques improved, Cohen et al. (2005) discovered a statistically significant ($p = 0.007$) association between the presence of *P. acnes* in cultures of radical prostatectomy samples (35% of culture positive samples) and acute and chronic inflammation in the prostate gland, and suggested that an asymptomatic infection with *Propionibaterium acnes* may play a role in the development of prostate adenocarcinoma.

Studies have provided evidence for the potential of infection as a cause of the inflammation seen in prostate cancer. History of sexually transmitted infections is considered a risk factor for the development of malignancy (Dennis and Dawson, 2002). Additionally, single nucleotide polymorphisms in immune response-related genes have also been linked to increased risk of prostate oncogenesis, including macrophage scavenger receptor 1 (MSR-1), toll-like receptors (TLRs) 1, 4, 6 and 10 which are involved in the recognition of bacterial invaders, and ribonuclease L (RNaseL), linked to response to viral infection (Carpten et al., 2002; Xu et al., 2002; Zheng et al., 2004; Sun et al., 2005). Furthermore, increased plasma levels of a number of cytokines are also seen in prostate cancer, and especially in castration therapy-resistant cancer, including interleukin (IL)-1β, IL-6 (with significantly higher expression in prostate cancer tissues compared to disease-free controls), IL-8, tumour necrosis factor (TNF-α) (Nakashima et al., 1995; Veltri et al., 1999; Wise et al., 2000; Giri et al., 2001).

The role of an infectious agent is also supported by the similarity of multifocal inflammation observed in prostate cancer relative to other malignancies with a known infective cause including gastric cancer induced by *Helicobacter pylori*, hepatocellular carcinoma initiated by hepatitis infection, and human papilloma virus (HPV)-related cervical cancer (Larson et al., 1997; Colombo, 2000; Faraji and Frank, 2002).

The isolation of *P. acnes* from the prostate by Cohen et al. (2005) highlighted a perfect candidate for an infectious agent which could have the potential to drive oncogenesis by causing a chronic asymptomatic infection. Due to *P. acnes*' requirement for anaerobic growth conditions and long incubation times, as well as resistance to commonly used lysis enzymes, such as lysozyme, *P. acnes* is difficult to detect using routine culturing techniques and with routinely used nucleic acid extraction procedures, which is why its presence in the prostate was not discovered earlier. Prostate cancer is a disease with high incidence, and if a bacterium is involved in its origin, it would tend towards a higher prevalence. This is another characteristic met by *P. acnes* as it is a member of the normal skin flora and the urinary tract microflora (Shannon et al., 2006a; Grice and Segre, 2011). The bacterium also has the ability to evade the immune system, as it can survive intracellularly in macrophages; this would allow it to cause a long-lasting infection (Fischer et al., 2013). Finally, there are similarities in the immune response seen in acne (which has also been linked to *P. acnes)* and prostate cancer. Both are linked to a delayed type hypersensitivity reaction, including increased levels of macrophages and $CD4^+$ T helper (T_H) cells (McClinton et al., 1990; Jeremy et al., 2003; Shannon et al., 2006b).

Following the initial discovery by Cohen et al. (2005) and with the development of superior sequencing systems, multiple studies have since confirmed the presence of *P. acnes* in the prostate (Alexeyev et al., 2006; Sfanos et al., 2008; Chen and Wei, 2015; Cavarretta et al., 2017). Using fluorescent *in situ* hybridization, Alexeyev et al. (2007) demonstrated that *P. acnes* can be found both intracellularly and as extracellular biofilm-like aggregates; employing an immunohistochemical approach, Bae et al. (2014) showed the presence of *P. acnes* in both epithelial cells and macrophages. The presence of *P. acnes* was also found to be associated with a 4-fold increase of the risk of developing prostate cancer (OR: 4.5; 95%; CI: 1.93-11.26) (Davidsson et al., 2016). A number of *in vitro* infection models have also been employed, demonstrating that *P. acnes* has the potential to cause cancer-promoting gene dysregulation in prostate

epithelial cells, including changes in vimentin levels, secretion of prostate cancer-related cytokines, dysregulation of nuclear factor-kappa B (NF-κB) and Janus kinase/signal transducer and activator of transcription 3 (JAK/STAT3) signalling, and cell cycle alterations (Drott et al., 2010; Fassi Fehri et al., 2011; Mak et al., 2012; Davidsson et al., 2016; Sayanjali et al., 2016). A recent study, using primary prostate cells suggested that *P. acnes* infection may have a cancer-protective role, while using the same strain was previously used by the same group to demonstrate cancer-inducing behaviour in the RWPE-1 cell line (Fassi Fehri et al., 2011; Mak et al., 2012; Sayanjali et al., 2016).

6.2. *Summary of findings*

6.2.1. Predominant isolates

The predominant sequence of prostate isolates identified using the 'Belfast' $MLST_8$ scheme was identified as sequence type 5 (ST5), comprising 33% of all prostate isolates in the database.

6.2.2. Stable infection model

Optimising the infection model limited the extrinsic factors which affect the prostate epithelial cells during experiments, to allow the direct effects of *P. acnes* on the host cells to be investigated, and provided a stable foundation for follow up experiments. It also enabled us to highlight any caveats associated with this particular *in vitro* infection model, which may prove important in the context of previously published work where this method was used.

6.2.3. Ability for intracellular survival

P. acnes strains 00035, NCTC737, ST27 (type IA_1) and B3 (type IB) appear to have a significantly higher ability to invade prostate epithelial cells, compared to the remaining phylogenetic types examined.

6.2.4. Phylotype-specific response to infection

The optimised acute and chronic infection models demonstrated stable eukaryotic cell and viability counts, in both acute and chronic infections and the cells remained viable for the duration of the experiments. There were two groups of bacterial behaviour observed in the 5% CO_2 humid environment – type IA_1 strains (00035 and NCTC737) and phylotype IB (strain B3) showed growth in this environment, while ST27 and types II, III and *P. granulosum* demonstrated a decrease in numbers. Thus, the RWPE-1 cells

remained challenged with bacteria for 30 days only in experiments with the former group. This is an important observation in the context of chronic infection experiments, as it highlights differences in behaviour between phylogroups.

All strains initiated an acute immune response, evaluated using qPCR, with the magnitude of upregulation being higher in phylotypes IA_1 and IB. The prostate-derived type III strain showed the highest number of downregulated inflammatory genes, highlighting the phylotype-specific response observed. Dysregulation of the epithelial-mesenchymal transition (EMT) genes studied is not consistent between time points, however, a trend is seen with significant increase in more EMT-related genes by phylotypes IA_1 and IB and more decreases in expression induced by types II, III and *P. granulosum.* A similar pattern is observed when the gene dysregulation of chronic infection models was studied. The dysregulation patterns, however, are not consistent with what would be expected if cells were undergoing EMT.

Anchorage-independent growth is seen in only one of the chronic infection models, and a trend towards increased migration was seen in cells infected with NCTC737 (24 hours post-wound creation), CFU2 and *P. granulosum* (48 hours post-wound creation).

6.2.5. Strain 00035 (type IA1) as a cancer inducing agent?

Cells infected with the type IA_1 strain were the only infection model to shown anchorage-independent growth in soft agar assays. This infection was also the only one to show downregulation of E-cadherin/*CDH1*, which is a marker of "cadherin switch" and EMT. The initial decrease seen at day 15 of a chronic infection was not observed in the qPCR experiment (Chapter 4, Section 4.3.2.3), however, a trend towards a decrease was seen in the qPCR array (-1.59-fold downregulation, $p = 0.0156$, Chapter 5, Section 5.3.2). By the day 30 timepoint, a significant decrease of -2.1-fold was seen. The dysregulation in numerous pathways, including phosphoinositide 3-kinase/protein kinase B (PI3K/AKT), apoptosis, cell cycle, Wnt/β-catenin and androgen-independent growth all point towards cancer-inducing dysregulation caused by this strain.

6.2.6. CFU2 (type III) and its potential cancer-protective role

The CFU2-infection model demonstrated a dysregulation pattern consistent with cancer-protective behaviour, including increased apoptosis-inducing gene expression and increased androgen-dependence.

6.2.7. Strain B3 (type IB)

The type IB strain investigated caused a statistically significant change in the expression of only one gene in infected prostate RWPE-1 cells compared to non-infected controls. Previous work investigating the effect of *P. acnes* infection on primary prostate epithelial cells indicated that thiopeptide-producing *P. acnes* strains (phylogroup IB), have the ability to cause cell cycle arrest and thus prevent cancer-progression, likely by inhibiting *FOXM1* (Sayanjali et al., 2016). The results in this thesis agree with these findings. In contrast, previous publications using the same type IB strain in an RWPE-1 immortalised cells line infection model have suggested that this phylogroup may induce cancer progression, however, the differences in incubation times for chronic infections and the multiplicity of infection (MOI) used could serve as an explanation for the discrepancies in observations (Mak et al., 2012; Fischer et al., 2013; Sayanjali et al., 2016).

6.3. *Study aims*

The aims of this study were outlined in Section 1.6 and were addressed over the course of this thesis.

Aim 1 – Genotypic analysis of prostate cancer-associated phylogenetic types of *P. acnes*

In Chapter 3, multilocus sequence typing (MLST) analysis, using a typing scheme developed by McDowell et al. (2013), was performed on a small group of available prostate isolates. The strains investigated belonged to different phylogenetic groups and to different STs, which are globally disseminated and highly prevalent in the human population, except for the two type IB strains which both belong to the same ST5. When the strains identified in this thesis are combined with the strains in the database available online, strains belonging to ST5 comprise 33% of all prostate isolates identified using the 'Belfast' $MLST_8$ typing scheme, highlighting the potential importance of this sequence type (McDowell et al., 2013). This contrasts with previous findings where type II was the prevalent isolates from the prostate (at approximately 50%, followed by type IA_1), however, the authors investigated multiple biopsies from a patient and each positive sample was counted as a separate isolate, thus inflating the number of samples investigated (Davidsson et al., 2016). The study included a total of 100 patients, with 60% being positive for *P. acnes*, however, a total number of 182 isolated were

investigated; if a patient's results were positive for *P. acnes* of the same type in multiple biopsy cores, it is likely that it is the same organisms isolated from all, rather than a separate infection (Davidsson et al., 2016). Thus, considering each isolated type from a patient rather that every individual sample, would have been more representative of the prevalence of the different phylogenetic types. Furthermore, as no washes of the sampled tissues are indicated in the methodology, the possibility for contamination cannot definitively excluded.

With the large number of published whole genomes of *P. acnes* and general advancement in the field, the creation of a database uniting the different MLST schemes available and thus the work performed by different groups would offer easier access to information and could provide better insight into the significance of the prevalence of certain sequence types both on prostate cancer but also in a wider context. Developing an *in silico* PCR script to analyse available whole genome sequences based on the available MLST schemes, would make access to such information even easier.

Aim 2 – Optimisation of *in vitro* infection model

A number of extensive optimisation experiments were performed in Chapter 3. These initial experiments were extremely valuable and critical for further analysis, as previous published studies have not investigated in detail cellular and bacterial behaviour within this *in vitro* assay, and in general have not demonstrated clear validation of the infection models used.

Investigating the optimal seeding density for the RWPE-1 prostate epithelial cells was necessary to limit any external factors, such as over-confluence, with potential to interfere in the study of the effects of *P. acnes* on the cells. If the cells were allowed to become over-confluent, increased death rate could occur, which may be interpreted to be as a direct consequence of infection.

Additionally, at each passage, the cells were split to the optimal seeding density (100,000 cells/ml), rather than at a set ratio, which was to again ensure that only the infection's effects upon the cells would be recorded while limiting the impact of additional extrinsic factors. Specifically, if infection with one strain induced the cells to proliferate faster, while another strain caused them to proliferate more slowly, and the cells were split at a set ratio, it could cause the faster-dividing cells to be seeded at near

confluence, while at the same time it could cause the slower-growing cells to have their growth delayed even further due to loss of contact-dependent signalling. These effects would be amplified at each passage.

Another difference from the majority of publications is the MOI 15:1 selected for our experiments, compared to MOI 50:1 used in other key studies (Fassi Fehri et al., 2011; Mak et al., 2012; Sayanjali et al., 2016). While our results showed that there is no statistically significant difference in bacterial counts between cells infected with MOI 15:1 and MOI 50:1 at days 10, 20 and 30 of a long-term infection models, the difference in the effect of the lower MOI would be seen in short-term infections. Additionally, the higher MOI could initiate changes in the cells during the first few days of infections (e.g. a stronger inflammatory response), before any media changes or passages. However, an MOI 15:1 is closer to the numbers observed in prostatectomy samples than MOI 50:1, and was thus selected for the experiments. MOI 15:1 is still an artificially high multiplicity of infection compared to *in vivo* scenarios.

To perform accurate intracellular bacterial counts, eradication of extracellular bacteria is necessary. Previous published studies have not indicated whether bacteria remain viable following antibiotic treatment or whether negative controls were used to interrogate this possibility, thus the reported intracellular counts could have been overestimated (Mak et al., 2012; Fischer et al., 2013). Our results showed that regardless of the combinations of antibiotics and incubation times used, viable bacteria do indeed remain viable in the media, prior to lysing the eukaryotic cells to release intracellular bacteria. As a result, the number of bacteria present in the medium following treatment was taken into account, and subtracted from future counts, to allow more accurate intracellular counts to be reported. In addition to the possibility that the bacteria found in the media are released by dying eukaryotic cells during the treatment and thus the antibiotic has not had enough time to target them effectively, it is plausible that biofilm formation on the surface of the culture dishes interfered with the antibiotic activity (Holmberg et al., 2009b; Dessinioti and Katsambas, 2017). If biofilms are then disturbed during the removal of the medium for bacterial counts, this could lead to the presence of bacteria reported in the medium. Previous studies have shown that all phylogenetic types (excluding type III, as the study was conducted before the identification of this type) of *P. acnes* skin and prosthetic infection isolates can form biofilm and when a

biofilm was formed they had higher resistance levels to commonly used antibiotics compared to planktonic cells (Coenye et al., 2007b; Holmberg et al., 2009b; Achermann et al., 2014). An investigation into the ability of the prostate isolates to form biofilm would be needed to confirm this possibility.

Another set of experiments which required the addition of antibiotics was soft agar assays. Our results showed that, as expected, if no antibiotics are used in soft agar assays with infected cells, bacterial colonies form in the assay. On the other hand, when antibiotics were used (at a final concentration 20 µg/ml erythromycin), a significant decrease was seen in the number of colonies formed by the prostate cancer cell line 22Rv1. As bacterial colonies cannot easily be distinguished from colonies formed by cells due to anchorage independent growth (difference in the edges of the colonies could be seen when observed under the microscope, with the bacterial colonies having smoother edges), antibiotics are critical for the successful and accurate representation of the results. However, the use of antibiotics may have decreased the number of observed colonies in the 00035 assay, and could have prevented the formation of colonies in the remainder of the soft agar assays performed.

The selection of a stable housekeeping gene is necessary for the accurate relative quantification analysis of qPCR data. Our findings in Chapter 3 showed that *HPRT1* is the most stable housekeeping gene in this cell culture model, and it also has a higher stability value than a combination of genes. This issue was highlighted once again in Chapter 5, when a selection of 5 housekeeping genes was interrogated as potential endogenous references for qPCR experiments. In agreement with the previous experiment, *HPRT1* was once again shown to be the most stable housekeeping gene. However, the results also did show a significant dysregulation of two potential housekeeping genes (*GAPDH*, upregulated 10.85-fold, and *B2M*, downregulated -2.77-fold, both in the 00035 infection model). Two previous studies exist examining the gene dysregulation as a result of *P. acnes* infection in a model using the RWPE-1 cell line. Mak et al. (2012) do not specify the housekeeping gene used for normalization to identify fold-change expression in a microarray, while a study conducted by Fassi Fehri et al. (2011) used *GAPDH* for microarray normalization. No information about housekeeping gene optimisation is mentioned in the studies, which highlights a potential issue with

the calculated fold-change, especially as the *GAPDH* dysregulation we observed here is more than 10-fold.

An extensive troubleshooting process led to the identification of an issue with the detection antibodies in the Peprotech ELISA kits. As a result of these findings, time and financial constraints, it was not possible to independently confirm the molecular results presented in the latter chapters. However, previous studies have demonstrated cytokine upregulation of IL-6 and IL-8 at the protein level in similar infection models, thus the data presented in this thesis is in line with previous findings (Fassi Fehri et al., 2011; Davidsson et al., 2016).

Overall, the experiments performed in Chapter 3 achieved the essential aim of optimising the methods to be used in future chapters. This work also highlighted potential weaknesses in previous studies and ensured robust data to address the overarching aims

Aim 3 – Investigation of the potential of *P. acnes* phylogenetic types to drive oncogenesis

Chapter 4 focused on an investigation of how infection affects the RWPE-1 cells, including viability counts, performed for the duration of the experiments, molecular dysregulation of inflammatory and EMT-related genes, anchorage-independent growth, migration and its ability to induce proliferation in endothelial cells. *P. acnes* bacterial counts in the infection models and the cytotoxicity of the different strains were also assessed, as well as intracellular counts for each strain used.

For experiments, strains representing each phylogenetic type which have been linked to prostate cancer were used. Previous studies have reported that strains belonging to phylotype II are commonly isolated from the prostatectomy samples, however, our study did not discover any type II strains (Mak et al., 2013b; Davidsson et al., 2016). This is most likely a result of the small sample size available here. Due to the unavailability of a prostate isolate type II, the reference strain NCTC10390 was used as a proxy in experiments, assuming type II strains would behave in similar ways. However, as seen with the behaviour of the different type IA_1 strains (most notably in the case of NCTC737 and 00035 versus ST27), this is not always the case, and any conclusions would need to be confirmed with a prostate-derived type II strain.

Strains from the IA_2 and IC phylotypes were not investigated in this study, as they are not associated with prostate infections (Mak et al., 2013b). Strains NCTC737, ST27 and *P. granulosum* were used as controls: NCTC737 (type IA_1, ST1) as the most widely studied representative of the *P. acnes* species; ST27 as a health-associated strain; *P. granulosum*, as a related member of the cutaneous *Propionibacterium* genus, which has also been isolated from the prostate (Mak et al., 2013b). *P. avidum*, another cutaneous *P. acnes* relative, was also trialled as a control, however, it led to the death of the RWPE-1 cells by the 72-hour time point of infection.

The intracellular counts showed that most *P. acnes* strains (00035, NCTC737, ST27 and B3) have the ability to become intracellular in the prostate epithelial cells, with the number of bacteria which become intracellular differing between strains. The results were presented with extracellular bacteria subtracted, to ensure accurate representation.

The ability of *P. acnes* to invade epithelial cells, and also to remain viable in macrophages, raises a number of questions about the importance of 'intracellularity' in this infection model and its involvement in cancer development. While *in vitro* studies have shown that *P. acnes* can remain viable in a range of cell lines, including macrophages, conflicting conclusions exist about whether the organism can reproduce intracellularly (Fischer et al., 2013; Nakamura et al., 2016). What is the significance of intracellularly infected cells in the context of this infection model? Does cancer originate in the cells which harbour intracellular infection or in surrounding cells, which become cancerous as a result of secretions produced by the infected cell? What is the effect or media changes and passages on the number of challenged cells?

An experiment designed to address the first question could also identify infected cells and isolate them using flow cytometry. Similar experiments have been performed previously to investigate the ability of *Mycobacterium tuberculosis* (a distant *P. acnes* relative; both belong to the *Actinomycetales* order) to survive intracellularly in macrophages, using CD14 (co-receptor of TLR4 and MD2) and CD119 (interferon gamma receptor 1 or IFNGR1) as targets (Sharma et al., 2012). The infected cells could be selected out of the population and cultured independently to investigate the direct effect of infection on the RWPE-1 cells. If it is the case that only one of the subgroups is affected by infection, then performing analysis of a culture including both would lead to

loss of significance of the results. Thus, studying the two subpopulations separately could give insight of dysregulation, which would otherwise be hidden in the mixture of cells.

Another limitation of the infection model is the potential loss of cells and bacteria as a result of passages and media changes. As seen in strains NCTC10390 and CFU2, during the acute infections, both demonstrate steady numbers for the duration of the experiments. However, in the long-term infection the numbers of both decrease overtime. If conditioned medium containing any bacteria was collected, centrifuged to pellet the bacteria and bacteria resuspended in fresh medium and added to the newly split cells, it would answer the question whether the drop in numbers in the case of CFU2 and NCTC10390 is due to bacterial death, or as a result of them being washed off. This decrease in bacterial counts has not previously been investigated and it is unclear whether it is an *in vitro* artefact or it is something that is also applicable to an *in vivo* situation.

Another potential issue is the loss of RWPE-1 cells during passages. Setting up the infection models in a small vessel, e.g. 6-well plate and then increasing the size of the vessel at each passage and keeping all the cells, rather than disposing of a large proportion of them, would limit the loss of any cells which could harbour mutations resulting from rare events induced by infection, and would allow them to continue proliferating until apoptosis occurs.

The investigation of the cytotoxic properties of the different phylogenetic types of *P. acnes* and *P. granulosum* revealed that they did not appear to be cytotoxic to the RWPE-1 cells. The highest cytotoxicity levels are observed in strains 00035 (highest value 8.7% at 24 hours) and B3 (highest value 10.2 at 72 hours).

Dysregulation of the inflammatory genes investigated here is seen in all strains in the acute infections, and in most infection models during the long-term infections, showing chronic immune response. Some of the EMT genes are also dysregulated in the acute infection, but the most notable change is seen in cells infected with 00035 at day 30 when a decrease in the expression levels of E-cadherin (*CDH1*) is seen, signalling a possible “cadherin switch”. This, together with 00035 being the only infection model to demonstrate anchorage-independent growth, suggests that cells chronically infected

with the type IA_1 strain 00035 are undergoing early cellular transformation and are beginning to acquire cancer hallmarks. These findings are in line with the observations from Chapter 5, which also support a potential role of 00035 in driving oncogenesis by promoting proliferation and survival, inhibiting apoptosis, and inducing androgen-independent growth, characteristics of advanced treatment-resistance tumours.

Two studies have been published analysing the transcript levels of a range of genes in long term infection models of prostate epithelial cells with *P. acnes.* The experimental design in those studies differed from the methodology used here, however, comparison can still be made, focusing on the trends seen.

The studies performed by Mak et al. (2012) and Fassi Fehri et al. (2011) used a type IB strain (P6, ST119) for their analysis, and selected an MOI 50:1, which differs from the MOI optimised in Chapter 3 of this thesis. Both studies used microarrays to assess gene dysregulation in a 24-hour infection of RWPE-1 cells There are four genes in common between the microarray used by Mak et al. (2012) and the genes investigated in Chapter 4 – *IL1B*, *IL6*, *IL8* and *TNF*. P6 caused an upregulation of 4.5-fold, and an increase in this study was seen when the cells were infected with strains 00035, ST27, B3, NCTC10390 and *P. granulosum*, with varying levels of increase (ranging between 130-fold for 00035 and 2.1-fold for NCTC10390; 40-fold for B3). A milder increase was seen in *IL1B*, with cells infected with P6 showing upregulation of 2.8-fold, which is close to the levels observed here with 2.5-fold increase for cells infected with ST27, and 2.4-fold for B3. *IL6* levels were upregulated in all infections. Finally, while P6 caused an insignificant change in *TNF* levels, it was upregulated in all infection models tested in Chapter 4. The study conducted by Fassi Fehri et al. (2011) also showed significant upregulation of *IL1B*, *IL6* and *IL8* expression 24 hours post-infection, with values of 3.1-fold, 5.8-fold and 8.6-fold, respectively.

Interestingly, despite the higher MOI used by Mak et al. (2012) and Fassi Fehri et al. (2011), the upregulation in inflammatory genes observed in both studies is significantly lower than what was seen in Chapter 4. A possible explanation is the different methodologies employed to assess differences in expression levels (microarrays vs qPCR). Additionally, as mentioned above, the selection of *GAPDH* as a housekeeping gene may have played a role in the values calculated in the two studies.

Fassi Fehri et al. (2011) also investigated gene dysregulation in a long-term infection model, defined as 21-days. They observed a mild upregulation in *IL1B*, *IL6* and *IL8* of 2.1-fold, 2.9-fold and 4.6-fold, respectively. These values demonstrate similar trends to what was observed in the infection models with types IA_1 and II in Chapter 4 at day 15.

Immunofluorescence was used here to quantify protein expression of E-cadherin and vimentin. However, this method can be used to identify bacterial presence, for example by using *P. acnes* specific antibodies such as QUBPa1 (specific for phylogenetic type I) , and could help localise the infection; alternatively, the method could also be used to identify infected cells utilising the antibodies used in flow cytometry experiments described above (targets CD14 and CD119) (McDowell et al., 2005; Sharma et al., 2012).

MTT assays were employed to assess the ability of conditioned medium from chronic infection models to initiate angiogenesis in endothelial cells.

The MTT assay used is not a proliferation assay but rather measures cell metabolic activity, thus increased or decreased MTT production, does not necessarily mean increased proliferation. The MTT assay was used as it was cost effective for an initial pilot study investigation into the angiogenic potential of chronic infection models.

The results from the MTT assay experiments showed no overall difference between proliferation in cells treated with conditioned medium from infected versus non-infected prostate epithelial cells. The results can be confirmed using a dedicated proliferation assay such as Ki67 or Bromodeoxyuridine (BrdU). The Ki67 assay uses an antibody to target the Ki67 protein which is only expressed in proliferating cells (and absent in cells in the G_0 phase) (Kim and Sederstrom, 2015). BrdU is a nucleotide analogue which replaces thymidine during DNA replication; BrdU can then be targeted by antibodies, leading to the detection of all actively proliferating cells (Messele et al., 2000). Additionally, an apoptosis assay, such as terminal deoxynucleotidyl transferase (**T**dt) d**U**TP **n**ick **e**nd **l**abelling (TUNEL, which binds fragmenting DNA during apoptosis and can be tagged with a fluorochrome and measured) or annexin 5 (which binds dead cells and can be quantified using flow cytometry) could be used to investigate whether any apoptosis is present which is not detected by the MTT assay (Kyrylkova et al., 2012; Lakshmanan and Batra, 2013).

In addition to confirming whether the endothelial cells have increased proliferation or increased apoptosis, further investigation could focus on how treatment with conditioned medium affects the ability of endothelial cells to form tubules in an appropriate extracellular matrix (DeCicco-Skinner et al., 2014). A scratch assay can also be used to assess migration of endothelial cells following treatment with conditioned medium (Guo et al., 2014).

The experiments in Chapter 4 addressed the aim and provided a detailed comparison of the effects of different strains on the RWPE-1 cells and highlighted strain 00035 as a potential pro-oncogenic strain. The data from Chapter 4 was also used as a basis of the selection of strains 00035 (type IA_1), B3 (type IB), and CFU2 (type III) to be interrogated at the molecular level by qPCR array in Chapter 5.

Aim 4 – Analysis of prostate cancer-related genes following infection

In Chapter 5, a commercially available qPCR array was used to investigate the dysregulation of prostate-cancer related genes induced by infection with the three strains selected in Chapter 4 in comparison to uninfected controls.

While the qPCR array used here provides information about the expression of 84 prostate cancer-related genes, the number of genes and the restricted gene selection are an obvious limitation of the array. While some genes are of interest, including those involved in apoptosis, cell cycle control and in fatty acid synthesis, others do not carry valuable information, e.g. gonadotropin-releasing hormone (*GNRH1*, involved in hormone secretion in the brain).

An alternative approach to analysing the transcriptome and comparing changes in expression between infection models and to untreated controls would be RNA sequencing (RNAseq). This method provides unbiased detection of expressed transcripts and it is not limited by template availability. It is highly specific and it offers the capability to detect novel transcripts and novel sequence variants (Marioni et al., 2008). While the data analysis is more complex, requiring the use of multiple bioinformatics tools and sophisticated programming skills, the resulting data gives a complete analysis of all transcripts in the cell and would allow the detection of differentially expressed genes. It could also permit a more thorough investigation of gene expression within pathways – while the qPCR array only has a limited number of representative genes within a

pathway, RNAseq could provide transcript information about all genes involved in the process.

The study performed by Fassi Fehri et al. (2011) mentioned above, also contains three gene which are common between the microarray they used, and the qPCR used here to analysed gene dysregulation. The three genes the studies have in common are *IL6*, prostaglandin-endoperoxide synthase (*PTGS2*) and vascular endothelial growth factor a (*VEGFA*). The dysregulation seen in *IL6* and *PTGS2* is only significant in cells infected with the type IA_1 00035 (1811.96-fold and 14.62-fold, respectively) which is significantly higher than the upregulation seen in the previous study at 2.9-fold and 2-fold for *IL6* and *PTGS2*, respectively (Fassi Fehri et al., 2011). The findings of increased levels of *PTGS2* (encoding cyclooxygenase-2, COX-2) is line with expectations, as COX-2 has previously been shown to be upregulated in prostate adenocarcinomas (Gupta et al., 2000; Uotila et al., 2001). Production of COX-2 is known to be upregulated if inflammation is present, and in the case of *H. pylori* infection, the bacterium has been shown to induce its production (McCarthy et al., 1999; Badary et al., 2017). A similar observation is made here, with COX-2 being upregulated as a result of infection; this suggests the possibility for *P. acnes* infection to drive oncogenesis via upregulation of COX-2.

In the study by Fassi Fehri et al. (2011) *VEGFA* levels at 21-days were not significantly different, compared to untreated controls (i.e. less than 2-fold change). In contrast, in our study the levels of *VEGFA* are 3.77-fold upregulated for the 00035 infection and 2.23-fold for the CFU2, it is possible that 6 days later that increase in expression would be lost, however, it is worth noting once again that different phylotypes and MOIs are being compared. While upregulation of *VEGFA*, a known inducer of angiogenesis is seen in two of the infection models (type IA_1 00035 and type III CFU2), when the potential of infected cells to induce proliferation of endothelial cells was investigated in Chapter 4, no such induction was seen. The most likely explanation is the fact that the qPCR assays were performed at 15 days post-infection, while the endothelial cells were treated with medium from RWPE-1 cells infected for 30 days, and thus the transcript information is not reflective of the processed in the cell at the later timepoint.

The data from experiments in Chapter 5 address the aim and led to findings, suggesting that the type IA_1 strain causes dysregulation related to cancer progression, while CFU2 (type III) leads to gene expression patterns implying cancer-protective effects.

6.4. *The role of the immune system*

The prostate, similarly to the intestine, is an immunocompetent organ, meaning that a range of immune cells are present within it (including $CD4^+$ T cell, $CD20^+$ B cells, macrophages) (Hussein et al., 2009). Another thing that distinguishes prostate cells from other cell types is that due to the accumulation of high levels of zinc ions they have a truncated Krebs cycle. As a result, prostate cells do not produce energy using cellular respiration and unlike other cells in the body, they are not exposed to reactive oxygen species (ROS), a by-product of respiration. This makes prostate more sensitive to ROS-induced DNA damage, compared to other cell types.

If the infection model included inflammatory cells, they would be affected by the secreted inflammatory genes, and as a result, ROS may be released, exposing the prostate cells to high levels of a carcinogen they have not encountered before. Additionally, the immune cells would attempt to eradicate the infection with *P. acnes*, with macrophages engulfing the bacteria and the bacteria remaining viable intracellularly, as previously reported (Fischer et al., 2013). All in all, if macrophages were involved, the infection model would behave differently, and it would be more likely that a cancer-inducing event would occur, such as the excretion of matrix metalloproteases (MMPs) by the immune cells and ROS damage to the cells as a result of the attempt to eradicate infection.

While small changes in response of the endothelial cells are seen when treated with medium from infected prostate cells, the macrophage is a key player in angiogenesis whose involvement is not investigated in this study. Monocytes are recruited to the cancer site by hypoxic cells (which release macrophage chemoattractant protein-1 (MCP-1)); there the monocytes would differentiate into tumour associated macrophages; the macrophages also release pro-apoptotic signals, just like the cancer cells, and also induce the production of IL-6 and MCP-1, both of which lead to the summoning of monocytes, initiating an activation loop (Roca et al., 2009). Additionally, the macrophages also secrete MMP2, MMP7, MMP9, MMP12, and cathepsin proteases (Lewis and Pollard, 2006; Gocheva et al., 2010; Mason and Joyce, 2011; Small et al., 2013). The MMPs play a role in extracellular matrix remodelling and also stimulate the proliferation rate and migration of endothelial cells (Lu et al., 2012; Guo et al., 2013). Cathepsin also plays a pro-angiogenic role, as the inhibition of macrophage cathepsin

causes arrest in the development of cancer-associated blood vessels; cathepsin has also been shown to induce tumour proliferation, invasiveness and metastasis (Small et al., 2013; Olson and Joyce, 2015).

Taken together, these observations highlight the important role of the inflammatory response in infection-induced cancer.

6.5. *Future work*

6.5.1. Are epigenetic modifications involved?

Studies of the mechanism *H. pylori* utilises to cause gastric carcinoma have discovered that the infection has the ability to cause DNA methylation, thus silencing genes necessary for the function of healthy cells (Nardone et al., 2007). An example observed was methylation (resulting in silencing) of the *CDH1* gene when *H. pylori* infection was present and loss of the methylation if the infection was eradicated (Chan et al., 2003; Leung et al., 2006). Such a methylation-induced loss of E-cadherin would allow cells to undergo a "cadherin switch" and become motile, initiating cellular transformation.

To investigate whether any epigenetic changes are present following infection and initial screen of global methylation levels would present a snapshot of the epigenome. However, it is theoretically possible that the results of a global methylation analysis could be the same between treatments while the genes affected differ. Thus, a bisulfide treatment approach, followed by whole genome sequencing would provide information about the methylation status of all genes in the cells which could easily be compared between infections and to untreated controls.

6.5.2. Can infection speed up cancer progression?

Investigation of the effects of *P. acnes* infection on cancer cell lines could provide insight in whether the bacterium could speed up cancer progression once the disease has developed. Infecting prostate cancer cell lines, for example the androgen-sensitive cell line LNCaP and investigating whether *P. acnes* infection could lead to androgen-independent growth.

To investigate any dysregulation of the androgen receptor in the RWPE-1 cell line treatment with synthetic androgen is necessary, as it is currently unknown whether *P. acnes* infection has an effect on the androgen receptor function. As the RWPE-1 cells require stimulation to produce the androgen receptor, culturing infection models and

uninfected controls in complete keratinocyte serum-free medium supplemented with synthetic androgen (e.g. mibolerone) would allow the investigation of androgen receptor dysregulation.

6.5.3. Development of a superior infection model

The culture of a single cell type in a monolayer and the addition of bacteria is a simple way to investigate the direct response in the epithelial cells, however, it is not representative of an *in vivo* situation. Using primary cells, rather than an immortalised cell line, would allow the investigation of dysregulation caused by infection in an environment representative of *in vivo* situation. Improving the currently used infection model would provide new ways to study interaction between bacteria and between different cell types.

A further limitation of the currently established infection models is that by focusing on a single cell line it does not address the tumour heterogeneity seen *in vivo*. Using primary cells for infection models could help investigate the effect on infection on a heterogenic population of cells. Clonal selection of chronically cells could lead to the generation of distinct cell lines demonstrating differential expression as a result of infection. Furthermore, single cell could be used to better study the heterogeneity within the cell population in infection models.

A simple approach would be to create variations of the experiments in Chapter 4 (where endothelial cells were treated with medium from infection models), using different cell lines. For example, what effect would be observed if the monocytic cell line THP-1 was treated with medium from *P. acnes*-infected RWPE-1 prostate epithelial cells? Alternatively, what would the effect be on the HDMEC cells if they were treated with conditioned medium from infected THP-1 cells? And what if conditioned medium from the RPWE-1 cells was exposed to the THP-1 cell line, and then conditioned medium from this experiment was used on the HDMEC cells?

A more complex approach would be to set up co-culture experiments, for example with RWPE-1 prostate epithelial cells and THP-1 monocytes and then initiate a *P. acnes* infection. While optimising the co-culture infection model would be a challenge, the results would be more representative of an *in vivo* situation.

In the body, multiple cell types work together; cells are not in monolayers but form structures. The development of flow-cytometry technology has allowed for FACS-sorted cells to be cultured to form 3D prostate organoid cultures (Chua et al., 2014; Gao et al., 2014; Karthaus et al., 2014; Drost et al., 2016). These organoids can then be used for the generation of complex co-culture experiments with stromal or inflammatory cells. Optimising an *in vitro* infection model of *P. acnes* infection of a 3D prostate organoid, co-cultured with inflammatory cells would offer an environment closer to that observed *in vivo* compared to the currently used monolayer monoculture (Fatehullah et al., 2016). As murine prostates greatly differ from the human prostate gland, the usage of complex organoid cultures may be the only way to accurately study the effect of infection on the gland and the role it plays in oncogenesis (Grabowska et al., 2014).

6.6. *Conclusion*

The results from this study clearly demonstrate that there is a strain-specific response when prostate epithelial cells are challenged with different *P. acnes* isolates. The results of infection models with strain 00035 in particular, support a potential role of *P. acnes* in prostate oncogenesis.

Opponents of the role of *P. acnes* in the development of prostate cancer have suggested that the presence of the bacterium in prostatectomy samples and biopsies could be a result of contamination which has occurred during the procedure. However, as the phylogenetic types of *P. acnes* isolated from the prostate (predominantly types IB and II) differ from those commonly isolated from the skin (IA_1), it is unlikely that contamination is the source of the bacterium. Additionally, with improved culturing techniques, care is taken to wash the tissue sample thoroughly and only to culture bacteria present within the tissue itself.

Stratified medicine aims to identify the most appropriate treatment for each individual based on pre-disposing factors. Being able to prescribe the correct treatment to a patient, guaranteeing that they would respond to the selected treatment is not only cost effective, but it also prevents the physical and emotional suffering of the patient. As prostate cancer is a complex multifactorial disease, infection as a potential modifiable risk factor presents an attractive opportunity to use it as a biomarker for the

identification of a subgroup of men harbouring an infection which could potentially lead to cancer.

There is currently no simple way to diagnose prostate cancer. While the PSA test used highlights possible cases of the disease, its low specificity and sensitivity mean uncertainty for the patients, and a high risk of unnecessary biopsy based on the test result. The only way for a prostate cancer to be diagnosed currently is through a prostate biopsy.

With *P. acnes* infection being a potential cause of prostate oncogenesis, there is a need for the development of a test which could identify men harbouring an asymptomatic infection of the prostate. At present, the only way to identify the presence of infection is via a biopsy. Developing a blood or urine test which can distinguish between carrier of the bacterium from the general population, and which can also identify the phylogenetic type of the bacterium present, would allow the stratification of the subgroup of men who are at risk of developing prostate cancer as a result of *P. acnes* infection. As seen here, the phylotype specific response to infection in prostate cells, confirms the existence of prostate cancer-inducing and suggest the possibility for cancer-protective strains. The ability to identify these cancer-causing strains, such as 00035, via a test, would allow patients to be stratified into groups and those at risk could receive preventative antibiotic treatment eradicating the bacterium prior to oncogenesis; in contrast, in patients who have a cancer-protective strain (similar to CFU2), then no action would be needed. This separation based on specific pathogen characteristics would be similar to what is observed in the case of HPV-related oncogenesis, where only some viral types (e.g. HPV-16, HPV-18, etc.) have been lined to malignancy (Woodman et al., 2007).

In addition to a screening test, the development of a vaccine would protect men from the harmful effects of being colonised with a potentially cancerous strain of *P. acnes.* Recently, a vaccine targeting the *P. acnes* Christie–Atkins–Munch-Petersen (CAMP) factor was developed and used successfully to treat *in vivo P. acnes* skin infections in animal models (Liu et al., 2011). Similar vaccine could be optimised to target the harmful prostate-associated *P. acnes* strains and preventing them from potentially causing cancer.

This study is the basis necessary for the development of such screening tests and vaccines as it demonstrates that the specific phylogenetic types of *P. acnes* have the potential to act as a causative agent in prostate cancer.

Appendices

Appendix A: Publications

The following manuscript was published during this PhD programme:

Barnard, E., Liu, J., **Yankova, E.**, Cavalcanti, S.M., Magalhães, M., Li, H., Patrick, S., and McDowell, A. (2016). Strains of the *Propionibacterium acnes* type III lineage are associated with the skin condition progressive macular hypomelanosis. *Scientific reports* 6, 31968, doi:10.1038/srep31968

Appendix B: Gene dysregulation in short-term infection models

Figures of the fold-change in expression of inflammatory and epithelial-mesenchymal transition (EMT) genes used in short-term infection models.

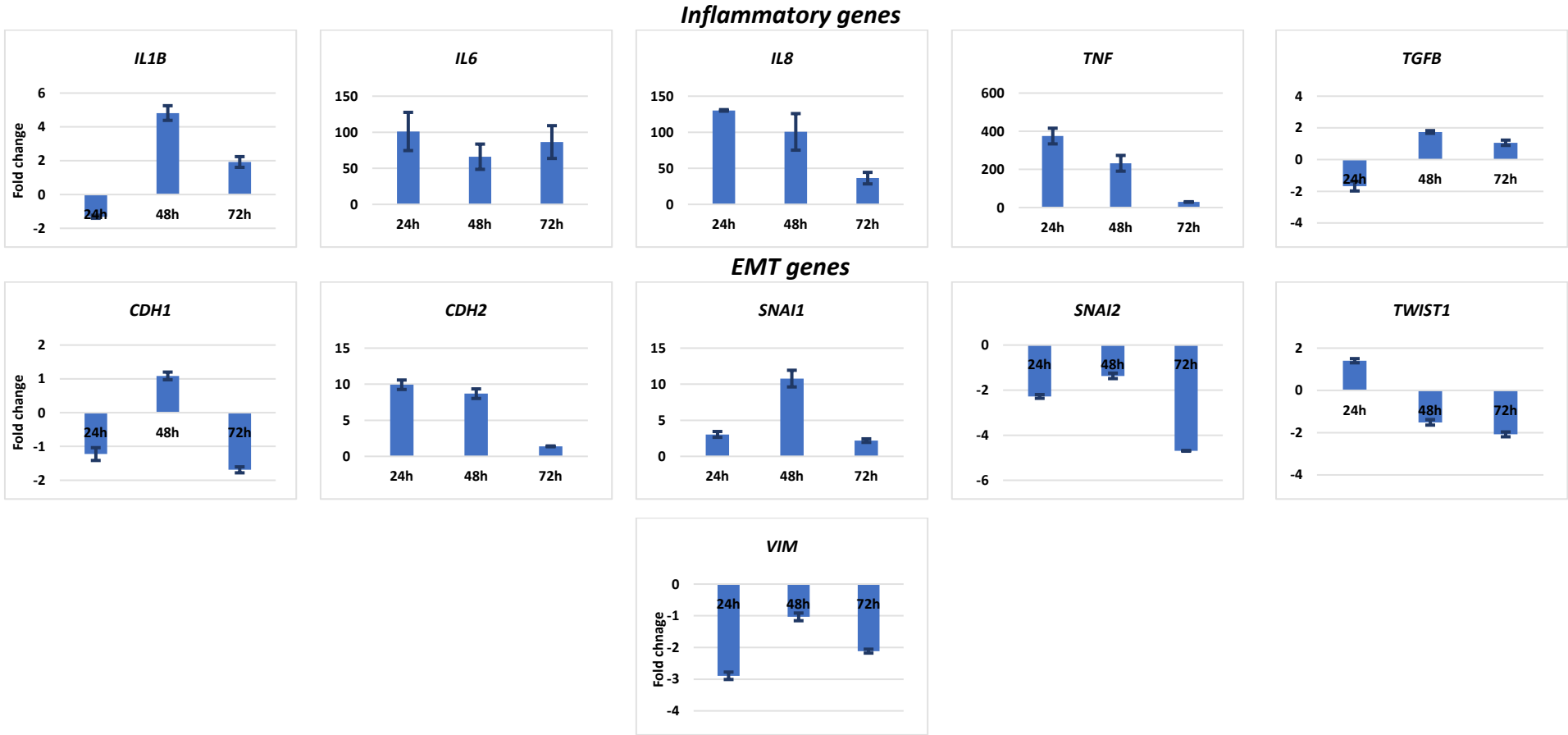

Appendix B Figure 1. Dysregulation in 00035 short-term infection model.

Ratio difference in the expression of each gene in infected RWPE-1 prostate epithelial cells, calculated by normalising to uninfected controls, with HPRT as a housekeeping gene. Data is presented as presented as mean fold change of three biological replicates, +/- standard error.

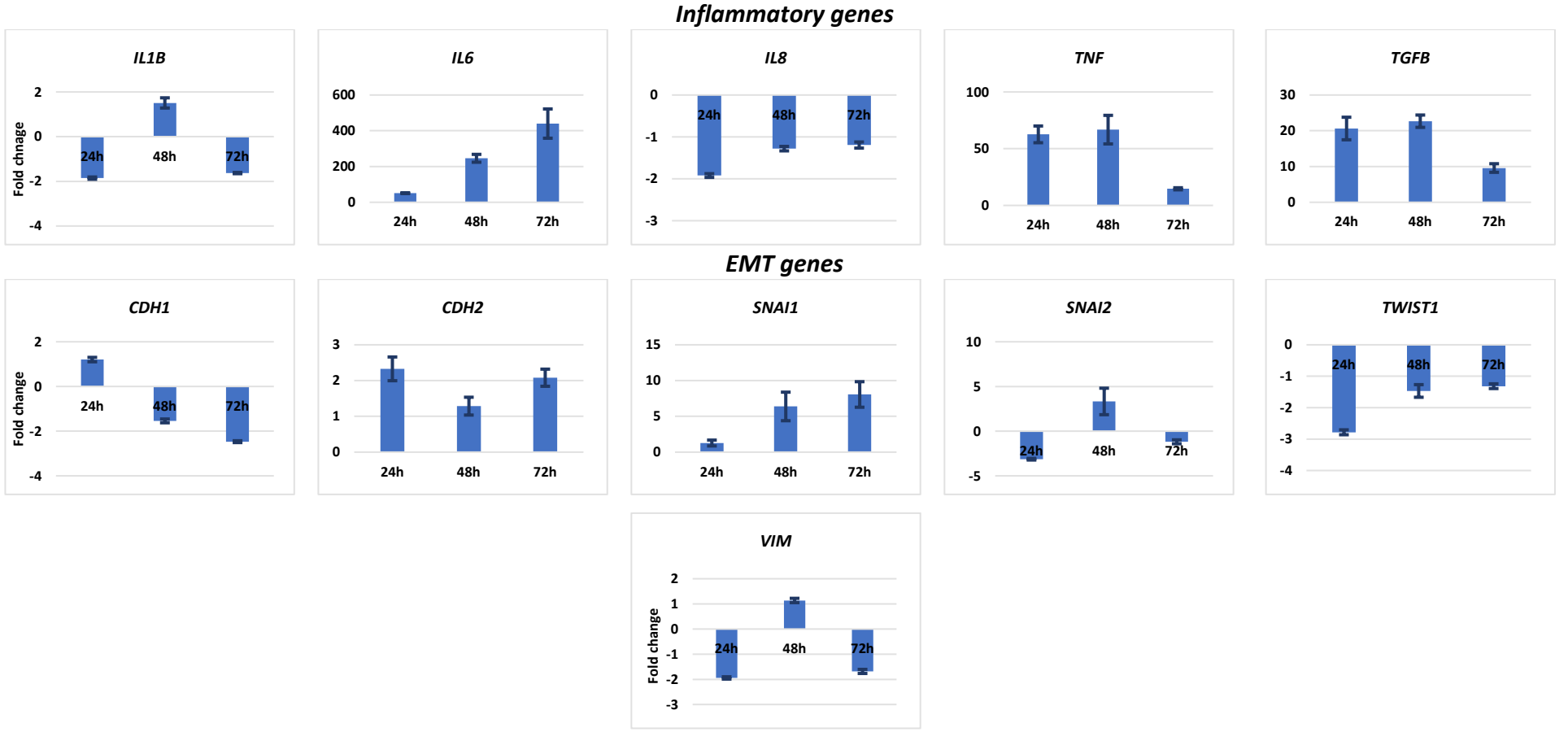

Appendix B Figure 2. Dysregulation in NCTC737 short-term infection model.

Ratio difference in the expression of each gene in infected RWPE-1 prostate epithelial cells, calculated by normalising to uninfected controls, with HPRT as a housekeeping gene. Data is presented as presented as mean fold change of three biological replicates, +/- standard error.

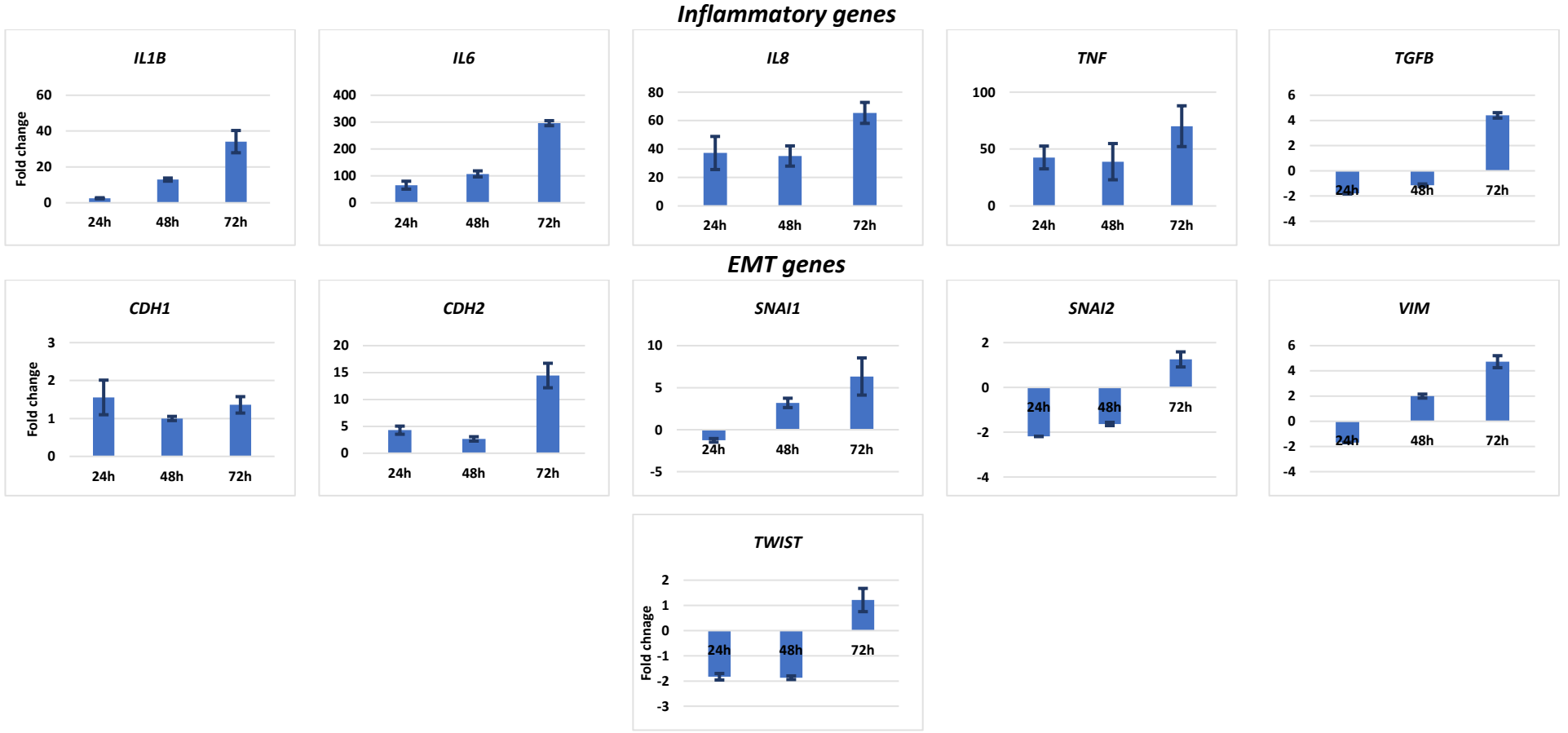

Appendix B Figure 3. Dysregulation in ST27 short-term infection model.

Ratio difference in the expression of each gene in infected RWPE-1 prostate epithelial cells, calculated by normalising to uninfected controls, with HPRT as a housekeeping gene. Data is presented as presented as mean fold change of three biological replicates, +/- standard error.

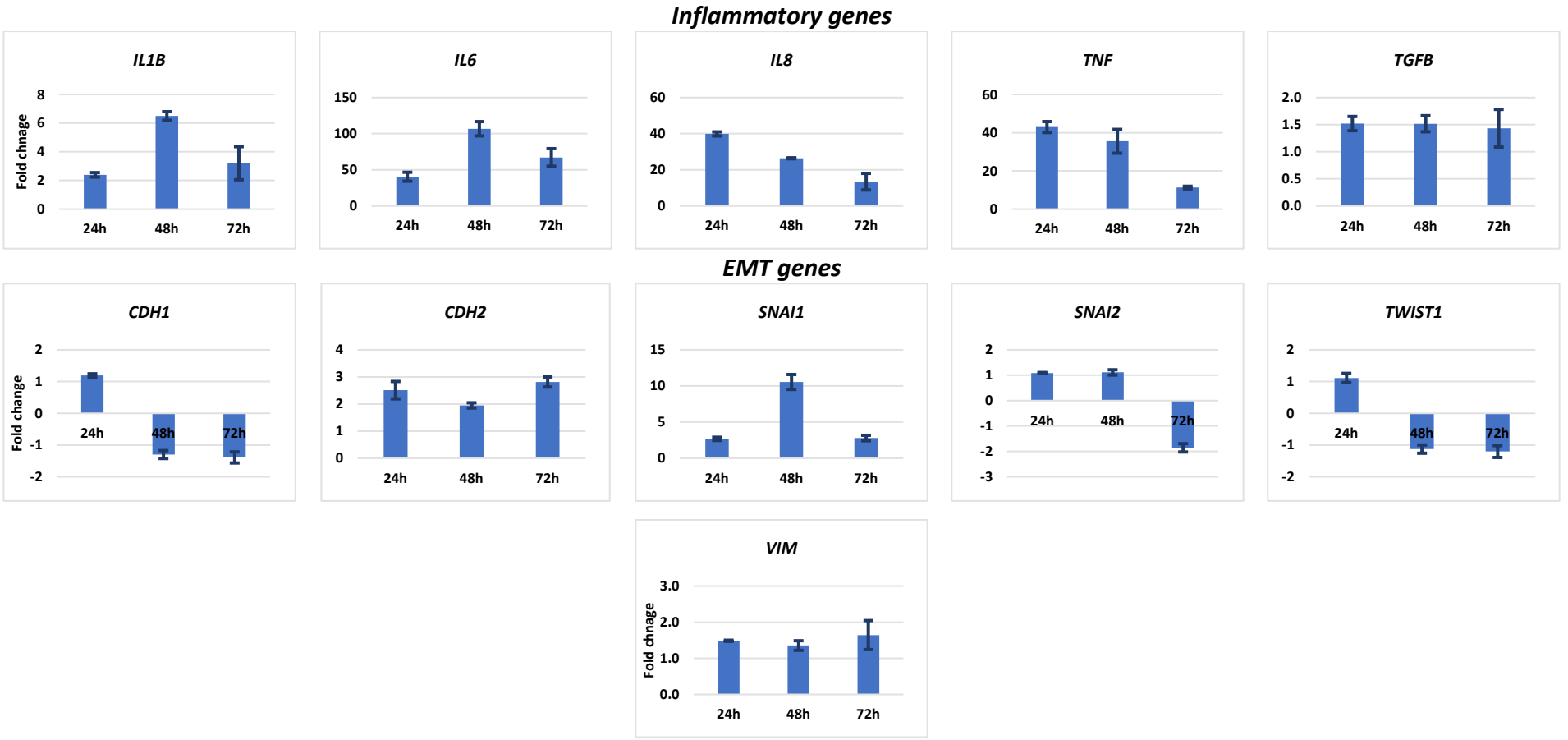

Appendix B Figure 4. Dysregulation in B3 short-term infection model.

Ratio difference in the expression of each gene in infected RWPE-1 prostate epithelial cells, calculated by normalising to uninfected controls, with HPRT as a housekeeping gene. Data is presented as presented as mean fold change of three biological replicates, +/- standard error.

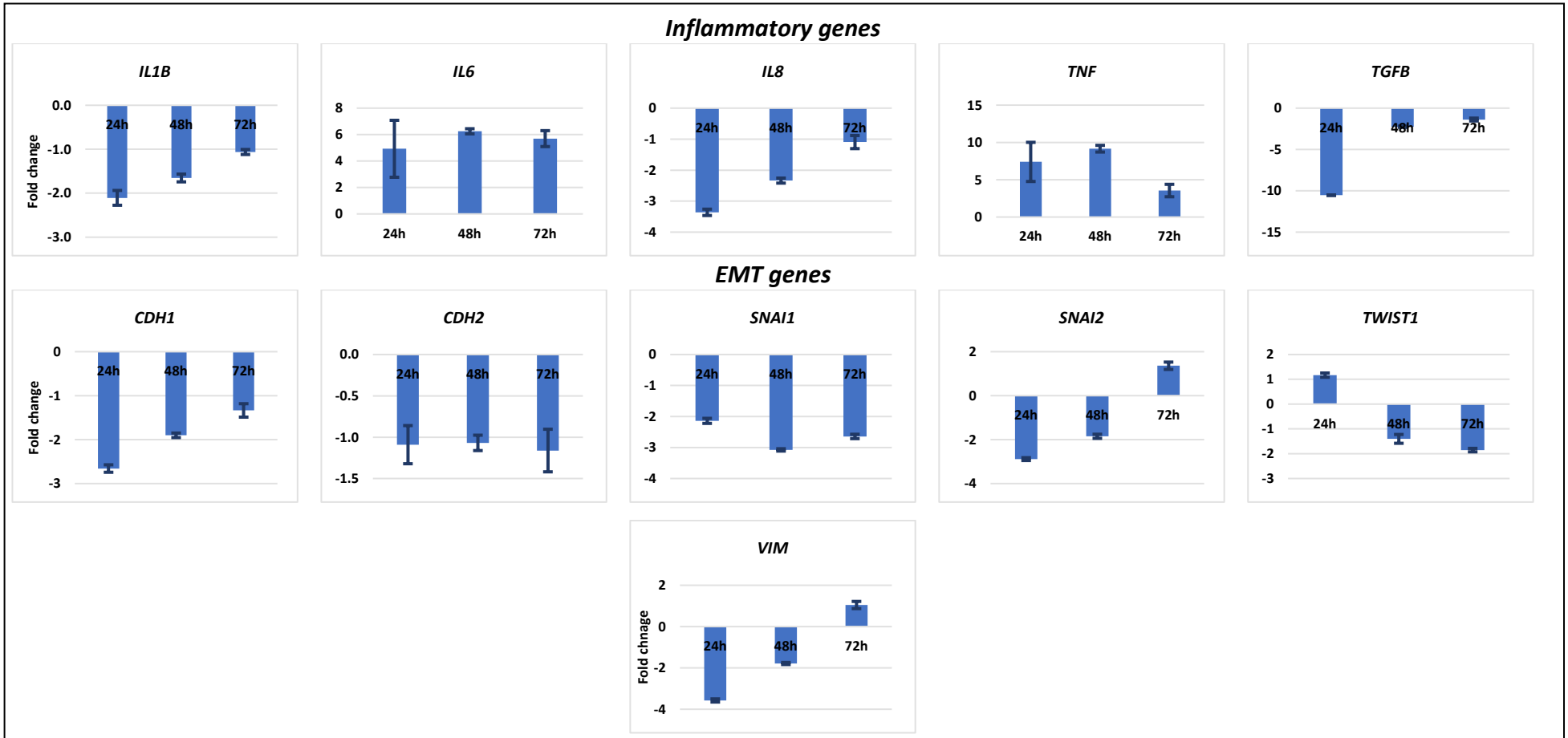

Appendix B Figure 5. Dysregulation in NCTC10390 short-term infection model.

Ratio difference in the expression of each gene in infected RWPE-1 prostate epithelial cells, calculated by normalising to uninfected controls, with HPRT as a housekeeping gene. Data is presented as presented as mean fold change of three biological replicates, +/- standard error.

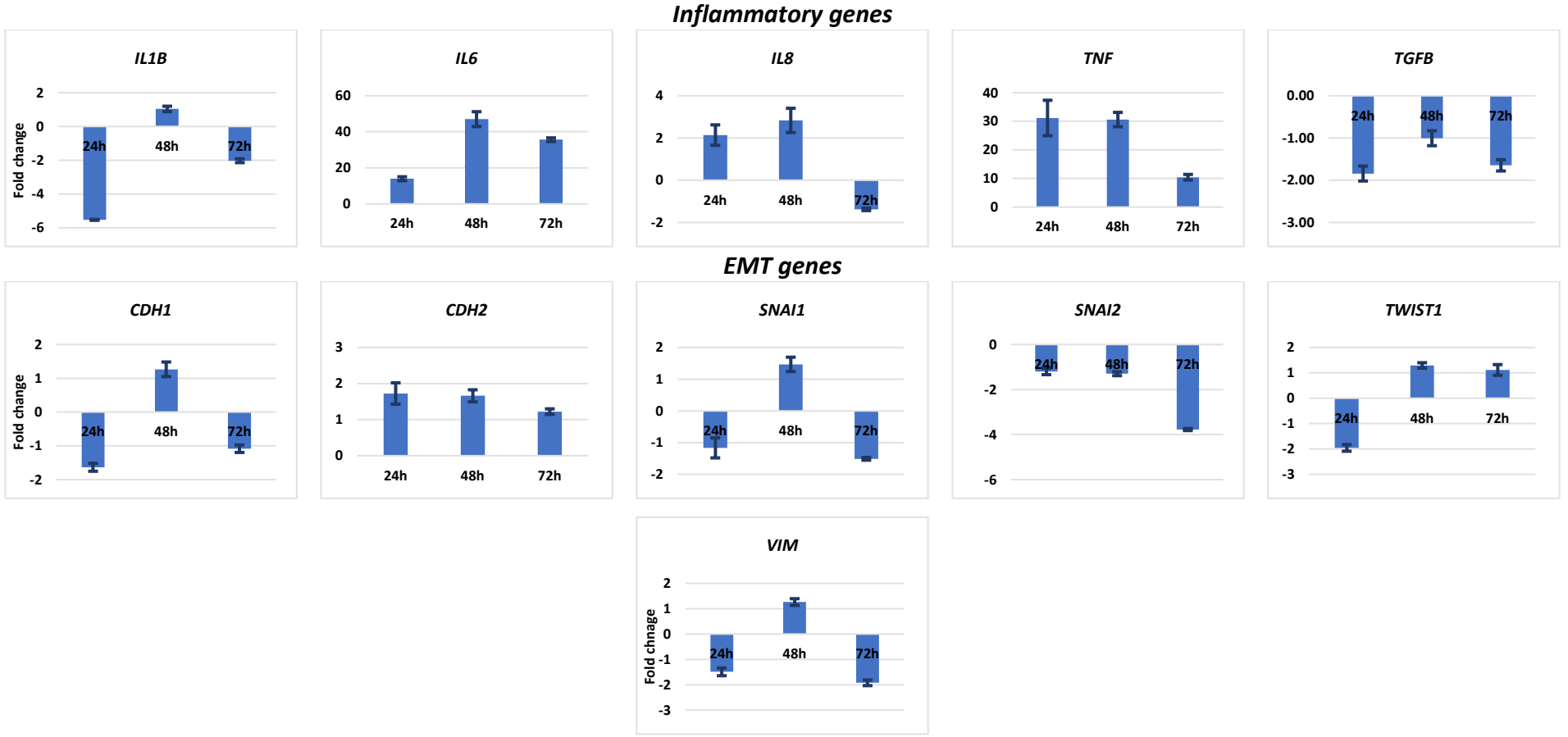

Appendix B Figure 6. Dysregulation in CFU2 short-term infection model.

Ratio difference in the expression of each gene in infected RWPE-1 prostate epithelial cells, calculated by normalising to uninfected controls, with HPRT as a housekeeping gene. Data is presented as presented as mean fold change of three biological replicates, +/- standard error.

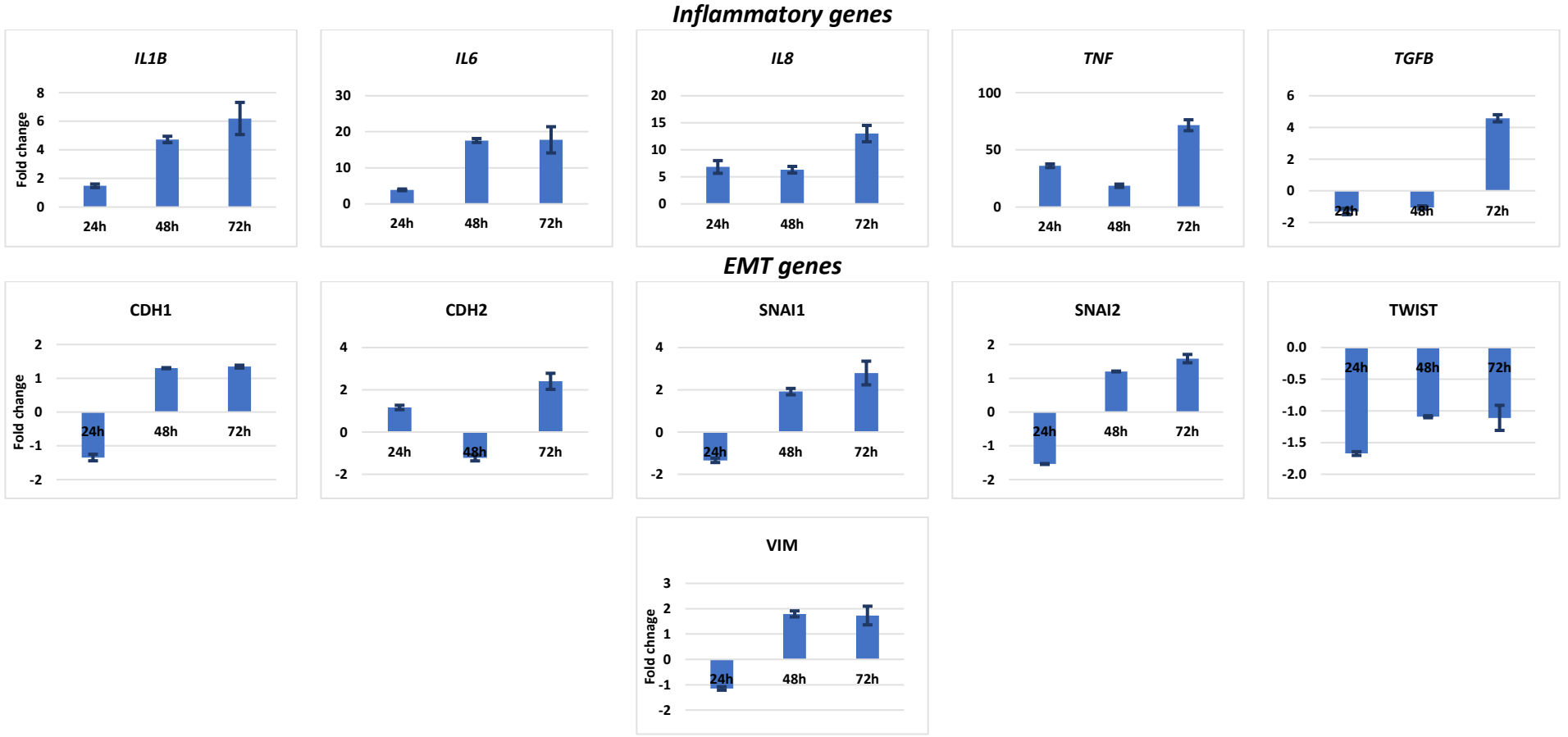

Appendix B Figure 7. Dysregulation in P. granulosum short-term infection model.

Ratio difference in the expression of each gene in infected RWPE-1 prostate epithelial cells, calculated by normalising to uninfected controls, with HPRT as a housekeeping gene. Data is presented as presented as mean fold change of three biological replicates, +/- standard error.

Appendix C: Gene dysregulation in long-term infection models

Figures of the fold-change in expression of inflammatory and epithelial-mesenchymal transition (EMT) genes used in short-term infection models.

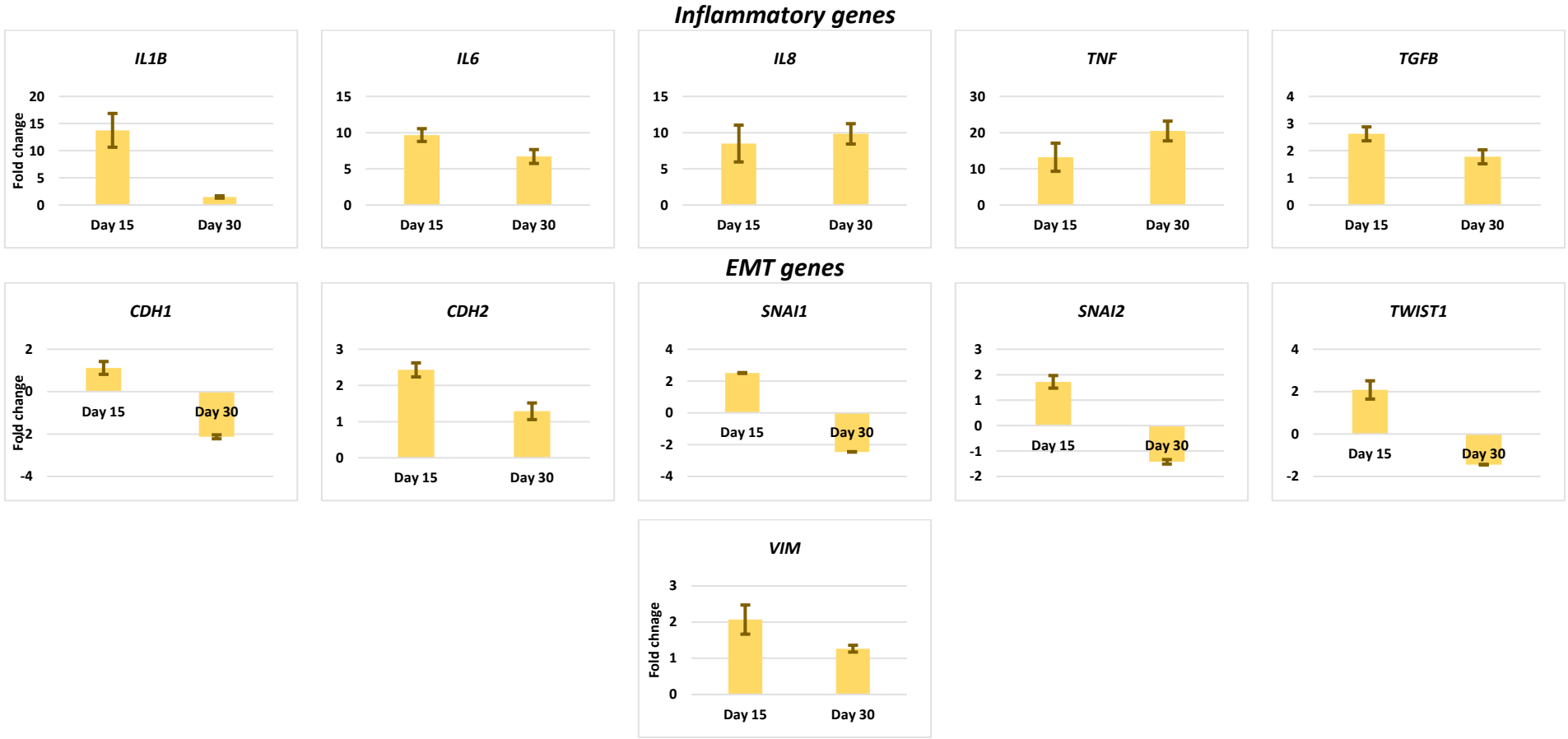

Appendix C Figure 1. Dysregulation in 00035 long-term infection model.

Ratio difference in the expression of each gene in infected RWPE-1 prostate epithelial cells, calculated by normalising to uninfected controls, with HPRT as a housekeeping gene. Data is presented as presented as mean fold change of three biological replicates, +/- standard error.

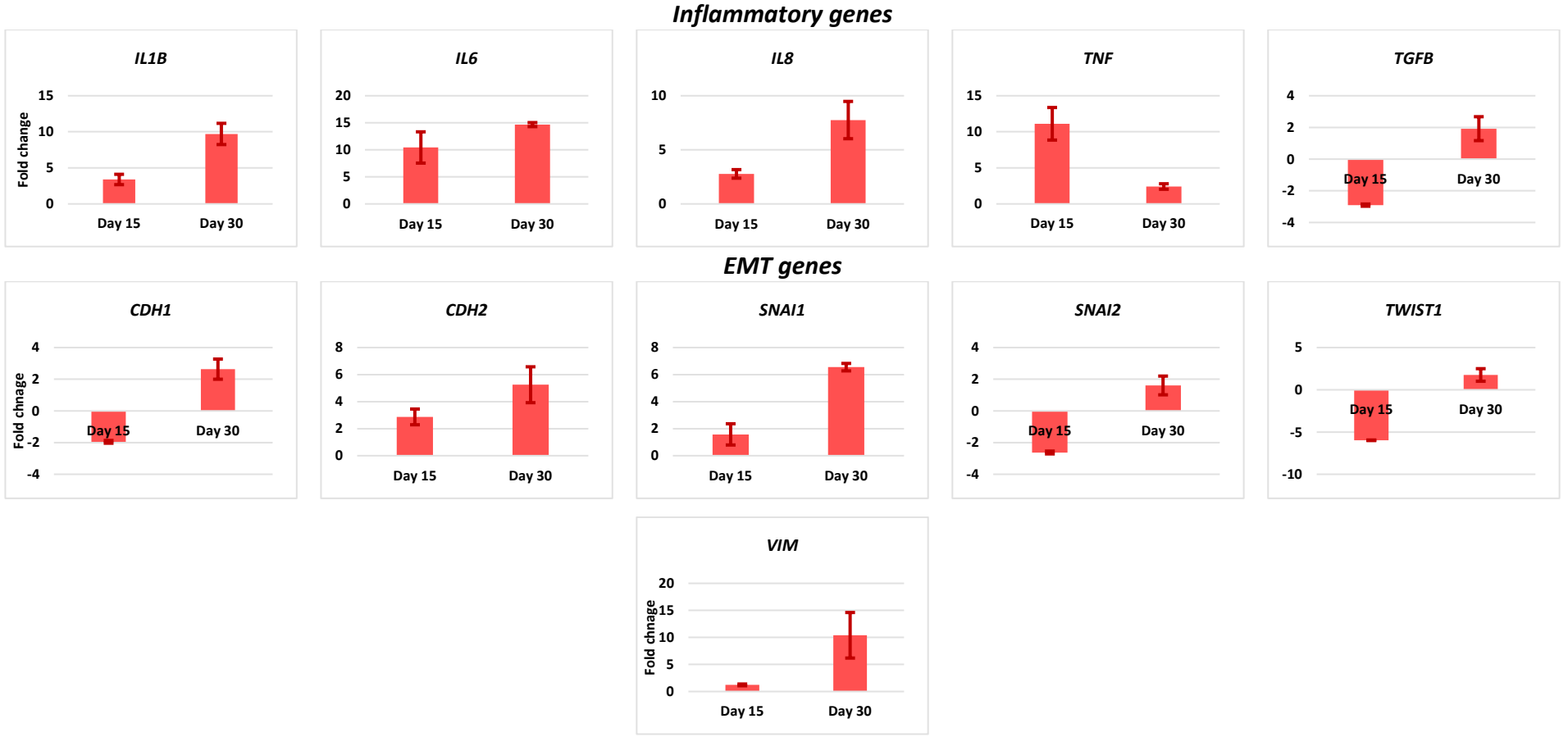

Appendix C Figure 2. Dysregulation in NCTC737 long-term infection model.

Ratio difference in the expression of each gene in infected RWPE-1 prostate epithelial cells, calculated by normalising to uninfected controls, with HPRT as a housekeeping gene. Data is presented as presented as mean fold change of three biological replicates, +/- standard error.

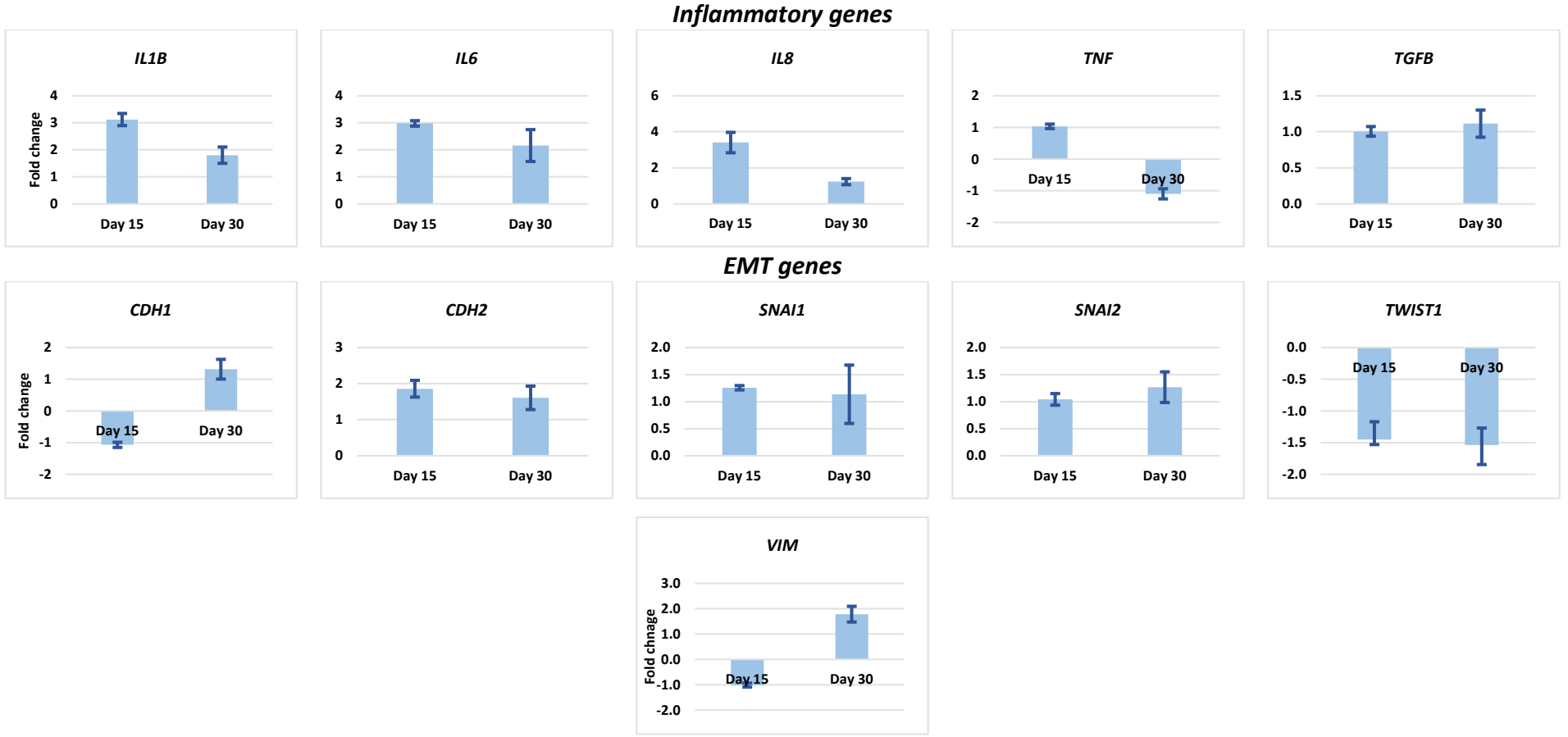

Appendix C Figure 3. Dysregulation in ST27 long-term infection model.

Ratio difference in the expression of each gene in infected RWPE-1 prostate epithelial cells, calculated by normalising to uninfected controls, with HPRT as a housekeeping gene. Data is presented as presented as mean fold change of three biological replicates, +/- standard error.

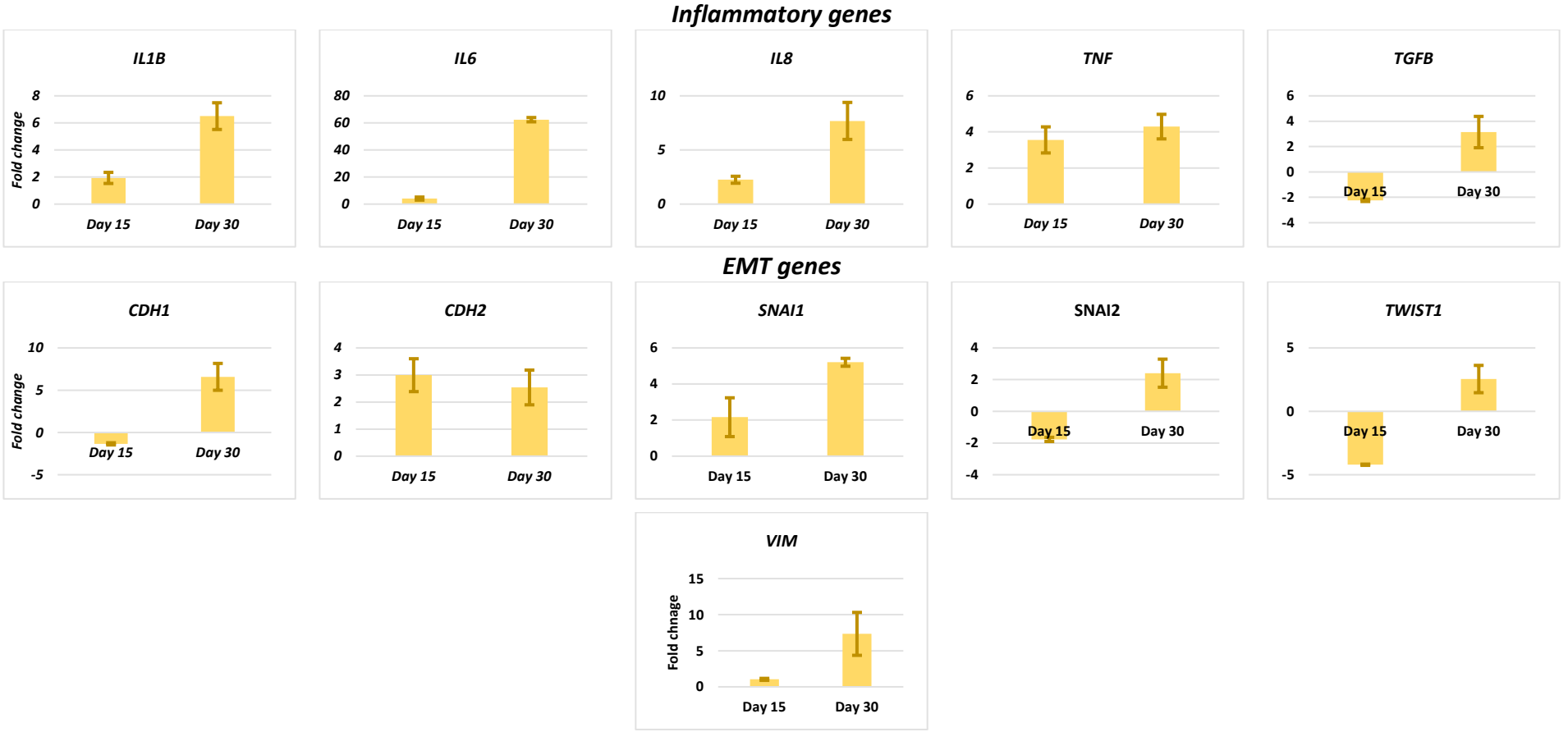

Appendix C Figure 4. Dysregulation in B3 long-term infection model.

Ratio difference in the expression of each gene in infected RWPE-1 prostate epithelial cells, calculated by normalising to uninfected controls, with HPRT as a housekeeping gene. Data is presented as presented as mean fold change of three biological replicates, +/- standard error.

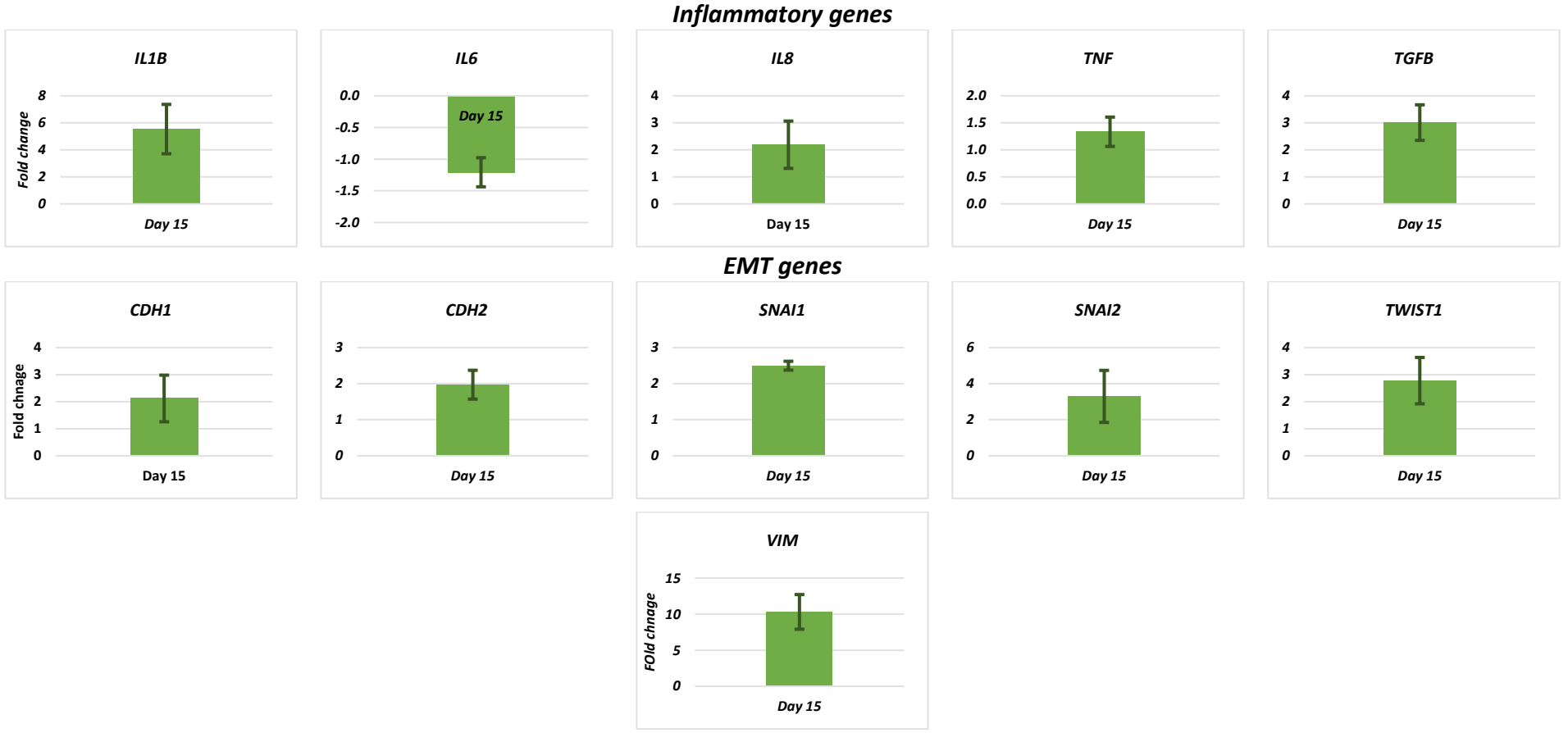

Appendix C Figure 5. Dysregulation in NCTC10390 long-term infection model.

Ratio difference in the expression of each gene in infected RWPE-1 prostate epithelial cells, calculated by normalising to uninfected controls, with HPRT as a housekeeping gene. Data is presented as presented as mean fold change of three biological replicates, +/- standard error.

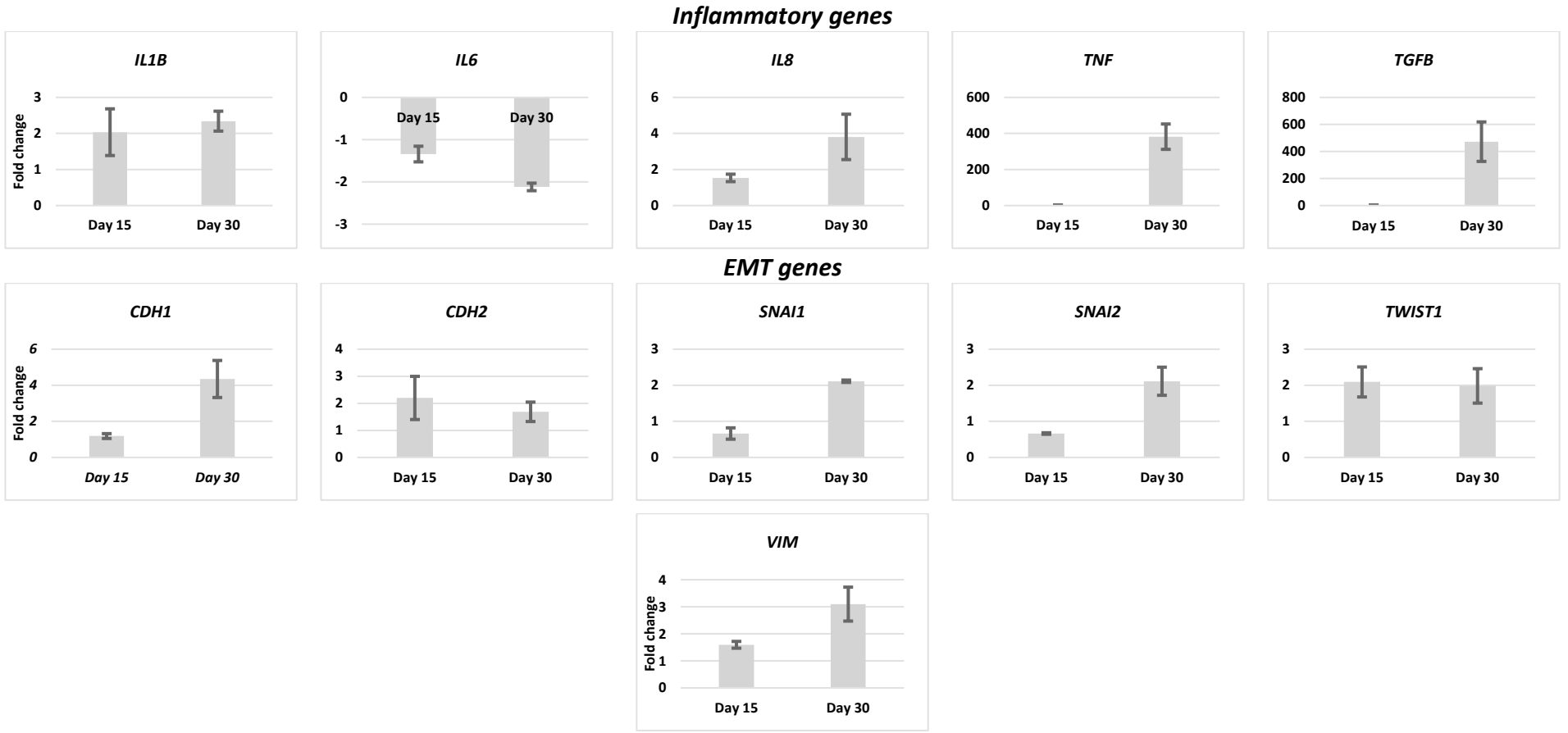

Appendix C Figure 6. Dysregulation in CFU2 long-term infection model.

Ratio difference in the expression of each gene in infected RWPE-1 prostate epithelial cells, calculated by normalising to uninfected controls, with HPRT as a housekeeping gene. Data is presented as presented as mean fold change of three biological replicates, +/- standard error.

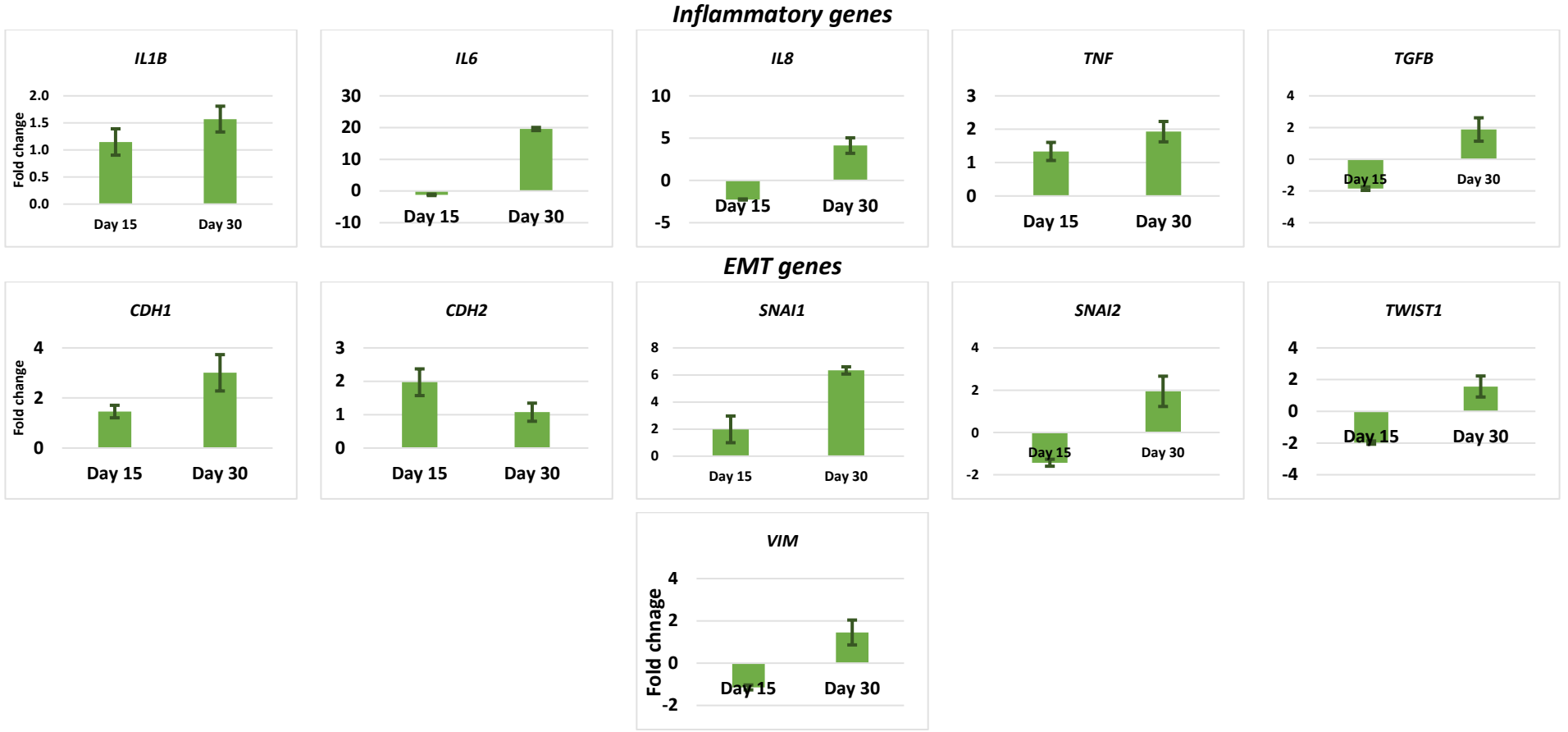

Appendix C Figure 7. Dysregulation in P. granulosum long-term infection model.
Ratio difference in the expression of each gene in infected RWPE-1 prostate epithelial cells, calculated by normalising to uninfected controls, with HPRT as a housekeeping gene. Data is presented as presented as mean fold change of three biological replicates, +/- standard error.

Appendix D: Pathways analysis for qPCR array experiments

Pathway analysis and gene ontology analysis performed using STRING (Szklarczyk et al., 2017).

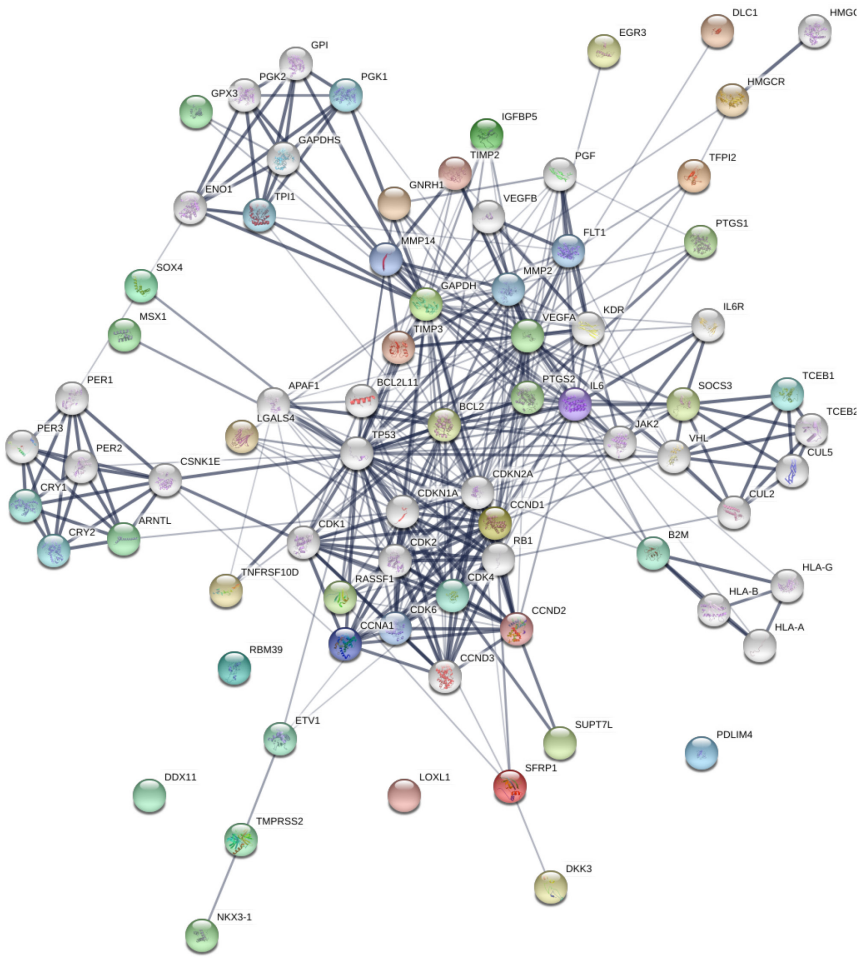

Appendix D Figure 1. STRING analysis of 00035 qPCR array results

STRING analysis performed using medium confidence (0.400) and all active interaction sources with lines representing "confidence". Total number of nodes: 66.

Biological Process (GO)			
Pathway ID	**Pathway description**	**No. genes**	**False discovery rate**
GO:0051726	regulation of cell cycle	22	1.59e-10
GO:0070887	cellular response to chemical stimulus	31	1.59e-10
GO:0048511	rhythmic process	14	8.68e-10
GO:0070482	response to oxygen levels	14	8.68e-10
GO:0009628	response to abiotic stimulus	22	1.25e-09
Molecular Function (GO)			
Pathway ID	**Pathway description**	**No. genes**	**False discovery rate**
GO:0005515	protein binding	41	1.78e-09
GO:0019899	enzyme binding	20	2.72e-06
GO:0031625	ubiquitin protein ligase binding	8	0.000383
GO:0004693	cyclin-dep. protein S/T kinase activity	4	0.00228
GO:0005488	binding	49	0.00239

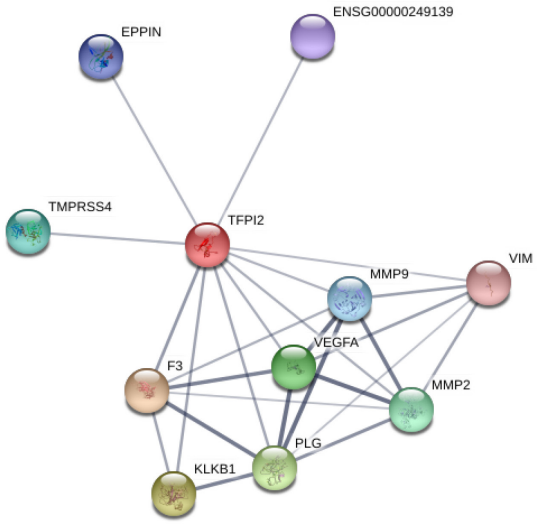

Appendix D Figure 2. STRING analysis of B3 qPCR array results

STRING analysis performed using medium confidence (0.400) and all active interaction sources with lines representing "confidence". Total number of nodes: 11.

Biological Process (GO)			
Pathway ID	**Pathway description**	**No. genes**	**False discovery rate**
GO:0030162	regulation of proteolysis	7	7.54e-05
GO:0052548	regulation of endopeptidase activity	6	7.54e-05
GO:0010951	-ve regulation of endopeptidase activity	5	0.000226
GO:0022617	extracellular matrix disassembly	4	0.000627
GO:0051919	positive regulation of fibrinolysis	2	0.00242
Molecular Function (GO)			
Pathway ID	**Pathway description**	**No. genes**	**False discovery rate**
GO:0004252	serine-type endopeptidase activity	4	0.000816
GO:0004175	endopeptidase activity	5	0.00123
GO:0004867	S-type endopeptidase inhibitor activity	3	0.00805

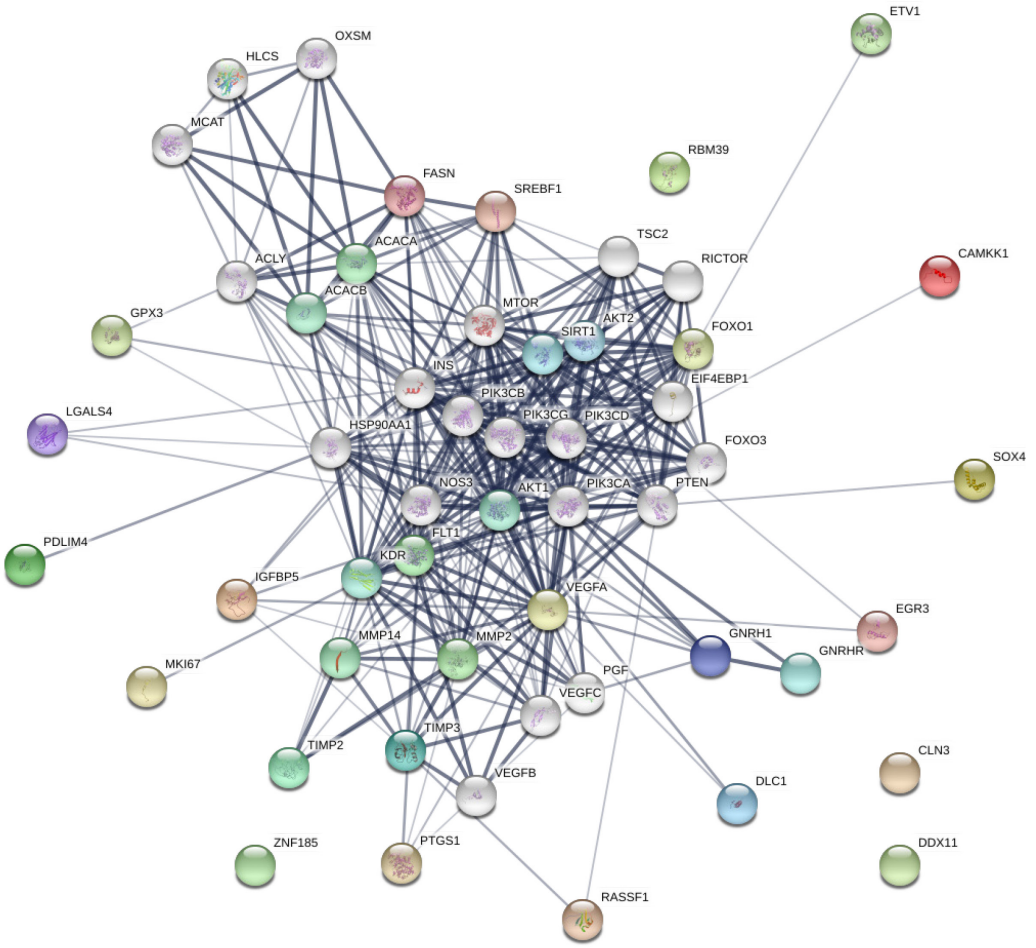

Appendix D Figure 3. STRING analysis of CFU2 qPCR array results

STRING analysis performed using medium confidence (0.400) and all active interaction sources with lines representing "confidence". Total number of nodes: 53.

Biological Process (GO)			
Pathway ID	**Pathway description**	**No. genes**	**False discovery rate**
GO:0007169	transmembrane receptor protein tyrosine kinase signalling pathway	22	1.47e-15
GO:0010033	response to organic substance cellular	33	1.47e-15
GO:0071310	response to organic substance	30	1.47e-15
GO:0048010	VEGFR signalling pathway	13	3.24e-15
GO:0009719	response to endogenous stimulus	26	2.28e-14
Molecular Function (GO)			
Pathway ID	**Pathway description**	**No. genes**	**False discovery rate**
GO:0046934	phosphatidylinositol-4,5-bisphosphate 3-kinase activity	4	8.26e-08
GO:0035005	1-phosphatidylinositol-4-phosphate 3-kinase activity	4	1.92e-06
GO:0016303	1-phosphatidylinositol-3-kinase activity	4	6.86e-06
GO:0043168	anion binding	23	1.08e-05
GO:0097367	carbohydrate derivative binding	21	1.16e-05

References

Abdulghani, J., Gu, L., Dagvadorj, A., Lutz, J., Leiby, B., Bonuccelli, G., Lisanti, M.P., Zellweger, T., Alanen, K., Mirtti, T*., et al.* (2008). Stat3 Promotes Metastatic Progression of Prostate Cancer. The American journal of pathology *172*, 1717-1728.

Abe, C., Iwai, K., Mikami, R., and Hosoda, Y. (1984). Frequent isolation of *Propionibacterium acnes* from sarcoidosis lymph nodes. Zentralblatt fur Bakteriologie, Mikrobiologie, und Hygiene Series A, Medical microbiology, infectious diseases, virology, parasitology *256*, 541-547.

Abhinand, C.S., Raju, R., Soumya, S.J., Arya, P.S., and Sudhakaran, P.R. (2016). VEGF-A/VEGFR2 signaling network in endothelial cells relevant to angiogenesis. Journal of Cell Communication and Signaling *10*, 347-354.

Achermann, Y., Goldstein, E.J.C., Coenye, T., and Shirtliff, M.E. (2014). *Propionibacterium acnes*: from Commensal to Opportunistic Biofilm-Associated Implant Pathogen. Clinical microbiology reviews *27*, 419-440.

Adler, H.L., McCurdy, M.A., Kattan, M.W., Timme, T.L., Scardino, P.T., and Thompson, T.C. (1999). Elevated levels of circulating interleukin-6 and transforming growth factor-beta 1 in patiens with metastatic prostatic carcinoma. The Journal of urology *161*, 182-187.

Aggarwal, B.B., Gupta, S.C., and Kim, J.H. (2012). Historical perspectives on tumor necrosis factor and its superfamily: 25 years later, a golden journey. Blood *119*, 651-665.

Agostini, L., Martinon, F., Burns, K., McDermott, M.F., Hawkins, P.N., and Tschopp, J. (2004). NALP3 forms an IL-1beta-processing inflammasome with increased activity in Muckle-Wells autoinflammatory disorder. Immunity *20*, 319-325.

Ahlbom, A., Lichtenstein, P., Malmstrom, H., Feychting, M., Hemminki, K., and Pedersen, N.L. (1997). Cancer in twins: Genetic and nongenetic familial risk factors. Journal of the National Cancer Institute *89*, 287-293.

Ahmed, N., Maines-Bandiera, S., Quinn, M.A., Unger, W.G., Dedhar, S., and Auersperg, N. (2006). Molecular pathways regulating EGF-induced epithelio-mesenchymal transition in human ovarian surface epithelium. American journal of physiology Cell physiology *290*, C1532-1542.

Alberici, P., and Fodde, R. (2006). The role of the APC tumor suppressor in chromosomal instability. Genome dynamics *1*, 149-170.

Albert, H.B., Manniche, C., Sorensen, J.S., and Deleuran, B.W. (2008). Antibiotic treatment in patients with low-back pain associated with Modic changes Type 1 (bone oedema): a pilot study. British journal of sports medicine *42*, 969-973.

Albert, H.B., Sorensen, J.S., Christensen, B.S., and Manniche, C. (2013). Antibiotic treatment in patients with chronic low back pain and vertebral bone edema (Modic type 1 changes):

a double-blind randomized clinical controlled trial of efficacy. European Spine Journal *22*, 697-707.

Alberti, C., Pinciroli, P., Valeri, B., Ferri, R., Ditto, A., Umezawa, K., Sensi, M., Canevari, S., and Tomassetti, A. (2012). Ligand-dependent EGFR activation induces the co-expression of IL-6 and PAI-1 via the NFκB pathway in advanced-stage epithelial ovarian cancer. Oncogene *31*, 4139-4149.

Albertsen, P.C., Moore, D.F., Shih, W., Lin, Y., Li, H., and Lu-Yao, G.L. (2011). Impact of Comorbidity on Survival Among Men With Localized Prostate Cancer. Journal of Clinical Oncology *29*, 1335-1341.

Albini, A., Tosetti, F., Li, V.W., Noonan, D.M., and Li, W.W. (2012). Cancer prevention by targeting angiogenesis. *9*, 498.

Aldave, A.J., Stein, J.D., Deramo, V.A., Shah, G.K., Fischer, D.H., and Maguire, J.I. (1999). Treatment strategies for postoperative *Propionibacterium acnes* endophthalmitis. Ophthalmology *106*, 2395-2401.

Alessi, D.R., Andjelkovic, M., Caudwell, B., Cron, P., Morrice, N., Cohen, P., and Hemmings, B.A. (1996). Mechanism of activation of protein kinase B by insulin and IGF-1. The EMBO journal *15*, 6541-6551.

Alexeyev, O., Bergh, J., Marklund, I., Thellenberg-Karlsson, C., Wiklund, F., Gronberg, H., Bergh, A., and Elgh, F. (2006). Association between the presence of bacterial 16S RNA in prostate specimens taken during transurethral resection of prostate and subsequent risk of prostate cancer (Sweden). Cancer causes & control: CCC *17*, 1127-1133.

Alexeyev, O.A., Marklund, I., Shannon, B., Golovleva, I., Olsson, J., Andersson, C., Eriksson, I., Cohen, R., and Elgh, F. (2007). Direct visualization of *Propionibacterium acnes* in prostate tissue by multicolor fluorescent in situ hybridization assay. Journal of clinical microbiology *45*, 3721-3728.

Allen, J.E., and El-Deiry, W.S. (2012). Regulation of the human TRAIL gene. Cancer biology & therapy *13*, 1143-1151.

Alonso, L., and Fuchs, E. (2003). Stem cells in the skin: waste not, Wnt not. Genes & development *17*, 1189-1200.

Aman, M.J., Lamkin, T.D., Okada, H., Kurosaki, T., and Ravichandran, K.S. (1998). The Inositol Phosphatase SHIP Inhibits Akt/PKB Activation in B Cells. Journal of Biological Chemistry *273*, 33922-33928.

Amaral, J.D., Xavier, J.M., Steer, C.J., and Rodrigues, C.M. (2010). The role of p53 in apoptosis. Discovery medicine *9*, 145-152.

Amieva, M., and Peek, R.M., Jr. (2016). Pathobiology of *Helicobacter pylori*-Induced Gastric Cancer. Gastroenterology *150*, 64-78.

Andersen, C.L., Jensen, J.L., and Orntoft, T.F. (2004). Normalization of real-time quantitative reverse transcription-PCR data: a model-based variance estimation approach to identify genes suited for normalization, applied to bladder and colon cancer data sets. Cancer research *64*, 5245-5250.

Armstrong, C.W., Maxwell, P.J., Ong, C.W., Redmond, K.M., McCann, C., Neisen, J., Ward, G.A., Chessari, G., Johnson, C., Crawford, N.T.*, et al.* (2016). PTEN deficiency promotes macrophage infiltration and hypersensitivity of prostate cancer to IAP antagonist/radiation combination therapy. Oncotarget *7*, 7885-7898.

Armulik, A., Genové, G., and Betsholtz, C. (2011). Pericytes: Developmental, Physiological, and Pathological Perspectives, Problems, and Promises. Developmental Cell *21*, 193-215.

Arnold, M., Karim-Kos, H.E., Coebergh, J.W., Byrnes, G., Antilla, A., Ferlay, J., Renehan, A.G., Forman, D., and Soerjomataram, I. (2015). Recent trends in incidence of five common cancers in 26 European countries since 1988: Analysis of the European Cancer Observatory. European journal of cancer *51*, 1164-1187.

Arnoux, V., Nassour, M., L'Helgoualc'h, A., Hipskind, R.A., and Savagner, P. (2008). Erk5 controls Slug expression and keratinocyte activation during wound healing. Molecular biology of the cell *19*, 4738-4749.

Asmarinah, A., Paradowska-Dogan, A., Kodariah, R., Tanuhardja, B., Waliszewski, P., Mochtar, C.A., Weidner, W., and Hinsch, E. (2014). Expression of the Bcl-2 family genes and complexes involved in the mitochondrial transport in prostate cancer cells. International journal of oncology *45*, 1489-1496.

Azab, S., Osama, A., and Rafaat, M. (2012). Does normalizing PSA after successful treatment of chronic prostatitis with high PSA value exclude prostatic biopsy? Translational Andrology and Urology *1*, 148-152.

Azare, J., Leslie, K., Al-Ahmadie, H., Gerald, W., Weinreb, P.H., Violette, S.M., and Bromberg, J. (2007). Constitutively Activated Stat3 Induces Tumorigenesis and Enhances Cell Motility of Prostate Epithelial Cells through Integrin β6. Molecular and cellular biology *27*, 4444-4453.

Babior, B.M. (2000). Phagocytes and oxidative stress. The American journal of medicine *109*, 33-44.

Badary, D.M., Rahma, M.Z.A.A., Ashmawy, A.M., and Hafez, M.Z. (2017). *H. pylori* infection increases gastric mucosal COX2 and mTOR expression in chronic gastritis: Implications for cancer progression? Pathophysiology *24*, 205-211.

Bae, Y., Ito, T., Iida, T., Uchida, K., Sekine, M., Nakajima, Y., Kumagai, J., Yokoyama, T., Kawachi, H., Akashi, T.*, et al.* (2014). Intracellular *Propionibacterium acnes* infection in glandular

epithelium and stromal macrophages of the prostate with or without cancer. PloS one *9*, e90324.

Baena, E., Shao, Z., Linn, D.E., Glass, K., Hamblen, M.J., Fujiwara, Y., Kim, J., Nguyen, M., Zhang, X., Godinho, F.J*., et al.* (2013). ETV1 directs androgen metabolism and confers aggressive prostate cancer in targeted mice and patients. Genes & development *27*, 683-698.

Baer, C., Squadrito, M.L., Iruela-Arispe, M.L., and De Palma, M. (2013). Reciprocal interactions between endothelial cells and macrophages in angiogenic vascular niches. Experimental cell research *319*, 1626-1634.

Baggiolini, M., Walz, A., and Kunkel, S.L. (1989). Neutrophil-activating peptide-1/interleukin 8, a novel cytokine that activates neutrophils. The Journal of clinical investigation *84*, 1045-1049.

Bahk, J.Y., Hyun, J.S., Lee, H., Kim, M.O., Cho, G.J., Lee, B.H., and Choi, W.S. (1998). Expression of gonadotropin-releasing hormone (GnRH) and GnRH receptor mRNA in prostate cancer cells and effect of GnRH on the proliferation of prostate cancer cells. Urological research *26*, 259-264.

Bai, D., Ueno, L., and Vogt, P.K. (2009). Akt-mediated regulation of NFκB and the essentialness of NFκB for the oncogenicity of PI3K and Akt. International journal of cancer Journal international du cancer *125*, 2863-2870.

Balkwill, F. (2003). Chemokine biology in cancer. Seminars in immunology *15*, 49-55.

Baluk, P., Hashizume, H., and McDonald, D.M. (2005). Cellular abnormalities of blood vessels as targets in cancer. Curr Opin Genet Dev *15*, 102-111.

Barnard, E., Liu, J., Yankova, E., Cavalcanti, S.M., Magalhães, M., Li, H., Patrick, S., and McDowell, A. (2016). Strains of the *Propionibacterium acnes* type III lineage are associated with the skin condition progressive macular hypomelanosis. Scientific reports *6*, 31968.

Barnard, E., Nagy, I., Hunyadkurti, J., Patrick, S., and McDowell, A. (2015). Multiplex Touchdown PCR for Rapid Typing of the Opportunistic Pathogen *Propionibacterium acnes*. Journal of clinical microbiology *53*, 1149-1155.

Barry, M.J., Fowler, F.J., Jr., O'Leary, M.P., Bruskewitz, R.C., Holtgrewe, H.L., Mebust, W.K., and Cockett, A.T. (1992). The American Urological Association symptom index for benign prostatic hyperplasia. The Measurement Committee of the American Urological Association. The Journal of urology *148*, 1549-1557; discussion 1564.

Barton, G.M., and Medzhitov, R. (2003). Toll-like receptor signaling pathways. Science *300*, 1524-1525.

Bartsch, G., Frick, J., Rüegg, I., Bucher, M., Holliger, O., Oberholzer, M., and Rohr, H.P. (1979). Electron Microscopic Stereological Analysis of the Normal Human Prostate and of Benign Prostatic Hyperplasia. The Journal of urology *122*, 481-486.

Batlle, E., Sancho, E., Franci, C., Dominguez, D., Monfar, M., Baulida, J., and Garcia De Herreros, A. (2000). The transcription factor Snail is a repressor of E-cadherin gene expression in epithelial tumour cells. Nature cell biology *2*, 84-89.

Beagle, B., and Fruman, David A. (2011). A Lipid Kinase Cousin Cooperates to Promote Cancer. Cancer cell *19*, 693-695.

Beckers, A., Organe, S., Timmermans, L., Scheys, K., Peeters, A., Brusselmans, K., Verhoeven, G., and Swinnen, J.V. (2007). Chemical inhibition of acetyl-CoA carboxylase induces growth arrest and cytotoxicity selectively in cancer cells. Cancer research *67*, 8180-8187.

Beers, M.F., and Morrisey, E.E. (2011). The three R's of lung health and disease: repair, remodeling, and regeneration. The Journal of clinical investigation *121*, 2065-2073.

Beier, R., Burgin, A., Kiermaier, A., Fero, M., Karsunky, H., Saffrich, R., Moroy, T., Ansorge, W., Roberts, J., and Eilers, M. (2000). Induction of cyclin E-cdk2 kinase activity, E2F-dependent transcription and cell growth by Myc are genetically separable events. The EMBO journal *19*, 5813-5823.

Bellacosa, A., de Feo, D., Godwin, A.K., Bell, D.W., Cheng, J.Q., Altomare, D.A., Wan, M., Dubeau, L., Scambia, G., Masciullo, V.*, et al.* (1995). Molecular alterations of the AKT2 oncogene in ovarian and breast carcinomas. International journal of cancer Journal international du cancer *64*, 280-285.

Ben-Neriah, Y., and Karin, M. (2011). Inflammation meets cancer, with NF-κB as the matchmaker. Nat Immunol *12*, 715-723.

Bender, A.T., Ostenson, C.L., Giordano, D., and Beavo, J.A. (2004). Differentiation of human monocytes *in vitro* with granulocyte-macrophage colony-stimulating factor and macrophage colony-stimulating factor produces distinct changes in cGMP phosphodiesterase expression. Cellular signalling *16*, 365-374.

Bergers, G., and Benjamin, L.E. (2003). Tumorigenesis and the angiogenic switch. Nature reviews Cancer *3*, 401-410.

Berx, G., Becker, K.F., Hofler, H., and van Roy, F. (1998). Mutations of the human E-cadherin (CDH1) gene. Human mutation *12*, 226-237.

Bird, A.P. (1986). CpG-rich islands and the function of DNA methylation. Nature *321*, 209-213.

Blobe, G.C., Schiemann, W.P., and Lodish, H.F. (2000). Role of Transforming Growth Factor β in Human Disease. New England Journal of Medicine *342*, 1350-1358.

Blumenfeld, W., Tucci, S., and Narayan, P. (1992). Incidental lymphocytic prostatitis. Selective involvement with nonmalignant glands. The American journal of surgical pathology *16*, 975-981.

Bogoyevitch, M.A., Ngoei, K.R.W., Zhao, T.T., Yeap, Y.Y.C., and Ng, D.C.H. (2010). c-Jun N-terminal kinase (JNK) signaling: Recent advances and challenges. Biochimica et Biophysica Acta (BBA) - Proteins and Proteomics *1804*, 463-475.

Bolla, M., Gonzalez, D., Warde, P., Dubois, J.B., Mirimanoff, R.O., Storme, G., Bernier, J., Kuten, A., Sternberg, C., Gil, T.*, et al.* (1997). Improved survival in patients with locally advanced prostate cancer treated with radiotherapy and goserelin. The New England journal of medicine *337*, 295-300.

Bollrath, J., Phesse, T.J., von Burstin, V.A., Putoczki, T., Bennecke, M., Bateman, T., Nebelsiek, T., Lundgren-May, T., Canli, Ö., Schwitalla, S.*, et al.* (2009). gp130-Mediated Stat3 Activation in Enterocytes Regulates Cell Survival and Cell-Cycle Progression during Colitis-Associated Tumorigenesis. Cancer cell *15*, 91-102.

Bonetto, A., Aydogdu, T., Kunzevitzky, N., Guttridge, D.C., Khuri, S., Koniaris, L.G., and Zimmers, T.A. (2011). STAT3 activation in skeletal muscle links muscle wasting and the acute phase response in cancer cachexia. PloS one *6*, e22538.

Borowicz, S., Van Scoyk, M., Avasarala, S., Karuppusamy Rathinam, M.K., Tauler, J., Bikkavilli, R.K., and Winn, R.A. (2014). The Soft Agar Colony Formation Assay. Journal of Visualized Experiments: JoVE.

Boström, K. (1971). Chronic Inflammation of Human Male Accessory Sex Glands and its Effect on the Morphology of the Spermatozoa. Scandinavian journal of urology and nephrology *5*, 133-140.

Bourboulia, D., Han, H.Y., Jensen-Taubman, S., Gavil, N., Isaac, B., Wei, B., Neckers, L., and Stetler-Stevenson, W.G. (2013). TIMP-2 modulates cancer cell transcriptional profile and enhances E-cadherin/beta-catenin complex expression in A549 lung cancer cells. Oncotarget *4*, 163-173.

Bratland, A., Ragnhildstveit, E., Bjornland, K., Andersen, K., Maelandsmo, G.M., Fodstad, O., Saatcioglu, F., and Ree, A.H. (2003). The metalloproteinase inhibitor TIMP-2 is down-regulated by androgens in LNCaP prostate carcinoma cells. Clinical & experimental metastasis *20*, 541-547.

Braumuller, H., Wieder, T., Brenner, E., Aszmann, S., Hahn, M., Alkhaled, M., Schilbach, K., Essmann, F., Kneilling, M., Griessinger, C.*, et al.* (2013). T-helper-1-cell cytokines drive cancer into senescence. Nature *494*, 361-365.

Brenner, D., Blaser, H., and Mak, T.W. (2015). Regulation of tumour necrosis factor signalling: live or let die. Nature reviews Immunology *15*, 362-374.

Brewington, J.J., McPhail, G.L., and Clancy, J.P. (2016). Lumacaftor alone and combined with ivacaftor: preclinical and clinical trial experience of F508del CFTR correction. Expert review of respiratory medicine *10*, 5-17.

Brodlie, M., Haq, I.J., Roberts, K., and Elborn, J.S. (2015). Targeted therapies to improve CFTR function in cystic fibrosis. Genome medicine *7*, 101.

Bromberg, J.F., Wrzeszczynska, M.H., Devgan, G., Zhao, Y., Pestell, R.G., Albanese, C., and Darnell, J.E., Jr. (1999). Stat3 as an oncogene. Cell *98*, 295-303.

Bruggemann, H., Henne, A., Hoster, F., Liesegang, H., Wiezer, A., Strittmatter, A., Hujer, S., Durre, P., and Gottschalk, G. (2004). The complete genome sequence of *Propionibacterium acnes*, a commensal of human skin. Science *305*, 671-673.

Bruick, R.K., and McKnight, S.L. (2001). A Conserved Family of Prolyl-4-Hydroxylases That Modify HIF. Science *294*, 1337-1340.

Brunet, A., Bonni, A., Zigmond, M.J., Lin, M.Z., Juo, P., Hu, L.S., Anderson, M.J., Arden, K.C., Blenis, J., and Greenberg, M.E. (1999). Akt Promotes Cell Survival by Phosphorylating and Inhibiting a Forkhead Transcription Factor. Cell *96*, 857-868.

Bryant, R.J., Sjoberg, D.D., Vickers, A.J., Robinson, M.C., Kumar, R., Marsden, L., Davis, M., Scardino, P.T., Donovan, J., Neal, D.E.*, et al.* (2015). Predicting high-grade cancer at ten-core prostate biopsy using four kallikrein markers measured in blood in the ProtecT study. Journal of the National Cancer Institute *107*.

Bubendorf, L., Schopfer, A., Wagner, U., Sauter, G., Moch, H., Willi, N., Gasser, T.C., and Mihatsch, M.J. (2000). Metastatic patterns of prostate cancer: an autopsy study of 1,589 patients. Human pathology *31*, 578-583.

Bundrick, W., Heron, S.P., Ray, P., Schiff, W.M., Tennenberg, A.M., Wiesinger, B.A., Wright, P.A., Wu, S.C., Zadeikis, N., and Kahn, J.B. (2003). Levofloxacin versus ciprofloxacin in the treatment of chronic bacterial prostatitis: a randomized double-blind multicenter study. Urology *62*, 537-541.

Burstein, H.J. (2005). The distinctive nature of HER2-positive breast cancers. The New England journal of medicine *353*, 1652-1654.

Bushman, W. (2009). Etiology, epidemiology, and natural history of benign prostatic hyperplasia. Urol Clin North Am *36*, 403-415, v.

Cairns, P., Okami, K., Halachmi, S., Halachmi, N., Esteller, M., Herman, J.G., Jen, J., Isaacs, W.B., Bova, G.S., and Sidransky, D. (1997). Frequent inactivation of PTEN/MMAC1 in primary prostate cancer. Cancer research *57*, 4997-5000.

Caldeira, J.R.F., Prando É, C., Quevedo, F.C., Neto, F.A.M., Rainho, C.A., and Rogatto, S.R. (2006). CDH1 promoter hypermethylation and E-cadherin protein expression in infiltrating breast cancer. BMC cancer *6*, 48.

Callaghan, B., Lydon, H., Roelants, S.L.K.W., Van Bogaert, I.N.A., Marchant, R., Banat, I.M., and Mitchell, C.A. (2016). Lactonic Sophorolipids Increase Tumor Burden in Apcmin+/- Mice. PloS one *11*, e0156845.

Cano, A., Perez-Moreno, M.A., Rodrigo, I., Locascio, A., Blanco, M.J., del Barrio, M.G., Portillo, F., and Nieto, M.A. (2000). The transcription factor Snail controls epithelial-mesenchymal transitions by repressing E-cadherin expression. Nature cell biology *2*, 76-83.

Carl, V.S., Gautam, J.K., Comeau, L.D., and Smith, M.F., Jr. (2004). Role of endogenous IL-10 in LPS-induced STAT3 activation and IL-1 receptor antagonist gene expression. Journal of leukocyte biology *76*, 735-742.

Carpten, J., Nupponen, N., Isaacs, S., Sood, R., Robbins, C., Xu, J., Faruque, M., Moses, T., Ewing, C., Gillanders, E.*, et al.* (2002). Germline mutations in the ribonuclease L gene in families showing linkage with HPC1. Nature genetics *30*, 181-184.

Carswell, E.A., Old, L.J., Kassel, R.L., Green, S., Fiore, N., and Williamson, B. (1975). An endotoxin-induced serum factor that causes necrosis of tumors. Proceedings of the National Academy of Sciences of the United States of America *72*, 3666-3670.

Castro, E., Goh, C., Olmos, D., Saunders, E., Leongamornlert, D., Tymrakiewicz, M., Mahmud, N., Dadaev, T., Govindasami, K., Guy, M.*, et al.* (2013). Germline BRCA mutations are associated with higher risk of nodal involvement, distant metastasis, and poor survival outcomes in prostate cancer. Journal of clinical oncology: official journal of the American Society of Clinical Oncology *31*, 1748-1757.

Catlett-Falcone, R., Landowski, T.H., Oshiro, M.M., Turkson, J., Levitzki, A., Savino, R., Ciliberto, G., Moscinski, L., Fernandez-Luna, J.L., Nunez, G.*, et al.* (1999). Constitutive activation of Stat3 signaling confers resistance to apoptosis in human U266 myeloma cells. Immunity *10*, 105-115.

Catz, S.D., and Johnson, J.L. (2003). BCL-2 in prostate cancer: A minireview. Apoptosis *8*, 29-37.

Cavarretta, I., Ferrarese, R., Cazzaniga, W., Saita, D., Lucianò, R., Ceresola, E.R., Locatelli, I., Visconti, L., Lavorgna, G., Briganti, A.*, et al.* (2017). The Microbiome of the Prostate Tumor Microenvironment. European urology.

Centenera, M.M., Harris, J.M., Tilley, W.D., and Butler, L.M. (2008). Minireview: The Contribution of Different Androgen Receptor Domains to Receptor Dimerization and Signaling. Molecular endocrinology *22*, 2373-2382.

Chakravarti, A., DeSilvio, M., Zhang, M., Grignon, D., Rosenthal, S., Asbell, S.O., Hanks, G., Sandler, H.M., Khor, L.Y., Pollack, A.*, et al.* (2007). Prognostic Value of p16 in Locally Advanced Prostate Cancer: A Study Based on Radiation Therapy Oncology Group Protocol 9202. Journal of clinical oncology: official journal of the American Society of Clinical Oncology *25*, 3082-3089.

Chan, A.O., Lam, S., Wong, B.C., Wong, W., Yuen, M., Yeung, Y., Hui, W., Rashid, A., and Kwong, Y. (2003). Promoter methylation of E-cadherin gene in gastric mucosa associated with *Helicobacter pylori* infection and in gastric cancer. Gut *52*, 502-506.

Chan, J.M., and Giovannucci, E.L. (2001). DietVegetables, Fruits, Associated Micronutrients, and Risk of Prostate Cancer. Epidemiologic reviews *23*, 82-86.

Chappell, W.H., Lehmann, B.D., Terrian, D.M., Abrams, S.L., Steelman, L.S., and McCubrey, J.A. (2012). p53 expression controls prostate cancer sensitivity to chemotherapy and the MDM2 inhibitor Nutlin-3. Cell cycle *11*, 4579-4588.

Chen, R.J., Ho, Y.S., Guo, H.R., and Wang, Y.J. (2008a). Rapid activation of Stat3 and ERK1/2 by nicotine modulates cell proliferation in human bladder cancer cells. Toxicological sciences: an official journal of the Society of Toxicology *104*, 283-293.

Chen, R.W., Saunders, P.A., Wei, H., Li, Z., Seth, P., and Chuang, D.M. (1999). Involvement of glyceraldehyde-3-phosphate dehydrogenase (GAPDH) and p53 in neuronal apoptosis: evidence that GAPDH is upregulated by p53. The Journal of neuroscience: the official journal of the Society for Neuroscience *19*, 9654-9662.

Chen, R.Z., Pettersson, U., Beard, C., Jackson-Grusby, L., and Jaenisch, R. (1998). DNA hypomethylation leads to elevated mutation rates. Nature *395*, 89-93.

Chen, S.-H., Murphy, D., Lassoued, W., Thurston, G., Feldman, M.D., and Lee, W.M.F. (2008b). Activated STAT3 is a mediator and biomarker of VEGF endothelial activation. Cancer biology & therapy *7*, 1994-2003.

Chen, T., Wang, L.H., and Farrar, W.L. (2000). Interleukin 6 activates androgen receptor-mediated gene expression through a signal transducer and activator of transcription 3-dependent pathway in LNCaP prostate cancer cells. Cancer research *60*, 2132-2135.

Chen, Y., and Wei, J. (2015). Identification of Pathogen Signatures in Prostate Cancer Using RNA-seq. PloS one *10*.

Chen, Y., Zhang, Q., Wang, Q., Li, J., Sipeky, C., Xia, J., Gao, P., Hu, Y., Zhang, H., Yang, X*., et al.* (2017). Genetic association analysis of the RTK/ERK pathway with aggressive prostate cancer highlights the potential role of CCND2 in disease progression. Scientific reports *7*.

Cheng, L., Montironi, R., Bostwick, D.G., Lopez-Beltran, A., and Berney, D.M. (2012). Staging of prostate cancer. Histopathology *60*, 87-117.

Christie, K., Atkins, N.E., and Munch-Petersen, E. (1944). A Note on a Lytic Phenomenon Shown by Group B Streptococci. Aust J Exp Biol Med Sci *22*.

Chua, C.W., Shibata, M., Lei, M., Toivanen, R., Barlow, L.J., Bergren, S.K., Badani, K.K., McKiernan, J.M., Benson, M.C., Hibshoosh, H*., et al.* (2014). Single luminal epithelial progenitors can generate prostate organoids in culture. Nature cell biology *16*, 951-961, 951-954.

Chui, S.Y., Clay, T.M., Lyerly, H.K., and Morse, M.A. (2005). The Development of Therapeutic and Preventive Vaccines for Gastric Cancer and *Helicobacter pylori*. Cancer Epidemiology Biomarkers & Prevention *14*, 1883-1889.

Clayton, J.J., Baig, W., Reynolds, G.W., and Sandoe, J.A. (2006). Endocarditis caused by Propionibacterium species: a report of three cases and a review of clinical features and diagnostic difficulties. Journal of medical microbiology *55*, 981-987.

Coenye, T., Peeters, E., and Nelis, H.J. (2007a). Biofilm formation by *Propionibacterium acnes* is associated with increased resistance to antimicrobial agents and increased production of putative virulence factors. Research in microbiology *158*, 386-392.

Coenye, T., Peeters, E., and Nelis, H.J. (2007b). Biofilm formation by *Propionibacterium acnes* is associated with increased resistance to antimicrobial agents and increased production of putative virulence factors. Research in microbiology *158*, 386-392.

Cohen, R.J., Shannon, B.A., McNeal, J.E., Shannon, T., and Garrett, K.L. (2005). *Propionibacterium acnes* associated with inflammation in radical prostatectomy specimens: a possible link to cancer evolution? The Journal of urology *173*, 1969-1974.

Cohen, T., Nahari, D., Cerem, L.W., Neufeld, G., and Levi, B.Z. (1996). Interleukin 6 induces the expression of vascular endothelial growth factor. The Journal of biological chemistry *271*, 736-741.

Colombo, M. (2000). Hepatocellular carcinoma in patients with HCV. Best Practice & Research Clinical Gastroenterology *14*, 327-339.

Conacci-Sorrell, M., Simcha, I., Ben-Yedidia, T., Blechman, J., Savagner, P., and Ben-Ze'ev, A. (2003). Autoregulation of E-cadherin expression by cadherin–cadherin interactions. the roles of β-catenin signaling, Slug, and MAPK *163*, 847-857.

Consortium, T.G.P. (2012). An integrated map of genetic variation from 1,092 human genomes. Nature *491*, 56-65.

Cory, S., Huang, D.C.S., and Adams, J.M. (2003). The Bcl-2 family: roles in cell survival and oncogenesis. Oncogene *22*, 8590-8607.

Costello, L.C., and Franklin, R.B. (2000). The intermediary metabolism of the prostate: a key to understanding the pathogenesis and progression of prostate malignancy. Oncology *59*, 269-282.

Costello, L.C., and Franklin, R.B. (2006). The clinical relevance of the metabolism of prostate cancer; zinc and tumor suppression: connecting the dots. Molecular cancer *5*, 17.

Cotman, S.L., and Staropoli, J.F. (2012). The juvenile Batten disease protein, CLN3, and its role in regulating anterograde and retrograde post-Golgi trafficking. Clinical lipidology *7*, 79-91.

Coussens, L.M., and Werb, Z. (2002). Inflammation and cancer. Nature *420*, 860-867.

Csukas, Z., Banizs, B., and Rozgonyi, F. (2004). Studies on the cytotoxic effects of *Propionibacterium acnes* strains isolated from cornea. Microbial pathogenesis *36*, 171-174.

Cui, J., Rohr, L.R., Swanson, G., Speights, V.O., Maxwell, T., and Brothman, A.R. (2001). Hypermethylation of the caveolin-1 gene promoter in prostate cancer. The Prostate *46*, 249-256.

D'Angelo, R.C., Liu, X.-W., Najy, A.J., Jung, Y.S., Won, J., Chai, K.X., Fridman, R., and Kim, H.-R.C. (2014). TIMP-1 via TWIST1 Induces EMT Phenotypes in Human Breast Epithelial Cells. Molecular Cancer Research *12*, 1324-1333.

Dakubo, G.D., Parr, R.L., Costello, L.C., Franklin, R.B., and Thayer, R.E. (2006). Altered metabolism and mitochondrial genome in prostate cancer. Journal of Clinical Pathology *59*, 10-16.

Dang, C.V. (2013). MYC, Metabolism, Cell Growth, and Tumorigenesis. Cold Spring Harbor perspectives in medicine *3*.

Dannenberg, A.J., Altorki, N.K., Boyle, J.O., Dang, C., Howe, L.R., Weksler, B.B., and Subbaramaiah, K. (2001). Cyclo-oxygenase 2: a pharmacological target for the prevention of cancer. The Lancet Oncology *2*, 544-551.

Datta, S.R., Dudek, H., Tao, X., Masters, S., Fu, H., Gotoh, Y., and Greenberg, M.E. (1997). Akt phosphorylation of BAD couples survival signals to the cell-intrinsic death machinery. Cell *91*, 231-241.

Dauer, D.J., Ferraro, B., Song, L., Yu, B., Mora, L., Buettner, R., Enkemann, S., Jove, R., and Haura, E.B. (2005). Stat3 regulates genes common to both wound healing and cancer. Oncogene *24*, 3397-3408.

Davidsson, S., Mölling, P., Rider, J.R., Unemo, M., Karlsson, M.G., Carlsson, J., Andersson, S.-O., Elgh, F., Söderquist, B., and Andrén, O. (2016). Frequency and typing of *Propionibacterium acnes* in prostate tissue obtained from men with and without prostate cancer. Infectious agents and cancer *11*, 26.

Davis, R.J. (1994). MAPKs: new JNK expands the group. Trends in biochemical sciences *19*, 470-473.

Dayer, J.M., and Choy, E. (2010). Therapeutic targets in rheumatoid arthritis: the interleukin-6 receptor. Rheumatology *49*, 15-24.

de Araújo, V.C., Furuse, C., Cury, P.R., Altemani, A., and de Araújo, N.S. (2008). STAT3 expression in salivary gland tumours. Oral Oncology *44*, 439-445.

de Bono, J.S., Logothetis, C.J., Molina, A., Fizazi, K., North, S., Chu, L., Chi, K.N., Jones, R.J., Goodman, O.B.J., Saad, F.*, et al.* (2011). Abiraterone and Increased Survival in Metastatic Prostate Cancer. New England Journal of Medicine *364*, 1995-2005.

De Francesco, E.M., Bonuccelli, G., Maggiolini, M., Sotgia, F., and Lisanti, M.P. (2017). Vitamin C and Doxycycline: a synthetic lethal combination therapy targeting metabolic flexibility in cancer stem cells (CSCs). Oncotarget.

De Marzo, A.M., Platz, E.A., Sutcliffe, S., Xu, J., Gronberg, H., Drake, C.G., Nakai, Y., Isaacs, W.B., and Nelson, W.G. (2007). Inflammation in prostate carcinogenesis. Nature reviews Cancer *7*, 256-269.

De Nunzio, C., Kramer, G., Marberger, M., Montironi, R., Nelson, W., Schroder, F., Sciarra, A., and Tubaro, A. (2011). The controversial relationship between benign prostatic hyperplasia and prostate cancer: the role of inflammation. European urology *60*, 106-117.

De Palma, M., Biziato, D., and Petrova, T.V. (2017). Microenvironmental regulation of tumour angiogenesis. Nature reviews Cancer *17*, 457-474.

De Vincenzo, R., Conte, C., Ricci, C., Scambia, G., and Capelli, G. (2014). Long-term efficacy and safety of human papillomavirus vaccination. International Journal of Women's Health *6*, 999-1010.

Dechow, T.N., Pedranzini, L., Leitch, A., Leslie, K., Gerald, W.L., Linkov, I., and Bromberg, J.F. (2004). Requirement of matrix metalloproteinase-9 for the transformation of human mammary epithelial cells by Stat3-C. Proceedings of the National Academy of Sciences of the United States of America *101*, 10602-10607.

DeCicco-Skinner, K.L., Henry, G.H., Cataisson, C., Tabib, T., Gwilliam, J.C., Watson, N.J., Bullwinkle, E.M., Falkenburg, L., O'Neill, R.C., Morin, A.*, et al.* (2014). Endothelial Cell Tube Formation Assay for the In Vitro Study of Angiogenesis. Journal of Visualized Experiments: JoVE.

Demaria, M., and Poli, V. (2012). PKM2, STAT3 and HIF-1α: The Warburg's vicious circle. Jak-stat *1*, 194-196.

Demidenko, Z.N., Fojo, T., and Blagosklonny, M.V. (2005). Complementation of two mutant p53: Implications for loss of heterozygosity in cancer. FEBS letters *579*, 2231-2235.

Denmeade, S.R., and Isaacs, J.T. (2002). A history of prostate cancer treatment. Nature reviews Cancer *2*, 389-396.

Dennis, L.K., and Dawson, D.V. (2002). Meta-analysis of measures of sexual activity and prostate cancer. Epidemiology *13*, 72-79.

Dennis, L.K., Lynch, C.F., and Torner, J.C. (2002). Epidemiologic association between prostatitis and prostate cancer. Urology *60*, 78-83.

Denys, G.A., Jerris, R.C., Swenson, J.M., and Thornsberry, C. (1983). Susceptibility of *Propionibacterium acnes* clinical isolates to 22 antimicrobial agents. Antimicrobial agents and chemotherapy *23*, 335-337.

Dessinioti, C., and Katsambas, A. (2017). *Propionibacterium acnes* and antimicrobial resistance in acne. Clinics in dermatology *35*, 163-167.

Dessinioti, C., and Katsambas, A.D. (2010). The role of *Propionibacterium acnes* in acne pathogenesis: facts and controversies. Clinics in dermatology *28*, 2-7.

Dhanasekaran, D.N., and Reddy, E.P. (2008). JNK signaling in apoptosis. Oncogene *27*, 6245-6251.

Dhillon, A.S., Hagan, S., Rath, O., and Kolch, W. (2009). MAP kinase signalling pathways in cancer. Oncogene *26*, 3279-3290.

Di Carlo, E., Magnasco, S., D'Antuono, T., Tenaglia, R., and Sorrentino, C. (2007). The prostate-associated lymphoid tissue (PALT) is linked to the expression of homing chemokines CXCL13 and CCL21. The Prostate *67*, 1070-1080.

di Sant'Agnese, P.A. (1998). Neuroendocrine cells of the prostate and neuroendocrine differentiation in prostatic carcinoma: a review of morphologic aspects. Urology *51*, 121-124.

Dinarello, C.A. (1998). Interleukin-1 beta, interleukin-18, and the interleukin-1 beta converting enzyme. Annals of the New York Academy of Sciences *856*, 1-11.

Dinarello, C.A. (2011). Interleukin-1 in the pathogenesis and treatment of inflammatory diseases. Blood *117*, 3720-3732.

Disis, M.L. (2010). Immune Regulation of Cancer. Journal of Clinical Oncology *28*, 4531-4538.

Dodson, C.C., Craig, E.V., Cordasco, F.A., Dines, D.M., Dines, J.S., Dicarlo, E., Brause, B.D., and Warren, R.F. (2010). *Propionibacterium acnes* infection after shoulder arthroplasty: a diagnostic challenge. Journal of shoulder and elbow surgery / American Shoulder and Elbow Surgeons et al. *19*, 303-307.

Drobnjak, M., Osman, I., Scher, H.I., Fazzari, M., and Cordon-Cardo, C. (2000). Overexpression of Cyclin D1 Is Associated with Metastatic Prostate Cancer to Bone. Clinical Cancer Research *6*, 1891-1895.

Drost, J., Karthaus, W.R., Gao, D., Driehuis, E., Sawyers, C.L., Chen, Y., and Clevers, H. (2016). Organoid culture systems for prostate epithelial and cancer tissue. Nat Protocols *11*, 347-358.

Drott, J.B., Alexeyev, O., Bergstrom, P., Elgh, F., and Olsson, J. (2010). *Propionibacterium acnes* infection induces upregulation of inflammatory genes and cytokine secretion in prostate epithelial cells. BMC microbiology *10*, 126.

Dunn, G.P., Old, L.J., and Schreiber, R.D. (2004). The Three Es of Cancer Immunoediting. Annual review of immunology *22*, 329-360.

Edwards, J., and Bartlett, J.M.S. (2005). The androgen receptor and signal-transduction pathways in hormone-refractory prostate cancer. Part 1: modifications to the androgen receptor. BJU international *95*, 1320-1326.

Efesoy, O., Bozlu, M., Çayan, S., and Akbay, E. (2013). Complications of transrectal ultrasound-guided 12-core prostate biopsy: a single center experience with 2049 patients. Turkish journal of urology *39*, 6-11.

Egger, G., Liang, G., Aparicio, A., and Jones, P.A. (2004). Epigenetics in human disease and prospects for epigenetic therapy. Nature *429*, 457-463.

Eilers, M., and Eisenman, R.N. (2008). Myc's broad reach. Genes & development *22*, 2755-2766.

Eischen, C.M., Woo, D., Roussel, M.F., and Cleveland, J.L. (2001). Apoptosis Triggered by Myc-Induced Suppression of Bcl-XL or Bcl-2 Is Bypassed during Lymphomagenesis. Molecular and cellular biology *21*, 5063-5070.

Eishi, Y. (2013). Etiologic link between sarcoidosis and *Propionibacterium acnes*. Respiratory investigation *51*, 56-68.

Eishi, Y., Suga, M., Ishige, I., Kobayashi, D., Yamada, T., Takemura, T., Takizawa, T., Koike, M., Kudoh, S., Costabel, U*., et al.* (2002). Quantitative analysis of mycobacterial and propionibacterial DNA in lymph nodes of Japanese and European patients with sarcoidosis. Journal of clinical microbiology *40*, 198-204.

El-Mahdy, T.S., Abdalla, S., El-Domany, R., Mohamed, M.S., Ross, J.I., and Snelling, A.M. (2010). Detection of a new *erm(X)*-mediated antibiotic resistance in Egyptian cutaneous propionibacteria. Anaerobe *16*, 376-379.

Elinav, E., Nowarski, R., Thaiss, C.A., Hu, B., Jin, C., and Flavell, R.A. (2013). Inflammation-induced cancer: crosstalk between tumours, immune cells and microorganisms. Nature reviews Cancer *13*, 759-771.

English, H.F., Santen, R.J., and Isaacs, J.T. (1987). Response of glandular versus basal rat ventral prostatic epithelial cells to androgen withdrawal and replacement. The Prostate *11*, 229-242.

Ernst, P.B., and Gold, B.D. (2000). The disease spectrum of *Helicobacter pylori*: the immunopathogenesis of gastroduodenal ulcer and gastric cancer. Annual review of microbiology *54*, 615-640.

Esposito, K., Chiodini, P., Capuano, A., Bellastella, G., Maiorino, M.I., Parretta, E., Lenzi, A., and Giugliano, D. (2013). Effect of metabolic syndrome and its components on prostate cancer risk: Meta-analysis. Journal of endocrinological investigation *36*, 132-139.

Evans, G.S., and Chandler, J.A. (1987). Cell proliferation studies in the rat prostate: II. The effects of castration and androgen-induced regeneration upon basal and secretory cell proliferation. The Prostate *11*, 339-351.

Faraji, E.I., and Frank, B.B. (2002). Multifocal atrophic gastritis and gastric carcinoma. Gastroenterology clinics of North America *31*, 499-516.

Farge, E. (2003). Mechanical Induction of Twist in the *Drosophila* Foregut/Stomodeal Primordium. Current Biology *13*, 1365-1377.

Fassi Fehri, L., Mak, T.N., Laube, B., Brinkmann, V., Ogilvie, L.A., Mollenkopf, H., Lein, M., Schmidt, T., Meyer, T.F., and Bruggemann, H. (2011). Prevalence of *Propionibacterium acnes* in diseased prostates and its inflammatory and transforming activity on prostate epithelial cells. International journal of medical microbiology: IJMM *301*, 69-78.

Fatehullah, A., Tan, S.H., and Barker, N. (2016). Organoids as an in vitro model of human development and disease. Nature cell biology *18*, 246-254.

Felcht, M., Luck, R., Schering, A., Seidel, P., Srivastava, K., Hu, J., Bartol, A., Kienast, Y., Vettel, C., Loos, E.K.*, et al.* (2012). Angiopoietin-2 differentially regulates angiogenesis through TIE2 and integrin signaling. The Journal of clinical investigation *122*, 1991-2005.

Fischer, N., Mak, T.N., Shinohara, D.B., Sfanos, K.S., Meyer, T.F., and Bruggemann, H. (2013). Deciphering the intracellular fate of *Propionibacterium acnes* in macrophages. BioMed research international *2013*, 603046.

Fizazi, K., Tran, N., Fein, L., Matsubara, N., Rodriguez-Antolin, A., Alekseev, B.Y., Ozguroglu, M., Ye, D., Feyerabend, S., Protheroe, A.*, et al.* (2017). Abiraterone plus Prednisone in Metastatic, Castration-Sensitive Prostate Cancer. The New England journal of medicine.

Flavin, R., Peluso, S., Nguyen, P.L., and Loda, M. (2010). Fatty acid synthase as a potential therapeutic target in cancer. Future oncology *6*, 551-562.

Focaccetti, C., Bruno, A., Magnani, E., Bartolini, D., Principi, E., Dallaglio, K., Bucci, E.O., Finzi, G., Sessa, F., Noonan, D.M.*, et al.* (2015). Effects of 5-Fluorouracil on Morphology, Cell Cycle, Proliferation, Apoptosis, Autophagy and ROS Production in Endothelial Cells and Cardiomyocytes. PloS one *10*.

Fosslien, E. (2001). Review: molecular pathology of cyclooxygenase-2 in cancer-induced angiogenesis. Annals of clinical and laboratory science *31*, 325-348.

Franco, A.T., Israel, D.A., Washington, M.K., Krishna, U., Fox, J.G., Rogers, A.B., Neish, A.S., Collier-Hyams, L., Perez-Perez, G.I., Hatakeyama, M.*, et al.* (2005). Activation of beta-catenin by carcinogenic *Helicobacter pylori*. Proceedings of the National Academy of Sciences of the United States of America *102*, 10646-10651.

Franklin, R.B., Milon, B., Feng, P., and Costello, L.C. (2005). Zinc and zinc transporters in normal prostate and the pathogenesis of prostate cancer. Frontiers in bioscience: a journal and virtual library *10*, 2230-2239.

Frisch, S.M., Schaller, M., and Cieply, B. (2013). Mechanisms that link the oncogenic epithelial–mesenchymal transition to suppression of anoikis. Journal of cell science *126*, 21-29.

Furukawa, A., Uchida, K., Ishige, Y., Ishige, I., Kobayashi, I., Takemura, T., Yokoyama, T., Iwai, K., Watanabe, K., Shimizu, S.*, et al.* (2009). Characterization of *Propionibacterium acnes*

isolates from sarcoid and non-sarcoid tissues with special reference to cell invasiveness, serotype, and trigger factor gene polymorphism. Microbial pathogenesis *46*, 80-87.

Gallo, O., Franchi, A., Magnelli, L., Sardi, I., Vannacci, A., Boddi, V., Chiarugi, V., and Masini, E. (2001). Cyclooxygenase-2 Pathway Correlates with VEGF Expression in Head and Neck Cancer. Implications for Tumor Angiogenesis and Metastasis. Neoplasia *3*, 53-61.

Gann, P.H., Hennekens, C.H., Sacks, F.M., Grodstein, F., Giovannucci, E.L., and Stampfer, M.J. (1994). Prospective study of plasma fatty acids and risk of prostate cancer. Journal of the National Cancer Institute *86*, 281-286.

Gao, D., Vela, I., Sboner, A., Iaquinta, P.J., Karthaus, W.R., Gopalan, A., Dowling, C., Wanjala, J.N., Undvall, E.A., Arora, V.K.*, et al.* (2014). Organoid cultures derived from patients with advanced prostate cancer. Cell *159*, 176-187.

Garcia-Tobilla, P., Solorzano, S.R., Salido-Guadarrama, I., Gonzalez-Covarrubias, V., Morales-Montor, G., Diaz-Otanez, C.E., and Rodriguez-Dorantes, M. (2016). SFRP1 repression in prostate cancer is triggered by two different epigenetic mechanisms. Gene *593*, 292-301.

Gartel, A.L., Ye, X., Goufman, E., Shianov, P., Hay, N., Najmabadi, F., and Tyner, A.L. (2001). Myc represses the p21(WAF1/CIP1) promoter and interacts with Sp1/Sp3. Proceedings of the National Academy of Sciences of the United States of America *98*, 4510-4515.

Gebert, B., Fischer, W., Weiss, E., Hoffmann, R., and Haas, R. (2003). *Helicobacter pylori* vacuolating cytotoxin inhibits T lymphocyte activation. Science *301*, 1099-1102.

Genot, E.M., Arrieumerlou, C., Ku, G., Burgering, B.M.T., Weiss, A., and Kramer, I.M. (2000). The T-Cell Receptor Regulates Akt (Protein Kinase B) via a Pathway Involving Rac1 and Phosphatidylinositide 3-Kinase. Molecular and cellular biology *20*, 5469-5478.

Gerstenbluth, R.E., Seftel, A.D., MacLennan, G.T., Rao, R.N., Corty, E.W., Ferguson, K., and Resnick, M.I. (2002). Distribution of chronic prostatitis in radical prostatectomy specimens with up-regulation of bcl-2 in areas of inflammation. The Journal of urology *167*, 2267-2270.

Giacinti, C., and Giordano, A. (2006). RB and cell cycle progression. Oncogene *25*, 5220-5227.

Gilany, K., Minai-Tehrani, A., Savadi-Shiraz, E., Rezadoost, H., and Lakpour, N. (2015). Exploring the human seminal plasma proteome: an unexplored gold mine of biomarker for male infertility and male reproduction disorder. Journal of reproduction & infertility *16*, 61-71.

Gilgunn, S., Conroy, P.J., Saldova, R., Rudd, P.M., and O'Kennedy, R.J. (2013). Aberrant PSA glycosylation – a sweet predictor of prostate cancer. Nat Rev Urol *10*, 99-107.

Giovannucci, E., Rimm, E.B., Colditz, G.A., Stampfer, M.J., Ascherio, A., Chute, C.G., and Willett, W.C. (1993). A prospective study of dietary fat and risk of prostate cancer. Journal of the National Cancer Institute *85*, 1571-1579.

Giri, D., Ozen, M., and Ittmann, M. (2001). Interleukin-6 is an autocrine growth factor in human prostate cancer. The American journal of pathology *159*, 2159-2165.

Gleason, D.F., and Mellinger, G.T. (1974). Prediction of prognosis for prostatic adenocarcinoma by combined histological grading and clinical staging. The Journal of urology *111*, 58-64.

Gocheva, V., Wang, H.W., Gadea, B.B., Shree, T., Hunter, K.E., Garfall, A.L., Berman, T., and Joyce, J.A. (2010). IL-4 induces cathepsin protease activity in tumor-associated macrophages to promote cancer growth and invasion. Genes & development *24*, 241-255.

Gonzalgo, M.L., and Isaacs, W.B. (2003). Molecular pathways to prostate cancer. The Journal of urology *170*, 2444-2452.

Gorlach, A., and Bonello, S. (2008). The cross-talk between NF-kappaB and HIF-1: further evidence for a significant liaison. The Biochemical journal *412*, e17-19.

Grabowska, M.M., DeGraff, D.J., Yu, X., Jin, R.J., Chen, Z., Borowsky, A.D., and Matusik, R.J. (2014). Mouse Models of Prostate Cancer: Picking the Best Model for the Question. Cancer metastasis reviews *33*, 377-397.

Greenhalgh, C.J., and Hilton, D.J. (2001). Negative regulation of cytokine signaling. Journal of leukocyte biology *70*, 348-356.

Grell, M., Douni, E., Wajant, H., Lohden, M., Clauss, M., Maxeiner, B., Georgopoulos, S., Lesslauer, W., Kollias, G., Pfizenmaier, K*., et al.* (1995). The transmembrane form of tumor necrosis factor is the prime activating ligand of the 80 kDa tumor necrosis factor receptor. Cell *83*, 793-802.

Grice, E.A., and Segre, J.A. (2011). The skin microbiome. Nature reviews Microbiology *9*, 244-253.

Grille, S.J., Bellacosa, A., Upson, J., Klein-Szanto, A.J., van Roy, F., Lee-Kwon, W., Donowitz, M., Tsichlis, P.N., and Larue, L. (2003). The protein kinase Akt induces epithelial mesenchymal transition and promotes enhanced motility and invasiveness of squamous cell carcinoma lines. Cancer research *63*, 2172-2178.

Gronberg, H., Damber, L., and Damber, J.E. (1994). Studies of genetic-factors in prostate-cancer in a twin population. J Urology *152*, 1484-1487.

Gross, G.A., Turesky, R.J., Fay, L.B., Stillwell, W.G., Skipper, P.L., and Tannenbaum, S.R. (1993). Heterocyclic aromatic amine formation in grilled bacon, beef and fish and in grill scrapings. Carcinogenesis *14*, 2313-2318.

Gross, M., Top, I., Laux, I., Katz, J., Curran, J., Tindell, C., and Agus, D. (2007). β-2-Microglobulin Is an Androgen-Regulated Secreted Protein Elevated in Serum of Patients with Advanced Prostate Cancer. Clinical Cancer Research *13*, 1979-1986.

Guilford, P., Hopkins, J., Harraway, J., McLeod, M., McLeod, N., Harawira, P., Taite, H., Scoular, R., Miller, A., and Reeve, A.E. (1998). E-cadherin germline mutations in familial gastric cancer. Nature *392*, 402-405.

Guo, C., Buranych, A., Sarkar, D., Fisher, P.B., and Wang, X.-Y. (2013). The role of tumor-associated macrophages in tumor vascularization. Vascular Cell *5*, 20.

Guo, S., Lok, J., Liu, Y., Hayakawa, K., Leung, W., Xing, C., Ji, X., and Lo, E.H. (2014). Assays to Examine Endothelial Cell Migration, Tube Formation, and Gene Expression Profiles. Methods in molecular biology *1135*, 393-402.

Gupta, S., Srivastava, M., Ahmad, N., Bostwick, D.G., and Mukhtar, H. (2000). Over-expression of cyclooxygenase-2 in human prostate adenocarcinoma. The Prostate *42*, 73-78.

Guschin, D., Rogers, N., Briscoe, J., Witthuhn, B., Watling, D., Horn, F., Pellegrini, S., Yasukawa, K., Heinrich, P., and Stark, G.R. (1995). A major role for the protein tyrosine kinase JAK1 in the JAK/STAT signal transduction pathway in response to interleukin-6. The EMBO journal *14*, 1421-1429.

Haenszel, W., and Kurihara, M. (1968). Studies of Japanese migrants. I. Mortality from cancer and other diseases among Japanese in the United States. Journal of the National Cancer Institute *40*, 43-68.

Hager, M.H., Solomon, K.R., and Freeman, M.R. (2006). The role of cholesterol in prostate cancer. Current opinion in clinical nutrition and metabolic care *9*, 379-385.

Hanahan, D., and Weinberg, Robert A. (2011a). Hallmarks of Cancer: The Next Generation. Cell *144*, 646-674.

Hanahan, D., and Weinberg, R.A. (2011b). Hallmarks of cancer: the next generation. Cell *144*, 646-674.

Harada, K., Tsuneyama, K., Sudo, Y., Masuda, S., and Nakanuma, Y. (2001). Molecular identification of bacterial 16S ribosomal RNA gene in liver tissue of primary biliary cirrhosis: is *Propionibacterium acnes* involved in granuloma formation? Hepatology *33*, 530-536.

Haraldsdottir, S., Hampel, H., Wei, L., Wu, C., Frankel, W., Bekaii-Saab, T., de la Chapelle, A., and Goldberg, R.M. (2014). Prostate cancer incidence in males with Lynch syndrome. Genetics in medicine: official journal of the American College of Medical Genetics *16*, 553-557.

Haussler, O. (1999). Cell proliferation, apoptosis, oncogene, and tumor suppressor genes status in adenosis with comparison to benign prostatic hyperplasia, prostatic intraepithelial neoplasia, and cancer. Human pathology *30*, 1077-1086.

Hay, N., and Sonenberg, N. (2004). Upstream and downstream of mTOR. Genes & development *18*, 1926-1945.

Hayden, M.S., and Ghosh, S. (2008). Shared Principles in NF-κB Signaling. Cell *132*, 344-362.

Heemers, H., Maes, B., Foufelle, F., Heyns, W., Verhoeven, G., and Swinnen, J.V. (2001). Androgens stimulate lipogenic gene expression in prostate cancer cells by activation of the sterol regulatory element-binding protein cleavage activating protein/sterol regulatory element-binding protein pathway. Molecular endocrinology *15*, 1817-1828.

Heerboth, S., Housman, G., Leary, M., Longacre, M., Byler, S., Lapinska, K., Willbanks, A., and Sarkar, S. (2015). EMT and tumor metastasis. Clinical and Translational Medicine *4*.

Heidenreich, A., Bellmunt, J., Bolla, M., Joniau, S., Mason, M., Matveev, V., Mottet, N., Schmid, H.P., van der Kwast, T., Wiegel, T.*, et al.* (2011). EAU guidelines on prostate cancer. Part 1: screening, diagnosis, and treatment of clinically localised disease. European urology *59*, 61-71.

Heinrich, P.C., Behrmann, I., Haan, S., Hermanns, H.M., Muller-Newen, G., and Schaper, F. (2003). Principles of interleukin (IL)-6-type cytokine signalling and its regulation. The Biochemical journal *374*, 1-20.

Heinrich, P.C., Behrmann, I., Muller-Newen, G., Schaper, F., and Graeve, L. (1998). Interleukin-6-type cytokine signalling through the gp130/Jak/STAT pathway. The Biochemical journal *334 (Pt 2)*, 297-314.

Hemminki, K. (2012). Familial risk and familial survival in prostate cancer. World Journal of Urology *30*, 143-148.

Hirsch, E., Ciraolo, E., Franco, I., Ghigo, A., and Martini, M. (2014). PI3K in cancer-stroma interactions: bad in seed and ugly in soil. Oncogene *33*, 3083-3090.

Hobisch, A., Eder, I.E., Putz, T., Horninger, W., Bartsch, G., Klocker, H., and Culig, Z. (1998). Interleukin-6 regulates prostate-specific protein expression in prostate carcinoma cells by activation of the androgen receptor. Cancer research *58*, 4640-4645.

Hochreiter, W.W., Duncan, J.L., and Schaeffer, A.J. (2000). Evaluation of the bacterial flora of the prostate using a 16S rRNA gene based polymerase chain. The Journal of urology *163*, 127-130.

Hoeben, A., Landuyt, B., Highley, M.S., Wildiers, H., Van Oosterom, A.T., and De Bruijn, E.A. (2004). Vascular Endothelial Growth Factor and Angiogenesis. Pharmacological Reviews *56*, 549-580.

Hoeffler, U. (1977). Enzymatic and hemolytic properties of *Propionibacterium acnes* and related bacteria. Journal of clinical microbiology *6*, 555-558.

Hoesel, B., and Schmid, J.A. (2013). The complexity of NF-kappaB signaling in inflammation and cancer. Molecular cancer *12*, 86.

Hoffman, R.M. (2011). Screening for Prostate Cancer. New England Journal of Medicine *365*, 2013-2019.

Hoffmeyer, K., Raggioli, A., Rudloff, S., Anton, R., Hierholzer, A., Del Valle, I., Hein, K., Vogt, R., and Kemler, R. (2012). Wnt/β-Catenin Signaling Regulates Telomerase in Stem Cells and Cancer Cells. Science *336*, 1549-1554.

Hojilla, C.V., Kim, I., Kassiri, Z., Fata, J.E., Fang, H., and Khokha, R. (2007). Metalloproteinase axes increase β-catenin signaling in primary mouse mammary epithelial cells lacking TIMP3. Journal of cell science *120*, 1050-1060.

Holmberg, A., Lood, R., Morgelin, M., Soderquist, B., Holst, E., Collin, M., Christensson, B., and Rasmussen, M. (2009a). Biofilm formation by *Propionibacterium acnes* is a characteristic of invasive isolates. Clinical microbiology and infection: the official publication of the European Society of Clinical Microbiology and Infectious Diseases *15*, 787-795.

Holmberg, A., Lood, R., Mörgelin, M., Söderquist, B., Holst, E., Collin, M., Christensson, B., and Rasmussen, M. (2009b). Biofilm formation by *Propionibacterium acnes* is a characteristic of invasive isolates. Clinical Microbiology and Infection *15*, 787-795.

Homma, J.Y., Abe, C., Chosa, H., Ueda, K., Saegusa, J., Nakayama, M., Homma, H., Washizaki, M., and Okano, H. (1978). Bacteriological investigation on biopsy specimens from patients with sarcoidosis. The Japanese journal of experimental medicine *48*, 251-255.

Horvath, B., Hunyadkurti, J., Voros, A., Fekete, C., Urban, E., Kemeny, L., and Nagy, I. (2012). Genome sequence of *Propionibacterium acnes* type II strain ATCC 11828. Journal of bacteriology *194*, 202-203.

Howlader, N., Noone, A., Krapcho, M., Neyman, N., Aminou, R., Waldron, W., Altekruse, S., Kosary, C., Ruhl, J., Tatalovich, Z*., et al.* (2011). SEER Cancer Statistics Review, 1975-2008, National Cancer Institute. Bethesda, MD, based on November 2010 SEER data submission (http://seer.cancer.gov/csr/1975_2008/).

Hsing, A.W., Tsao, L., and Devesa, S.S. (2000). International trends and patterns of prostate cancer incidence and mortality. International journal of cancer Journal international du cancer *85*, 60-67.

Hu, X., Li, B., Li, X., Zhao, X., Wan, L., Lin, G., Yu, M., Wang, J., Jiang, X., Feng, W*., et al.* (2014). Transmembrane TNF-α Promotes Suppressive Activities of Myeloid-Derived Suppressor Cells via TNFR2. The Journal of Immunology *192*, 1320-1331.

Huang, R.Y.-J., Guilford, P., and Thiery, J.P. (2012). Early events in cell adhesion and polarity during epithelial-mesenchymal transition. Journal of cell science *125*, 4417-4422.

Huang, S.P., Wu, M.S., Shun, C.T., Wang, H.P., Lin, M.T., Kuo, M.L., and Lin, J.T. (2004). Interleukin-6 increases vascular endothelial growth factor and angiogenesis in gastric carcinoma. Journal of biomedical science *11*, 517-527.

Huang, T.T., Wuerzberger-Davis, S.M., Wu, Z.-H., and Miyamoto, S. (2003). Sequential Modification of NEMO/IKKγ by SUMO-1 and Ubiquitin Mediates NF-κB Activation by Genotoxic Stress. Cell *115*, 565-576.

Huber, M.A., Azoitei, N., Baumann, B., Grunert, S., Sommer, A., Pehamberger, H., Kraut, N., Beug, H., and Wirth, T. (2004). NF-kappaB is essential for epithelial-mesenchymal transition and metastasis in a model of breast cancer progression. The Journal of clinical investigation *114*, 569-581.

Huggins, C., Stevens, R.E., Jr, and Hodges, C.V. (1941). Studies on prostatic cancer: Ii. the effects of castration on advanced carcinoma of the prostate gland. Archives of Surgery *43*, 209-223.

Hunninghake, G.W., Costabel, U., Ando, M., Baughman, R., Cordier, J.F., du Bois, R., Eklund, A., Kitaichi, M., Lynch, J., Rizzato, G.*, et al.* (1999). ATS/ERS/WASOG statement on sarcoidosis. American Thoracic Society/European Respiratory Society/World Association of Sarcoidosis and other Granulomatous Disorders. Sarcoidosis, vasculitis, and diffuse lung diseases: official journal of WASOG / World Association of Sarcoidosis and Other Granulomatous Disorders *16*, 149-173.

Hunyadkurti, J., Feltoti, Z., Horvath, B., Nagymihaly, M., Voros, A., McDowell, A., Patrick, S., Urban, E., and Nagy, I. (2011). Complete genome sequence of *Propionibacterium acnes* type IB strain 6609. Journal of bacteriology *193*, 4561-4562.

Hussain, S., Slevin, M., Mesaik, M.A., Choudhary, M.I., Elosta, A.H., Matou, S., Ahmed, N., West, D., and Gaffney, J. (2008). Cheiradone: a vascular endothelial cell growth factor receptor antagonist. BMC Cell Biology *9*, 7.

Hussein, M.-R.A., Al-Assiri, M., and Musalam, A.O. (2009). Phenotypic characterization of the infiltrating immune cells in normal prostate, benign nodular prostatic hyperplasia and prostatic adenocarcinoma. Experimental and Molecular Pathology *86*, 108-113.

Hwang, S.-H., Lee, B.-H., Choi, S.-H., Kim, H.-J., Won, K.J., Lee, H.M., Rhim, H., Kim, H.-C., and Nah, S.-Y. (2016). Effects of gintonin on the proliferation, migration, and tube formation of human umbilical-vein endothelial cells: involvement of lysophosphatidic-acid receptors and vascular-endothelial-growth-factor signaling. Journal of Ginseng Research *40*, 325-333.

Ichim, G., and Tait, S.W.G. (2016). A fate worse than death: apoptosis as an oncogenic process. Nature reviews Cancer *16*, 539-548.

Ingham, E., Holland, K.T., Gowland, G., and Cunliffe, W.J. (1981). Partial purification and characterization of lipase (EC 3.1.1.3) from *Propionibacterium acnes*. Journal of general microbiology *124*, 393-401.

Issuree, P.D., Maretzky, T., McIlwain, D.R., Monette, S., Qing, X., Lang, P.A., Swendeman, S.L., Park-Min, K.H., Binder, N., Kalliolias, G.D.*, et al.* (2013). iRHOM2 is a critical pathogenic mediator of inflammatory arthritis. The Journal of clinical investigation *123*, 928-932.

Ittmann, M., Huang, J., Radaelli, E., Martin, P., Signoretti, S., Sullivan, R., Simons, B.W., Ward, J.M., Robinson, B.D., Chu, G.C.*, et al.* (2013). Animal models of human prostate cancer: The Consensus Report of the New York Meeting of the Mouse Models of Human Cancers Consortium Prostate Pathology Committee. Cancer research *73*, 2718-2736.

Ivanovic, V., Melman, A., Davis-Joseph, B., Valcic, M., and Geliebter, J. (1995). Elevated plasma levels of TGF-beta 1 in patients with invasive prostate cancer. Nature medicine *1*, 282-284.

Jaiswal, A.S., and Narayan, S. (2008). A novel function of adenomatous polyposis coli (APC) in regulating DNA repair. Cancer letters *271*, 272-280.

Jarnicki, A., Putoczki, T., and Ernst, M. (2010). Stat3: linking inflammation to epithelial cancer - more than a "gut" feeling? Cell division *5*, 14.

Jeremy, A.H., Holland, D.B., Roberts, S.G., Thomson, K.F., and Cunliffe, W.J. (2003). Inflammatory events are involved in acne lesion initiation. The Journal of investigative dermatology *121*, 20-27.

Jeronimo, C., Henrique, R., Hoque, M.O., Mambo, E., Ribeiro, F.R., Varzim, G., Oliveira, J., Teixeira, M.R., Lopes, C., and Sidransky, D. (2004). A quantitative promoter methylation profile of prostate cancer. Clinical cancer research: an official journal of the American Association for Cancer Research *10*, 8472-8478.

Johnson, G.L., and Nakamura, K. (2007). The c-jun kinase/stress-activated pathway: Regulation, function and role in human disease. Biochimica et Biophysica Acta (BBA) - Molecular Cell Research *1773*, 1341-1348.

Johnson, J.L., and Cummins, C.S. (1972). Cell wall composition and deoxyribonucleic acid similarities among the anaerobic coryneforms, classical propionibacteria, and strains of Arachnia propionica. Journal of bacteriology *109*, 1047-1066.

Johnson, L.A., Kanak, M.A., Kajdacsy-Balla, A., Pestaner, J.P., and Bagasra, O. (2010). Differential zinc accumulation and expression of human zinc transporter 1 (hZIP1) in prostate glands. Methods (San Diego, Calif) *52*, 316-321.

Jolley, K.A., Chan, M.-S., and Maiden, M.C. (2004). mlstdbNet – distributed multi-locus sequence typing (MLST) databases. BMC bioinformatics *5*, 86.

Jones, P.A., and Laird, P.W. (1999). Cancer epigenetics comes of age. Nature genetics *21*, 163-167.

Jones, P.A., and Takai, D. (2001). The role of DNA methylation in mammalian epigenetics. Science *293*, 1068-1070.

Jones, S.A., Scheller, J., and Rose-John, S. (2011). Therapeutic strategies for the clinical blockade of IL-6/gp130 signaling. The Journal of clinical investigation *121*, 3375-3383.

Jordà, M., Olmeda, D., Vinyals, A., Valero, E., Cubillo, E., Llorens, A., Cano, A., and Fabra, À. (2005). Upregulation of MMP-9 in MDCK epithelial cell line in response to expression of the Snail transcription factor. Journal of cell science *118*, 3371-3385.

Jung-Hynes, B., Huang, W., Reiter, R.J., and Ahmad, N. (2010). Melatonin resynchronizes dysregulated circadian rhythm circuitry in human prostate cancer cells. Journal of pineal research *49*, 60-68.

Jung, H., Choe, Y., Kim, H., Park, N., Son, G.H., Khang, I., and Kim, K. (2003). Involvement of CLOCK:BMAL1 heterodimer in serum-responsive mPer1 induction. Neuroreport *14*, 15-19.

Kalliolias, G.D., and Ivashkiv, L.B. (2016). TNF biology, pathogenic mechanisms and emerging therapeutic strategies. Nat Rev Rheumatol *12*, 49-62.

Kamisango, K., Saiki, I., Tanio, Y., Okumura, H., Araki, Y., Sekikawa, I., Azuma, I., and Yamamura, Y. (1982). Structures and biological activities of peptidoglycans of Listeria monocytogenes and *Propionibacterium acnes*. Journal of biochemistry *92*, 23-33.

Kanda, N., Seno, H., Konda, Y., Marusawa, H., Kanai, M., Nakajima, T., Kawashima, T., Nanakin, A., Sawabu, T., Uenoyama, Y.*, et al.* (2004). STAT3 is constitutively activated and supports cell survival in association with survivin expression in gastric cancer cells. Oncogene *23*, 4921-4929.

Karami, S., Young, H.A., and Henson, D.E. (2007). Earlier age at diagnosis: Another dimension in cancer disparity? Cancer Detection and Prevention *31*, 29-34.

Karin, M. (2009). NF-kappaB as a critical link between inflammation and cancer. Cold Spring Harbor perspectives in biology *1*, a000141.

Karin, M., Cao, Y., Greten, F.R., and Li, Z.W. (2002). NF-kappaB in cancer: from innocent bystander to major culprit. Nature reviews Cancer *2*, 301-310.

Karthaus, W.R., Iaquinta, P.J., Drost, J., Gracanin, A., van Boxtel, R., Wongvipat, J., Dowling, C.M., Gao, D., Begthel, H., Sachs, N.*, et al.* (2014). Identification of multipotent luminal progenitor cells in human prostate organoid cultures. Cell *159*, 163-175.

Kato, Y., Tapping, R.I., Huang, S., Watson, M.H., Ulevitch, R.J., and Lee, J.D. (1998). Bmk1/Erk5 is required for cell proliferation induced by epidermal growth factor. Nature *395*, 713-716.

Keku, T.O., McCoy, A.N., and Azcarate-Peril, A.M. (2013). *Fusobacterium* spp. and colorectal cancer: cause or consequence? Trends in microbiology *21*, 506-508.

Kessenbrock, K., Plaks, V., and Werb, Z. (2010). Matrix Metalloproteinases: Regulators of the Tumor Microenvironment. Cell *141*, 52-67.

Khan, F.U., Ihsan, A.U., Khan, H.U., Jana, R., Wazir, J., Khongorzul, P., Waqar, M., and Zhou, X. (2017). Comprehensive overview of prostatitis. Biomedicine & Pharmacotherapy *94*, 1064-1076.

Khor, L.Y., Bae, K., Pollack, A., Hammond, M.E., Grignon, D.J., Venkatesan, V.M., Rosenthal, S.A., Ritter, M.A., Sandler, H.M., Hanks, G.E.*, et al.* (2007). COX-2 expression predicts prostate-cancer outcome: analysis of data from the RTOG 92-02 trial. The Lancet Oncology *8*, 912-920.

Kikuchi, A., and Yamamoto, H. (2008). Tumor formation due to abnormalities in the β-catenin-independent pathway of Wnt signaling. Cancer Science *99*, 202-208.

Kim, D., Kim, S., Koh, H., Yoon, S.-O., Chung, A.-S., Cho, K.S., and Chung, J. (2001). Akt/PKB promotes cancer cell invasion via increased motility and metalloproteinase production. The FASEB Journal *15*, 1953-1962.

Kim, E.H., Larson, J.A., and Andriole, G.L. (2016). Management of Benign Prostatic Hyperplasia. Annual review of medicine *67*, 137-151.

Kim, J.H., Cox, M.E., and Wasan, K.M. (2014). Effect of simvastatin on castration-resistant prostate cancer cells. Lipids in Health and Disease *13*, 56.

Kim, K.H., and Sederstrom, J.M. (2015). Assaying cell cycle status using flow cytometry. Current protocols in molecular biology / edited by Frederick M Ausubel et al. *111*, 28.26.21-28.26.11.

Kim, K.J., Cho, C.S., and Kim, W.U. (2012). Role of placenta growth factor in cancer and inflammation. Experimental & Molecular Medicine *44*, 10-19.

Klement, J.F., Rice, N.R., Car, B.D., Abbondanzo, S.J., Powers, G.D., Bhatt, P.H., Chen, C.H., Rosen, C.A., and Stewart, C.L. (1996). IkappaBalpha deficiency results in a sustained NF-kappaB response and severe widespread dermatitis in mice. Molecular and cellular biology *16*, 2341-2349.

Klotz, L., Zhang, L., Lam, A., Nam, R., Mamedov, A., and Loblaw, A. (2010). Clinical results of long-term follow-up of a large, active surveillance cohort with localized prostate cancer. Journal of clinical oncology: official journal of the American Society of Clinical Oncology *28*, 126-131.

Knall, C., Worthen, G.S., and Johnson, G.L. (1997). Interleukin 8-stimulated phosphatidylinositol-3-kinase activity regulates the migration of human neutrophils independent of extracellular signal-regulated kinase and p38 mitogen-activated protein kinases. Proceedings of the National Academy of Sciences of the United States of America *94*, 3052-3057.

Knudsen, K.E., and Penning, T.M. (2010). Partners in crime: deregulation of AR activity and androgen synthesis in prostate cancer. Trends Endocrinol Metab *21*, 315-324.

Konduri, S.D., Tasiou, A., Chandrasekar, N., and Rao, J.S. (2001). Overexpression of tissue factor pathway inhibitor-2 (TFPI-2), decreases the invasiveness of prostate cancer cells in vitro. International journal of oncology *18*, 127-131.

Konishi, N., Shimada, K., Nakamura, M., Ishida, E., Ota, I., Tanaka, N., and Fujimoto, K. (2008). Function of JunB in transient amplifying cell senescence and progression of human prostate cancer. Clinical cancer research: an official journal of the American Association for Cancer Research *14*, 4408-4416.

Kostic, Aleksandar D., Chun, E., Robertson, L., Glickman, Jonathan N., Gallini, Carey A., Michaud, M., Clancy, Thomas E., Chung, Daniel C., Lochhead, P., Hold, Georgina L.*, et al.* (2013). *Fusobacterium nucleatum* Potentiates Intestinal Tumorigenesis and Modulates the Tumor-Immune Microenvironment. Cell host & microbe *14*, 207-215.

Krieger, J.N., Lee, S.W.H., Jeon, J., Cheah, P.Y., Liong, M.L., and Riley, D.E. (2008). Epidemiology of prostatitis. International journal of antimicrobial agents *31*, 85-90.

Krieger, J.N., Nyberg, L., Jr., and Nickel, J.C. (1999). NIH consensus definition and classification of prostatitis. Jama *282*, 236-237.

Kristal, A.R., Price, D.K., Till, C., Schenk, J.M., Neuhouser, M.L., Ockers, S., Lin, D.W., Thompson, I.M., and Figg, W.D. (2010). Androgen receptor CAG repeat length is not associated with the risk of incident symptomatic benign prostatic hyperplasia: results from the Prostate Cancer Prevention Trial. The Prostate *70*, 584-590.

Kumar, R., Herold, J.L., Schady, D., Davis, J., Kopetz, S., Martinez-Moczygemba, M., Murray, B.E., Han, F., Li, Y., Callaway, E.*, et al.* (2017). *Streptococcus gallolyticus* subsp. gallolyticus promotes colorectal tumor development. PLoS pathogens *13*, e1006440.

Kuroda, K., Nakashima, J., Kanao, K., Kikuchi, E., Miyajima, A., Horiguchi, Y., Nakagawa, K., Oya, M., Ohigashi, T., and Murai, M. (2007). Interleukin 6 is associated with cachexia in patients with prostate cancer. Urology *69*, 113-117.

Kypta, R.M., and Waxman, J. (2012). Wnt/beta-catenin signalling in prostate cancer. Nat Rev Urol *9*, 418-428.

Kyrylkova, K., Kyryachenko, S., Leid, M., and Kioussi, C. (2012). Detection of Apoptosis by TUNEL Assay. In Odontogenesis: Methods and Protocols, C. Kioussi, ed. (Totowa, NJ: Humana Press), pp. 41-47.

LaGory, E.L., and Giaccia, A.J. (2016). The ever-expanding role of HIF in tumour and stromal biology. Nature cell biology *18*, 356-365.

Lakshmanan, I., and Batra, S.K. (2013). Protocol for Apoptosis Assay by Flow Cytometry Using Annexin V Staining Method. Bio-protocol *3*.

Lang, S., and Palmer, M. (2003). Characterization of *Streptococcus agalactiae* CAMP factor as a pore-forming toxin. The Journal of biological chemistry *278*, 38167-38173.

Larsen, L., and Ropke, C. (2002). Suppressors of cytokine signalling: SOCS. APMIS: acta pathologica, microbiologica, et immunologica Scandinavica *110*, 833-844.

Larson, A.A., Liao, S.Y., Stanbridge, E.J., Cavenee, W.K., and Hampton, G.M. (1997). Genetic alterations accumulate during cervical tumorigenesis and indicate a common origin for multifocal lesions. Cancer research *57*, 4171-4176.

Larue, L., and Bellacosa, A. (2005). Epithelial-mesenchymal transition in development and cancer: role of phosphatidylinositol 3' kinase//AKT pathways. Oncogene *24*, 7443-7454.

Law, N.C., White, M.F., and Hunzicker-Dunn, M.E. (2016). G protein-coupled receptors (GPCRs) That Signal via Protein Kinase A (PKA) Cross-talk at Insulin Receptor Substrate 1 (IRS1) to Activate the phosphatidylinositol 3-kinase (PI3K)/AKT Pathway. Journal of Biological Chemistry *291*, 27160-27169.

Lawler, J. (2002). Thrombospondin-1 as an endogenous inhibitor of angiogenesis and tumor growth. Journal of cellular and molecular medicine *6*, 1-12.

Lee, H., Herrmann, A., Deng, J.-H., Kujawski, M., Niu, G., Li, Z., Forman, S., Jove, R., Pardoll, D.M., and Yu, H. (2009). Persistently Activated Stat3 Maintains Constitutive NF-κB Activity in Tumors. Cancer cell *15*, 283-293.

Lee, J.C., Muller, C.H., Rothman, I., Agnew, K.J., Eschenbach, D., Ciol, M.A., Turner, J.A., and Berger, R.E. (2003). Prostate biopsy culture findings of men with chronic pelvic pain syndrome do not differ from those of healthy controls. The Journal of urology *169*, 584-587; discussion 587-588.

Lee, M.K., Pardoux, C., Hall, M.C., Lee, P.S., Warburton, D., Qing, J., Smith, S.M., and Derynck, R. (2007). TGF-beta activates Erk MAP kinase signalling through direct phosphorylation of ShcA. The EMBO journal *26*, 3957-3967.

Lemarchand, L., Kolonel, L.N., Wilkens, L.R., Myers, B.C., and Hirohata, T. (1994). ANIMAL FAT CONSUMPTION AND PROSTATE-CANCER - A PROSPECTIVE-STUDY IN HAWAII. Epidemiology *5*, 276-282.

Lemmon, M.A., and Schlessinger, J. (2010). Cell signaling by receptor-tyrosine kinases. Cell *141*, 1117-1134.

Lengauer, C., Kinzler, K.W., and Vogelstein, B. (1998). Genetic instabilities in human cancers. Nature *396*, 643-649.

Leung, W.K., Man, E.P., Yu, J., Go, M.Y., To, K.F., Yamaoka, Y., Cheng, V.Y., Ng, E.K., and Sung, J.J. (2006). Effects of *Helicobacter pylori* eradication on methylation status of E-cadherin gene in noncancerous stomach. Clinical cancer research: an official journal of the American Association for Cancer Research *12*, 3216-3221.

Lewis, C.E., and Pollard, J.W. (2006). Distinct role of macrophages in different tumor microenvironments. Cancer research *66*, 605-612.

Lewis, J.S., Landers, R.J., Underwood, J.C., Harris, A.L., and Lewis, C.E. (2000). Expression of vascular endothelial growth factor by macrophages is up-regulated in poorly vascularized areas of breast carcinomas. The Journal of pathology *192*, 150-158.

Li, L.C., Zhao, H., Nakajima, K., Oh, B.R., Ribeiro Filho, L.A., Carroll, P., and Dahiya, R. (2001). Methylation of the E-cadherin gene promoter correlates with progression of prostate cancer. The Journal of urology *166*, 705-709.

Lieu, C., Heymach, J., Overman, M., Tran, H., and Kopetz, S. (2011). Beyond VEGF: Inhibition of the Fibroblast Growth Factor Pathway and Antiangiogenesis. Clinical Cancer Research *17*, 6130-6139.

Lightfoot, N., Conlon, M., Kreiger, N., Sass-Kortsak, A., Purdham, J., and Darlington, G. (2004). Medical history, sexual, and maturational factors and prostate cancer risk. Annals of epidemiology *14*, 655-662.

Lilja, H. (1985). A kallikrein-like serine protease in prostatic fluid cleaves the predominant seminal vesicle protein. The Journal of clinical investigation *76*, 1899-1903.

Lilja, H., Oldbring, J., Rannevik, G., and Laurell, C.B. (1987). Seminal vesicle-secreted proteins and their reactions during gelation and liquefaction of human semen. The Journal of clinical investigation *80*, 281-285.

Lilja, H., Ulmert, D., and Vickers, A.J. (2008). Prostate-specific antigen and prostate cancer: prediction, detection and monitoring. Nature reviews Cancer *8*, 268-278.

Lin, Y., Fukuchi, J., Hiipakka, R.A., Kokontis, J.M., and Xiang, J. (2007). Up-regulation of Bcl-2 is required for the progression of prostate cancer cells from an androgen-dependent to an androgen-independent growth stage. Cell research *17*, 531-536.

Linke, S.P., Clarkin, K.C., Di Leonardo, A., Tsou, A., and Wahl, G.M. (1996). A reversible, p53-dependent G0/G1 cell cycle arrest induced by ribonucleotide depletion in the absence of detectable DNA damage. Genes & development *10*, 934-947.

Linkermann, A., and Green, D.R. (2014). Necroptosis. The New England journal of medicine *370*, 455-465.

Liou, G.-Y., and Storz, P. (2010). Reactive oxygen species in cancer. Free Radical Research *44*, 479-496.

Lippman, S.M., Klein, E.A., Goodman, P.J., Lucia, M.S., Thompson, I.M., Ford, L.G., Parnes, H.L., Minasian, L.M., Gaziano, J.M., Hartline, J.A.*, et al.* (2009). Effect of selenium and vitamin E on risk of prostate cancer and other cancers: the Selenium and Vitamin E Cancer Prevention Trial (SELECT). Jama *301*, 39-51.

Liu, N., Huang, J., Sun, S., Zhou, Z., Zhang, J., Gao, F., and Sun, Q. (2015). Expression of matrix metalloproteinase-9, cyclooxygenase-2 and vascular endothelial growth factor are increased in gastrointestinal stromal tumors. International Journal of Clinical and Experimental Medicine *8*, 6495-6501.

Liu, P.F., Nakatsuji, T., Zhu, W., Gallo, R.L., and Huang, C.M. (2011). Passive Immunoprotection Targeting a Secreted CAMP Factor of *Propionibacterium acnes* as a Novel Immunotherapeutic for Acne Vulgaris. Vaccine *29*, 3230-3238.

Liu, Q., Zhang, Y., Mao, H., Chen, W., Luo, N., Zhou, Q., Chen, W., and Yu, X. (2012). A Crosstalk between the Smad and JNK Signaling in the TGF-β-Induced Epithelial-Mesenchymal Transition in Rat Peritoneal Mesothelial Cells. PloS one *7*, e32009.

Livak, K.J., and Schmittgen, T.D. (2001). Analysis of Relative Gene Expression Data Using Real-Time Quantitative PCR and the 2−ΔΔCT Method. Methods (San Diego, Calif) *25*, 402-408.

Lodygin, D., Epanchintsev, A., Menssen, A., Diebold, J., and Hermeking, H. (2005). Functional epigenomics identifies genes frequently silenced in prostate cancer. Cancer research *65*, 4218-4227.

Loeb, S., and Catalona, W.J. (2014). The Prostate Health Index: a new test for the detection of prostate cancer. Therapeutic Advances in Urology *6*, 74-77.

Lomholt, H.B., and Kilian, M. (2010). Population genetic analysis of *Propionibacterium acnes* identifies a subpopulation and epidemic clones associated with acne. PloS one *5*, e12277.

Lonergan, P., and Tindall, D. (2011). Androgen receptor signaling in prostate cancer development and progression. Journal of Carcinogenesis *10*, 20-20.

Lu, N.Z., Wardell, S.E., Burnstein, K.L., Defranco, D., Fuller, P.J., Giguere, V., Hochberg, R.B., McKay, L., Renoir, J.-M., Weigel, N.L.*, et al.* (2006). International Union of Pharmacology. LXV. The Pharmacology and Classification of the Nuclear Receptor Superfamily: Glucocorticoid, Mineralocorticoid, Progesterone, and Androgen Receptors. Pharmacological Reviews *58*, 782-797.

Lu, P., Weaver, V.M., and Werb, Z. (2012). The extracellular matrix: A dynamic niche in cancer progression. The Journal of cell biology *196*, 395-406.

Luppi, F., Longo, A.M., de Boer, W.I., Rabe, K.F., and Hiemstra, P.S. (2007). Interleukin-8 stimulates cell proliferation in non-small cell lung cancer through epidermal growth factor receptor transactivation. Lung cancer *56*, 25-33.

Lust, J.A., Donovan, K.A., Kline, M.P., Greipp, P.R., Kyle, R.A., and Maihle, N.J. (1992). Isolation of an mRNA encoding a soluble form of the human interleukin-6 receptor. Cytokine *4*, 96-100.

Ma, Q., Fu, W., Li, P., Nicosia, S.V., Jenster, G., Zhang, X., and Bai, W. (2009). FoxO1 Mediates PTEN Suppression of Androgen Receptor N- and C-Terminal Interactions and Coactivator Recruitment. Molecular endocrinology *23*, 213-225.

MacManus, C.F., Pettigrew, J., Seaton, A., Wilson, C., Maxwell, P.J., Berlingeri, S., Purcell, C., McGurk, M., Johnston, P.G., and Waugh, D.J. (2007). Interleukin-8 signaling promotes translational regulation of cyclin D in androgen-independent prostate cancer cells. Molecular cancer research: MCR *5*, 737-748.

Maehama, T., and Dixon, J.E. (1998). The tumor suppressor, PTEN/MMAC1, dephosphorylates the lipid second messenger, phosphatidylinositol 3,4,5-trisphosphate. The Journal of biological chemistry *273*, 13375-13378.

Maekita, T., Nakazawa, K., Mihara, M., Nakajima, T., Yanaoka, K., Iguchi, M., Arii, K., Kaneda, A., Tsukamoto, T., Tatematsu, M*., et al.* (2006). High levels of aberrant DNA methylation in *Helicobacter pylori*-infected gastric mucosae and its possible association with gastric cancer risk. Clinical cancer research: an official journal of the American Association for Cancer Research *12*, 989-995.

Mak, T.N., Fischer, N., Laube, B., Brinkmann, V., Metruccio, M.M., Sfanos, K.S., Mollenkopf, H.J., Meyer, T.F., and Bruggemann, H. (2012). *Propionibacterium acnes* host cell tropism contributes to vimentin-mediated invasion and induction of inflammation. Cellular microbiology *14*, 1720-1733.

Mak, T.N., Sfanos, K.S., and Brüggemann, H. (2013a). Draft Genome Sequences of Two Strains of *Propionibacterium acnes* Isolated from Radical Prostatectomy Specimens. Genome announcements *1*.

Mak, T.N., Yu, S.H., De Marzo, A.M., Bruggemann, H., and Sfanos, K.S. (2013b). Multilocus sequence typing (MLST) analysis of *Propionibacterium acnes* isolates from radical prostatectomy specimens. The Prostate *73*, 770-777.

Makoukji, J., Raad, M., Genadry, K., El-Sitt, S., Makhoul, N.J., Saad Aldin, E., Nohra, E., Jabbour, M., Sangaralingam, A., Chelala, C*., et al.* (2015). Association between CLN3 (Neuronal

Ceroid Lipofuscinosis, CLN3 Type) Gene Expression and Clinical Characteristics of Breast Cancer Patients. Frontiers in oncology *5*.

Malhotra, S., and Kincade, P.W. (2009). Wnt-Related Molecules and Signaling Pathway Equilibrium in Hematopoiesis. Cell Stem Cell *4*, 27-36.

Manning, B.D., and Cantley, L.C. (2007). AKT/PKB Signaling: Navigating Downstream. Cell *129*, 1261-1274.

Manns, M.P., Buti, M., Gane, E., Pawlotsky, J.M., Razavi, H., Terrault, N., and Younossi, Z. (2017). Hepatitis C virus infection. Nature reviews Disease primers *3*, 17006.

Mao, D., Che, J., Han, S., Zhao, H., Zhu, Y., and Zhu, H. (2015). RNAi-mediated knockdown of the CLN3 gene inhibits proliferation and promotes apoptosis in drug-resistant ovarian cancer cells. Molecular medicine reports *12*, 6635-6641.

Marioni, J.C., Mason, C.E., Mane, S.M., Stephens, M., and Gilad, Y. (2008). RNA-seq: An assessment of technical reproducibility and comparison with gene expression arrays. Genome research *18*, 1509-1517.

Marples, R.R., Downing, D.T., and Kligman, A.M. (1971). Control of free fatty acids in human surface lipids by *Corynebacterium acnes*. The Journal of investigative dermatology *56*, 127-131.

Marrack, P., McKee, A.S., and Munks, M.W. (2009). Towards an understanding of the adjuvant action of aluminium. Nature reviews Immunology *9*, 287-293.

Martin-Belmonte, F., and Perez-Moreno, M. (2012). Epithelial cell polarity, stem cells and cancer. Nature reviews Cancer *12*, 23-38.

Maruyama, J., Naguro, I., Takeda, K., and Ichijo, H. (2009). Stress-activated MAP kinase cascades in cellular senescence. Current medicinal chemistry *16*, 1229-1235.

Masciocchi, D., Gelain, A., Villa, S., Meneghetti, F., and Barlocco, D. (2011). Signal transducer and activator of transcription 3 (STAT3): a promising target for anticancer therapy. Future medicinal chemistry *3*, 567-597.

Mason, S.D., and Joyce, J.A. (2011). Proteolytic networks in cancer. Trends in cell biology *21*, 228-237.

Massague, J. (2004). G1 cell-cycle control and cancer. Nature *432*, 298-306.

Matsuda, K., Yoshida, K., Taya, Y., Nakamura, K., Nakamura, Y., and Arakawa, H. (2002). p53AIP1 regulates the mitochondrial apoptotic pathway. Cancer research *62*, 2883-2889.

Matsusaka, K., Funata, S., Fukayama, M., and Kaneda, A. (2014). DNA methylation in gastric cancer, related to *Helicobacter pylori* and Epstein-Barr virus. World journal of gastroenterology: WJG *20*, 3916-3926.

Maxwell, P.J., Coulter, J., Walker, S.M., McKechnie, M., Neisen, J., McCabe, N., Kennedy, R.D., Salto-Tellez, M., Albanese, C., and Waugh, D.J.J. (2013). Potentiation of Inflammatory

CXCL8 Signalling Sustains Cell Survival in PTEN-deficient Prostate Carcinoma. European urology *64*, 177-188.

May, M.J., and Ghosh, S. (1998). Signal transduction through NF-κB. Immunology Today *19*, 80-88.

McCarron, S.L., Edwards, S., Evans, P.R., Gibbs, R., Dearnaley, D.P., Dowe, A., Southgate, C., Easton, D.F., Eeles, R.A., and Howell, W.M. (2002). Influence of cytokine gene polymorphisms on the development of prostate cancer. Cancer research *62*, 3369-3372.

McCarthy, C.J., Crofford, L.J., Greenson, J., and Scheiman, J.M. (1999). Cyclooxygenase-2 expression in gastric antral mucosa before and after eradication of *Helicobacter pylori* infection. The American journal of gastroenterology *94*, 1218-1223.

McClinton, S., Miller, I.D., and Eremin, O. (1990). An immunohistochemical characterisation of the inflammatory cell infiltrate in benign and malignant prostatic disease. British journal of cancer *61*, 400-403.

McDowell, A., Barnard, E., Nagy, I., Gao, A., Tomida, S., Li, H., Eady, A., Cove, J., Nord, C.E., and Patrick, S. (2012a). An expanded multilocus sequence typing scheme for *Propionibacterium acnes*: investigation of 'pathogenic', 'commensal' and antibiotic resistant strains. PloS one *7*, e41480.

McDowell, A., Gao, A., Barnard, E., Fink, C., Murray, P.I., Dowson, C.G., Nagy, I., Lambert, P.A., and Patrick, S. (2011). A novel multilocus sequence typing scheme for the opportunistic pathogen *Propionibacterium acnes* and characterization of type I cell surface-associated antigens. Microbiology *157*, 1990-2003.

McDowell, A., Hunyadkurti, J., Horvath, B., Voros, A., Barnard, E., Patrick, S., and Nagy, I. (2012b). Draft genome sequence of an antibiotic-resistant *Propionibacterium acnes* strain, PRP-38, from the novel type IC cluster. Journal of bacteriology *194*, 3260-3261.

McDowell, A., Nagy, I., Magyari, M., Barnard, E., and Patrick, S. (2013). The opportunistic pathogen *Propionibacterium acnes*: insights into typing, human disease, clonal diversification and CAMP factor evolution. PloS one *8*, e70897.

McDowell, A., Perry, A.L., Lambert, P.A., and Patrick, S. (2008). A new phylogenetic group of *Propionibacterium acnes*. Journal of medical microbiology *57*, 218-224.

McDowell, A., Valanne, S., Ramage, G., Tunney, M.M., Glenn, J.V., McLorinan, G.C., Bhatia, A., Maisonneuve, J.F., Lodes, M., Persing, D.H*., et al.* (2005). *Propionibacterium acnes* types I and II represent phylogenetically distinct groups. Journal of clinical microbiology *43*, 326-334.

McErlean, S.B. (2008). Identification and Characterisation of a Genetic Signature for Invasion in Breast Cancer Cells (University of Ulster).

McNeal, J.E. (1968). Regional Morphology and Pathology of The Prostate. American Journal of Clinical Pathology *49*, 347-357.

McNeal, J.E. (1981). The zonal anatomy of the prostate. The Prostate *2*, 35-49.

McNeal, J.E. (1988). Normal histology of the prostate. The American journal of surgical pathology *12*, 619-633.

McNeal, J.E., Redwine, E.A., Freiha, F.S., and Stamey, T.A. (1988). Zonal distribution of prostatic adenocarcinoma. Correlation with histologic pattern and direction of spread. The American journal of surgical pathology *12*, 897-906.

Mendez, M.G., Kojima, S.-I., and Goldman, R.D. (2010). Vimentin induces changes in cell shape, motility, and adhesion during the epithelial to mesenchymal transition. The FASEB Journal *24*, 1838-1851.

Merrimen, J.L., Evans, A.J., and Srigley, J.R. (2013). Preneoplasia in the prostate gland with emphasis on high grade prostatic intraepithelial neoplasia. Pathology *45*, 251-263.

Messele, T., Roos, M.T.L., Hamann, D., Koot, M., Fontanet, A.L., Miedema, F., Schellekens, P.T.A., and Rinke de Wit, T.F. (2000). Nonradioactive Techniques for Measurement of In Vitro T-Cell Proliferation: Alternatives to the [(3)H]Thymidine Incorporation Assay. Clinical and Diagnostic Laboratory Immunology *7*, 687-692.

Micalizzi, D.S., Farabaugh, S.M., and Ford, H.L. (2010). Epithelial-Mesenchymal Transition in Cancer: Parallels Between Normal Development and Tumor Progression. Journal of Mammary Gland Biology and Neoplasia *15*, 117-134.

Micheau, O., and Tschopp, J. (2003). Induction of TNF receptor I-mediated apoptosis via two sequential signaling complexes. Cell *114*, 181-190.

Miles, A.A., Misra, S.S., and Irwin, J.O. (1938). The estimation of the bactericidal power of the blood. The Journal of hygiene *38*, 732-749.

Millan-Rodriguez, F., Palou, J., Bujons-Tur, A., Musquera-Felip, M., Sevilla-Cecilia, C., Serrallach-Orejas, M., Baez-Angles, C., and Villavicencio-Mavrich, H. (2006). Acute bacterial prostatitis: two different sub-categories according to a previous manipulation of the lower urinary tract. World J Urol *24*, 45-50.

Millman, I., Scott, A.W., and Halbherr, T. (1977). Antitumor activity of *Propionibacterium acnes* (*Corynebacterium parvum*) and isolated cytoplasmic fractions. Cancer research *37*, 4150-4155.

Milovanovic, T., Planutis, K., Nguyen, A., Marsh, J.L., Lin, F., Hope, C., and Holcombe, R.F. (2004). Expression of Wnt genes and frizzled 1 and 2 receptors in normal breast epithelium and infiltrating breast carcinoma. International journal of oncology *25*, 1337-1342.

Mink, S.R., Hodge, A., Agus, D.B., Jain, A., and Gross, M.E. (2010). Beta-2-microglobulin expression correlates with high-grade prostate cancer and specific defects in androgen signaling. The Prostate *70*, 1201-1210.

Miscia, S., Marchisio, M., Grilli, A., Di Valerio, V., Centurione, L., Sabatino, G., Garaci, F., Zauli, G., Bonvini, E., and Di Baldassarre, A. (2002). Tumor necrosis factor alpha (TNF-alpha) activates Jak1/Stat3-Stat5B signaling through TNFR-1 in human B cells. Cell growth & differentiation: the molecular biology journal of the American Association for Cancer Research *13*, 13-18.

Miskin, J.E., Farrell, A.M., Cunliffe, W.J., and Holland, K.T. (1997). *Propionibacterium acnes*, a resident of lipid-rich human skin, produces a 33 kDa extracellular lipase encoded by gehA. Microbiology *143 (Pt 5)*, 1745-1755.

Mitsuhashi, K., Nosho, K., Sukawa, Y., Matsunaga, Y., Ito, M., Kurihara, H., Kanno, S., Igarashi, H., Naito, T., Adachi, Y.*, et al.* (2015). Association of *Fusobacterium* species in pancreatic cancer tissues with molecular features and prognosis. Oncotarget *6*, 7209-7220.

Mohsen, A.H., Price, A., Ridgway, E., West, J.N., Green, S., and McKendrick, M.W. (2001). *Propionibacterium acnes* endocarditis in a native valve complicated by intraventricular abscess: a case report and review. Scandinavian journal of infectious diseases *33*, 379-380.

Monga, S.P.S. (2011). Role of Wnt/β-catenin signaling in liver metabolism and cancer. The International Journal of Biochemistry & Cell Biology *43*, 1021-1029.

Montagut, C., and Settleman, J. (2009). Targeting the RAF–MEK–ERK pathway in cancer therapy. Cancer letters *283*, 125-134.

Montgomery, R.B., Mostaghel, E.A., Vessella, R., Hess, D.L., Kalhorn, T.F., Higano, C.S., True, L.D., and Nelson, P.S. (2008). Maintenance of Intratumoral Androgens in Metastatic Prostate Cancer: A Mechanism for Castration-Resistant Tumor Growth. Cancer research *68*, 4447-4454.

Mortara, L., Benest, A.V., Bates, D.O., and Noonan, D.M. (2017). Can the co-dependence of the immune system and angiogenesis facilitate pharmacological targeting of tumours? Current opinion in pharmacology *35*, 66-74.

Mottet, N., Bellmunt, J., Bolla, M., Briers, E., Cumberbatch, M.G., De Santis, M., Fossati, N., Gross, T., Henry, A.M., Joniau, S.*, et al.* (2017). EAU-ESTRO-SIOG Guidelines on Prostate Cancer. Part 1: Screening, Diagnosis, and Local Treatment with Curative Intent. European urology *71*, 618-629.

Moyer, V.A. (2012). Screening for prostate cancer: U.S. Preventive Services Task Force recommendation statement. Annals of internal medicine *157*, 120-134.

Muraoka-Cook, R.S., Dumont, N., and Arteaga, C.L. (2005). Dual role of transforming growth factor beta in mammary tumorigenesis and metastatic progression. Clinical cancer research: an official journal of the American Association for Cancer Research *11*, 937s-943s.

Murtola, T.J., Syvala, H., Pennanen, P., Blauer, M., Solakivi, T., Ylikomi, T., and Tammela, T.L. (2012). The importance of LDL and cholesterol metabolism for prostate epithelial cell growth. PloS one *7*, e39445.

Nagy, T.A., Frey, M.R., Yan, F., Israel, D.A., Polk, D.B., and Peek, R.M., Jr. (2009). *Helicobacter pylori* regulates cellular migration and apoptosis by activation of phosphatidylinositol 3-kinase signaling. The Journal of infectious diseases *199*, 641-651.

Nakamura, T., Furukawa, A., Uchida, K., Ogawa, T., Tamura, T., Sakonishi, D., Wada, Y., Suzuki, Y., Ishige, Y., Minami, J.*, et al.* (2016). Autophagy Induced by Intracellular Infection of *Propionibacterium acnes*. PloS one *11*, e0156298.

Nakano, H., Shindo, M., Sakon, S., Nishinaka, S., Mihara, M., Yagita, H., and Okumura, K. (1998). Differential regulation of IκB kinase α and β by two upstream kinases, NF-κB-inducing kinase and mitogen-activated protein kinase/ERK kinase kinase-1. Proceedings of the National Academy of Sciences *95*, 3537-3542.

Nakao, A., Imamura, T., Souchelnytskyi, S., Kawabata, M., Ishisaki, A., Oeda, E., Tamaki, K., Hanai, J., Heldin, C.H., Miyazono, K.*, et al.* (1997). TGF-beta receptor-mediated signalling through Smad2, Smad3 and Smad4. The EMBO journal *16*, 5353-5362.

Nakashima, J., Tachibana, M., Ueno, M., Baba, S., and Tazaki, H. (1995). Tumor necrosis factor and coagulopathy in patients with prostate cancer. Cancer research *55*, 4881-4885.

Nakatani, K., Thompson, D.A., Barthel, A., Sakaue, H., Liu, W., Weigel, R.J., and Roth, R.A. (1999). Up-regulation of Akt3 in Estrogen Receptor-deficient Breast Cancers and Androgen-independent Prostate Cancer Lines. Journal of Biological Chemistry *274*, 21528-21532.

Nakatsuji, T., Tang, D.C., Zhang, L., Gallo, R.L., and Huang, C.M. (2011). *Propionibacterium acnes* CAMP factor and host acid sphingomyelinase contribute to bacterial virulence: potential targets for inflammatory acne treatment. PloS one *6*, e14797.

Nakaya, Y., and Sheng, G. (2008). Epithelial to mesenchymal transition during gastrulation: An embryological view. Development, Growth & Differentiation *50*, 755-766.

Nardone, G., Compare, D., De Colibus, P., de Nucci, G., and Rocco, A. (2007). *Helicobacter pylori* and epigenetic mechanisms underlying gastric carcinogenesis. Digestive diseases (Basel, Switzerland) *25*, 225-229.

Narod, S.A., Neuhausen, S., Vichodez, G., Armel, S., Lynch, H.T., Ghadirian, P., Cummings, S., Olopade, O., Stoppa-Lyonnet, D., Couch, F.*, et al.* (2008). Rapid progression of prostate cancer in men with a BRCA2 mutation. British journal of cancer *99*, 371-374.

Nelson, W.G., De Marzo, A.M., and Isaacs, W.B. (2003). Prostate Cancer. New England Journal of Medicine *349*, 366-381.

Nemeth, M.J., Mak, K.K., Yang, Y., and Bodine, D.M. (2009). β-Catenin Expression in the Bone Marrow Microenvironment Is Required for Long-Term Maintenance of Primitive Hematopoietic Cells. STEM CELLS *27*, 1109-1119.

Newman, A.C., and Hughes, C.C.W. (2012). Macrophages and angiogenesis: a role for Wnt signaling. Vascular Cell *4*, 13.

Niault, T.S., and Baccarini, M. (2010). Targets of Raf in tumorigenesis. Carcinogenesis *31*, 1165-1174.

Nickel, J.C., Downey, J., Young, I., and Boag, S. (1999). Asymptomatic inflammation and/or infection in benign prostatic hyperplasia. BJU international *84*, 976-981.

Ninomiya-Tsuji, J., Kishimoto, K., Hiyama, A., Inoue, J.-i., Cao, Z., and Matsumoto, K. (1999). The kinase TAK1 can activate the NIK-IκB as well as the MAP kinase cascade in the IL-1 signalling pathway. Nature *398*, 252-256.

Nisticò, P., Bissell, M.J., and Radisky, D.C. (2012). Epithelial-Mesenchymal Transition: General Principles and Pathological Relevance with Special Emphasis on the Role of Matrix Metalloproteinases. Cold Spring Harbor perspectives in biology *4*.

Norman, A.W., and Henry, H.L. (2015). Chapter 12 - Androgens. In Hormones (Third Edition) (San Diego: Academic Press), pp. 255-273.

Oeckinghaus, A., and Ghosh, S. (2009). The NF-kappaB family of transcription factors and its regulation. Cold Spring Harbor perspectives in biology *1*, a000034.

Ohl, F., Jung, M., Xu, C., Stephan, C., Rabien, A., Burkhardt, M., Nitsche, A., Kristiansen, G., Loening, S.A., Radonić, A.*, et al.* (2005). Gene expression studies in prostate cancer tissue: which reference gene should be selected for normalization? Journal of Molecular Medicine *83*, 1014-1024.

Olson, O.C., and Joyce, J.A. (2015). Cysteine cathepsin proteases: regulators of cancer progression and therapeutic response. Nature Reviews Cancer *15*, 712.

Olsson, J., Drott, J.B., Laurantzon, L., Laurantzon, O., Bergh, A., and Elgh, F. (2012). Chronic prostatic infection and inflammation by *Propionibacterium acnes* in a rat prostate infection model. PloS one *7*, e51434.

Opitz, O.G., Suliman, Y., Hahn, W.C., Harada, H., Blum, H.E., and Rustgi, A.K. (2001). Cyclin D1 overexpression and p53 inactivation immortalize primary oral keratinocytes by a telomerase-independent mechanism. The Journal of clinical investigation *108*, 725-732.

Otalora, B.B., Madrid, J.A., Alvarez, N., Vicente, V., and Rol, M.A. (2008). Effects of exogenous melatonin and circadian synchronization on tumor progression in melanoma-bearing C57BL6 mice. Journal of pineal research *44*, 307-315.

Otto, T., and Sicinski, P. (2017). Cell cycle proteins as promising targets in cancer therapy. Nature reviews Cancer *17*, 93-115.

Pahl, H.L. (1999). Activators and target genes of Rel/NF-kappaB transcription factors. Oncogene *18*, 6853-6866.

Panigrahy, D. (2010). Inhibition of tumor angiogenesis by oral etoposide. *1*, 739-746.

Park, B.K., Zeng, X., and Glazer, R.I. (2001). Akt1 induces extracellular matrix invasion and matrix metalloproteinase-2 activity in mouse mammary epithelial cells. Cancer research *61*, 7647-7653.

Park, O.K., Schaefer, T.S., and Nathans, D. (1996). In vitro activation of Stat3 by epidermal growth factor receptor kinase. Proceedings of the National Academy of Sciences *93*, 13704-13708.

Park, S.H., Kim, K.E., Hwang, H.Y., and Kim, T.Y. (2003). Regulatory effect of SOCS on NF-kappaB activity in murine monocytes/macrophages. DNA Cell Biol *22*, 131-139.

Parsonnet, J., Friedman, G.D., Vandersteen, D.P., Chang, Y., Vogelman, J.H., Orentreich, N., and Sibley, R.K. (1991). *Helicobacter pylori* infection and the risk of gastric carcinoma. The New England journal of medicine *325*, 1127-1131.

Pasparakis, M., and Vandenabeele, P. (2015). Necroptosis and its role in inflammation. Nature *517*, 311-320.

Patel, D.A., Bock, C.H., Schwartz, K., Wenzlaff, A.S., Demers, R.Y., and Severson, R.K. (2005). Sexually transmitted diseases and other urogenital conditions as risk factors for prostate cancer: a case--control study in Wayne County, Michigan. Cancer causes & control: CCC *16*, 263-273.

Pećina-Šlaus, N. (2010). Wnt signal transduction pathway and apoptosis: a review. Cancer Cell International *10*, 22.

Peinado, H., Olmeda, D., and Cano, A. (2007). Snail, Zeb and bHLH factors in tumour progression: an alliance against the epithelial phenotype? Nature reviews Cancer *7*, 415-428.

Pepper, M.S. (1997). Transforming growth factor-beta: vasculogenesis, angiogenesis, and vessel wall integrity. Cytokine & growth factor reviews *8*, 21-43.

Perez-Roger, I., Kim, S.H., Griffiths, B., Sewing, A., and Land, H. (1999). Cyclins D1 and D2 mediate myc-induced proliferation via sequestration of p27(Kip1) and p21(Cip1). The EMBO journal *18*, 5310-5320.

Perkins, N.D., and Gilmore, T.D. (2006). Good cop, bad cop: the different faces of NFκB. Cell Death Differ *13*, 759-772.

Phin, S., Moore, M.W., and Cotter, P.D. (2013). Genomic Rearrangements of PTEN in Prostate Cancer. Frontiers in oncology *3*.

Pierconti, F., Martini, M., Pinto, F., Cenci, T., Capodimonti, S., Calarco, A., Bassi, P.F., and Larocca, L.M. (2011). Epigenetic silencing of SOCS3 identifies a subset of prostate cancer with an aggressive behavior. The Prostate *71*, 318-325.

Pilepich, M.V., Caplan, R., Byhardt, R.W., Lawton, C.A., Gallagher, M.J., Mesic, J.B., Hanks, G.E., Coughlin, C.T., Porter, A., Shipley, W.U.*, et al.* (1997). Phase III trial of androgen suppression using goserelin in unfavorable-prognosis carcinoma of the prostate treated with definitive radiotherapy: report of Radiation Therapy Oncology Group Protocol 85-31. Journal of clinical oncology: official journal of the American Society of Clinical Oncology *15*, 1013-1021.

Pilepich, M.V., Krall, J.M., al-Sarraf, M., John, M.J., Doggett, R.L., Sause, W.T., Lawton, C.A., Abrams, R.A., Rotman, M., Rubin, P.*, et al.* (1995). Androgen deprivation with radiation therapy compared with radiation therapy alone for locally advanced prostatic carcinoma: a randomized comparative trial of the Radiation Therapy Oncology Group. Urology *45*, 616-623.

Pimienta, G., and Pascual, J. (2007). Canonical and Alternative MAPK Signaling. Cell cycle *6*, 2628-2632.

Pinsky, P.F., Kramer, B.S., Crawford, E.D., Grubb, R.L., Urban, D.A., Andriole, G.L., Chia, D., Levin, D.L., and Gohagan, J.K. (2006). Prostate volume and prostate-specific antigen levels in men enrolled in a large screening trial. Urology *68*, 352-356.

Pinto, D., and Clevers, H. (2005). Wnt control of stem cells and differentiation in the intestinal epithelium. Experimental cell research *306*, 357-363.

Placzek, W.J., Wei, J., Kitada, S., Zhai, D., Reed, J.C., and Pellecchia, M. (2010). A survey of the anti-apoptotic Bcl-2 subfamily expression in cancer types provides a platform to predict the efficacy of Bcl-2 antagonists in cancer therapy. Cell Death and Dis *1*, e40.

Plonis, J., Nakazawa-Miklasevica, M., Malevskis, A., Vaganovs, P., Pildava, S., Vjaters, E., Gardovskis, J., and Miklasevics, E. (2015). Survival rates of familial and sporadic prostate cancer patients. Experimental oncology *37*, 154-155.

Plotnikov, A., Zehorai, E., Procaccia, S., and Seger, R. (2011). The MAPK cascades: Signaling components, nuclear roles and mechanisms of nuclear translocation. Biochimica et Biophysica Acta (BBA) - Molecular Cell Research *1813*, 1619-1633.

Polakis, P. (2007). The many ways of Wnt in cancer. Current Opinion in Genetics & Development *17*, 45-51.

Polakis, P. (2012). Drugging Wnt signalling in cancer. The EMBO journal *31*, 2737-2746.

Pommier, Y., Leo, E., Zhang, H., and Marchand, C. (2010). DNA Topoisomerases and Their Poisoning by Anticancer and Antibacterial Drugs. Chemistry & Biology *17*, 421-433.

Presti, J.C. (2007). Prostate biopsy strategies. Nat Clin Pract Urol *4*, 505-511.

Price, P.J., and Gregory, E.A. (1982). Relationship between in vitro growth promotion and biophysical and biochemical properties of the serum supplement. In Vitro *18*, 576-584.

Probert, L. (2015). TNF and its receptors in the CNS: The essential, the desirable and the deleterious effects. Neuroscience *302*, 2-22.

Pugh, C.W., and Ratcliffe, P.J. (2003). Regulation of angiogenesis by hypoxia: role of the HIF system. Nature medicine *9*, 677-684.

Puto, L.A., Brognard, J., and Hunter, T. (2015). Transcriptional Repressor DAXX Promotes Prostate Cancer Tumorigenicity via Suppression of Autophagy. The Journal of biological chemistry *290*, 15406-15420.

Putzi, M.J., and De Marzo, A.M. (2000). Morphologic transitions between proliferative inflammatory atrophy and high-grade prostatic intraepithelial neoplasia. Urology *56*, 828-832.

Qin, Y., Capaldo, C., Gumbiner, B.M., and Macara, I.G. (2005). The mammalian Scribble polarity protein regulates epithelial cell adhesion and migration through E-cadherin. The Journal of cell biology *171*, 1061-1071.

Qiu, S.D., Young, C.Y., Bilhartz, D.L., Prescott, J.L., Farrow, G.M., He, W.W., and Tindall, D.J. (1990). In situ hybridization of prostate-specific antigen mRNA in human prostate. The Journal of urology *144*, 1550-1556.

Quail, D.F., and Joyce, J.A. (2013). Microenvironmental regulation of tumor progression and metastasis. Nature medicine *19*, 1423-1437.

Ragde, H., Grado, G.L., Nadir, B., and Elgamal, A.-A. (2000). Modern prostate brachytherapy. CA: a cancer journal for clinicians *50*, 380-393.

Raheem, O.A., Cohen, S.A., Parsons, J.K., Palazzi, K.L., and Kane, C.J. (2015). A Family History of Lethal Prostate Cancer and Risk of Aggressive Prostate Cancer in Patients Undergoing Radical Prostatectomy. Scientific reports *5*, 10544.

Rakoff-Nahoum, S., and Medzhitov, R. (2009). Toll-like receptors and cancer. Nature reviews Cancer *9*, 57-63.

Ramage, G., Tunney, M.M., Patrick, S., Gorman, S.P., and Nixon, J.R. (2003). Formation of *Propionibacterium acnes* biofilms on orthopaedic biomaterials and their susceptibility to antimicrobials. Biomaterials *24*, 3221-3227.

Raman, M., Chen, W., and Cobb, M.H. (2007). Differential regulation and properties of MAPKs. Oncogene *26*, 3100-3112.

Ramsay, C., Pickard, R., Robertson, C., Close, A., Vale, L., Armstrong, N., Barocas, D.A., Eden, C.G., Fraser, C., Gurung, T*., et al.* (2012). Systematic review and economic modelling of the relative clinical benefit and cost-effectiveness of laparoscopic surgery and robotic

surgery for removal of the prostate in men with localised prostate cancer. Health Technol Assess *16*, 313.

Ramsey, B.W., Davies, J., McElvaney, N.G., Tullis, E., Bell, S.C., Drevinek, P., Griese, M., McKone, E.F., Wainwright, C.E., Konstan, M.W.*, et al.* (2011). A CFTR potentiator in patients with cystic fibrosis and the G551D mutation. The New England journal of medicine *365*, 1663-1672.

Randazzo, M., Muller, A., Carlsson, S., Eberli, D., Huber, A., Grobholz, R., Manka, L., Mortezavi, A., Sulser, T., Recker, F.*, et al.* (2016). A positive family history as a risk factor for prostate cancer in a population-based study with organised prostate-specific antigen screening: results of the Swiss European Randomised Study of Screening for Prostate Cancer (ERSPC, Aarau). BJU international *117*, 576-583.

Ravitz, M.J., and Wenner, C.E. (1997). Cyclin-dependent kinase regulation during G1 phase and cell cycle regulation by TGF-beta. Advances in cancer research *71*, 165-207.

Rawson, J.B., Mrkonjic, M., Daftary, D., Dicks, E., Buchanan, D.D., Younghusband, H.B., Parfrey, P.S., Young, J.P., Pollett, A., Green, R.C.*, et al.* (2011). Promoter methylation of Wnt5a is associated with microsatellite instability and BRAF V600E mutation in two large populations of colorectal cancer patients. British journal of cancer *104*, 1906-1912.

Raymaekers, K., Stegen, S., van Gastel, N., and Carmeliet, G. (2015). The vasculature: a vessel for bone metastasis. BoneKEy Rep.

Rehman, A., Baloch, N.U., and Janahi, I.A. (2015). Lumacaftor-Ivacaftor in Patients with Cystic Fibrosis Homozygous for Phe508del CFTR. The New England journal of medicine *373*, 1783.

Rhee, C.S., Sen, M., Lu, D., Wu, C., Leoni, L., Rubin, J., Corr, M., and Carson, D.A. (2002). Wnt and frizzled receptors as potential targets for immunotherapy in head and neck squamous cell carcinomas. Oncogene *21*, 6598-6605.

Ricote, M., García-Tuñón, I., Bethencourt, F.R., Fraile, B., Paniagua, R., and Royuela, M. (2004). Interleukin-1 (IL-1α and IL-1β) and its receptors (IL-1RI, IL-1RII, and IL-1Ra) in prostate carcinoma. Cancer *100*, 1388-1396.

Ritter, S.L., and Hall, R.A. (2009). Fine-tuning of GPCR activity by receptor-interacting proteins. Nature reviews Molecular cell biology *10*, 819-830.

Robbins, H.A., Engels, E.A., Pfeiffer, R.M., and Shiels, M.S. (2015). Age at cancer diagnosis for blacks compared with whites in the United States. Journal of the National Cancer Institute *107*.

Roca, H., Varsos, Z.S., Sud, S., Craig, M.J., Ying, C., and Pienta, K.J. (2009). CCL2 and Interleukin-6 Promote Survival of Human CD11b+ Peripheral Blood Mononuclear Cells and Induce M2-type Macrophage Polarization. Journal of Biological Chemistry *284*, 34342-34354.

Rodríguez-Berriguete, G., Torrealba, N., Ortega, M.A., Martínez-Onsurbe, P., Olmedilla, G., Paniagua, R., Guil-Cid, M., Fraile, B., and Royuela, M. (2015). Prognostic value of inhibitors of apoptosis proteins (IAPs) and caspases in prostate cancer: caspase-3 forms and XIAP predict biochemical progression after radical prostatectomy. BMC cancer *15*, 809.

Ross, J.I., Eady, E.A., Cove, J.H., and Cunliffe, W.J. (1998). 16S rRNA mutation associated with tetracycline resistance in a gram-positive bacterium. Antimicrobial agents and chemotherapy *42*, 1702-1705.

Ross, J.I., Eady, E.A., Cove, J.H., Jones, C.E., Ratyal, A.H., Miller, Y.W., Vyakrnam, S., and Cunliffe, W.J. (1997). Clinical resistance to erythromycin and clindamycin in cutaneous propionibacteria isolated from acne patients is associated with mutations in 23S rRNA. Antimicrobial agents and chemotherapy *41*, 1162-1165.

Rowles, J.L., 3rd, Ranard, K.M., Smith, J.W., An, R., and Erdman, J.W., Jr. (2017). Increased dietary and circulating lycopene are associated with reduced prostate cancer risk: a systematic review and meta-analysis. Prostate cancer and prostatic diseases.

Rubinstein, Mara R., Wang, X., Liu, W., Hao, Y., Cai, G., and Han, Yiping W. (2013). *Fusobacterium nucleatum* Promotes Colorectal Carcinogenesis by Modulating E-Cadherin/β-Catenin Signaling via its FadA Adhesin. Cell host & microbe *14*, 195-206.

Rui, L., Yuan, M., Frantz, D., Shoelson, S., and White, M.F. (2002). SOCS-1 and SOCS-3 block insulin signaling by ubiquitin-mediated degradation of IRS1 and IRS2. The Journal of biological chemistry *277*, 42394-42398.

Ryan, C.J., Smith, A., Lal, P., Satagopan, J., Reuter, V., Scardino, P., Gerald, W., and Scher, H.I. (2006). Persistent prostate-specific antigen expression after neoadjuvant androgen depletion: An early predictor of relapse or incomplete androgen suppression. Urology *68*, 834-839.

Rylova, S.N., Amalfitano, A., Persaud-Sawin, D.A., Guo, W.X., Chang, J., Jansen, P.J., Proia, A.D., and Boustany, R.M. (2002). The CLN3 gene is a novel molecular target for cancer drug discovery. Cancer research *62*, 801-808.

Sabatini, D.M. (2006). mTOR and cancer: insights into a complex relationship. Nature reviews Cancer *6*, 729-734.

Sakr, W.A., Macoska, J.A., Benson, P., Grignon, D.J., Wolman, S.R., Pontes, J.E., and Crissman, J.D. (1994). Allelic loss in locally metastatic, multisampled prostate cancer. Cancer research *54*, 3273-3277.

Sampedro, M.F., Piper, K.E., McDowell, A., Patrick, S., Mandrekar, J.N., Rouse, M.S., Steckelberg, J.M., and Patel, R. (2009). Species of Propionibacterium and *Propionibacterium acnes*

phylotypes associated with orthopedic implants. Diagnostic microbiology and infectious disease *64*, 138-145.

Sanchez-Chapado, M., Olmedilla, G., Cabeza, M., Donat, E., and Ruiz, A. (2003). Prevalence of prostate cancer and prostatic intraepithelial neoplasia in Caucasian Mediterranean males: an autopsy study. The Prostate *54*, 238-247.

Sartor, C.I., Dziubinski, M.L., Yu, C.L., Jove, R., and Ethier, S.P. (1997). Role of epidermal growth factor receptor and STAT-3 activation in autonomous proliferation of SUM-102PT human breast cancer cells. Cancer research *57*, 978-987.

Savvidis, C., and Koutsilieris, M. (2012). Circadian Rhythm Disruption in Cancer Biology. Molecular medicine *18*, 1249-1260.

Sayanjali, B., Christensen, G.J., Al-Zeer, M.A., Mollenkopf, H.J., Meyer, T.F., and Bruggemann, H. (2016). *Propionibacterium acnes* inhibits FOXM1 and induces cell cycle alterations in human primary prostate cells. International journal of medical microbiology: IJMM.

Schaefer, L.K., Ren, Z., Fuller, G.N., and Schaefer, T.S. (2002). Constitutive activation of Stat3alpha] in brain tumors: localization to tumor endothelial cells and activation by the endothelial tyrosine kinase receptor (VEGFR-2). Oncogene *21*, 2058-2065.

Scheid, M.P., and Woodgett, J.R. (2001). PKB/AKT: functional insights from genetic models. Nature reviews Molecular cell biology *2*, 760-768.

Schiffman, M., Doorbar, J., Wentzensen, N., de Sanjose, S., Fakhry, C., Monk, B.J., Stanley, M.A., and Franceschi, S. (2016). Carcinogenic human papillomavirus infection. Nature reviews Disease primers *2*, 16086.

Schmid, J.A., and Birbach, A. (2008). IκB kinase β (IKKβ/IKK2/IKBKB)—A key molecule in signaling to the transcription factor NF-κB. Cytokine & growth factor reviews *19*, 157-165.

Schneider, C.A., Rasband, W.S., and Eliceiri, K.W. (2012). NIH Image to ImageJ: 25 years of image analysis. Nature methods *9*, 671-675.

Scholz, C.F., Jensen, A., Lomholt, H.B., Bruggemann, H., and Kilian, M. (2014). A novel high-resolution single locus sequence typing scheme for mixed populations of *Propionibacterium acnes* in vivo. PloS one *9*, e104199.

Scholz, C.F.P., and Kilian, M. (2016). The natural history of cutaneous propionibacteria, and reclassification of selected species within the genus *Propionibacterium* to the proposed novel genera *Acidipropionibacterium* gen. nov., *Cutibacterium* gen. nov. and *Pseudopropionibacterium* gen. nov. International journal of systematic and evolutionary microbiology *66*, 4422-4432.

Scott, N.F. (2009). Investigating the Key Regulators of Invasion and Metastasis in a Breast Cancer Cell Line Model (University of Ulster).

Sen, R., and Baltimore, D. (1986). Multiple nuclear factors interact with the immunoglobulin enhancer sequences. Cell *46*, 705-716.

Seoane, J., Pouponnot, C., Staller, P., Schader, M., Eilers, M., and Massague, J. (2001). TGFβ influences Myc, Miz-1 and Smad to control the CDK inhibitor p15INK4b. Nature cell biology *3*, 400-408.

Seong, M.K., Lee, J.Y., Byeon, J., Sohn, Y.J., Seol, H., Lee, J.K., Kim, E.K., Kim, H.A., and Noh, W.C. (2015). Bcl-2 is a highly significant prognostic marker of hormone-receptor-positive, human epidermal growth factor receptor-2-negative breast cancer. Breast cancer research and treatment *150*, 141-148.

Serrano-Gomez, S.J., Maziveyi, M., and Alahari, S.K. (2016). Regulation of epithelial-mesenchymal transition through epigenetic and post-translational modifications. Molecular cancer *15*.

Sfanos, K.S., and De Marzo, A.M. (2012). Prostate cancer and inflammation: the evidence. Histopathology *60*, 199-215.

Sfanos, K.S., Sauvageot, J., Fedor, H.L., Dick, J.D., De Marzo, A.M., and Isaacs, W.B. (2008). A molecular analysis of prokaryotic and viral DNA sequences in prostate tissue from patients with prostate cancer indicates the presence of multiple and diverse microorganisms. The Prostate *68*, 306-320.

Shang, Y., Myers, M., and Brown, M. (2002). Formation of the Androgen Receptor Transcription Complex. Molecular Cell *9*, 601-610.

Shannon, B.A., Cohen, R.J., and Garrett, K.L. (2006a). Polymerase chain reaction-based identification of *Propionibacterium acnes* types isolated from the male urinary tract: evaluation of adolescents, normal adults and men with prostatic pathology. BJU international *98*, 388-392.

Shannon, B.A., Garrett, K.L., and Cohen, R.J. (2006b). Links between *Propionibacterium acnes* and prostate cancer. Future oncology *2*, 225-232.

Shao, Y., Hu, D., and Chen, J. (2008). A study on effect of bFGF, EGF and NGF on growth of cultured human corneal endothelial cells. Yan ke xue bao = Eye science *24*, 9-12.

Sharma, M., Bose, M., Abhimanyu, Sharma, L., Diwakar, A., Kumar, S., Gaur, S.N., and Banavalikar, J.N. (2012). Intracellular survival of *Mycobacterium tuberculosis* in macrophages is modulated by phenotype of the pathogen and immune status of the host. International Journal of Mycobacteriology *1*, 65-74.

Shaul, Y.D., and Seger, R. (2007). The MEK/ERK cascade: From signaling specificity to diverse functions. Biochimica et Biophysica Acta (BBA) - Molecular Cell Research *1773*, 1213-1226.

Shibuya, M. (2011). Vascular Endothelial Growth Factor (VEGF) and Its Receptor (VEGFR) Signaling in Angiogenesis: A Crucial Target for Anti- and Pro-Angiogenic Therapies. Genes & cancer *2*, 1097-1105.

Shimizu, H., Ross, R.K., Bernstein, L., Yatani, R., Henderson, B.E., and Mack, T.M. (1991). Cancers of the prostate and breast among Japanese and white immigrants in Los Angeles County. British journal of cancer *63*, 963-966.

Shimono, A., Okuda, T., and Kondoh, H. (1999). N-myc-dependent repression of ndr1, a gene identified by direct subtraction of whole mouse embryo cDNAs between wild type and N-myc mutant. Mechanisms of development *83*, 39-52.

Shinohara, D.B., Vaghasia, A.M., Yu, S.H., Mak, T.N., Brüggemann, H., Nelson, W.G., De Marzo, A.M., Yegnasubramanian, S., and Sfanos, K.S. (2013). A Mouse Model of Chronic Prostatic Inflammation Using a Human Prostate Cancer-Derived Isolate of *Propionibacterium acnes*. The Prostate *73*, 1007-1015.

Shtutman, M., Zhurinsky, J., Simcha, I., Albanese, C., D'Amico, M., Pestell, R., and Ben-Ze'ev, A. (1999). The cyclin D1 gene is a target of the beta-catenin/LEF-1 pathway. Proceedings of the National Academy of Sciences of the United States of America *96*, 5522-5527.

Siegel, R.L., Miller, K.D., and Jemal, A. (2017). Cancer statistics, 2017. CA: a cancer journal for clinicians *67*, 7-30.

Simpson, K.J., Selfors, L.M., Bui, J., Reynolds, A., Leake, D., Khvorova, A., and Brugge, J.S. (2008). Identification of genes that regulate epithelial cell migration using an siRNA screening approach. Nature cell biology *10*, 1027-1038.

Siveen, K.S., Sikka, S., Surana, R., Dai, X., Zhang, J., Kumar, A.P., Tan, B.K.H., Sethi, G., and Bishayee, A. (2014). Targeting the STAT3 signaling pathway in cancer: Role of synthetic and natural inhibitors. Biochimica et Biophysica Acta (BBA) - Reviews on Cancer *1845*, 136-154.

Small, D.M., Burden, R.E., Jaworski, J., Hegarty, S.M., Spence, S., Burrows, J.F., McFarlane, C., Kissenpfennig, A., McCarthy, H.O., Johnston, J.A*., et al.* (2013). Cathepsin S from both tumor and tumor-associated cells promote cancer growth and neovascularization. International journal of cancer Journal international du cancer *133*, 2102-2112.

Smittenaar, C.R., Petersen, K.A., Stewart, K., and Moitt, N. (2016). Cancer incidence and mortality projections in the UK until 2035. British journal of cancer *115*, 1147-1155.

Smyth, M.J., Dunn, G.P., and Schreiber, R.D. (2006). Cancer Immunosurveillance and Immunoediting: The Roles of Immunity in Suppressing Tumor Development and Shaping Tumor Immunogenicity. Advances in Immunology *90*, 1-50.

Soderquist, B., Holmberg, A., and Unemo, M. (2010). *Propionibacterium acnes* as an etiological agent of arthroplastic and osteosynthetic infections--two cases with specific clinical presentation including formation of draining fistulae. Anaerobe *16*, 304-306.

Sohn, S.J., Thompson, J., and Winoto, A. (2007). Apoptosis during negative selection of autoreactive thymocytes. Current Opinion in Immunology *19*, 510-515.

Soler, A., Serra, H., Pearce, W., Angulo, A., Guillermet-Guibert, J., Friedman, L.S., Viñals, F., Gerhardt, H., Casanovas, O., Graupera, M.*, et al.* (2013). Inhibition of the p110α isoform of PI 3-kinase stimulates nonfunctional tumor angiogenesis. The Journal of experimental medicine *210*, 1937-1945.

Somani, S., Grinbaum, A., and Slomovic, A.R. (1997). Postoperative endophthalmitis: incidence, predisposing surgery, clinical course and outcome. Canadian journal of ophthalmology Journal canadien d'ophtalmologie *32*, 303-310.

Sooriakumaran, P., and Kaba, R. (2005). The risks and benefits of cyclo-oxygenase-2 inhibitors in prostate cancer: A review. International Journal of Surgery *3*, 278-285.

Soos, G., Tsakiris, I., Szanto, J., Turzo, C., Haas, P.G., and Dezso, B. (2005). The prevalence of prostate carcinoma and its precursor in Hungary: an autopsy study. European urology *48*, 739-744.

Staal, S.P. (1987). Molecular cloning of the akt oncogene and its human homologues AKT1 and AKT2: amplification of AKT1 in a primary human gastric adenocarcinoma. Proceedings of the National Academy of Sciences of the United States of America *84*, 5034-5037.

Stanbrough, M., Bubley, G.J., Ross, K., Golub, T.R., Rubin, M.A., Penning, T.M., Febbo, P.G., and Balk, S.P. (2006). Increased Expression of Genes Converting Adrenal Androgens to Testosterone in Androgen-Independent Prostate Cancer. Cancer research *66*, 2815-2825.

Steinberg, G.D., Carter, B.S., Beaty, T.H., Childs, B., and Walsh, P.C. (1990). Family history and the risk of prostate cancer. The Prostate *17*, 337-347.

Stewart, R.W., Lizama, S., Peairs, K., Sateia, H.F., and Choi, Y. (2017). Screening for prostate cancer. Seminars in Oncology *44*, 47-56.

Stirling, A., Worthington, T., Rafiq, M., Lambert, P.A., and Elliott, T.S.J. (2001). Association between sciatica and *Propionibacterium acnes*. The Lancet *357*, 2024-2025.

Stockmann, C., Schadendorf, D., Klose, R., and Helfrich, I. (2014). The Impact of the Immune System on Tumor: Angiogenesis and Vascular Remodeling. Frontiers in oncology *4*.

Strieter, R.M. (2002). Interleukin-8: a very important chemokine of the human airway epithelium. American Journal of Physiology - Lung Cellular and Molecular Physiology *283*, L688-L689.

Strieter, R.M., Polverini, P.J., Kunkel, S.L., Arenberg, D.A., Burdick, M.D., Kasper, J., Dzuiba, J., Van Damme, J., Walz, A., Marriott, D.*, et al.* (1995). The functional role of the ELR motif in CXC chemokine-mediated angiogenesis. The Journal of biological chemistry *270*, 27348-27357.

Stronach, E.A., Chen, M., Maginn, E.N., Agarwal, R., Mills, G.B., Wasan, H., and Gabra, H. (2011). DNA-PK Mediates AKT Activation and Apoptosis Inhibition in Clinically Acquired Platinum Resistance. Neoplasia *13*, 1069-1080.

Stuart, G.R., Holcroft, J., de Boer, J.G., and Glickman, B.W. (2000). Prostate mutations in rats induced by the suspected human carcinogen 2-aminol-methyl-6-phenylimidazo 4,5-b pyridine. Cancer research *60*, 266-268.

Subramaniam, A., Shanmugam, M.K., Perumal, E., Li, F., Nachiyappan, A., Dai, X., Swamy, S.N., Ahn, K.S., Kumar, A.P., Tan, B.K.H.*, et al.* (2013). Potential role of signal transducer and activator of transcription (STAT)3 signaling pathway in inflammation, survival, proliferation and invasion of hepatocellular carcinoma. Biochimica et Biophysica Acta (BBA) - Reviews on Cancer *1835*, 46-60.

Sugarman, B., Aggarwal, B., Hass, P., Figari, I., Palladino, M., and Shepard, H. (1985). Recombinant human tumor necrosis factor-alpha: effects on proliferation of normal and transformed cells in vitro. Science *230*, 943-945.

Sugie, S., Mukai, S., Yamasaki, K., Kamibeppu, T., Tsukino, H., and Kamoto, T. (2015). Significant Association of Caveolin-1 and Caveolin-2 with Prostate Cancer Progression. Cancer genomics & proteomics *12*, 391-396.

Sun, J., Wiklund, F., Zheng, S.L., Chang, B., Balter, K., Li, L., Johansson, J.E., Li, G., Adami, H.O., Liu, W.*, et al.* (2005). Sequence variants in Toll-like receptor gene cluster (TLR6-TLR1-TLR10) and prostate cancer risk. Journal of the National Cancer Institute *97*, 525-532.

Sun, L., Wang, H., Wang, Z., He, S., Chen, S., Liao, D., Wang, L., Yan, J., Liu, W., Lei, X.*, et al.* (2012). Mixed lineage kinase domain-like protein mediates necrosis signaling downstream of RIP3 kinase. Cell *148*, 213-227.

Sun, M., Wang, G., Paciga, J.E., Feldman, R.I., Yuan, Z.Q., Ma, X.L., Shelley, S.A., Jove, R., Tsichlis, P.N., Nicosia, S.V.*, et al.* (2001). AKT1/PKBalpha kinase is frequently elevated in human cancers and its constitutive activation is required for oncogenic transformation in NIH3T3 cells. The American journal of pathology *159*, 431-437.

Sun, X., Huang, J., Homma, T., Kita, D., Klocker, H., Schafer, G., Boyle, P., and Ohgaki, H. (2009). Genetic Alterations in the PI3K Pathway in Prostate Cancer. Anticancer Research *29*, 1739-1743.

Suriano, G., Oliveira, C., Ferreira, P., Machado, J.C., Bordin, M.C., De Wever, O., Bruyneel, E.A., Moguilevsky, N., Grehan, N., Porter, T.R.*, et al.* (2003). Identification of CDH1 germline

missense mutations associated with functional inactivation of the E-cadherin protein in young gastric cancer probands. Human molecular genetics *12*, 575-582.

Suwanabol, P.A., Seedial, S.M., Zhang, F., Shi, X., Si, Y., Liu, B., and Kent, K.C. (2012). TGF-β and Smad3 modulate PI3K/Akt signaling pathway in vascular smooth muscle cells. American Journal of Physiology - Heart and Circulatory Physiology *302*, H2211-H2219.

Suzuki, H., Emi, M., Komiya, A., Fujiwara, Y., Yatani, R., Nakamura, Y., and Shimazaki, J. (1995). Localization of a tumor suppressor gene associated with progression of human prostate cancer within a 1.2 Mb region of 8p22-p21.3. Genes, chromosomes & cancer *13*, 168-174.

Szklarczyk, D., Morris, J.H., Cook, H., Kuhn, M., Wyder, S., Simonovic, M., Santos, A., Doncheva, N.T., Roth, A., Bork, P.*, et al.* (2017). The STRING database in 2017: quality-controlled protein-protein association networks, made broadly accessible. Nucleic acids research *45*, D362-d368.

Taga, T., Hibi, M., Hirata, Y., Yamasaki, K., Yasukawa, K., Matsuda, T., Hirano, T., and Kishimoto, T. (1989). Interleukin-6 triggers the association of its receptor with a possible signal transducer, gp130. Cell *58*, 573-581.

Tahara, T., Hirata, I., Nakano, N., Tahara, S., Horiguchi, N., Kawamura, T., Okubo, M., Ishizuka, T., Yamada, H., Yoshida, D.*, et al.* Potential link between *Fusobacterium* enrichment and DNA methylation accumulation in the inflammatory colonic mucosa in ulcerative colitis (Oncotarget. 2017 Sep 22;8(37):61917-26. doi:10.18632/oncotarget.18716.).

Takeda, D.Y., and Dutta, A. (2005). DNA replication and progression through S phase. *24*, 2827-2843.

Talley, N.J., Zinsmeister, A.R., Weaver, A., DiMagno, E.P., Carpenter, H.A., Perez-Perez, G.I., and Blaser, M.J. (1991). Gastric adenocarcinoma and *Helicobacter pylori* infection. Journal of the National Cancer Institute *83*, 1734-1739.

Tan, P., Fuchs, S.Y., Chen, A., Wu, K., Gomez, C., Ronai, Z.e., and Pan, Z.-Q. (1999). Recruitment of a ROC1–CUL1 Ubiquitin Ligase by Skp1 and HOS to Catalyze the Ubiquitination of IκBα. Molecular Cell *3*, 527-533.

Tancrede, C. (1992). Role of human microflora in health and disease. European journal of clinical microbiology & infectious diseases: official publication of the European Society of Clinical Microbiology *11*, 1012-1015.

Tannock, I.F., de Wit, R., Berry, W.R., Horti, J., Pluzanska, A., Chi, K.N., Oudard, S., Theodore, C., James, N.D., Turesson, I.*, et al.* (2004). Docetaxel plus prednisone or mitoxantrone plus prednisone for advanced prostate cancer. The New England journal of medicine *351*, 1502-1512.

Theveneau, E., and Mayor, R. (2012). Cadherins in collective cell migration of mesenchymal cells. Current Opinion in Cell Biology *24*, 677-684.

Thomas, S.J., Snowden, J.A., Zeidler, M.P., and Danson, S.J. (2015). The role of JAK/STAT signalling in the pathogenesis, prognosis and treatment of solid tumours. British journal of cancer *113*, 365-371.

Thomason, J.L., Schreckenberger, P.C., Spellacy, W.N., Riff, L.J., and LeBeau, L.J. (1984). Clinical and microbiological characterization of patients with nonspecific vaginosis associated with motile, curved anaerobic rods. The Journal of infectious diseases *149*, 801-809.

Thompson, I.M., Ankerst, D., Chi, C., and et al. (2005). Operating characteristics of prostate-specific antigen in men with an initial psa level of 3.0 ng/ml or lower. Jama *294*, 66-70.

Thornton, T.M., and Rincon, M. (2009). Non-Classical P38 Map Kinase Functions: Cell Cycle Checkpoints and Survival. International Journal of Biological Sciences *5*, 44-52.

Thun, M.J., Henley, S.J., and Patrono, C. (2002). Nonsteroidal anti-inflammatory drugs as anticancer agents: mechanistic, pharmacologic, and clinical issues. Journal of the National Cancer Institute *94*, 252-266.

Tomlins, S.A., Rhodes, D.R., Perner, S., Dhanasekaran, S.M., Mehra, R., Sun, X.-W., Varambally, S., Cao, X., Tchinda, J., Kuefer, R*., et al.* (2005). Recurrent Fusion of *TMPRSS2* and ETS Transcription Factor Genes in Prostate Cancer. Science *310*, 644-648.

Tomshine, J.C., Severson, S.R., Wigle, D.A., Sun, Z., Beleford, D.A.T., Shridhar, V., and Horazdovsky, B.F. (2009). Cell Proliferation and Epidermal Growth Factor Signaling in Non-small Cell Lung Adenocarcinoma Cell Lines Are Dependent on Rin1. Journal of Biological Chemistry *284*, 26331-26339.

Tsareva, S.A., Moriggl, R., Corvinus, F.M., Wiederanders, B., Schütz, A., Kovacic, B., and Friedrich, K. (2007). Signal Transducer and Activator of Transcription 3 Activation Promotes Invasive Growth of Colon Carcinomas through Matrix Metalloproteinase Induction. Neoplasia *9*, 279-291.

Tsaur, I., Renninger, M., Hennenlotter, J., Oppermann, E., Munz, M., Kuehs, U., Stenzl, A., and Schilling, D. (2013). Reliable housekeeping gene combination for quantitative PCR of lymph nodes in patients with prostate cancer. Anticancer Res *33*, 5243-5248.

Tse, B.W.C., Scott, K.F., and Russell, P.J. (2012). Paradoxical Roles of Tumour Necrosis Factor-Alpha in Prostate Cancer Biology. Prostate Cancer *2012*, 8.

Tsodikov, A., Gulati, R., Heijnsdijk, E.M., and et al. (2017). REconciling the effects of screening on prostate cancer mortality in the erspc and plco trials. Annals of internal medicine.

Tsuda, K., Yamanaka, K., Linan, W., Miyahara, Y., Akeda, T., Nakanishi, T., Kitagawa, H., Kakeda, M., Kurokawa, I., Shiku, H*., et al.* (2011). Intratumoral Injection of *Propionibacterium*

acnes Suppresses Malignant Melanoma by Enhancing Th1 Immune Responses. PloS one *6*, e29020.

Tsujii, M., and DuBois, R.N. (1995). Alterations in cellular adhesion and apoptosis in epithelial cells overexpressing prostaglandin endoperoxide synthase 2. Cell *83*, 493-501.

Tucci, M., Scagliotti, G.V., and Vignani, F. (2015). Metastatic castration-resistant prostate cancer: time for innovation. Future oncology *11*, 91-106.

Tunney, M.M., Patrick, S., Gorman, S.P., Nixon, J.R., Anderson, N., Davis, R.I., Hanna, D., and Ramage, G. (1998). Improved detection of infection in hip replacements. A currently underestimated problem. The Journal of bone and joint surgery British volume *80*, 568-572.

Turner, M.D., Nedjai, B., Hurst, T., and Pennington, D.J. (2014). Cytokines and chemokines: At the crossroads of cell signalling and inflammatory disease. Biochimica et Biophysica Acta (BBA) - Molecular Cell Research *1843*, 2563-2582.

Uhlen, M., Zhang, C., Lee, S., Sjöstedt, E., Fagerberg, L., Bidkhori, G., Benfeitas, R., Arif, M., Liu, Z., Edfors, F*., et al.* (2017). A pathology atlas of the human cancer transcriptome. Science *357*.

Ullah, I., Subbarao R , B., and Rho G , J. (2015). Human mesenchymal stem cells - current trends and future prospective. Bioscience Reports *35*.

Uotila, P., Valve, E., Martikainen, P., Nevalainen, M., Nurmi, M., and Härkönen, P. (2001). Increased expression of cyclooxygenase-2 and nitric oxide synthase-2 in human prostate cancer. Urological research *29*, 25-28.

Valanne, S., McDowell, A., Ramage, G., Tunney, M.M., Einarsson, G.G., O'Hagan, S., Wisdom, G.B., Fairley, D., Bhatia, A., Maisonneuve, J.F*., et al.* (2005). CAMP factor homologues in *Propionibacterium acnes*: a new protein family differentially expressed by types I and II. Microbiology *151*, 1369-1379.

Vallée, A., Guillevin, R., and Vallée, J.-N. (2017). Vasculogenesis and angiogenesis initiation under normoxic conditions through Wnt/β-catenin pathway in gliomas. In Reviews in the Neurosciences.

van Cruijsen, H., Giaccone, G., and Hoekman, K. (2005). Epidermal growth factor receptor and angiogenesis: Opportunities for combined anticancer strategies. International journal of cancer Journal international du cancer *117*, 883-888.

Van de Sande, T., Roskams, T., Lerut, E., Joniau, S., Van Poppel, H., Verhoeven, G., and Swinnen, J.V. (2005). High-level expression of fatty acid synthase in human prostate cancer tissues is linked to activation and nuclear localization of Akt/PKB. The Journal of pathology *206*, 214-219.

van Poppel, H., and Nilsson, S. (2008). Testosterone Surge: Rationale for Gonadotropin-Releasing Hormone Blockers? Urology *71*, 1001-1006.

Vanaja, D.K., Ballman, K.V., Morlan, B.W., Cheville, J.C., Neumann, R.M., Lieber, M.M., Tindall, D.J., and Young, C.Y. (2006). PDLIM4 repression by hypermethylation as a potential biomarker for prostate cancer. Clinical cancer research: an official journal of the American Association for Cancer Research *12*, 1128-1136.

Vandesompele, J., De Preter, K., Pattyn, F., Poppe, B., Van Roy, N., De Paepe, A., and Speleman, F. (2002). Accurate normalization of real-time quantitative RT-PCR data by geometric averaging of multiple internal control genes. Genome Biology *3*, research0034.0031.

Veltri, R.W., Miller, M.C., Zhao, G., Ng, A., Marley, G.M., Wright, G.L., Jr., Vessella, R.L., and Ralph, D. (1999). Interleukin-8 serum levels in patients with benign prostatic hyperplasia and prostate cancer. Urology *53*, 139-147.

Venter, J.C., Adams, M.D., Myers, E.W., Li, P.W., Mural, R.J., Sutton, G.G., Smith, H.O., Yandell, M., Evans, C.A., Holt, R.A*., et al.* (2001). The sequence of the human genome. Science *291*, 1304-1351.

Verze, P., Cai, T., and Lorenzetti, S. (2016). The role of the prostate in male fertility, health and disease. Nat Rev Urol *13*, 379-386.

Vincent, T., Neve, E.P.A., Johnson, J.R., Kukalev, A., Rojo, F., Albanell, J., Pietras, K., Virtanen, I., Philipson, L., Leopold, P.L*., et al.* (2009). A SNAIL1-SMAD3/4 transcriptional repressor complex promotes TGF-β mediated epithelial-mesenchymal transition. Nature cell biology *11*, 943-950.

Vivanco, I., and Sawyers, C.L. (2002). The phosphatidylinositol 3-Kinase-AKT pathway in human cancer. Nature reviews Cancer *2*, 489-501.

Vleminckx, K., Vakaet, L., Mareel, M., Fiers, W., and Van Roy, F. (1991). Genetic manipulation of E-cadherin expression by epithelial tumor cells reveals an invasion suppressor role. Cell *66*, 107-119.

Vocke, C.D., Pozzatti, R.O., Bostwick, D.G., Florence, C.D., Jennings, S.B., Strup, S.E., Duray, P.H., Liotta, L.A., Emmert-Buck, M.R., and Linehan, W.M. (1996). Analysis of 99 microdissected prostate carcinomas reveals a high frequency of allelic loss on chromosome 8p12-21. Cancer research *56*, 2411-2416.

Vörös, A., Horváth, B., Hunyadkürti, J., McDowell, A., Barnard, E., Patrick, S., and Nagy, I. (2012). Complete genome sequences of three *Propionibacterium acnes* isolates from the type IA(2) cluster. Journal of bacteriology *194*, 1621-1622.

Wagenlehner, F.M.E., Elkahwaji, J.E., Algaba, F., Bjerklund-Johansen, T., Naber, K.G., Hartung, R., and Weidner, W. (2007). The role of inflammation and infection in the pathogenesis of prostate carcinoma. BJU international *100*, 733-737.

Wagenlehner, F.M.E., Pilatz, A., Bschleipfer, T., Diemer, T., Linn, T., Meinhardt, A., Schagdarsurengin, U., Dansranjavin, T., Schuppe, H.-C., and Weidner, W. (2013). Bacterial prostatitis. World Journal of Urology *31*, 711-716.

Wagner, E.F., and Nebreda, A.R. (2009). Signal integration by JNK and p38 MAPK pathways in cancer development. Nature reviews Cancer *9*, 537-549.

Wang, D., Li, Z., Messing, E.M., and Wu, G. (2005). The SPRY domain-containing SOCS box protein 1 (SSB-1) interacts with MET and enhances the hepatocyte growth factor-induced Erk-Elk-1-serum response element pathway. The Journal of biological chemistry *280*, 16393-16401.

Wang, L., Du, F., and Wang, X. (2008a). TNF-alpha induces two distinct caspase-8 activation pathways. Cell *133*, 693-703.

Wang, S., Li, X., Parra, M., Verdin, E., Bassel-Duby, R., and Olson, E.N. (2008b). Control of endothelial cell proliferation and migration by VEGF signaling to histone deacetylase 7. Proceedings of the National Academy of Sciences *105*, 7738-7743.

Wang, W., Bergh, A., and Damber, J.E. (2009). Morphological transition of proliferative inflammatory atrophy to high-grade intraepithelial neoplasia and cancer in human prostate. The Prostate *69*, 1378-1386.

Wang, W.L., Everett, E.D., Johnson, M., and Dean, E. (1977). Susceptibility of *Propionibacterium acnes* to seventeen antibiotics. Antimicrobial agents and chemotherapy *11*, 171-173.

Webster, M.R., and Weeraratna, A.T. (2013). A Wnt-er Migration: The Confusing Role of β-Catenin in Melanoma Metastasis. Science signaling *6*, pe11-pe11.

Weerasinghe, P., Li, Y., Guan, Y., Zhang, R., Tweardy, D.J., and Jing, N. (2008). T40214/PEI Complex, a Potent Therapeutics for Prostate Cancer that Targets STAT3 Signaling. The Prostate *68*, 1430-1442.

Wegiel, B., Bjartell, A., Culig, Z., and Persson, J.L. (2008). Interleukin-6 activates PI3K/Akt pathway and regulates cyclin A1 to promote prostate cancer cell survival. International journal of cancer Journal international du cancer *122*, 1521-1529.

Wegiel, B., Bjartell, A., Ekberg, J., Gadaleanu, V., Brunhoff, C., and Persson, J.L. (2005). A role for cyclin A1 in mediating the autocrine expression of vascular endothelial growth factor in prostate cancer. Oncogene *24*, 6385-6393.

Weidner, W., Schiefer, H.G., Krauss, H., Jantos, C., Friedrich, H.J., and Altmannsberger, M. (1991). Chronic prostatitis: a thorough search for etiologically involved microorganisms in 1,461 patients. Infection *19 Suppl 3*, S119-125.

Westerhof, W., Relyveld, G.N., Kingswijk, M.M., de Man, P., and Menke, H.E. (2004). *Propionibacterium acnes* and the pathogenesis of progressive macular hypomelanosis. Archives of dermatology *140*, 210-214.

Weston, C.R., and Davis, R.J. (2007). The JNK signal transduction pathway. Current Opinion in Cell Biology *19*, 142-149.

Wheelock, M.J., Shintani, Y., Maeda, M., Fukumoto, Y., and Johnson, K.R. (2008). Cadherin switching. Journal of cell science *121*, 727-735.

Whitmore, W.F., Jr., Hilaris, B., and Grabstald, H. (1972). Retropubic implantation to iodine 125 in the treatment of prostatic cancer. The Journal of urology *108*, 918-920.

Whittemore, A.S., Kolonel, L.N., Wu, A.H., John, E.M., Gallagher, R.P., Howe, G.R., Burch, J.D., Hankin, J., Dreon, D.M., West, D.W.*, et al.* (1995). Prostate Cancer in Relation to Diet, Physical Activity, and Body Size in Blacks, Whites, and Asians in the United States and Canada. JNCI: Journal of the National Cancer Institute *87*, 652-661.

Whyte, J.L., Smith, A.A., and Helms, J.A. (2012). Wnt Signaling and Injury Repair. Cold Spring Harbor perspectives in biology *4*.

Wise, G.J., Marella, V.K., Talluri, G., and Shirazian, D. (2000). Cytokine variations in patients with hormone treated prostate cancer. The Journal of urology *164*, 722-725.

Wong, S.C.C., Lo, S.F.E., Lee, K.C., Yam, J.W.P., Chan, J.K.C., and Wendy Hsiao, W.L. (2002). Expression of frizzled-related protein and Wnt-signalling molecules in invasive human breast tumours. The Journal of pathology *196*, 145-153.

Wong, Y.N., Ferraldeschi, R., Attard, G., and de Bono, J. (2014). Evolution of androgen receptor targeted therapy for advanced prostate cancer. Nat Rev Clin Oncol *11*, 365-376.

Woodman, C.B.J., Collins, S.I., and Young, L.S. (2007). The natural history of cervical HPV infection: unresolved issues. Nature Reviews Cancer *7*, 11.

Woodruff, M.F., and Boak, J.L. (1966). Inhibitory effect of injection of *Corynebacterium parvum* on the growth of tumour transplants in isogenic hosts. British journal of cancer *20*, 345-355.

Wrana, J.L., Attisano, L., Wieser, R., Ventura, F., and Massague, J. (1994). Mechanism of activation of the TGF-β receptor. Nature *370*, 341-347.

Wu, D., Zhau, H.E., Huang, W.C., Iqbal, S., Habib, F.K., Sartor, O., Cvitanovic, L., Marshall, F.F., Xu, Z., and Chung, L.W.K. (2007). cAMP-responsive element-binding protein regulates vascular endothelial growth factor expression: implication in human prostate cancer bone metastasis. Oncogene *26*, 5070-5077.

Wu, K., Fuchs, S.Y., Chen, A., Tan, P., Gomez, C., Ronai, Z., and Pan, Z.Q. (2000). The SCF(HOS/beta-TRCP)-ROC1 E3 ubiquitin ligase utilizes two distinct domains within CUL1 for substrate targeting and ubiquitin ligation. Molecular and cellular biology *20*, 1382-1393.

Wu, X., Daniels, G., Lee, P., and Monaco, M.E. (2014). Lipid metabolism in prostate cancer. American Journal of Clinical and Experimental Urology *2*, 111-120.

Wu, Y., Deng, J., Rychahou, P.G., Qiu, S., Evers, B.M., and Zhou, B.P. (2009). Stabilization of Snail by NF-κB Is Required for Inflammation-Induced Cell Migration and Invasion. Cancer cell *15*, 416-428.

Wullschleger, S., Loewith, R., and Hall, M.N. (2006). TOR Signaling in Growth and Metabolism. Cell *124*, 471-484.

Xiao, G., Harhaj, E.W., and Sun, S.-C. (2001). NF-κB-Inducing Kinase Regulates the Processing of NF-κB2 p100. Molecular Cell *7*, 401-409.

Xiong, H., Zhang, Z.-G., Tian, X.-Q., Sun, D.-F., Liang, Q.-C., Zhang, Y.-J., Lu, R., Chen, Y.-X., and Fang, J.-Y. (2008). Inhibition of JAK1, 2/STAT3 Signaling Induces Apoptosis, Cell Cycle Arrest, and Reduces Tumor Cell Invasion in Colorectal Cancer Cells. Neoplasia *10*, 287-297.

Xu, J., Lamouille, S., and Derynck, R. (2009). TGF-beta-induced epithelial to mesenchymal transition. Cell research *19*, 156-172.

Xu, J., Zheng, S.L., Komiya, A., Mychaleckyj, J.C., Isaacs, S.D., Hu, J.J., Sterling, D., Lange, E.M., Hawkins, G.A., Turner, A.*, et al.* (2002). Germline mutations and sequence variants of the macrophage scavenger receptor 1 gene are associated with prostate cancer risk. Nature genetics *32*, 321-325.

Yamamura, K., Baba, Y., Nakagawa, S., Mima, K., Miyake, K., Nakamura, K., Sawayama, H., Kinoshita, K., Ishimoto, T., Iwatsuki, M.*, et al.* (2016). Human Microbiome *Fusobacterium Nucleatum* in Esophageal Cancer Tissue Is Associated with Prognosis. Clinical cancer research: an official journal of the American Association for Cancer Research *22*, 5574-5581.

Yamaoka, M., Hara, T., and Kusaka, M. (2010). Overcoming Persistent Dependency on Androgen Signaling after Progression to Castration-Resistant Prostate Cancer. Clinical Cancer Research *16*, 4319-4324.

Yang, F., Sun, L., Li, Q., Han, X., Lei, L., Zhang, H., and Shang, Y. (2012). SET8 promotes epithelial-mesenchymal transition and confers TWIST dual transcriptional activities. The EMBO journal *31*, 110-123.

Yang, G., Murashige, Danielle S., Humphrey, Sean J., and James, David E. (2015). A Positive Feedback Loop between Akt and mTORC2 via SIN1 Phosphorylation. Cell reports *12*, 937-943.

Yang, J., Liao, X., Agarwal, M.K., Barnes, L., Auron, P.E., and Stark, G.R. (2007). Unphosphorylated STAT3 accumulates in response to IL-6 and activates transcription by binding to NFkappaB. Genes & development *21*, 1396-1408.

Yang, J., Liu, X., Bhalla, K., Kim, C.N., Ibrado, A.M., Cai, J., Peng, T.-I., Jones, D.P., and Wang, X. (1997a). Prevention of Apoptosis by Bcl-2: Release of Cytochrome c from Mitochondria Blocked. Science *275*, 1129-1132.

Yang, J., Mani, S.A., Donaher, J.L., Ramaswamy, S., Itzykson, R.A., Come, C., Savagner, P., Gitelman, I., Richardson, A., and Weinberg, R.A. (2004). Twist, a Master Regulator of Morphogenesis, Plays an Essential Role in Tumor Metastasis. Cell *117*, 927-939.

Yang, M.-H., Hsu, D.S.-S., Wang, H.-W., Wang, H.-J., Lan, H.-Y., Yang, W.-H., Huang, C.-H., Kao, S.-Y., Tzeng, C.-H., Tai, S.-K*., et al.* (2010). Bmi1 is essential in Twist1-induced epithelial-mesenchymal transition. Nature cell biology *12*, 982-992.

Yang, M.-H., Wu, M.-Z., Chiou, S.-H., Chen, P.-M., Chang, S.-Y., Liu, C.-J., Teng, S.-C., and Wu, K.-J. (2008). Direct regulation of TWIST by HIF-1α promotes metastasis. Nature cell biology *10*, 295-305.

Yang, X., Khosravi-Far, R., Chang, H.Y., and Baltimore, D. (1997b). Daxx, a novel Fas-binding protein that activates JNK and apoptosis. Cell *89*, 1067-1076.

Yeh, P.Y., Yeh, K.-H., Chuang, S.-E., Song, Y.C., and Cheng, A.-L. (2004). Suppression of MEK/ERK Signaling Pathway Enhances Cisplatin-induced NF-κB Activation by Protein Phosphatase 4-mediated NF-κB p65 Thr Dephosphorylation. Journal of Biological Chemistry *279*, 26143-26148.

Yilmaz, M., and Christofori, G. (2009). EMT, the cytoskeleton, and cancer cell invasion. Cancer and Metastasis Reviews *28*, 15-33.

Yook, J.I., Li, X.-Y., Ota, I., Fearon, E.R., and Weiss, S.J. (2005). Wnt-dependent Regulation of the E-cadherin Repressor Snail. Journal of Biological Chemistry *280*, 11740-11748.

Yook, J.I., Li, X.-Y., Ota, I., Hu, C., Kim, H.S., Kim, N.H., Cha, S.Y., Ryu, J.K., Choi, Y.J., Kim, J*., et al.* (2006). A Wnt-Axin2-GSK3β cascade regulates Snail1 activity in breast cancer cells. Nature cell biology *8*, 1398-1406.

Yoon, B.I., Kim, S., Han, D.S., Ha, U.S., Lee, S.J., Kim, H.W., Han, C.H., and Cho, Y.H. (2012). Acute bacterial prostatitis: how to prevent and manage chronic infection? Journal of infection and chemotherapy: official journal of the Japan Society of Chemotherapy *18*, 444-450.

Yoon, S., and Seger, R. (2006). The extracellular signal-regulated kinase: Multiple substrates regulate diverse cellular functions. Growth Factors *24*, 21-44.

Yoshida, A., Yoshida, S., Ishibashi, T., Kuwano, M., and Inomata, H. (1999). Suppression of retinal neovascularization by the NF-kappaB inhibitor pyrrolidine dithiocarbamate in mice. Investigative ophthalmology & visual science *40*, 1624-1629.

Yow, M.A., Tabrizi, S.N., Severi, G., Bolton, D.M., Pedersen, J., Giles, G.G., and Southey, M.C. (2017). Characterisation of microbial communities within aggressive prostate cancer tissues. Infectious agents and cancer *12*.

Yu, H., and Jove, R. (2004). The STATs of cancer--new molecular targets come of age. Nature reviews Cancer *4*, 97-105.

Yu, H., Pardoll, D., and Jove, R. (2009). STATs in cancer inflammation and immunity: a leading role for STAT3. Nature reviews Cancer *9*, 798-809.

Zeller, V., Ghorbani, A., Strady, C., Leonard, P., Mamoudy, P., and Desplaces, N. (2007). *Propionibacterium acnes*: an agent of prosthetic joint infection and colonization. The Journal of infection *55*, 119-124.

Zhang, J., Chen, S., Zhang, W., Zhang, J., Liu, X., Shi, H., Che, H., Wang, W., Li, F., and Yao, L. (2008). Human differentiation-related gene NDRG1 is a Myc downstream-regulated gene that is repressed by Myc on the core promoter region. Gene *417*, 5-12.

Zhang, J.Y., Zhang, F., Hong, C.Q., Giuliano, A.E., Cui, X.J., Zhou, G.J., Zhang, G.J., and Cui, Y.K. (2015). Critical protein GAPDH and its regulatory mechanisms in cancer cells. Cancer Biology & Medicine *12*, 10-22.

Zhang, L., Altuwaijri, S., Deng, F., Chen, L., Lal, P., Bhanot, U.K., Korets, R., Wenske, S., Lilja, H.G., Chang, C*., et al.* (2009). NF-κB Regulates Androgen Receptor Expression and Prostate Cancer Growth. The American journal of pathology *175*, 489-499.

Zhao, J., Stockwell, T., Roemer, A., and Chikritzhs, T. (2016). Is alcohol consumption a risk factor for prostate cancer? A systematic review and meta–analysis. BMC cancer *16*, 845.

Zhao, X., Rong, L., Zhao, X., Li, X., Liu, X., Deng, J., Wu, H., Xu, X., Erben, U., Wu, P*., et al.* (2012). TNF signaling drives myeloid-derived suppressor cell accumulation. The Journal of clinical investigation *122*, 4094-4104.

Zheng, S.L., Augustsson-Balter, K., Chang, B., Hedelin, M., Li, L., Adami, H.O., Bensen, J., Li, G., Johnasson, J.E., Turner, A.R*., et al.* (2004). Sequence variants of toll-like receptor 4 are associated with prostate cancer risk: results from the CAncer Prostate in Sweden Study. Cancer research *64*, 2918-2922.

Zhong, Z., Wen, Z., and Darnell, J.E., Jr. (1994). Stat3: a STAT family member activated by tyrosine phosphorylation in response to epidermal growth factor and interleukin-6. Science *264*, 95-98.

Ziello, J.E., Jovin, I.S., and Huang, Y. (2007). Hypoxia-Inducible Factor (HIF)-1 Regulatory Pathway and its Potential for Therapeutic Intervention in Malignancy and Ischemia. The Yale journal of biology and medicine *80*, 51-60.

Zilfou, J.T., and Lowe, S.W. (2009). Tumor Suppressive Functions of p53. Cold Spring Harbor perspectives in biology *1*.

Zlotnik, A., and Yoshie, O. (2000). Chemokines: a new classification system and their role in immunity. Immunity *12*, 121-127.